Universitat de les
Illes Balears

DOCTORAL THESIS

2015

IMPROVING OSSEOINTEGRATION OF TITANIUM IMPLANTS BY A NOVEL BIOACTIVE COATING WITH UV-IRRADIATED 7- DEHYDROCHOLESTEROL

María Satué Sahún

Universitat de les Illes Balears

DOCTORAL THESIS

2015

Doctoral Programme of Biosciences

IMPROVING OSSEOINTEGRATION OF TITANIUM IMPLANTS BY A NOVEL BIOACTIVE COATING WITH UV-IRRADIATED 7- DEHYDROCHOLESTEROL

María Satué Sahún

Thesis Supervisor: Marta Monjo Cabrer, PhD

Thesis Supervisor: Joana Maria Ramis Morey, PhD

Doctor by the Universitat de les Illes Balears

With the approval of the supervisors

Marta Monjo Cabrer, PhD

Contracted Lecturer

Department of Fundamental Biology and Health Sciences, University of Balearic Islands, Palma (Spain)

Joana M. Ramis Morey, PhD

Adjunct Lecturer

Department of Fundamental Biology and Health Sciences, University of Balearic Islands, Palma (Spain)

The doctoral candidate

María Satué Sahún

Universitat de les Illes Balears

Dr Marta Monjo, contracted lecturer at the Department of Fundamental Biology and Health Sciences of the University of the Balearic Islands

And

Dr Joana Maria Ramis, adjunct lecturer at the Department of Fundamental Biology and Health Sciences of the University of the Balearic Islands

WE DECLARE:

That the thesis entitled *Improving osseointegration of titanium implants by a novel bioactive coating with UV-irradiated 7-dehydrocholesterol*, presented by María Satué Sahún to obtain a doctoral degree, has been completed under our supervision and meets the requirements to opt for an European Doctorate Mention.

For all intents and purposes, we hereby sign this document.

Marta Monjo Cabrer, PhD

Contracted Lecturer

Department of Fundamental Biology and Health Sciences, University of Balearic Islands, Palma (Spain)

Joana M. Ramis Morey, PhD

Adjunct Lecturer

Department of Fundamental Biology and Health Sciences, University of Balearic Islands, Palma (Spain)

Palma de Mallorca, 25 May 2015

A mis padres.

Agradecimientos/*Acknowledgments*

El trabajo presentado en esta tesis doctoral se ha llevado a cabo en el *Grupo de Terapia Celular e Ingeniería Tisular* del Instituto Universitario de Investigación en Ciencias de la Salud en la Universidad de las Islas Baleares y en el *Departamento de Biomateriales* de la Facultad de Odontología en la Universidad de Oslo. Durante estos años, muchas personas han contribuido, de una forma u otra, en la realización de esta tesis y por ello me gustaría expresar mi más sincero agradecimiento:

En primer lugar, quiero dar las gracias de corazón a mis directoras de tesis: la Dra. Marta Monjo y la Dra. Joana Maria Ramis, por haberme dado la oportunidad de introducirme en el mundo de la investigación y poder realizar el doctorado. Gracias por confiar en mí desde el primer día, por vuestro gran apoyo y dedicación, y por todo lo que me habéis enseñado durante estos años. Gracias por haberme guiado en este camino y por haberme ayudado a crecer tanto profesional como personalmente.

I would like to thank the co-authors who contributed to my thesis: Christiane Petzold, Staale Petter Lyngstadaas, Hans Jacob Ronold, Alba Córdoba and Manuel Gómez-Florit. A mis compañeros de laboratorio: Marina, Mar, Manu y Alba, por todo lo que he aprendido de vosotros, por vuestra ayuda y por todos los buenos momentos que hemos pasado en el laboratorio. Quiero agradecer a todos los compañeros del IUNICS y del Edificio Científico-Técnico, por su colaboración y ayuda con diferentes instrumentos, por su buen humor y por los buenos ratos de comidas y postres. *I would like to express my gratitude to all the Oslo team for the warm welcome that I received during my stay and for making the animal study possible.*

Quiero agradecer especialmente a mis amigas, por todo lo que hemos vivido juntas, por vuestro apoyo y vuestros ánimos a pesar de las distancias que nos separan. Sois geniales. También a todos los que han compartido estos años conmigo en Mallorca, gracias por vuestra acogida y por todo lo que hemos disfrutado juntos. Habéis conseguido que estos años en la isla hayan sido estupendos y difíciles de olvidar.

A toda mi familia. A mis padres y a mi hermana, porque siempre estáis a mi lado, apoyándome y animándome en todo momento. Gracias por todo vuestro amor y apoyo incondicional. Y por último a mi mallorquín preferido, por escucharme, comprenderme y siempre saberme sacar una sonrisa. Muchas gracias por todo. Os quiero.

María Satué

Barbastro, Mayo 2015

Index

Abbreviations

ACTA2	Smooth muscle actin alpha 2
ADAM8	A Disintegrin and metalloproteinase domain-containing protein 8
ALP	Alkaline phosphatase
ANOVA	Analysis of variance
BMPs	Bone morphogenic proteins
BMU	Basic multicellular units
CALCR	Calcitonin receptor
CaP	Calcium phosphate
CAR2	Carbonic anhydrase II
cDNA	Complementary deoxyribonucleic acid
CLSM	Confocal laser scanning microscopy
COL3A1	Collagen type III, alpha 1 chain
COLL1	Collagen type I
Cp	Crossing-point
CSF-1	Colony stimulating factor 1
CTSK	Cathepsine K
CYP24A1	1,25-Dihydroxyvitamin D_3 24-hydroxylase
CYP27A1	Vitamin D_3 25-hydroxylase
CYP27B1	25-Hydroxyvitamin D_3-1alpha-hydroxylase
D_2	Ergocalciferol
D_3	Cholecalciferol
DBP	Vitamin D binding protein
DC-STAMP	Dendritic-cell specific transmembrane protein
7-DHC	7-Dehydrocholesterol
DI	Deionized
DMS	Minimum significance difference
DNA	Deoxyribonucleic acid
dsDNA	Double-stranded DNA
ECM	Extracellular matrix
EDN1	Endothelin 1
ELISA	Enzyme-Linked ImmunoSorbent Assay

FITC	Fluorescein isothiocyanate
FN1	Fibronectin 1
FTIR	Fourier transform infrared spectroscopy
GAPDH	Glyceraldehyde-3-phosphate dehydrogenase
H^+ATPase	Proton ATPase
HGF	Human gingival fibroblast
HPLC	High performance liquid chromatography
hUC-MSC	Human umbilical cord mesenchymal stem cell
ICP-AES	Inductively coupled atomic plasma emission spectroscopy
IGF	Insulin-like growth factor
IL6	Interleukin-6
IL8	Interleukin-8
IL10	Interleukin-10
IR	Infrared
ITGAV	Integrin alpha-V
ITGB3	Integrin beta-3
LDH	Lactate dehydrogenase
M-CSF	Macrophage colony-stimulating factor
MIQE	Minimum information for Publication of Quantitative Real-Time PCR Experiments
MMPs	Matrix metalloproteinases
MSC	Mesenchymal stem cell
MTT	Tetrazolium salt
NARA	Norwegian Animal Research Authority
OC	Osteocalcin
$25(OH)D_3$	25-Hydroxyvitamin D_3
$1,25(OH)_2D_3$	Calcitriol
OPG	Osteoprotegerin
OSX	Osterix
PBS	Phosphate-buffered saline
PCR	Polymerase chain reaction
PDA	Photodiode array
PDGF	Platelet derived growth factor
pNPP	p-Nitrophenyl phosphate

$preD_3$	Previtamin D_3
PTFE	Polytetrafluoroethylene
PTH	Parathormone
qPCR	Quantitative PCR
RANKL	Receptor activator NFKB Ligand
RGD	Arginine-glycine-aspartate
RNA	Ribonucleic acid
RPA	Ribonucleases protective assay
RT-PCR	Real time reverse transcription polymerase chain reaction
RUNX2	Runt related gene
RXR	Retinoid X receptor
18S	Ribosomal RNA 18S
SEM	Scanning electron microscope
S.E.M.	Standard deviation of the mean
SPARC	Osteonectin
SPP1	Osteopontin
TGF-β	Transforming growth factor B
Ti	Titanium
TIMP1	Tissue inhibitor of metalloproteinase 1
TiO_2	Titanium dioxide
TNF-α	Tumor necrosis factor alpha
TRAP	Tartrate-resistant acid phosphatase
UNIANOVA	Univariate analysis of variance
UV	Ultraviolet
VDR	Vitamin D receptor
VDREs	Vitamin D response elements
VitE	α-Tocopherol

Improving osseointegration of titanium implants by a novel bioactive coating with UV-irradiated 7-dehydrocholesterol

PhD thesis, María Satué Sahún, University Institute for Health Sciences Research (IUNICS), University of Balearic Islands, Palma de Mallorca, Spain.

Abstract

Current implant research aims at producing innovative bioactive surfaces to restore function in compromised skeletal structures. Surface modification of titanium (Ti) implants aims for a better biological response to the material to improve osseointegration. Increasing evidences highlight the essential role of vitamin D in bone regeneration and the profound negative effects of its insufficiency on implant osseointegration. Indeed, vitamin D deficiency leads to bone resorption, osteoporosis and reduced mineralization. Unfortunately, there is a high prevalence of vitamin D deficiency across all age groups in worldwide populations, what is due to inadequate dietary intake and insufficient exposure to sunlight.

Calcitriol ($1,25(OH)_2D_3$), the biologically active form of vitamin D_3, is produced by a hydroxylation cascade, which is preceded by a photochemical activation. It starts when 7-dehydrocholesterol (7-DHC) is exposed in the skin to UVB irradiation, involving the conversion into previtamin D_3 ($preD_3$). Afterwards, this metabolite is transformed into cholecalciferol (D_3) and subsequently hydroxylated once in the liver and once in the kidneys to the end product. In this thesis, we demonstrated for the first time that the vitamin D precursor, 7-DHC, can be used to locally produce active vitamin D by osteoblastic cells and enhance their differentiation, when 7-DHC is coated on polystyrene surfaces and UV-irradiated before the cell culture. In addition, we proved the feasibility of using UV-irradiated 7-DHC to locally produce $preD_3$ at the surface of Ti implants, which entails an increased osteoblast differentiation *in vitro*. Further, the biological potential of the present surface modification was confirmed in primary cultures of human umbilical cord mesenchymal stem cells (hUC-MSCs), which were promoted to differentiate towards the osteogenic lineage.

Since 7-DHC is very labile to free radical oxidation, we proved the antioxidant properties of α-tocopherol (VitE) on preserving its stability. Furthermore, we improved the isomerization of $preD_3$ to D_3 on the Ti surface by adding an incubation of the coating at 23ºC for 48 hours after UV irradiation. Thus, UV-irradiated 7-DHC:VitE coated implants were tested in the murine preosteoclastic cell line RAW264.7 and further, in human gingival fibroblasts (HGFs). Interestingly, the bioactive coating inhibited osteoclastogenesis *in vitro*. Moreover, HGFs positively responded to these modified implants; the coating showed a positive action in the inflammatory response and in the ECM maturation/breakdown. Finally, an animal study verified its biological potential *in vivo*, the coating promoted the gene expression of the late bone formation marker osteocalcin (OC) in the peri-implant bone and increased ALP activity in the wound fluid. Additionally, the composition and bioactivity of the coating was maintained after 12 weeks when stored at 4ºC avoiding light, oxygen and moisture.

All in all, results from this thesis demonstrate that UV-activated 7-DHC:VitE coated Ti implants promote differentiation of cells involved in hard and soft tissues, indicating a better peri-implant integration. Thus, this novel bioactive coating may be considered as a new approach for dental implant therapies.

Resumen

La investigación actual sobre implantes tiene como objetivo producir superficies bioactivas innovadoras que restauren la función en estructuras esqueléticas comprometidas. La modificación de la superficie de implantes de titanio (Ti) pretende mejorar la respuesta biológica de los tejidos peri-implantarios y favorecer la osteointegración. Cada vez hay más evidencias que destacan el papel esencial de la vitamina D en la regeneración ósea y los efectos negativos que tiene su insuficiencia en la osteointegración del implante. De hecho, la deficiencia de vitamina D conlleva reabsorción ósea, osteoporosis y menor mineralización. Desafortunadamente, existe una gran prevalencia de deficiencia de vitamina D en todas las edades a nivel mundial, debido a una dieta inadecuada e insuficiente exposición solar.

El calcitriol ($1,25(OH)_2D_3$), la forma biológicamente activa de la vitamina D_3, se produce por una cascada de hidroxilaciones, precedida por una activación fotoquímica. Comienza cuando el 7-dehidrocolesterol (7-DHC) se expone a la radiación UVB en la piel, convirtiéndose en previtamina D_3 ($preD_3$). Posteriormente, éste se transforma en colecalciferol (D_3) y se hidroxila primero en el hígado y luego en los riñones hasta formar el producto final. En esta tesis, demostramos por primera vez que el precursor de la vitamina D, el 7-DHC, puede utilizarse para producir localmente vitamina D activa en células osteoblásticas e incrementar su diferenciación, cuando se recubren superficies de poliestireno con 7-DHC y se irradian con UV antes del cultivo celular. Además, comprobamos la posibilidad de usar 7-DHC irradiado con UV para producir $preD_3$ en la superficie de implantes de Ti, lo que incrementa la diferenciación de osteoblastos *in vitro*. Posteriormente, el potencial biológico de esta modificación fue confirmado en cultivos primarios de células madre mesenquimales de cordón umbilical humano (hUC-MSCs), que fueron inducidas hacia el linaje osteogénico.

Puesto que el 7-DHC es muy lábil a la oxidación por radicales libres, comprobamos las propiedades antioxidantes del α-tocoferol (VitE) en la preservación de su estabilidad. Además, mejoramos la isomerización de $preD_3$ a D_3 en la superficie de Ti al incubar el recubrimiento a 23ºC durante 48 horas tras la irradiación con UV. Estos implantes se testaron en la línea celular preosteoclástica murina RAW264.7, y en fibroblastos gingivales humanos (HGFs). Curiosamente, el recubrimiento bioactivo inhibió la osteoclastogénesis mientras que mostró una acción positiva en la respuesta inflamatoria y en la maduración/descomposición de la matriz extracelular en HGFs. Finalmente, un estudio animal verificó su potencial biológico *in vivo*, el recubrimiento incrementó la expresión génica del marcador tardío de formación ósea, osteocalcina (OC), en el hueso periimplantario y la actividad ALP en el fluido de la herida. Además, se comprobó que la composición y la bioactividad del recubrimiento se mantienen después de ser almacenados hasta 12 semanas a 4ºC, evitando la luz, el oxígeno y la humedad.

En conjunto, los resultados de esta tesis demuestran que los implantes de Ti recubiertos con 7-DHC y VitE, e irradiados con UV, promueven la diferenciación de células pertenecientes al tejido duro y blando, indicando una mejor integración. De este modo, este novedoso recubrimiento bioactivo podría ser considerado como una nueva estrategia para terapias con implantes dentales.

List of publications

This doctoral thesis is based on the following research manuscripts, which will be referred to by their Roman numbers in the text:

Paper I. Satué M. ; Córdoba A. ; Ramis J.M. ; Monjo M. UV-irradiated 7-Dehydrocholesterol coating on polystyrene surfaces is converted to active vitamin D by osteoblastic MC3T3-E1 cells. *Photochemical and Photobiological Sciences* (2013), 12(6) :1025-35; doi: 10.1039/c3pp50025j.

Impact factor (2013) : 2,939 (Q2).

Paper II. Satué M. ; Petzold C. ; Córdoba A. ; Ramis J.M. ; Monjo M. UV photoactivation of 7-dehydrocholesterol on titanium implants enhances osteoblast differentiation and decreases Rankl gene expression. *Acta Biomaterialia* (2013), 9(3) :5759-70; doi : 10.1016/j.actbio.2012.11.021.

Impact factor (2013) : 5,684 (Q1).

Paper III. Satué M. ; Ramis J.M. ; Monjo M. UV-activated 7-dehydrocholesterol coated titanium implants promote differentiation of human umbilical cord mesenchymal stem cells into osteoblasts. *Journal of Biomaterials Applications* (2015); doi:10.1177/0885328215582324.

Impact factor (2014) : 2,764 (Q2).

Paper IV. Satué M. ; Ramis J.M. ; Monjo M. Cholecalciferol synthesized after UV-activation of 7-dehdydrocholesterol onto titanium implants inhibits osteoclastogenesis in vitro. *Journal of Biomedical Materials Research: Part A* (2014); doi: 10.1002/jbm.a.35364.

Impact factor (2014) : 2,841 (Q1).

Paper V. Satué M*. ; Gómez-Florit M.* ; Monjo M. ; Ramis J.M. Improved human gingival fibroblast response to titanium implants coated with UV-irradiated vitamin D precursor and vitamin E (2015), *Manuscript.*

Paper VI. Satué M. ; Monjo M. ; Ronold H.J. ; Lyngstadaas S.P. ; Ramis J.M. Bioactive implants coated with vitamin D precursor: in vivo osteogenic potential and stability after storage (2015), *Manuscript.*

All publications were reproduced with kind permission of the respective journal.

** First and second author contributed equally to this study.*

1. Introduction

1. Introduction

1.1. Background of the study

The field of skeletal regeneration is a rapidly growing field of biomedicine with great potential to revolutionize health care treatments and address challenges for an increasing aging population. Bone is a constantly remodeling tissue that requires interaction between different cell types and it is controlled by several biochemical and mechanical factors (Vallet-Regí, 2014). Current research in implantable medical devices aims at improving the biological response to the biomaterial surface whilst accelerating the osseointegration process. One of the most common strategies for solving these drawbacks is the modification of the surface with biologically active compounds. Indeed, several studies immobilizing different growth factors, proteins or peptides have already been developed (Palmquist et al., 2010). Nevertheless, their use might entail some difficulties due to their bioactivity, bioavailability or stability. Thus, there is a real need for finding cheap, stable and bioactive modified surfaces with potential to regenerate the bone tissue and stimulate the biomaterial integration with the bone.

Among the numerous functions attributed to vitamin D, its primary function is to maintain the calcium and phosphate homeostasis (Norman, 2012). Indeed, its deficiency leads to bone resorption, osteoporosis and reduced bone mineralization (Lee et al., 2014; Lips and Van Schoor, 2011). Interestingly, its administration has positive effects on bone formation (Kärkkäinen et al., 2010; Priemel et al., 2010) and also other benefits including anticancer and antimmunomodulatory actions (Souberbielle et al., 2010). Although vitamin D is naturally synthesized from 7-DHC in our skin, and further hydroxylated in liver and kidney tissues, different cell types and tissues, including bone cells, are able to produce final active vitamin D (Hansdottir et al., 2008; Hewison et al., 2003; Bikle, 2004). Thus, this thesis presents the feasibility of using Ti implants coated with the vitamin D precursor, 7-DHC, and then UV-irradiated as it happens in the skin to initiate the vitamin D synthesis, with the aim of improving their osseointegration (Figure 1.1).

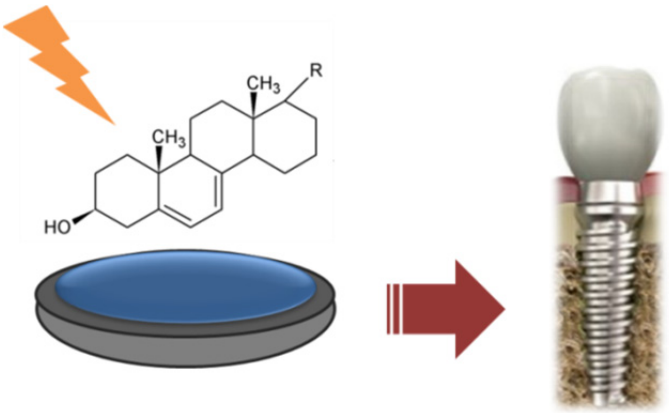

Figure 1.1. Graphical representation of the principal goal of this thesis: Development of a novel bioactive coating using UV-irradiated 7-DHC to promote osseointegration of orthopedical and dental implants on compromised skeletal structures.

1.2. Skeletal biology

The skeletal system is formed by bone and cartilage which are involved in two key functions: (i) a structural role, providing support and protection of vital internal organs, and (ii) a metabolic function, functioning as a mineral reservoir for the rest of the body, especially with regard to phosphate and calcium (Shea and Miller, 2005).

1.2.1. Bone tissue

Two types of bone tissue are observed in normal mature human skeleton: cortical (compact) bone and trabecular (cancellous or spongy) bone (Figure 1.2). Although both bones have the same composition and material properties, they have differences in density and mechanical properties (Hadjidakis and Androulakis 2006; Buckwalter et al. 1995; Silva 2012). Thus, the compressive strength of bone is proportional to its density, so the elasticity and compressive strength of cortical bone may be as much as 10 times greater than those of cancellous bone (Buckwalter et al., 1995).

Cortical bone is dense and compact (5-10 % porosity) and constitutes the outer part of all bones. It forms approximately 80% of the mature skeleton (Buckwalter et al., 1995). Most cortical bone is calcified and it provides strength whilst also participates in the modulation of prolonged mineral deficit (Hadjidakis and Androulakis, 2006). Furthermore, the compact structure leads cortical bone to fulfill mainly a mechanical and protective function (Mackiewicz et al., 2011).

Trabecular bone is very porous bone (75-95% porosity) that is found in the cuboidal bones, flat bones and the ends of long bones. Trabecular bone is much less dense and contributes to mechanical support and provides the initial mineral supply in deficiency states (Hadjidakis and Androulakis 2006; Buckwalter et al. 1995). This spongeous structure ensures the elasticity and stability of the skeleton and counters for the main part of bone metabolism (Mackiewicz et al., 2011).

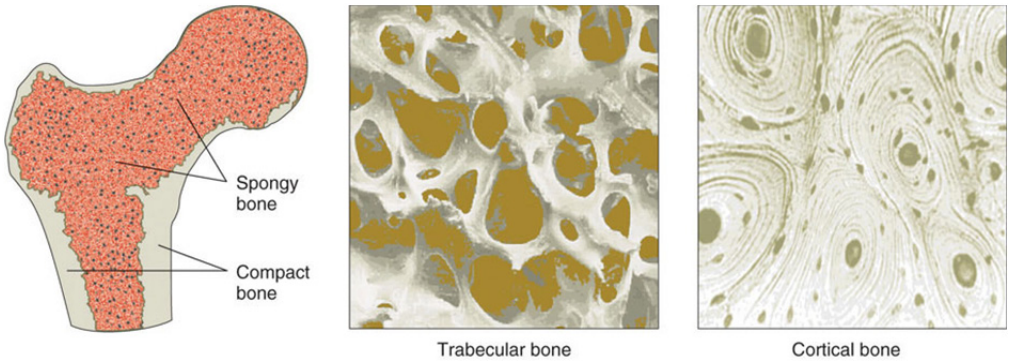

Figure 1.2. The two bone tissue types: trabecular and cortical (http://2012books.lardbucket.org/books/an-introduction-to-nutrition/s13-01-bone-structure-and-function.html).

Bone is a porous mineralized tissue formed by extracellular matrix (ECM), cells and water, like any other connective tissue (Table 1.1).

Table 1.1. Summary of main bone components (Baron, 2003; Fleisch, 2000).

Bone composition		
ECM	Inorganic matrix (~65%):	Hydroxyapatite and other ions (Na^{+}, Mg^{2+}, HPO_4^{2-}, HCO_3…)
	Organic matrix (~35%):	Collagen fibers (mainly Collagen type I) and noncollagenous proteins
Cells	Osteoblasts (<5% of total cells), bone lining cells; osteocytes (90-95%), osteoclasts (<1%), others (lymphocytes, MSCs).	
Water		

1.2.1.1. Bone matrix

The matrix of bone occupies a greater volume than cells. It is formed by 4 major components: type I collagen, non-collagenous proteins and non-protein components (organic matrix), and a salt of calcium and phosphorus which in its crystal structure most closely resembles that of hydroxyapatite (inorganic matrix). Collagen is by far the most abundant fibrous protein of the organic matrix. Thus, type I collagen fibers and noncollagenous proteins represent approximately 90% of the organic composition of the whole bone tissue (Hadjidakis and Androulakis, 2006). The collagen fibers provide flexibility and strength. Furthermore, they probably also serve as scaffolding on which nucleators are oriented (Robey, 2008). The major noncollagenous protein produced is OC (Gla protein) and it is involved in the regulation of bone formation (Hadjidakis and Androulakis, 2006). However, the role of many other noncollagen proteins present in the bone matrix has not been fully elucidated. The inorganic material is also known as mineralized matrix, and it consists of mostly crystals of hydroxyapatite which are found in the collagen fibers and in the matrix to provide rigid structure (Shea and Miller, 2005).

1.2.1.2. Bone cells

Bone tissue is a dynamic tissue that is constantly renewed. Thus, bone cells are constantly resizing and reshaping throughout growth and adulthood. Many different and specialized cells carry out the diverse functions of bone formation, resorption, mineral homeostasis and bone repair (Figure 1.3). These cells are derived from different progenitor pools that are under different molecular mechanisms (Robling et al., 2006). Thus, bone cells come from mesenchymal stem cells (osteoblasts, bone-lining cells and osteocytes) and hematopoietic stem cells (osteoclasts).

- ***Mesenchymal stem cells (MSCs)***

This stem cell population involves multipotent stromal cells that can differentiate into a variety of cells including bone cells (osteoblasts), cartilage cells (chondrocytes) and fat cells (adipocytes) (Nardi, N. Beyer; da Silva Meirelles, 2006).

Osteoblasts

Osteoblasts are responsible for bone formation. Their most apparent function is to synthesize bone matrix (osteoid), but they also control fluxes between the extracellular fluid and the osseous fluid. Osteoblasts are derived from local progenitors that proliferate prior to further differentiation (Shea and Miller, 2005). Thus, once osteoprogenitor cells (pre-osteoblastic cells) are stimulated, they are able to proliferate and differentiate into osteoblasts. Commitment of these cells to the osteblastic lineage depends on the specific activation of transcription factors. Several hormones, cytokines, and mechanical stimuli may affect bone turnover (Robling et al., 2006). For example, after a fracture, several events stimulate the proliferation and differentiation of these cells to participate in the fracture-healing. Once osteoblasts are active, they express high levels of alkaline phosphatase (ALP) and osteocalcin (OC), what reflects the rate of bone formation. They also secrete abundant type I collagen and other matrix proteins, which form osteoid. This organic phase of bone serves as a template for the subsequent deposit of mineral in the form of hydroxyapatite (Bellido et al., 2014). Furthermore, osteoblasts express colony-stimulating factor, receptor activator of nuclear factor kappa-B ligand (RANKL) and osteoprotegerin (OPG), which are related to osteoclastogenesis and bone resorption (Katagiri and Takahashi, 2002).

Bone lining cells

The majority of bone surfaces are not undergoing bone formation or resorption in the adult skeleton, but they are lined by a specialized cell, the bone lining cell. Bone lining cells are formed by osteoblasts that become flattened and cover the inactive bone surface. These cells are able to proliferate and regulate the calcium exchange between mineralized bone and the bone marrow. In fact, they are in close contact with osteocytes embedded in the bone matrix through gap junctions, suggesting their role in the support of nutrients and metabolic support of osteocytes (Shea and Miller, 2005). Bone lining cells can recover their ability to produce matrix in response to parathormone (PTH), what contributes to the rapid bone formation after administration of this hormone (Bellido et al., 2014). Another suggested role for bone lining cells is the initiation of osteoclast resorption (Everts et al., 2002).

Osteocytes

Osteocytes are the most abundant cells (90%) in the bone tissue (Bellido et al., 2014). These cells are formed from osteoblasts that become entombed and buried during bone formation (Shea and Miller, 2005). These cells are regularly distributed throughout the mineralized bone matrix and they maintain the mineral homeostasis. Although the metabolic activity of osteoblasts decreases once it is completely encased in the bone matrix, they still produce matrix proteins (Hadjidakis and Androulakis, 2006). Thus, although osteocytes do not normally express ALP, they do express OC and other bone matrix proteins that support intercellular adhesion and regulate exchange of mineral in the bone fluid. Furthermore, osteocytes may function as phagocytic cells because they contain lysosomes (Clarke, 2008). Another function attributed to these cells is to coordinate the function of osteoblasts and osteoclasts. Indeed, it has been suggested that they respond to mechanical load through a three-

dimensional network of osteocyte cell processes capable of sensing microdistorsions of the matrix and translating them into signals to control the bone cells activity (Raggatt and Partridge, 2010).

❖ ***Hematopoietic stem cells***

This stem cell population is involved in forming blood and immune cells in the body. It is a heterogenous population that gives rise to the myeloid (monocytes, macrophages, neutrophils, basophils, eosinophils, erythrocytes, megakaryocytes and dendritic cells) and lymphoid lineages (T-cells, B-cells and NK-cells) (Soysa et al., 2012). Macrophages from the hematopoietic stem cell line further give rise to osteoclasts, as detailed below.

Osteoclasts

The osteoclast is the only cell responsible for the bone resorption. Osteoclasts are multinucleated giant cells developed from hematopoietic stem cells residing in the marrow and spleen (Robling et al., 2006). Development of osteoclasts proceeds whithin a local microenvironmental milieu of bone that guide mononuclear preosteoclasts to bone matrix (Takahashi et al., 2008). Thus, the fusion of mononuclear preosteoclasts to multinuclear osteoclasts requires the presence of two cytokines, macrophage colony-stimulating factor (M-CSF) and the RANKL that are necessary for survival, expansion and differentiation of osteoclast precursor cells *in vitro* (Clarke, 2008; Raggatt and Partridge, 2010). Besides being a multinucleated cell, the mature osteoclast is characterized by the expression of tartrate-resistant acid phosphatase (TRAP) (Teitelbaum and Ross, 2003). Then, mature osteoclasts are activated, involving the reorganization of their cytoskeleton, known as actin ring, which surrounds the “ruffled border”, a specialized cell membrane that facilitates bone resorption (Väänänen and Zhao, 2008). Finally, activated osteoclasts resorb bone by acidification and proteolysis of the bone matrix and the hydroxyapatite crystals (Clarke, 2008).

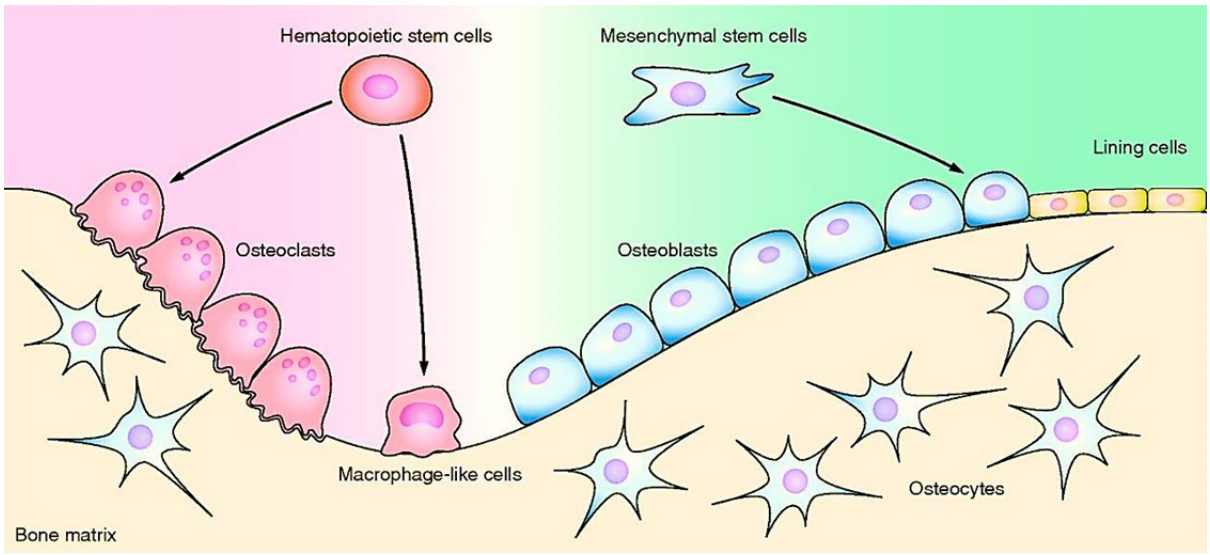

Figure 1.3. Mesenchymal and hematopoietic stem cells originate the different types of bone cells (Imai et al., 2013).

1.2.1.3. Bone formation, modeling and remodeling

Bone formation (osteogenesis) is the process of new bone formation by osteoblasts and it occurs in three successive phases: the production and the maturation of osteoid matrix, followed by mineralization of the matrix. Bone undergoes longitudinal and radial growth during life. In normal adult bone, these processes occur at the same rate so that the balance between matrix production and mineralization is equal. This process of healthy bone formation is carried out by two important processes: (i) intramembranous ossification (lay down of bone into the primitive connective tissue); and (ii) endochondral ossification (a cartilage model acts as a precursor) (Kini and Nandeesh, 2012). Further, bone development and maintenance are regulated by two processes, modeling and remodeling (Raggatt and Partridge, 2010).

Bone modeling (construction) controls growth and mechanically induced adaptation of bone which is formed by osteoblasts without prior bone resorption (Seeman, 2008). Thus modeling leads to gradual adjustment of the skeleton to forces that it encounters. Bone modeling occurs during growth and is responsible for gain in skeletal mass and changes in skeletal form.

Bone remodeling (reconstruction) is responsible for removal and repair of damaged bone to maintain integrity of skeletal system and mineral homeostasis. This process occurs throughout life and involves removal of old bone, replacement with new synthesized proteinaceous matrix and further mineralization to form new bone (Hadjidakis and Androulakis, 2006). This mainly occurs in the adult skeleton to maintain bone mass. This process involves the coupling of bone formation and bone resorption and occurs in both cortical and trabecular bone (Sims and Gooi, 2008). At the microscopic level, bone remodeling occurs in small areas of the cortical and trabecular surface known as “basic multicellular units” (BMU). There are 35 million BMU in the human skeleton and 3-4 million are activated each year, then the skeleton in completely renewed every 10 years (Fernández-Tresguerres-Hernández-Gil et al., 2006). Bone remodeling consists of the following phases (Figure 1.4):

Activation. The first step involves detection of an initiating remodeling signal, which can take several forms such as direct mechanical strain on the bone resulting in structural damage or hormone action on bone cells (Raggatt and Partridge, 2010). Then, bone surface is activated through retraction of the bone lining cells. This step involves the recruitment and activation of mononuclear monocyte-macrophage osteoclast precursors from the circulation that further are differentiated and fused to form large multinucleated osteoclasts.

Resorption. In addition to recruitment of osteoclast precursors, osteoblasts express the master osteoclastogenesis cytokines, colony stimulating factor (CSF-1), RANKL and OPG to promote proliferation and differentiation of osteoclast precursors to multinucleated osteoclasts. Osteoclasts are able to attach to the bone surface through $\alpha_v\beta_3$ integrin molecules creating an isolated microenvironment known as the “sealed zone” and further dissolve the mineral matrix (Raggatt and Partridge, 2010). Matrix metalloproteinases (MMPs) are secreted to degrade unmineralized osteoid and also growth factors contained within the matrix are released, such as transforming growth factor

(TGF-β), platelet derived growth factor (PDGF), insulin-like growth factor I and II (IGF-I and –II) (Fernández-Tresguerres-Hernández-Gil et al., 2006).

Reversal. There are several evidences indicating that the resorbed surface likely contains important signals for regulating recruitment of bone lining cells and osteoblasts. Thus, mononuclear cells are essential for conditioning the resorbed for subsequent osteoblast-mediated bone formation (Henriksen et al., 2009). Initially, these "reversal" cells were thought to belong to the monocyte/macrophage lineage but they belong to the osteoblast lineage (Raggatt and Partridge, 2010). The final role of these cells may be to receive or produce coupling signals that allow transition from bone resorption to bone formation.

Bone formation and mineralization. It is controversial the nature of the coupling signal that coordinates the bone formation. IGF-I and II and TGF-β seem to be key signals for recruitment of MSCs to sites of bone resorption (Raggatt and Partridge, 2010). Once MSCs or early osteoblast progenitors returned to the resorption lacunae, they differentiate and secrete molecules to form replacement bone. Preosteoblasts synthesize a cementing substance upon which the new tissue is attached and express bone morphogenetic proteins (BMPs) which are responsible for differentiation (Fernández-Tresguerres-Hernández-Gil et al., 2006). After few days, differentiated osteoblasts synthesize the osteoid to fill the perforated areas. Finally, hydroxyapatite is incorporated to the newly deposited osteoid (Raggatt and Partridge, 2010).

Quinesence. The remodeling cycle concludes when an equal quantify of resorbed bone has been replaced. It is still being investigating the termination signal that informs the final of the remodeling process (Raggatt and Partridge, 2010). In this stage, mature osteoblasts undergo apoptosis or become lining cells or osteocytes. Then the resting bone surface is reestablished and maintained until the next remodeling process is initiated.

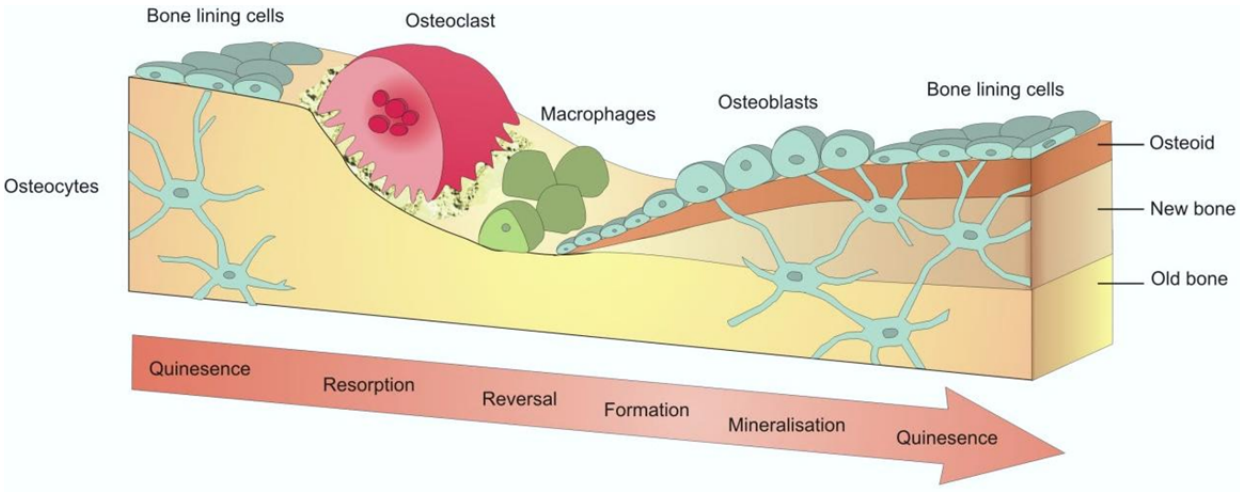

Figure 1.4. The bone remodeling cycle. Adapted from http://www.york.ac.uk/res/bonefromblood/background/boneremodelling.html.

1.2.2. Bone regeneration and repair

The bone mass in an adult human reaches its maximal level during a person's twenties but then gradually declines as the speed of bone resorption exceeds bone formation with increasing age (Jimi et al., 2012). Furthermore, many people suffer from bone defects, much of them which could be prevented. These bone defects often result from tumor resection, trauma, fractures, surgery or periodontitis, as well as from diseases such as osteoporosis or arthritis. Interestingly, unlike other tissues that repair predominantly through the production of scar, defects in bone tissue heal by forming new bone. Thus, osteogenesis is highly stimulated in injuries such as fractures.

The fracture healing begins immediately following the injury and ends following the remodeling of new bone. This process occurs in four overlapping steps (Figure 1.5):

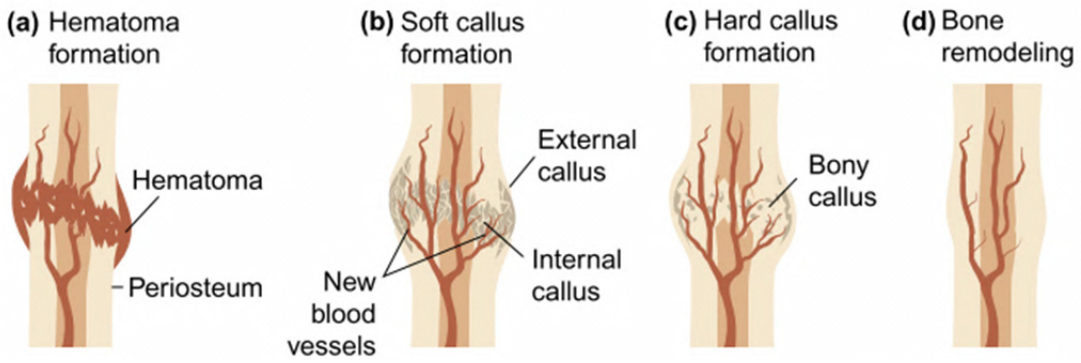

Figure 1.5. The stages of fracture repair Adapted from (Carano and Filvaroff 2003).

a) *Formation of hematoma.* After a bone is fractured, the damage to local vasculature produces a hematoma or a blood clot. This hematoma is formed by blood products, fibrin, growth factors and cytokines. This stage is also characterized by inflammation and local hypoxia (Shrivats et al., 2014).

b) *Soft callus formation.* This step is characterized by new vasculature formation. Local hypoxia stimulates the formation of new blood vessels (angiogenesis) what allows the recruitment of MSCs that differentiate into chondrocytes (cartilage matrix formation) and osteoblasts (new bone formation). A soft callus is formed to act as a fixation structure (Shrivats et al., 2014).

c) *Hard callus formation*. As repair progresses, the callus becomes mineralized, forming a hard callus. Chondrocytes undergo apoptosis and osteoblast deposit bone matrix (Carano and Filvaroff, 2003).

d) *Remodeling.* Final phase in which the fracture region is gradually modified to form new bone and resorb the excess callus. The vascular supply returns to a normal state.

Although this is the normal mechanism for bone to regenerate itself, there are some challenging bone conditions in which this process is impaired. Thus, unfortunately, the bone tissue is not able to regenerate and repair properly in patients with compromised skeletal structures, with poor bone

quality or quantity. For this reason, there is an urgent need for developing strategies to accelerate and improve the entire structure and function of the damaged tissue.

1.3. Endosseous titanium implants

Bone possesses the intrinsic capacity for regeneration during skeletal development and as part of its repair process. However, as mentioned above, there are some cases in which bone regeneration is impaired or it is required in large quantity for reconstruction of bone defects created by trauma, infection or skeletal abnormalities in compromised patients (Dimitriou et al., 2011). For these aforementioned cases, different biomaterials have been developed. Biomaterials field involves the creation of safer, more reliable, more inexpensive and bioactive materials for replacement of damaged or diseased human tissues. The degenerative diseases lead to degradation of the mechanical properties of the bone, what makes increase the necessity of artificial biomaterials to solve these problems. Furthermore, approximately 90% of population over the age of 40 suffer from these kind of degenerative diseases and aged people population has increased tremendously in recent years (Geetha et al., 2009). For these reasons, the development of appropriate materials for improving skeletal regeneration is a main concern at the moment for our increasing aging society.

Biomedical materials used for hard and soft tissue applications should meet the following requirements (Geetha et al., 2009; Tengvall and Lundström, 1992):

- High biocompatibility. It involves low intrinsic toxicity and inflammatory activation.
- Surface texture matching cellular adhesion without relative interfacial motion.
- Biofunctionality and osseointegrative potential, providing excellent mechanical properties.
- Corrosion and wear resistance.
- Bioadhesion to promote the bond between the biomaterial surface and the adjacent tissue. This should accelerate the healing period and avoid implant loosening.
- Prevention of bacterial adhesion.
- Low price is desirable.

Ti and its alloys fulfill these requirements to a high extent, especially when compared with other metallic biomaterials (Tengvall and Lundström, 1992). Thus, Ti is one of the best biomaterials known today and is extensively used for implantation. It has gradually replaced other metallic biomaterials like stainless steel in applications with high mechanical strength requirements (Tengvall and Lundström, 1992). In the 1940s, Ti was already mentioned as a bone-anchoring material and it was in the 1960s when it was used for prosthesis design and surgical procedure (Brånemark, 1977; P-I Brånemark et al., 1969). In general, Ti is found to be well tolerated and nearly an inert material in the human body due to its outstanding characteristics. Indeed, Ti possesses ideal properties such as high strength, low density, high resistance to corrosion, complete inertness to body environment, enhanced biocompatibility, low modulus and high capacity to join with bone and other tissues (Niinomi, 2003). In addition, pure Ti forms a very stable passive layer of titanium dioxide (TiO_2) in presence of oxygen molecules that provides superior biocompatibility. Indeed, this TiO_2 surface is of particular importance since it protects Ti from corrosion (Geetha et al., 2009).

There is a high interest in the application of Ti in several medical areas, such as the development of dental implants, joint replacement parts, bone fixation materials, artificial heart valves, etc. (Geetha et al., 2009). Commonly commercially available pure (c.p.) Ti is the basic material for purposes requiring lower mechanical strength whilst Ti-alloys such as TiAl6V4, Ti318 and Ti350 are used in applications when higher strength is desirable (Tengvall and Lundström 1992). However, although TiAl6V4 has long been a main medical Ti alloy for permanent implant applications, this alloy has a possible toxic effect resulting from released vanadium and aluminum. For this reason, vanadium- and aluminum-free alloys were further introduced for implant applications (Elias et al., 2008).

It was Brånemark who introduced the modern implants when he discovered what he named the osseointegration phenomenon for Ti implants that were completely attached to bone and difficult to remove (PI Brånemark et al., 1969). Osseointegration is therefore the stable anchorage of an implant achieved by direct bone-to-implant contact (Albrektsson and Johansson, 2001). This discovery started the exploration of dental and surgical applications of Ti alloys. It is the most important clinical goal of implant surgery, since osseointegrated implants significantly improve the long-term behavior of the implanted devices, decreasing the failure and loosening risks (Navarro et al., 2008). Although successful implant surgery requires the osseointegration of the implant within the surrounding tissues, it also requires osteoconduction in order to make the implant able to support bone growth over its surface (Salgado et al., 2004). After an implant placement, one of the first events is the adsorption of proteins and lipids from the blood to the implants surface (Wilson et al., 2005; Keselowsky et al., 2003). Then, MSCs colonize the implantation site and are exposed to inflammatory cytokines and growth factors to control the healing and tissue regeneration. Once the implant is fixed, osteogenesis should be promoted. Further, the next step involves the osteoclast action to resolve microcracks (Gittens et al., 2014).

Originally, endosseous implants were expected to perform their job simply through a mechanical anchorage with bone. However, early efforts had relatively high failure rates, mainly due to the formation of the fibrous connective tissue between the bone and the implant. Similarly, in the orthopedic implant field several reports have found fibrous capsules around implants, what was attributed to toxic wear debris phagocytosed by macrophages and other cells of the surrounding tissue (Cunningham et al., 2003). This fibrous capsule (Figure 1.6B) promotes micromotion and inflammation around the implant that usually leads to osteolysis and implant failure (Gittens et al., 2014). Another factor affecting osseointegration is the vascularization process, what refers to the provision of blood supply. Indeed, differentiation of osteogenic cells depends on tissue vascularity (Mavrogenis et al., 2009). Therefore, to achieve successful osseointegration, vascularization and a strong and direct integration between bone and implant is required, leading to an increased mechanical stability and lower probability of implant loosening (Figure 1.6C).

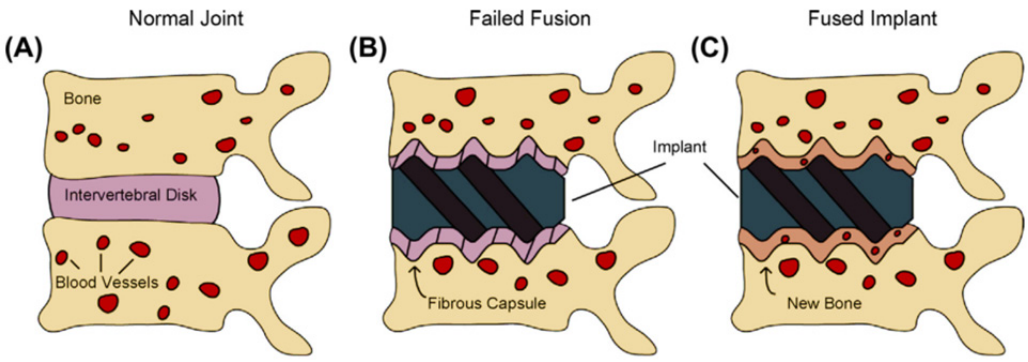

Figure 1.6. Schema of normal joint (A), failed fusion (B) and fused implant (C) (Gittens et al., 2014).

1.3.1. Dental implants

In the dental field, implants are usually made from commercially pure Ti or its alloys, due to their suitable weight-to-strength ratio and good biological performance (Gittens et al., 2014). The clinical success of an oral implant is related to its early osseointegration. Despite the high biocompatibility of Ti implants, they might be encapsulated by fibrous tissue. However, formation of this fibrous capsule can be avoided by promoting bone apposition directly onto the implant surface (Gittens et al., 2014). Therefore one the keys challenges in implantology is to develop a Ti implant with enhanced bioactivity to improve implant-host interactions, avoid fibrous tissue encapsulation and ensure osseointegration and long-term implant stability (Wang and Poh, 2013).

A dental implant is formed by the implant itself, which is in contact with the hard tissue and the abutment, which interacts with the soft tissue (Elias et al., 2008). For this reason, a successful dental implant requires its integration with periodontal tissues, which are formed by hard and soft tissues. An ideal dental implant (Figure 1.7) should therefore promote peri-implant bone healing and osseointegration, as described above, but also promote soft tissue healing around the implant abutment forming a biological seal between the oral cavity and the bone (Sculean et al., 2014). Since dental implants are placed in the mouth and interact with biological fluids and bacteria, both prosthetic biomechanical factors and patient hygiene are required for the implant long-term success (Le Guéhennec et al., 2007). Otherwise, bacterial adhesion and colonization of the teeth involve biofilm formation which further provokes an inflammatory response that can lead to implant loss. Thus, gingivitis and periodontitis are two of the most common chronic inflammatory diseases as result of the accumulation of bacteria on tooth surfaces (Bartold et al., 2000). Gingivitis involves an inflammation of the gingiva but without proper treatment it can lead to the more serious periodontitis, which can cause the destruction of both soft and hard tissues. Similarly, peri-implant diseases are characterized by an inflammatory reaction in the tissues surrounding an implant. Whilst the presence of inflammation in peri-implant mucositis is confined to the soft tissues surrounding a dental implant, peri-implantitis is characterized by an inflammatory process around an implant, including both soft tissue inflammation and progressive loss of the bone, that often leads to implant failure (Cochran and Froum, 2013).

The periodontium refers to these specialized tissues that support the teeth and provide protection against bacterial infection. This organ system is composed of two hard tissues (cementum and bone) and two soft tissues (periodontal ligament and gingiva), which maintain the function of the teeth (Bartold and Narayanan, 2006). The soft tissue that surrounds dental implants (gingiva) is comprised of one epithelial and one connective tissue component. The epithelial tissue resembles the functional epithelium around teeth while the connective tissue is involved in the repair of gingival tissues. Among the different cell types of the gingival connective tissue, fibroblasts account for most connective tissue cells and are responsible for the constant adaptation of the tissue. Thus, their principal function is to synthesize and maintain the components of the ECM of the connective tissue and participate in wound healing repair and regeneration (Bartold and Narayanan, 2006).

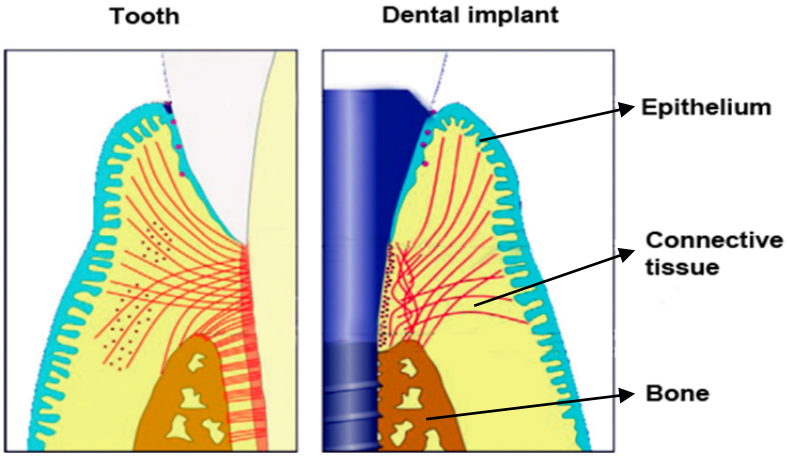

Figure 1.7. Osseointegrated dental implants serve as artificial teeth that are in direct contact with hard and soft tissues Adaptated from (Gruber and Bosshardt 2015).

The wound healing of the gingiva around a dental implant involves interplay between inflammatory cells, fibroblasts and the newly synthesized matrix. After the implant placement, a blood clot is formed to provide a fibrin network for bone cell migration. Indeed, within a short period of time, various plasma proteins, including fibrin, get adsorbed on the surface what promotes the migration of osteogenic cell populations towards the implant surface. Furthermore, during the initial remodeling, immune cells mediate early response followed by migration of phagocyte macrophages. They phagocytize bacteria and necrotic debris and release cell surface proteins and cytokines and pro-inflammatory mediators. One of the critical steps in the cell response to the dental implant is the attachment to the surface. With this aim, fibroblasts invade the fibrin network and form an ECM on the implant surface (Anil et al., 2005). Since fibroblasts require oxygen and nutrients for their activity, angiogenesis occurs at the same time that fibroblasts accumulate in the wound site. Next, the wound healing culminates with the remodeling of collagen to increases the strength of the wound. In this way, it can produce either repaired or regenerated tissue, depending on the biochemical factors of the microenvironment.

Thus, an ideal dental implant should promote the direct tissue-implant interaction and avoid the presence of the intervening connective tissue layer (Le Guéhennec et al., 2007). Furthermore, wound healing should prevent bacterial penetration, reduce inflammation and induce gingival fibroblast

proliferation to aid in the tissue regeneration process and avoid implant loss. Accordingly, current advances in periodontal therapies are based on the deep understanding of the fundamental cellular processes of periodontal regeneration and repair to enhance this regeneration process (Sculean et al., 2014).

1.3.2. Strategies for improving implant osseointegration

Different strategies aiming at improving biocompatibility, osteoconduction and osseointegration of Ti implants have been investigated. Thus, experimental evidences suggest that surface properties of Ti influence the initial cell adsorption, inflammation and cell response. However, these early molecular activities determining the tissue response at the peri-implant interface are not yet fully understood (Palmquist et al., 2010). Current research is being performed with the aim to modify the implant surface to make them more acceptable to bone cells and then, inducing the integration of the implanted device to bone whilst avoiding the fibrous encapsulation. The most used strategies to improve both short and long-term osseointegration of Ti implants include surface roughness modification and the incorporation of biological drugs to promote the bone healing in the peri-implant area (Le Guéhennec et al., 2007).

Roughness modification involves changes in surface topographies at the micro and nanometer level, what influences both the biomaterial biocompatibility and the cellular response (Sul et al., 2005). In particular, fibroblasts and epithelial cells adhere more strongly to smooth surfaces while osteoblasts increase their differentiation and matrix formation and mineralization on rough surfaces (Mendonça et al., 2008; Novaes et al., 2010). This observation leads to the conclusion that roughness modification could also influence protein adsorption, cellular activity or tissue response, which can be exploited to achieve a higher osseointegration process. For this reason, several techniques have been described to modify the surface roughness of metallic biomedical materials (Liu et al., 2010; Bauer et al., 2013). Furthermore, modification of the oxide thickness and compositions by using different mechanical, chemical and optical methods have also been described (Palmquist et al., 2010).

Numerous investigations confirm that the optimal microroughness for the hard tissue osseointegration ranges between 1-10 μm, since this range maximizes the bone-implant interaction (Bauer et al. 2013). The most common methods to meet this demand include blasting (by using TiO_2 o Al_2O_3 particles), acid-etching (mainly using HF), anodization (electrochemically growing a controlled TiO_2 layer on the Ti surface) and plasma-spraying (producing coatings at high temperatures with bioinert ceramics such as titania, zirconia or alumina) (Bauer et al. 2013). Furthermore, several studies have revealed that the modification of the implant surface at the nanometer level also influences on the biological response of bone cells (Zhao et al., 2007). Thus, modification of the surface through the formation of three-dimensional nanofiber structures is being used for guiding cell differentiation (McNamara et al., 2010).

The addition of bioactive molecules to the implant surface is other strategy applied to improve osseointegration of Ti implants. In fact, data suggest that Ti surface modifications with bioactive molecules enhances or accelerates the osteoblastic differentiation process (Novaes et al., 2010). Furthermore, the current research aiming at developing novel implants for compromised tissue

conditions entails the incorporation of biologically active molecules to recruit and deliver cells to the host site. To achieve this, different coatings are being applied to modify the implant surface. Among all engineering-based implant surface modifications, the calcium phosphate (CaP) and hydroxyapatite coatings have received significant attention as they may improve bone integration (Le Guéhennec et al. 2007; Palmquist et al. 2010). The interest of using them is that their chemical similarity to natural bone and that they can be applied by different industrial processing methods. Furthermore, CaP coatings increase the biocompatibility of bone-implant interface, implant anchorage and integration (Barrère et al., 2003).

Other example of biochemical modifications of biomaterial surfaces that is gaining popularity is the addition of growth factors. Growth factors immobilized on orthopedic devices have been reported to enhance osteoblastic activity and favor implant integration. In particular, bone morphogenetic proteins (BMPs), are considered as a potential strategy to enhance osteogenesis and induce specific cellular functions (Anil et al., 2005). However, critical factors such as the optimum dosage, exposure period and release kinetics have to be considered carefully to avoid the detrimental effects associated with their use (Wang and Poh, 2013). Other interesting approaches are the use of molecules that control bone remodeling, such as bisphosphonates (Josse et al., 2004), or the application of simvastatin to promote bone formation (Nyan et al., 2010).

Since the biological effects that surfaces have on cell attachment are mainly mediated by integrins that bind to sequences arginine-glycine-aspartate (RGD), these RGD sequences are being used as monolayer modifications to promote cell adhesion (García et al., 2002). Another strategy involves the addition of ECM proteins such as collagen, which enhances spreading of cells and speeding cell adhesion length (Geissler et al., 2000). Other approaches include the use of antibacterial coatings to prevent surgical site infections associated with implants, especially in dentistry (Anil et al., 2005).

However, some of the limiting factors of using these therapeutic drugs is the concentration used and their release which has to be progressive and not in a single burst (Le Guéhennec et al., 2007). Furthermore, thus far, none of these coatings are commercially available, since more research in this field is required to find their way into clinical practice. Therefore, the current development of new strategies on bioactive coatings would lead to a new generation of implants with improved osseointegration and bone healing properties.

1.4. Biological potential of vitamin D

It is widely known the importance of vitamin D in regulating calcium homeostasis in the body, which is critically important for normal mineralization of bone to prevent skeletal related diseases. Although the action of vitamin D traditionally known is to enhance calcium and phosphate absorption from the intestine, recent studies revealed that vitamin D also plays many additional extraskeletal functions. Indeed, it modulates the activity of hundreds, if not thousands, of genes in every tissue in the body, making it a potent regulator of antiproliferative, prodifferentiating, immunosuppressive and anti-inflammatory processes (Feldman et al., 2013).

1.4.1. Synthesis and metabolism

Vitamin D is a group of fat-soluble secosteroids whose principal function is the regulation of calcium and phosphate homeostasis in the body which is critically important for normal bone mineralization (Plum and DeLuca, 2010). In humans, vitamin D exists in two forms, vitamin D_3 (cholecalciferol), which is formed in the skin after exposure to sunlight, and vitamin D_2 (ergocalciferol) that is obtained from the diet. Although these two forms are handled similarly in the body, vitamin D_3 is more potent than vitamin D_2 (Heaney et al., 2011).

The natural synthesis of vitamin D in our body starts when human skin is exposed to sunlight (Figure 1.8). Ultraviolet B (UVB) light with wavelength of 290 to 320 nm is responsible of a photochemical activation of 7-DHC, the precursor of vitamin D_3. This reaction cleaves the B ring between carbon-9 and -10 to open the ring to form preD_3. Then, preD_3 undergoes a thermal isomerization of its three double bonds to form a more thermodynamically stable form, D_3. Thermal activation of preD_3 also gives rise to several non-vitamin D forms, including lumisterol, tachysterol and toxysterols. D_3 is an inactive prohormone that must be metabolized before it can function. To achieve this, D_3 is twice hydroxylated, once in the liver into 25-hydroxyvitamin D_3 (25(OH)D_3) and once in the kidney into 1,25-dihydroxyvitamin D_3 (1,25$(OH)_2D_3$). In the liver, several 25-hydroxylases have been implicated in this step, such as CYP27A1 and CYP2R1 (Jones G., 2011). 25(OH)D_3 is usually the chosen metabolite assayed to determine the vitamin D status of an individual since it is more abundant and stable than the final active metabolite (DeLuca, 2004). After liver hydroxylation, 25(OH)D_3 is carried in the blood stream bound to the vitamin D binding protein (DBP) and the kidney accomplishes the final hydroxylation through the 1α-hydroxylase (CYP27B1). Finally, the active metabolite 1,25$(OH)_2D_3$ enters the cell and binds to the vitamin D receptor (VDR) which can be found in several target tissues. Interestingly, the final active metabolite is able to regulate its own production by inducing its own destruction by stimulating the 24-hydroxylase enzyme (CYP24A1) (Omdahl et al., 2002).

Once 1,25$(OH)_2D_3$ is synthesized, it binds to the VDR and then dimerizes with the retinoid X receptor (RXR). The objective of the VDR-RXR complex is to bind to specific DNA sequences with high affinity for subsequent modulation of specific gene expression (Pike et al., 2012). These specific DNA sequences are known as vitamin D response elements (VDREs) and are found in the promoter regions of target genes. Interestingly, VDR is present in the nucleus of many tissues that are not related to calcium and phosphate metabolism, such as epidermal keratinocytes, T cells of the immune system, macrophages and monocytes. But the calcitriol function in these cells is not clearly known. Similarly, although the kidney was initially thought to be the sole organ responsible for producing 1,25$(OH)_2D_3$, not only renal synthesis is possible. Recent investigations have confirmed that other cells and tissues are able to convert 25(OH)D_3 to 1,25$(OH)_2D_3$. Indeed, several investigations confirmed the CYP27B1 expression in many extrarenal tissues, such as epithelial cells, macrophages, bone cells, gingival cells, endocrine glands, placenta, liver, brain and cancer cells (Bikle, 2009).

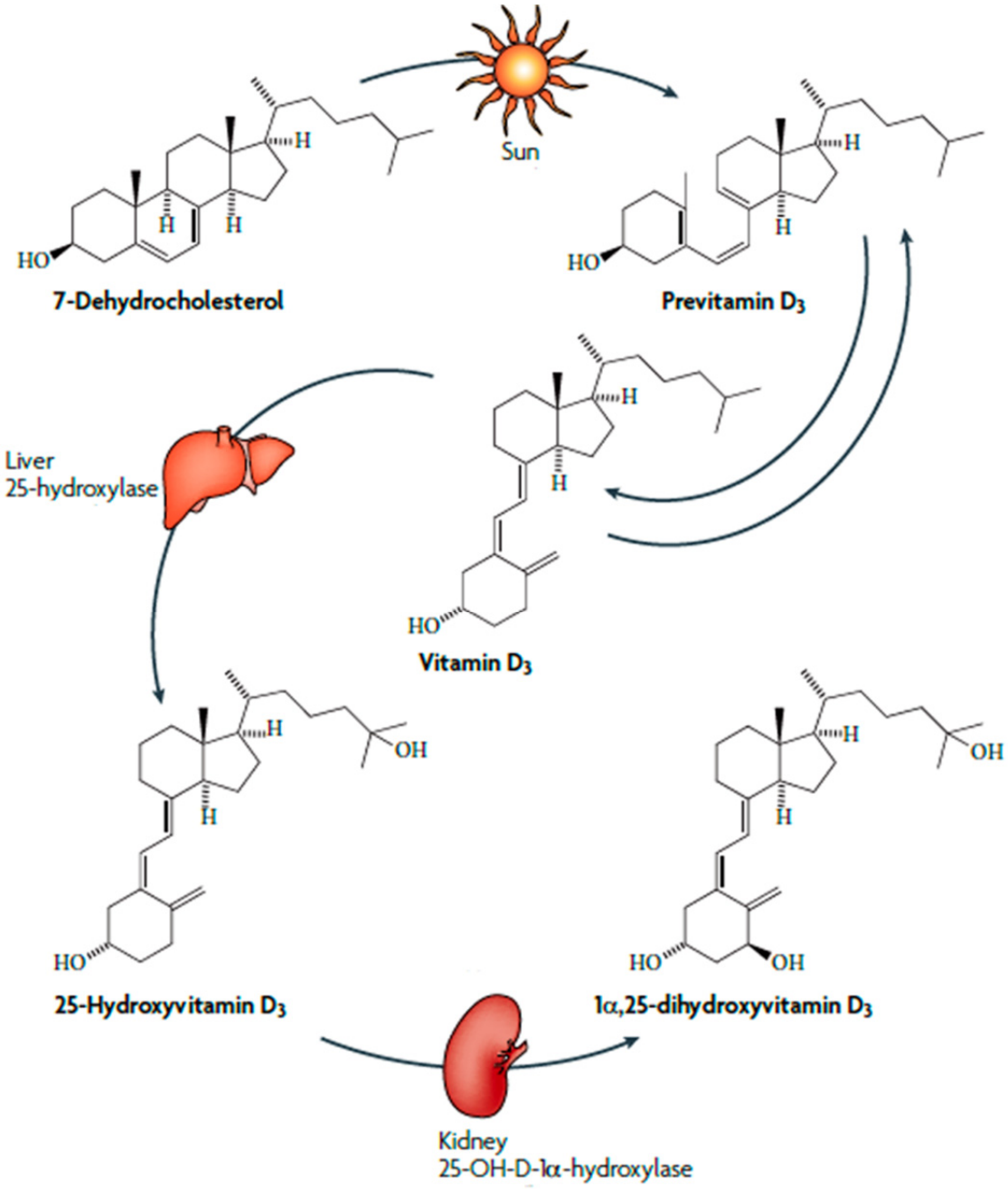

Figure 1.8. Pathway of the natural synthesis of vitamin D. Adapted from (Plum and DeLuca, 2010).

❖ ***Actions on bone***

The action of vitamin D in bone involves both formation and resorption. However, these actions on bone are complex and both direct and indirect effects have been described. Furthermore, direct actions are further complicated because vitamin D affects several cell types, including osteoblasts, bone stromal cells and osteoclasts (Feldman et al., 2013). Also the nature of vitamin D response depends on the differentiation state of bone cells (Arriagada et al., 2010). Osteoblasts express VDRs and the direct action of $1,25(OH)_2D_3$ on these cells include modulation of cell growth and stimulation of differentiation (Franceschi RT, 2011; Lian JB et al., 2011). Indeed, $1,25(OH)_2D_3$ induce osteoblasts to differentiate and synthesize matrix proteins and mineralized bone through the control of target genes, including ALP, OC, osteopontin (SPP1), the hydroxylases CYP27A1 and CYP27B1, RANKL or OPG (Pike et al., 2012; Bikle, 2009; Christakos, 2004). However, the fully understanding of the biological action of vitamin D in the bone is not clearly understood. Initially, $1,25(OH)_2D_3$ was thought to be a bone resorption inductor. Thus, it was said to induce RANKL expression in osteoblasts to further promote osteoclastogenesis (Suda et al., 1999). However, later studies proved that vitamin D compounds improved bone mineral density whilst reduce bone resorption by inhibiting osteoclastogenesis (Sairanen et al., 2000). This inhibitory action of vitamin D metabolites on osteoclastogenesis was believed to work through changes in the bone microenvironment (Takahashi et al., 2014). So far, there is much new knowledge regarding the biological mechanisms of vitamin D in bone cells. However, a full understanding of how vitamin D achieves these beneficial effects on the skeleton is still elusive.

1.4.2. Vitamin D and health

Vitamin D is essential for strong bones, muscles and overall health. However, several factors should be considered to maintain adequate vitamin D levels. First, a well-balanced diet is required to provide sufficient amounts of vitamin D. Food that contains substantial amounts of vitamin D includes liver, fatty fish and fish liver oils (DeLuca, 2013). Inadequate dietary intake of these foods can cause vitamin D deficiency. Furthermore, our body is able to produce vitamin D from its precursor, 7-DHC, which is photoactivated in our skin by the sun action. Nevertheless, this cutaneous synthesis depends on several factors, including latitude, seasonal variation, skin pigmentation, sunshine exposure and age (Feldman et al., 2013). Also other risk factors affecting vitamin D levels in our body comprise renal failure, alcoholism, obesity and some drug interactions with vitamin D levels (Feldman et al., 2013). Changes in the vitamin D levels due to the action of these factors have revealed several biological consequences, including disorders in both non-calcemic and skeletal tissues.

❖ ***Non-calcemic related disorders***

Besides its classical role in the bone metabolism, vitamin D has a variety of effects on other cells and disease states. Thus, vitamin D status has been linked to muscle decline and myopathy since vitamin D supplementation enhances muscle strength and ability (Verhaar et al., 2000). Chronic renal failure carries with it the loss of function of vitamin D endocrine system but recent evidences have suggested that therapy with $1,25(OH)_2D_3$ may delay the progress of the disease (Szeto et al., 2008). In

line with this, there is a high incidence of vascular disease and cardiovascular death in patients with renal failure (Thadhani, 2009). Furthermore, epidemiological studies showed that vitamin D treatment increased the life expectancy of these patients (Szeto et al., 2008). Furthermore, vitamin D also has a positive effect on skin disorders, including psoriasis and acne (Reichrath, 2007). The possibility that vitamin D may have a role in autoimmune diseases was confirmed since it can control proliferation of several immune-system cells. Thus, vitamin D has been speculated to be useful in some disorders such as multiple sclerosis, type I diabetes, inflammatory bowel disease, lupus erythematous or rheumatoid arthritis (Plum and DeLuca, 2010). Recently, vitamin D has been suggested to be beneficial for the treatment of periodontal diseases (Garcia, 2014; Garcia et al., 2011). Indeed, diminished levels of vitamin D have been found in patients with increased gingival inflammation (Stein et al., 2013). Thus, vitamin D may affect periodontium via an effect on bone mineral density or via immunomodulatory action (Martelli et al., 2014).

However, excess intake of vitamin D is toxic and can lead to hypervitaminosis. This condition leads to hypercalcaemia, with elevated serum calcium and phosphate what may cause soft tissue calcification. But vitamin D toxicity cannot result from the UV irradiation of the skin, as continued irradiation converts preD_3 to inactive products (Jones, 2008). Extrarenal production of vitamin D found in some pathological diseases such as lymphoma and tuberculosis are associated with hypercalcemia. Also many cases of hypercalcaemia are due to malignancy (Plum and DeLuca, 2010).

❖ ***Skeletal disorders***

Modifications in the vitamin D status can lead to several skeletal disorders. Thus, vitamin D deficiency causes an inadequate mineralization of the skeleton. In children, vitamin D deficiency results in rickets, which are characterized by deformations in the skeleton and weak and toneless muscles (Holick, 2005). In adults, vitamin D deficiency leads to osteomalacia that consists of a failure in the bone matrix mineralization (Duncan, 2013). Interestingly, administration of vitamin D results in the curing of both rickets and osteomalacia (Plum and DeLuca, 2010). Indeed, calcium salts and vitamin D preparations are available for the treatment of these diseases (Duncan, 2013).

Another bone disease produced by calcium and vitamin D deficiency is osteoporosis. The incidence of osteoporosis is currently increasing as result of the ageing population. This bone disease is a generalized skeletal disorder characterized by compromised bone strength, which predisposes to an increased risk of fractures (Inoue, 2005). Although the involvement of vitamin D in osteoporosis still remains under investigation, there is no doubt that adequate vitamin D intake is important in patients suffering from osteoporosis. Indeed, beneficial effects of vitamin D in treating osteoporosis have been demonstrated (Kubodera, 2009). Furthermore, vitamin D is often included with bisphosphonates or with calcium in the treatment of osteoporosis, since they do seem to reduce the fracture rate (Nishii, 2002; Tilyard et al., 1992). Vitamin D deficiency also leads to bone resorption, reduced bone mineralization and a higher risk of falls and fractures (Atkins et al., 2007; St-Arnaud, 2008). Interestingly, several studies have proved the effect of vitamin D on the osseointegration process. Indeed, various animal studies confirmed that vitamin D insufficiency impairs implant osseointegration whilst supplementation of vitamin D leads to peri-implant bone formation, as described in Table 1.2.

Table 1.2. Effect of vitamin D on the osseointegration process in several animal studies.

Reference	Animal model	Significance
Kelly et al. 2009	Sprague-Dawley rats	Vitamin D-deficient environment significantly impaired the establishment of Ti implant osseointegration *in vivo*.
Cho et al. 2011	New Zealand white rabbits	PLGA/1,25$(OH)_2D_3$ solution coating stimulated bone formation adjacent to the surface of implants inserted into bone.
Dvorak et al. 2012	Female ovariectomized Sprague-Dawley rats	Vitamin D-free diet had a negative impact on peri-implant bone formation in ovariectomized rats, which was compensated by vitamin D supplementation.
Zhou et al. 2012	Female ovariectomized Sprague-Dawley rats	1,25$(OH)_2D_3$ administration improved Ti implant osseointegration in osteoporotic rats.
Wu et al. 2013	Wistar rats, diabetes mellitus (DB) induced	D_3 and insulin combined supplementation promoted Ti implant osseointegration in DB rats.
Liu et al. 2014	C57BL mice	1,25$(OH)_2D_3$ supplementation was effective in improving the fixation of Ti implants in chronic kidney diseased mice.
Naito et al. 2014	New Zealand white rabbits	1,25$(OH)_2D_3$ coated implants presented a tendency to osseointegrate better than non-coated implants.

Due to the essential role of vitamin D in maintaining a healthy skeleton, vitamin D supplementation has already been considered for improving skeletal disorders and implant osseointegration, with positive proven results in these applications. However, to the best of our knowledge, the present thesis is the first study that develops a bioactive coating using the vitamin D precursor 7-DHC, UV-irradiated, instead of using the final active vitamin D metabolite. Having a coating that gives locally the precursor of vitamin D to the skeletal cells for their own production could be more effective in the modulation of the osseointegrative properties of such implant. Thus, using the vitamin D precursor could entail a number of benefits including minor risk of vitamin D toxicity in target cells and cheaper production as 7-DHC is easily available and low-priced compared with 1,25$(OH)_2D_3$.

2. Aims of research

2. Aims of research

The overall aim of this thesis was to develop a novel coating for Ti dental implants by using the vitamin D precursor to improve bone and soft tissue integration.

The work of this thesis can be divided in the following sections:

1. **Determination of vitamin D synthesis by osteoblastic cells from UV-irradiated 7-DHC and its feasibility as a bioactive coating for Ti implants.**

Our first aim was to determine whether osteoblastic cells were able to produce themselves final vitamin D from the external precursor 7-DHC and using UV irradiation. Thus, UV-irradiated 7-DHC coated polystyrene surfaces were tested for their biological potential in the murine preosteoblastic cell line MC3T3-E1 *(Paper I)*. In this study, different doses of 7-DHC were evaluated in order to determine the optimal concentration. Furthermore, we analyzed the expression of the whole enzymatic machinery required to synthesize the final vitamin D in these cells. HPLC analyses were used to determine the production of $preD_3$ after the UV-irradiation of 7-DHC and ELISA assays measured the 25-D_3 and 1,25-D_3 secretion in these cells. Similarly, Ti surfaces were coated with 7-DHC and further UV-irradiated to assess their effect on osteoblastic cells *(Paper II)*. In this case, different UV exposure times were analyzed in order to determine the optimal time for photoconversion of 7-DHC into $preD_3$. FTIR and HPLC analyses were performed to confirm changes in the ring structure and the conversion from 7-DHC to $preD_3$. In addition, the biological response to these modified implants was tested in MC3T3-E1 cells with regard to cytotoxicity, cell morphology, differentiation and mineralization.

2. **Improvement of the vitamin D synthesis on Ti surfaces and its biological effect on cells involved in hard and soft tissue integration *in vitro*.**

Once the potential of the bioactive coating was tested in osteoblastic cells, we aimed at evaluating its effect on the differentiation of hUC-MSCs towards the osteogenic lineage *(Paper III)*. Thus, we studied the biological response of hUC-MSCs in terms of cytotoxicity, cell morphology, gene expression of several markers related to osteoblast differentiation and finally, ALP activity and mineralization to examine osteoblast function.

Next, our goal was to improve the synthesis of D_3 over the Ti surface in two ways *(Paper IV)*. First, since 7-DHC and its metabolites are very labile, we added an antioxidant agent (vitamin E, VitE), to the 7-DHC coating to preserve their stability and to avoid their oxidation. Second, since the isomerization of $preD_3$ to D_3 is time and temperature dependent, we tested different incubation times and temperatures after the UV-irradiation of the coating. This incubation step was included to promote the thermal isomerization of $preD_3$ towards the D_3 metabolite, reducing therefore the isomerization of $preD_3$ towards secondary products (lumisterol, tachysterol and toxisterols).

The biological activity of this improved coating was then evaluated in pre-osteoclastic cells (RAW264.7 cell line) and HGFs. On one hand, we determined the response of RAW264.7 cells to UV-irradiated 7-DHC:VitE coated Ti implants by analyzing cytotoxicity, TRAP and actin immunostaining,

and the gene expression of osteoclast phenotypic, fusion, and activity markers *(Paper IV)*. On the other hand, the effect of UV-irradiated 7-DHC:VitE was assessed on HGF cell viability, morphology, gene expression and protein levels of specific markers involved in the ECM turnover and wound healing *(Paper V)*.

3. Evaluation of the biological response *in vivo* and stability analysis after storage.

Our ultimate goal was to investigate the *in vivo* potential of the bioactive implant surface here proposed. For this purpose, a rabbit animal study was selected to evaluate the osseointegration of UV-activated 7-DHC:VitE coated Ti implants after 8 weeks of healing using two doses, the optimal dose found *in vitro* and a dose ten times higher. The bone-to-implant attachment strength was evaluated and wound fluid (LDH activity, ALP activity and protein content) and bone tissue analyses (mRNA levels of bone markers) were performed. Furthermore, a stability study was carried out to determine the composition and bioactivity of the coating when stored up to 12 weeks. HPLC analyses quantified the coating composition whilst *in vitro* experiments using MC3T3-E1 cells were performed to evaluate their bioactivity after storage in terms of cytotoxicity, mRNA levels of bone markers and ALP activity *(Paper VI).*

The experimental work presented in this thesis was performed in the Cell Therapy and Tissue Engineering (TERCIT) group at the Research Institute on Health Science (IUNICS) at the University of Balearic Islands, except the animal study presented in *Paper VI*, which was carried out in the Department of Biomaterials at the University of Oslo. hUC-MSCs were a donation from the "Fundació Banc de Sang i Teixits de les Illes Balears".

3. Methodological considerations

3. Methodological considerations

This chapter intends to discuss methods used in this thesis by providing the advantages or disadvantages of the selected methods with regards to the aim of research. For a detailed description of the equipments, materials and specific methods used we refer to the "Material and Methods" sections of each individual paper *(Papers I-VI)*. Figure 3.1 gives an overview of the different methods used for the methodological approach.

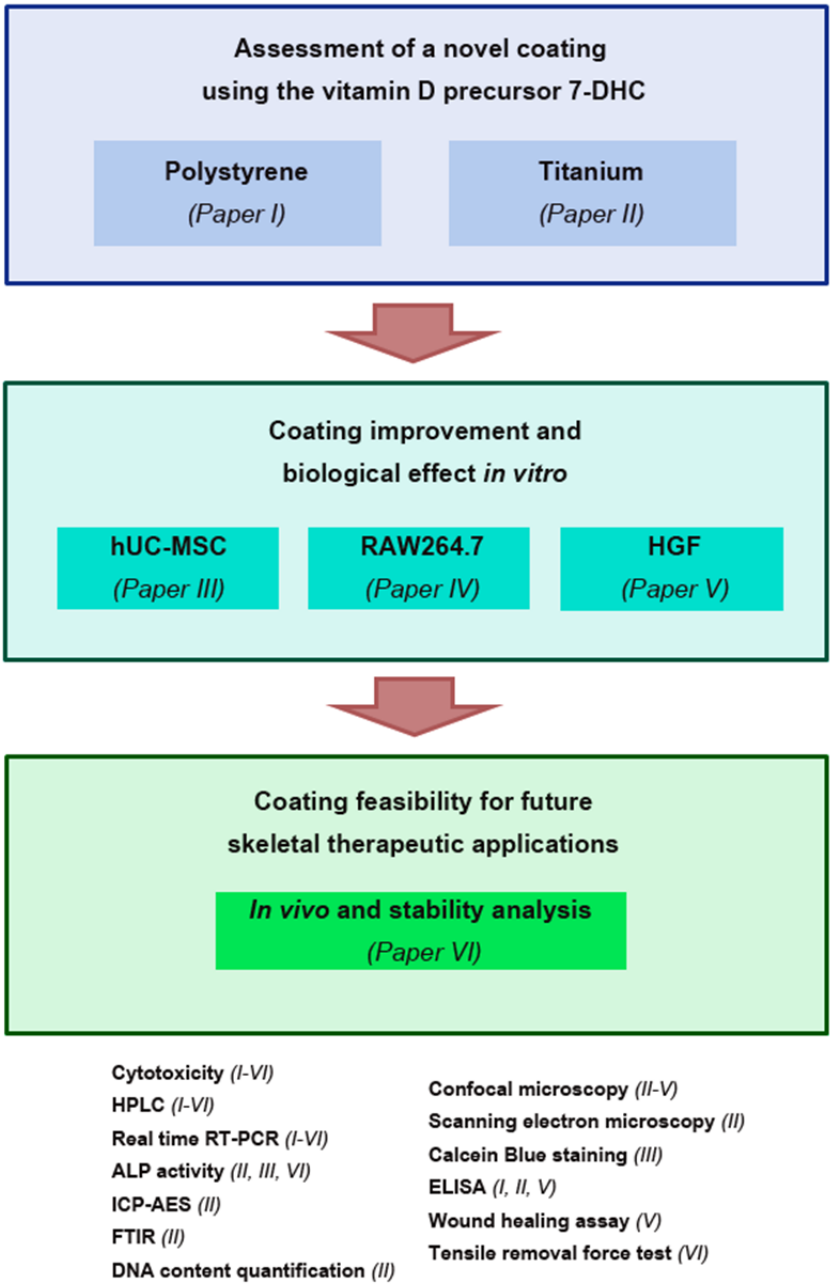

Figure 3.1. Overview of the methodological approach. Specific methods are listed and referred to the papers in which each method was performed. Roman numbers refer to the papers.

3.1. Preparation and optimization of the coating

During the development of the coating throughout this thesis, several variables affecting the resulting coating composition were taken into account. The following sections describe in detail the preparation of the coating and the considerations taken into account to improve its bioactivity and performance.

3.1.1. Materials

In this thesis, we first used polystyrene surfaces in order to validate osteoblast production of active vitamin D (1,25-D_3) in response to exogenous 7-DHC with and without UV irradiation (Paper I). This paper constitutes the basis for the next studies on titanium (Ti) disks to assess the feasibility of UV-irradiated 7-DHC as a bioactive coating for orthopedic and dental implants *(Papers II-VI)*. Ti was selected as the study material since it is the most common material used for endosseous implants due to its outstanding physical and biological properties (Niinomi, 2003). For the *in vitro* studies, Ti disks used were all made of grade 4 with a diameter of 6.25 mm and a height of 1.95 mm. All disks were machined from cp Ti rods and subsequently ground, polished and cleaned to completely remove debris. Briefly, Ti disks were washed in a glass beaker with deionized (DI) water for 30 s, with 70% ethanol for 30s, and in an ultrasonic bath in DI water at 40ºC for 5 min. The implants were subsequently placed in 40% NaOH solution in a water bath at 40ºC for 10 min, sonicated in DI water for 5 min and then washed with DI water until pH reached six. Afterwards, the implants were sonicated in DI water at 50ºC for 5 min, placed in 50% HNO_3 solution at 50ºC for 10 min and sonicated in DI water for another 5 min. Ti disks were then washed with DI water until pH reached six and stored in 70% ethanol prior to surface modification.

Whilst machined Ti implants are usually used for *in vitro* studies because they facilitate cell adhesion and proliferation, rough Ti implants are used for *in vivo* studies as they promote the osseointegration process (Le Guéhennec et al., 2007). Thus, for the *in vivo* study *(Paper VI)*, Ti disks were blasted with TiO_2 particles using 90-110 µm particle size fraction. Briefly, disks were mounted on a silicone holder and kept at a distance of approximately 20 mm from the jet nozzle and the particle stream hit the surface at an angle of 90º. The blasting process was carried out with repeated vertical and horizontal movements during 8 s and the air pressure used was 0.5 MPa. After blasting, Ti disks were cleaned with trichloroethylene in an ultrasonic bath for 30 min and then rinsed with 100% ethanol in an ultrasonic bath for 10 min (3 times). Cleaned disks were finally rinsed with DI water.

3.1.2. Coating with the vitamin D precursor

For the surface modification, 7-DHC (Sigma, St. Louis, MO) was dissolved in absolute ethanol and further filtered with a 0.22 mm pore size filter before use. Surfaces were coated with 10 µL of increasing doses of 7-DHC: 2×10^{-3} nmol, 2×10^{-2} nmol, 0.2 nmol, 2 nmol and 20 nmol per well *(Paper I)* or 0.2 nmol per Ti disk *(Paper II),* having the polystyrene well and the Ti disk the same surface area. For the *in vivo* analysis *(Paper VI*), a higher dose of 7-DHC (2 nmol/ Ti disk) was also

studied, as explained later in this section. UVB irradiation at the optimal wavelength and during the right time is an important factor for the synthesis of $preD_3$. Indeed, the use of long irradiation periods or long wavelengths can lead to the synthesis of irreversible or undesired products (Braun et al., 1991). For this reason, in this thesis we irradiated with a wavelength of 302 nm since it was previously reported to be the wavelength at which the maximum conversion of 7-DHC into $preD_3$ is achieved (Lehmann et al., 2001). Thus, a UV lamp (UVP, Upland, CA, USA) of 302 nm was used at an intensity of 6 mW cm^{-2}, either during 30 min *(Paper I)* or at increasing UV exposure times of 0, 5, 10, 15, 30 min *(Paper II)*. After this study, a 7-DHC dose of 0.2 nmol/Ti disk and a UV exposure time of 15 min were selected and applied for the coating of Ti disks and its biological evaluation in further studies *(Papers III-VI).*

During the development of this doctoral research, the coating composition was optimized by adding an antioxidant agent and by testing the incubation conditions after UV irradiation in order to promote the isomerization process towards D_3. On one hand, 7-DHC and its photoproducts are sensitive to light, heat and oxygen; indeed, 7-DHC is the most reactive lipid known to maintain a peroxidative free radical reaction (Porter, 2013). Thus, we hypothesized that the addition of VitE would reduce its oxidation. Then, 7-DHC was supplemented with VitE (Sigma, St. Louis, MO). The selection of VitE as the chosen antioxidant agent was due to its similar solubility properties to 7-DHC and to its positive effects on bone. Indeed, VitE suppresses the production of several cytokines involved in increased bone loss (Nazrun et al., 2012) and prevents bone resorption as oxygen-free radicals are linked to osteoclast formation and activation (Lee, 2005). Therefore different doses of VitE (20:1, 5:1, 1:1; 7-DHC:VitE) on a mass-to-mass (m:m) basis were evaluated *(Paper IV)*, as this antioxidant may have a prooxidant effect at high concentrations (Ouchi et al., 2009). On the other hand, since the isomerization of $preD_3$ into D_3 is a time and temperature reaction (Holick, 1981), we improved the final D_3 synthesis onto the Ti surfaces by including an incubation step, with controlled time and temperature conditions, after the UV-irradiation of 7-DHC:VitE. UV-irradiation of 7-DHC produces the formation of $preD_3$ which further isomerizes via heat to D_3 but also to other secondary products. In order to favour the isomerization process towards the D_3 metabolite, several temperatures (-20, 4 and 23ºC) and incubation times (0, 24, 48 and 96h) were tested in *Paper IV*.

Further investigations *in vitro (Papers V and VI)* were carried out using 10 µL of 0.2 nmol 7-DHC supplemented with VitE (1:1; m:m) per Ti disk and an incubation step for the coating (48h at 23ºC), immediately after the UV-activation process, as shown in Figure 3.2. The main limitation of these *in vitro* methods is the result of the direct extrapolation of *in vitro* data to the *in vivo* situation, since there exists numerous differences between *in vitro* and *in vivo* compound biokinetics that difficult the assessment of the concentration at which the compound is bioactive and relevant to *in vivo* dose levels (Davila et al., 1998). With the aim of obtaining a bioactive response *in vivo*, besides the dose studied *in vitro*, we also evaluated a higher dose of 7-DHC:VitE (2 nmols/Ti disk) in the *in vivo* experiment *(Paper VI)*.

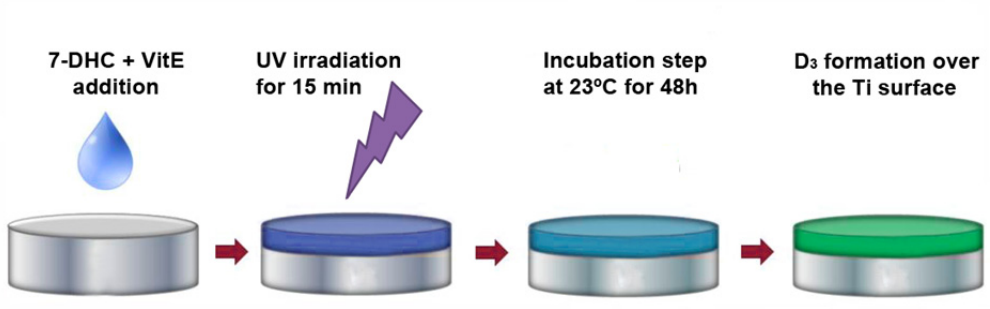

Figure 3.2 Final coating procedure for Ti implants. Addition of VitE and an incubation step with controlled time and temperature conditions were introduced in order to promote the D_3 synthesis over the Ti surface *(Papers IV, V and VI)*.

3.1.3. Storage conditions

Implants used in clinical practice need to maintain their stability for a certain period of time. On that basis, we evaluated the stability and bioactivity of the coating after storage up to 12 weeks (Paper VI). Thus, coated surfaces were stored avoiding light, oxygen and moisture at different temperatures (-20, 4 and 23ºC) for 21 days to assess the best storage condition. Next, modified implants were stored under the selected temperature conditions up to 12 weeks and their coating composition and biological activity were analysed *(Paper VI)*.

3.2. Chemical surface characterization

Surface characterization methods are important to measure critical chemical properties of biomaterial coatings. In this thesis, we determined the resulting metabolite composition of the UV-irradiated 7-DHC coated surfaces using high performance liquid chromatography (HPLC); whilst the changes in the chemistry of the coating after UV-irradiation were assessed through Fourier transform infrared spectroscopy (FTIR).

3.2.1. High performance liquid chromatography (HPLC)

HPLC was the technique used to quantify the coating composition in all the studies *(Papers I-VI)*. HPLC is an analytical technique with high separation power and sensitive detection that allows performing very precise and highly reproducible analysis. Alternatively, vitamin D metabolites have been measured by other techniques including gas chromatography-mass spectrometry (Hugh L. J. Makin, 1984) and Enzyme-Linked ImmunoSorbent Assay (ELISA) (see page 46). However, HPLC is considered to be the “gold standard” for measuring vitamin D metabolites compared with other techniques (Lensmeyer et al., 2006). Despite its advantages, HPLC can be costly since it requires larger quantities of expensive organics and it can also be complex to troubleshoot problems. But it is extremely accurate and efficient. For preparing the mobile phase, we used methanol (HPLC gradient grade), acetonitrile, tetrahydrofurane (Thermo Fisher Scientific, MA, USA) and high-purity DI Milli-Q

water (Millipore Corporation, Billerica, MA, USA). Individual stock standard solutions of 7-DHC, D_3 and VitE were prepared in methanol and stored at −20 °C.

The coating of each surface was extracted by adding 100 µL of 'methanol–acetonitrile–tetrahydrofurane–water' (67 : 16 : 2 : 15, v : v) to each well or Ti disk. The content of three replicate wells was mixed and an aliquot of 100 µL was injected into the HPLC system. The analysis was carried out using a Waters liquid chromatographic system (Milford, MA, USA), equipped with a refrigerated automatic injector WISP700 and a 600 pump system, connected to a Waters 996 photodiode array (PDA) detector. For data analysis, Empower software was used (Waters, Milford, MA, USA). Detection was carried out at 282 nm. Sample components were separated using a Nova Pak C18 column (Waters) which was previously set to 30 °C. Two solvents, A: 'methanol–acetonitrile–tetrahydrofurane–water' (67 : 16 : 2 : 15, v : v) and B: 'methanol– acetonitrile–tetrahydrofurane' (75 : 20 : 5, v : v), were used in the gradient elution mode as the mobile phase. The binary gradient used was as follows: from 5% B to 90% B in 3 minutes, held for 9.5 min at 90% B, from 90% B to 5% B in 1 minute and equilibrated between injections at the initial conditions for 5 min (total run time = 15 min + 5 min equilibration between injections). Quantification was performed by integration of the peak area of the corresponding analyte and interpolation of the peak area in the standard curves.

3.2.2. Fourier transform infrared spectroscopy (FTIR)

Assessment of the surface chemistry was performed in order to detect the effect of UV irradiation on vitamin D conversion. In this thesis *(Paper II)*, FTIR spectroscopy in reflective mode (DRIFT, Spectrum 100, Perkin Elmer, USA) was used to analyze structural changes of 7-DHC after 0, 15, 30 and 60 min of UV irradiation. This technique is highly sensitive and quick to achieve high quality spectrum. Furthermore, it offers higher signal-to-noise and speeds than spectrometers that use gratings (Chittur, 1998). FTIR uses light in the infrared (IR) region to excite the specimen and induce a change of the vibrational and rotational state of its molecules. Then, the specific vibrational frequency of a molecule defines which frequency of the IR light is absorbed. This signal is further detected by a detector allowing the identification of molecular components and structures (Smith, 2011). Ti disks were coated with 7-DHC or D_3 and UV-irradiated as previously described in Section 3.1.2. Untreated Ti disks equally UV-irradiated were considered as a background for the FTIR measurements. FTIR spectra were analyzed for typical absorbances connected to changes in chemical structure of 7-DHC and D_3 after UV exposure of the coatings. Spectrum program (version 6.3.2.0151, PerkinElmer, Inc. Waltham, USA) was used for data spectra analysis. Typical peak areas were fitted quantified with CasaXPS (version 2.3.15, Casa Software Ltd).

3.3. Biological surface characterization

Biological characterization of our modified surfaces was conducted by *in vitro* cell culture techniques using several cell types and analyzing the cell response to the surface modifications in terms of cytotoxicity, cell morphology, proliferation, differentiation, and mineralization and wound healing analyses. Finally, an animal study was carried out to evaluate the biological response to the modified surfaces *in vivo* and thus, compare the results with the previous *in vitro* ones. Taken

together, all the methods used in this work provide a detailed evaluation of the biological response to the vitamin D precursor coating under investigation.

3.3.1. Cell culture

This thesis used *in vitro* studies to evaluate the biological performance of Ti implants coated with the vitamin D precursor. The use of *in vitro* experiments provides a cost effective screening of the biocompatibility and bioactivity of different modified surfaces on the biological response. Also, *in vitro* studies give a simplified reflection of the *in vivo* situation in controlled defined conditions.

In this work, four different types of *in vitro* cell models were used, including cells involved in both hard (osteoblasts, mesenchymal stem cells and osteoclasts) and soft (gingival fibroblasts) tissues.

Osteoblasts

The murine osteoblast cell line MC3T3-E1 (Figure 3.3) was used *(Papers I, II and VI)*. This cell line comes from an established osteogenic cell line from newborn mouse calvaria that has the capacity to differentiate into osteoblast-like cells and to form calcified bone tissue (Sudo et al., 1983). The advantage of immortal cell lines over primary cells is the ease of culture and increased phenotypic stability with serial passages, what results in increased reproducibility of results in independently conducted experiments. However, immortal cells might show characteristics less close to actual *in vivo* situations. Interestingly, MC3T3-E1 pre-osteoblastic cells have been widely used to study bone tissue development *in vitro* because they undergo a developmental sequence of proliferation and differentiation similar to primary cells in culture (Peterson et al., 2004). Furthermore, MC3T3-E1 cells are often used as an *in vitro* model for the cell-material interaction studies (Czekanska et al., 2012). Therefore, this cell line was chosen as an *in vitro* model for studying the biological effect of our coating. Cells were cultured in alpha-MEM culture medium, which includes ascorbic acid and phosphate for cell mineralization.

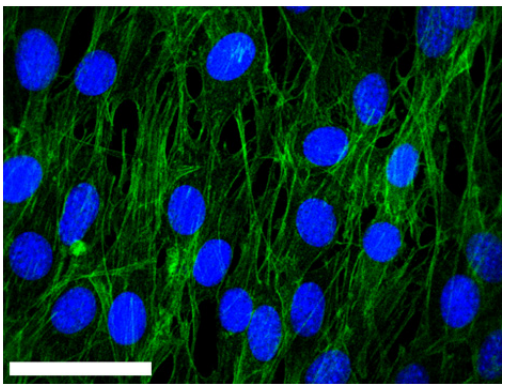

Figure 3.3. Typical elongated and spindle MC3T3-E1 cell morphology. Visualization by confocal microscope (scale bar = 50μm) of MC3T3-E1 cells cultured on Ti implants. Cell nuclei are shown in blue (DAPI staining) and actin filaments are shown in green (phalloidin-FITC staining).

Mesenchymal stem cells (MSCs)

In this thesis also primary cell cultures were used to evaluate the potential of modified surfaces to stimulate differentiation of MSCs commited to the osteogenic lineage *(Paper III)*. Although functionally differentiated primary cell cultures have a limited life span compared to cell lines, the use of primary cell cultures reflects better the *in vivo* situation. MSCs are multipotent cells with capacity to differentiate into a variety of cell lineages, including bone cells. MSCs are the main source of osteoprogenitor cells and are involved in normal skeletal homeostasis and bone regeneration (Deschaseaux et al., 2009).

Therefore, we used hUC-MSCs to evaluate the biological effect of our coating (Figure 3.4). hUC-MSCs were previously isolated from umbilical cords obtained in the process of human umbilical cord blood donations under the Concordia Cord Blood Donation program. Flow cytometry confirmed that the resulting cells isolated fulfilled the criteria of a MSC population (Dominici et al., 2006). Thus, cells did not express CD34, CD45, CD31, and HLA-DR, whereas were positive for CD105, CD90, and CD73. Variables among different donors were taken into account by using two different donors to improve validity of our data. In order to induce hUC-MSCs differentiation into the osteogenic lineage, cells were cultured in DMEM/Glutamax/Low glucose medium supplemented with dexamethasone (10 nM), ascorbic acid (50 µg/mL) and β-glycerophosphate (10 mM). These osteogenic supplements are known to be necessary for MSCs to differentiate to osteoblastic cells (Jaiswal et al., 1997).

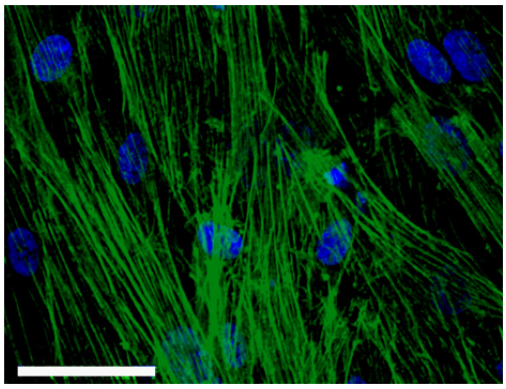

Figure 3.4. Human UC-MSC cell morphology when cultured with osteogenic supplements. Visualization by confocal microscope (scale bar = 50µm) of hUC-MSCs cultured on Ti implants. Cell nuclei are shown in blue (DAPI staining) and actin filaments are shown in green (phalloidin-FITC staining).

Osteoclasts

Successful osseointegration of an implant is accomplished by balanced bone remodeling in which both osteoblasts and osteoclasts play an essential role. Thus, murine macrophage cell line RAW264.7 (Figure 3.5) was used to evaluate the effect of modified implants on osteoclastogenesis *(Paper IV)*. RAW264.7 cell line is proven to be an important tool for *in vitro* studies of osteoclast formation and function, having particular advantages over the use of osteoclasts generated from bone marrow populations or directly isolated from murine bones (Collin-Osdoby and Osdoby, 2012). Furthermore, RAW264.7 cells allow a sensitive and rapid development into highly bone-resorptive osteoclasts expressing hallmark characteristics once RANKL stimulated. For these reasons, we chose

this cell line to study the effect of our coating on osteoclast behavior. RAW264.7 cells were cultured in DMEM medium and, after an overnight period, 4 ng/mL of RANKL were added to culture medium to stimulate osteoclast formation. After 4 days of cell culture with RANKL stimulation, osteoclast formation was observed in control surfaces.

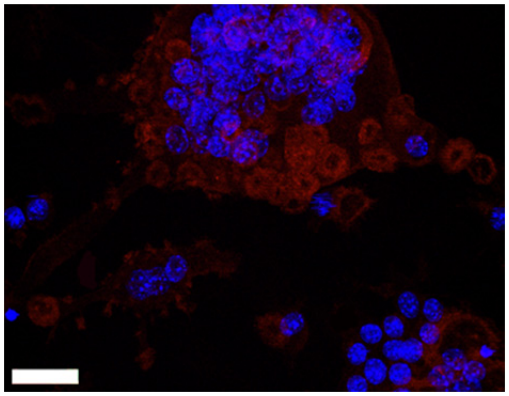

Figure 3.5. RAW264.7 cell morphology when cultured with RANKL addition. Visualization of RAW264.7 cells cultured on Ti implants by confocal microscope (Scale bar = 25μm). Formation of multinucleated cells and Trap expression was observed. Cell nuclei are shown in blue (DAPI staining) and Trap protein is shown in red (anti-Trap labeled with Cy3).

Gingival fibroblasts

As dental implants require the integration of the implant in both hard and soft tissue, we investigated the effect of our modified surfaces on HGFs. Although several cell types have been identified within gingival connective tissue, HGFs account for most connective tissue cells. HGFs (Figure 3.6) synthesize many ECM components and play a significant role in the constant adaptation of gingival connective tissue, the wound repopulation and the attachment to the implant after its installation (Bartold et al., 2000; Palaiologou et al., 2001; Abiko et al., 2004). Therefore, we evaluated the effect of modified Ti implants on HGF cell response *(Paper V)*. Since several donors must be considered when using primary cells, we used three different donors of primary HGFs (Provitro GmbH, Berlin, Germany).

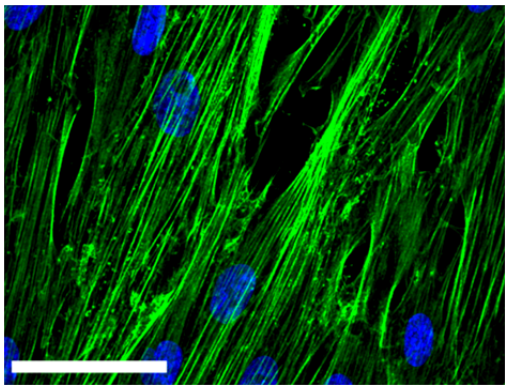

Figure 3.6. Characteristic fibroblastic cell morphology of HGFs. Visualization of extensive cell spreading over the Ti implant by confocal microscope (Scale bar = 50μm). Cell nuclei are shown in blue (DAPI staining) and actin filaments are shown in green (phalloidin-FITC staining).

3.3.2. Cell response evaluation

Assessment of cell response to biomaterial surfaces is the basis for understanding the biological potential of the studied coating. Thus, several cell responses such as cell viability, morphology, proliferation, differentiation, mineralization and wound healing were used to evaluate the modified surfaces providing basis for further selection of the coating with the best biological performance.

❖ ***Cell viability: Lactate dehydrogenase (LDH) activity***

One of the most important characteristics that a biomaterial must possess is biocompatibility (Van Tienhoven et al., 2006). LDH is a frequently used method to detect cell viability in bone (Acton, 2012). LDH is an intracellular enzyme that is released to the culture medium when the cell membrane becomes disrupted upon damage. It is a simple colorimetric assay that measures the LDH by assessing spectroscopically the rate of oxidation of NADH at 490 nm in the presence of pyruvate. This enzyme can be used to quantify cytotoxicity either *in vitro* or *in vivo*. Thus, tissue necrosis at the bone-implant interface can be determined using this method. Furthermore, by performing this assay, it is possible to measure the adverse effects induced by different treatments or biomaterials when are in contact with cells. For all these reasons, in this thesis we used this assay to assess the biocompatibility of the modified surfaces both *in vitro (Papers I-VI)* and *in vivo (Paper VI).*

Alternatively, the biocompatibility of the biomaterials can also be measured through the assessment of changes in membrane integrity by using trypan blue exclusion test or by using nucleic acid staining with propidium iodide or through assessment of the metabolic activity by the tetrazolium salt (MTT) assay.

❖ ***Cell morphology and proliferation***

Physico-chemical properties of biomaterials influence cell behavior, affecting their morphology and proliferation on the surface as well as regulating their cytoskeletal organization (Thevenot et al., 2008; Lin et al., 2011). Thus, in this thesis we evaluated cell morphology *(Papers II-V)* using confocal microscopy or scanning electron microscopy (SEM) and cell proliferation *(Paper II)* by quantifying the DNA content. Cell proliferation is also frequently measured by examining the metabolic activity of a population of cells through tetrazolium salts (MTT or WST-1) or resazurin. However, metabolic assays are subject to numerous variables, including their chemical dependency on the efficiency of metabolic enzymes, and are therefore not optimal methods for assessing cell proliferation (Quent et al., 2010).

Confocal laser scanning microscopy (CLSM)

Fluorescence imaging is a basic and useful tool for visualizing cells and tissues in biological sciences (Wu et al., 2010). This technique is based on labeling specimens with fluorophores. Fluorescence imaging can be performed with conventional fluorescence microscopy or with confocal microscopy. The first one is commonly used for fluorescence microscopy of thin fixed samples whilst confocal microscopy is more appropriate for thicker samples (Wu et al., 2010). CLSM is a very common method for fluorescence microscopy of fixed samples since it enables the collection of light

from a focal plane within a sample. Thus, it allows image capture at higher quality when compared with conventional fluorescent microscopy. Indeed, fine detail is often obscured by the haze and cannot be detected in a non-confocal fluorescent microscope (Corle and Kino, 1996). Therefore, we used in this thesis confocal microscopy (Leica DMI 4000B equipped with a Leica TCS SPE laser system) to visualize cell morphology of different cells cultured onto the modified Ti implants *(Papers II-V)*.

Scanning electron microscopy (SEM)

SEM is the most used electron microscopy approach to analyse cell surfaces. Images are obtained either by the secondary electrons generated following the interaction of an electron beam with the sample or by backscattering electrons (Figure 3.7). However, it requires the fixation of biological samples and therefore, the image produced does not reflect the natural state of the specimen. Also working under high vacuum state affects the specimen under investigation (Yaszemski MJ et al., 2003). One important advantage of SEM is that the whole surface of the cell can be visualized allowing accurate quantitative determination of the density of labelling (Souza, 2007). Thus, this approach provides information about sample surface composition at high magnification. In this thesis SEM was used for imaging the cell attachment and morphology to the modified Ti surfaces *(Paper II)*. To achieve this, cells were fixed and dried to preserve their structure under high vacuum conditions. Images of cells were captured using SEM Hitachi S-3400N (Hitachi High-Technologies Europe GmbH, Krefeld, Germany).

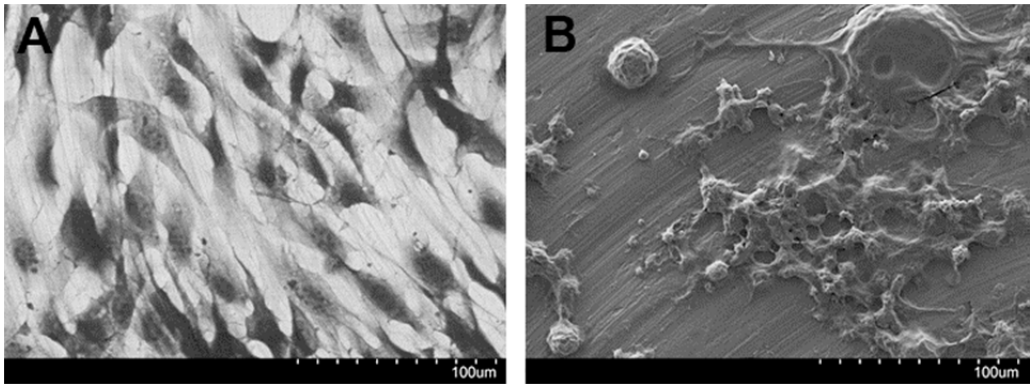

Figure 3.7. Visualization of MC3T3-E1 (A) and RAW264.7 (B) cell morphology using SEM. Images were obtained using environmental secondary electron detector (A) and backscattered electron detector (B).

DNA content quantification

The number of cells can be estimated from the quantification of the DNA content. Thus, this result provides information about the rate of cell proliferation. Although there are many different methods to quantitate DNA, most of them have disadvantages that preclude their use. For instance, absorbance measurements at 260 nm is the most commonly used method for DNA quantification but it suffers from the interfering absorbance of contaminating molecules that introduce high variability and error. Hoechst dye circumvents these problems and it is known to be an accurate, sensitive and specific method for quantifying DNA (Rao and Otto, 1992). Therefore, in this thesis we quantified the

DNA content *(Paper II)* using Hoechst dye. Fluorescence was measured at $\lambda_{excitation}$= 356 nm and $\lambda_{emission}$= 465 nm and the cell number was calculated using a linear standard curve.

❖ ***Real time reverse transcription polymerase chain reaction (Real-time RT-PCR)***

Several techniques can be used to detect specific mRNA sequences, including northern blot, in situ hybridization, conventional RT-PCR or real time RT-PCR. Among them, real-time PCR provides a quantitative, sensitive and fast method for the detection of specific mRNA sequences. In contrast to northern blot and ribonucleases protective assay (RPA), real-time PCR allows detection of mRNA sequences from very tiny amounts of sample, including the nanogram level. Furthermore, it offers many general technical advantages, such as reduced probabilities of variability and contamination, as well as online monitoring and the lack of need for post-reaction analyses. Thus, we used this method to evaluate the effect of our modified surfaces on cell behavior by analyzing the mRNA expression levels of different key markers *(Papers I-VI)*.

Total RNA was isolated from cells (*in vitro*) or bone tissue attached to extracted Ti implants (*in vivo*) by using a monophasic solution of phenol and guanidine thiocynate (TriPure®, Roche Diagnostics, Mannheim, Germany; TRIzol®, Invitrogen Life Technologies, Carlsbad, CA, USA). After RNA isolation, the same amount of total RNA in each experiment was retro-transcribed to its complementary DNA chain (cDNA) which was further used as template for real-time RT-PCR.

Retro-transcription of RNA to cDNA was primed by a mixture of random primers and oligo(dT) primers for the *in vitro* studies and random primers for the *in vivo* study. On the one hand, oligo(dT) primers allow the study of different targets from the same cDNA pool but also require full-length RNA. On the other hand, random hexamers allow synthesis of large pools of cDNA but the resulting amplification may not be quantitative if the mRNA target is at low levels. Thus, selection of appropriate RT primers depends on the target abundance, so we used these RT primers to guarantee synthesis of cDNA from RNA samples from tiny samples obtained *in vitro* and from the bone tissue *in vivo.* Next step includes the amplification of the specific cDNA-sequence by polymerase chain reaction (PCR) to a large amount of copies. In this step, specific primers for the target gene of study are required. In this thesis, specific primers for each target gene were designed using the Primer-Blast tool (http://www.ncbi.nlm.nih.gov/tools/primer-blast) and taking into account the considerations for designing primers for real-time PCR (Thornton and Basu, 2011). The main parameters to be considered when designing real-time PCR primers are as follows: (i) Primer length: The optimal length of primers is 18-24 pb, long enough to be specific but short enough to bind easily to the template; (ii) Product size: An ideal amplicon should be between 80-150 pb, to give enough time to polymerase to finish each amplification cycle. (iii) GC clamp: The 5' stability depends of how stable is the 5' end due to the amount of Gs or Cs present in the end of the primer. Having 1 or 2 GC clamps are ideal as it makes it more specific. (iv) Primer melting temperature: This temperature should be between 59 and 68ºC. (v) Primers should be designed to span an exon-exon junction in order to avoid false positive signals.

Real-time PCR monitors the reaction providing information of the amplification process at real time. To achieve this, a fluorescence dye or probe is introduced into the reaction and binds to each new copy of double-stranded DNA (dsDNA). Therefore, as PCR progresses, more amplified products are obtained and more fluorescent signal is produced as a result. Each reaction cycle is characterized by the crossing point (Cp) at which fluorescence first arise above defined background fluorescence. In this thesis, we used SYBR-Green as intercalating dye since it is the simplest method to detect amplicons. SYBR-Green intercalates into dsDNA thus increasing the fluorescent signal as SYBR-Green binds to the nascent dsDNA. The inconvenient of this dye is that it binds to any dsDNA, including primer-dimer or other non-specific reaction products (Bustin, 2000). Alternatively, other fluorescent probes used for real-time RT-PCR applications include fluorophores attached to primers and hybridization-probe based methods. However, the first ones usually require company-specific design software for optimal performance, and the second ones involve higher costs and occasional fragility of the probes.

Besides the target genes, reference or internal control genes are required to be analyzed to minimize differences in the amount of biological material and to compare mRNA concentrations across different samples. Normalization is an essential component of a reliable real-time PCR assay because it controls variations in extraction yield and efficacy of amplification (Bustin et al., 2009). These reference genes are constitutive genes required for the maintenance of basic cellular functions and expressed in all cells of an organism under normal and pathological conditions. Therefore these genes should have similar mRNA levels in all samples. However, some reference genes may vary depending on the experimental conditions. In the analyses performed in this thesis, three well described reference genes (Willems et al., 2006) were considered for normalization of mRNA levels: glyceraldehyde-3-phosphate dehydrogenase (GAPDH), ribosomal RNA 18S (18S) and β-actin. Stability of these reference genes was calculated using the Best-Keeper tool (Pfaffl et al., 2004). For the data analysis, we constructed standard curves for each target and reference gene by considering Cp values and cDNA concentrations. Therefore, all samples were normalized by the geometric mean of the expression levels of the reference genes and relative mRNA levels were calculated using the mathematical model described by Pfaffl (Pfaffl, 2001).

In order to perform and interprete the qPCR results in a reliable manner, we followed the considerations of the Minimum information for Publication of Quantitative Real-Time PCR Experiments (MIQE) guidelines. It describes the minimum information required to evaluate qPCR experiments in terms of nomenclature standardization and accuracy in the assay performance and further data analysis (Bustin et al., 2009). Thus, following these guidelines, we analyzed the mRNA levels of several markers along this thesis, depending on the cell type considered in each study. The function and importance of the different marker genes are described below (Tables 3.1 - 3-5):

Table 3.1. List of markers involved in osteogenic differentiation analyzed in the different studies.

Marker	Paper
ALP ***(Alkaline phosphatase)***	I, II
BMP2 ***(Bone morphogenic protein 2)***	I, II, III, VI
COLL1 ***(Collagen type I)***	I, II, III, VI
IGF1 ***(Insulin-like growth factor)***	VI
OC ***(Osteocalcin)***	I, II, III, VI
OSX ***(Osterix)***	I, II
RUNX2 ***(Runt related gene or CBFA1)***	III, VI
SPARC ***(Secreted protein acidic and rich in cysteine or Osteonectin)***	III
SPP1 ***(Secreted phosphoprotein 1 or Osteopontin)***	III

ALP

ALP is an early marker of osteoblast differentiation involved in hydroxyapatite deposition and its expression is increased during ECM maturation, just before mineralization is initiated (Stein et al., 1996; Golub et al., 1992).

BMP2

BMP2 plays a relevant role in osteogenesis since it regulates osteoblast phenotype development at different stages, stimulating osteoblast cell adhesion, migration, differentiation and bone matrix mineralization (Lai and Cheng, 2005).

COLL1

It is the most abundant type of all collagen ones. Its synthesis occurs at early stage (Stein et al., 1996) and it provides bone flexibility and strength. COLL1 serves as a scaffolding for mineral components (Robey, 2008).

IGF1

IGF plays a central role in cellular growth, differentiation, survival and cell cycle progression (Yakar et al., 2010). IGF1 participates in the acquisition and maintenance of bone (Yakar et al., 2002). Indeed, it appears to play a major role in bone remodeling and has a direct impact on linear bone growth.

OC

It is the major noncollagenous protein component of the bone ECM and is exclusively secreted by differentiated osteoblasts. OC regulates cell mineralization through binding to hydroxyapatite crystals (Boskey et al., 1998).

OSX

This transcription factor is required for osteoblastic differentiation and bone formation during bone development (Zhou et al., 2010). It acts down-stream of Runx2 to induce preosteoblastic differentiation into fully functional osteoblasts (Tu et al., 2006).

RUNX2

It is an early transcriptional factor involved in the MSC differentiation towards the osteogenic lineage (Yamaguchi et al., 2000). RUNX2 regulates the expression of ECM protein genes (Komori et al., 1997) and osteoblastogenesis (Jensen et al., 2010).

SPARC

SPARC is involved in matrix mineralization, wound healing, tissue remodeling and fibrosis (Davies et al., 2006). It binds selectively to both hydroxyapatite and collagen in the bone. Osteoblasts secrete SPARC during bone formation, linking the bone mineral and collagen phases (Termine et al., 1981).

SPP1

It is a noncollagenous protein present in bone matrix that plays a critical role in the maintenance of bone (Noda and Denhardt, 2008). SPP1 plays an important factor in bone remodeling since its role in anchoring osteoclasts to the mineral matrix of bone. It is expressed by both osteoblasts and osteoclasts (Sase et al., 2012).

Table 3.2. List of markers involved in osteoclastic differentiation and bone resorption analyzed in the different studies.

Marker	Paper
ADAM8 ***(A Disintegrin and metalloproteinase domain-containing protein 8)***	IV
CALCR ***(Calcitonin receptor)***	IV, VI
CAR2 ***(Carbonic anhydrase II)***	IV
CTSK ***(Cathepsine K)***	IV
DC-STAMP ***(Dendritic-cell specific transmembrane protein)***	IV
H^+ATPase ***(Proton ATPase)***	IV, VI
ITGAV ***(Integrin alpha-V)***	IV
ITGB3 ***(Integrin beta-3)***	IV
MMP9 ***(Matrix metalloproteinase-9)***	IV

ADAM8

ADAM8 is expressed at the later stages of osteoclast precursor differentiation. It enhances osteoclast precursor fusion resulting in the formation of multinucleated osteoclasts (Ishizuka et al., 2011).

CALCR

CALCR is a G protein-coupled cell receptor that binds to the hormone calcitonin, which is involved in osteoclast formation and bone resorption (Takahashi et al., 2008). Also, CALCR reduces osteoclast motility, spreading and bone resorbing activity (Horne and Baron, 2000).

CAR2

Carbonic anhydrases acidify the resorption lacuna in osteoclastic cells (Väänänen, 2008). CAR2 expression is characteristic for the early stage of osteoclast differentiation, providing protons for bone resorption (Lehenkari et al., 1998).

CTSK

It is a major proteinase in the degradation of bone matrix in the resorption lacuna. Indeed, it is responsible for the degradation of COLL1 in osteoclast-mediated bone resorption (Wilson et al., 2009). CTSK is highly expressed in osteoclasts and is secreted in the resorption lacuna (Väänänen, 2008).

DC-STAMP

It is an essential molecule for osteoclasts since it stimulates fusion and activation of osteoclasts (Takahashi, et al., 2008). DC-STAMP is expressed in osteoclasts but no in machopages (Yagi et al., 2005).

H^+ATPase

This proton pump is expressed in the membrane of bone resorbing osteoclasts and mediates the acidification of the extracellular environment in resorption lacunae (Farina and Gagliardi, 2002).

ITGAV

Integrins mediate cell-cell and cell-matrix interactions. Alpha-V integrins comprise a subset sharing common alpha-V subunit combined with 1 of 5 beta subunits. Osteoclasts express the $\alpha v\beta 3$ integrin, an adhesion receptor involved in bone resorption (McHugh et al., 2000). This integrin plays a key role in osteoclast resorption since it mediates osteoclast attachment and spreading *in vitro* (Nakamura et al., 1999).

ITGB3

ITGB3 is the beta subunit of $\alpha v\beta 3$ integrin. It seems to participate in the formation of the actin ring and normal ruffled border of osteoclasts (McHugh et al., 2000). Inhibition of ITGB3 *in vitro* decreased the ability of osteoclasts to bind and degrade bone (Nakamura et al., 1999; Engleman et al., 1997).

MMP9

MMPs may play a role in osteoclast migration, attachment/detachment and in regulating osteoclast behavior. In particular, MMP9 is a type IV collagenase that is highly expressed in

osteoclasts and plays an important role in degradation of ECM. However, the molecular mechanisms that regulate MMP-9 gene expression are unknown (Sundaram et al., 2007).

TRAP

TRAP is regarded as an important cytochemical marker of osteoclasts (Ballanti et al., 1997). It is localized in the transcytotic vesicles of resorbing osteoclasts and can generate highly destructive reactive oxygen species able to destroy collagen (Väänänen et al., 2000). Furthermore, it has been shown to partially dephosphorylate bone matrix phosphoproteins (Hayman et al., 2000).

Table 3.3. List of markers involved in bone remodelling analyzed in the different studies.

Marker	Paper
OPG ***(Osteoprotegerin)***	I, II, V
RANKL ***(Receptor Activator of Nuclear factor Kappa-β Ligand)***	I, II, V

OPG

OPG acts as a decoy receptor for RANKL and it is mainly produced by cells of the osteoblast lineage although it can also be produced by other cells in the bone marrow. It controls bone resorption by inhibiting the final differentiation and activation of osteoclasts and by inducing their apoptosis (Hadjidakis and Androulakis, 2006). Furthermore, HGFs have been reported to produce osteoclast-stimulating or inhibiting cytokines involved in bone resorption, including OPG, which influence in the pathogenesis of periodontal diseases (Yucel-Lindberg and Båge, 2013).

RANKL

RANKL is mainly expressed by both bone marrow stromal cells and osteoblastic cells. It facilitates osteoclast formation via direct binding to the tumor necrosis factor receptor superfamily member 11 A (RANK) receptor on osteoclasts (Bellido et al., 2014). As in the case of OPG, RANKL is also expressed by HGFs, playing a role in osteoclastic bone destruction in periodontal disease (Yucel-Lindberg and Båge, 2013).

Table 3.4. List of markers involved in inflammatory processes analyzed in the different studies.

Marker	Paper
IL6 ***(Interleukin-6)***	I, II, V, VI
IL8 ***(Interleukin-8)***	IV
IL10 ***(Interleukin-10)***	V
TNFα ***(Tumor necrosis factor alpha)***	VI

IL6

It is a pleiotropic cytokine that stimulates bone resorption by recruiting mature osteoclasts and by activating them through an autocrine mechanism (Fiorito et al., 2003; Tilg et al., 1994). IL6 also stimulates osteoblast differentiation and bone formation (Taguchi et al., 1998) and it is associated with inflammatory periodontal tissues (Bartold and Haynes, 1991).

IL8

It is a proinflammatory cytokine that promotes neutrophil migration (Dunlevy and Couchman, 1995). IL8 is implicated in inflammatory diseases including periodontitis, with elevated IL8 protein and mRNA levels in inflamed gingival tissue and patients with periodontitis (Yucel-Lindberg and Brunius, 2006).

IL10

IL10 is an anti-inflammatory cytokine that plays a major role in suppressing immune and inflammatory responses. It presents a protective role toward tissue destruction, especially in inflamed gingival tissues, in which it enhances autoimmune responses by increasing the number of anti-collagen secreting cells (Morandini et al., 2011).

TNFα

TNFα is secreted by macrophages, lymphocytes and monocytes and is considered one of the main cytokines related to inflammation and immune processes. Furthermore, it is involved in bone resorption by stimulating the differentiation and maturation of osteoclasts (Vitale and Ribeiro, 2007).

Table 3.5. List of markers involved in gingival fibroblast differentiation analyzed in the different studies.

Marker	Paper
ACTA2 ***(smooth muscle actin alpha 2)***	V
COL3A1 ***(type III collagen alpha 1 chain)***	V
EDN1 ***(Endothelin 1)***	V
FN1 ***(Fibronectin 1)***	V
MMP1 ***(Metalloproteinase 1)***	V
TGFβ1 ***(Transforming growth factor B1)***	V
TIMP1 ***(Tissue inhibitor of metalloproteinase 1)***	V

ACTA2

ACTA2 is found predominantly in smooth muscle but is also expressed in other specialized cells such as fibroblasts. It is important for cell motility and contraction processes during the wound healing (Rockey et al., 2013).

COL3A1

COL3A1 is mainly distributed in skin, tendon, aorta and cornea and is required for restoring a normal wound-healing process (Zoppi et al., 2004). Its expression increases during HGFs differentiation (Gómez-Florit et al., 2014) which is associated with scarless wound healing (Satish and Kathju, 2010).

EDN1

It stimulates fibroblast and smooth muscle cell proliferation and stimulates fibroblast collagen metabolism (Dawes et al., 1996). Indeed, EDN1 increases fibroblasts migration and confers on them a more contractile phenotype what might lead to aggressive oral malignances (Hinsley et al., 2012).

FN1

FN1 is an important ECM molecule that promotes cell adhesion and it is strictly related to focal adhesion and fibroblast activation (Guillem-Marti et al., 2013).

MMP1

MMPs constitute a class of proteolytic enzymes responsible for the metabolism of ECM components and are expressed by most fibroblast cell lines (Cury et al., 2007). MMP1 initiates degradation of collagen (Domeij et al., 2002) and activated pro-inflammatory mediators that sustain inflammation in the gingival tissue (Cury et al., 2007).

TGFB1

It is involved in cell proliferation, differentiation and matrix production. TGFB1 is also involved in the wound repair process (Ashcroft et al., 1997) and an increased expression of TGFB1 is related to fibrosis (Hsu et al., 2010).

TIMP1

TIMPs inhibit MMPs activity by binding the active site of proteinases. TIMP1 is produced by many connective tissue cells, which also produce MMPs. Imbalance in the activities of MMPs and TIMPs might be important in many pathologic conditions associated with excess deposition of ECM (Kikuchi et al., 1997).

❖ ***Enzyme-Linked ImmunoSorbent Assay (ELISA)***

ELISA is a sensitive immunoassay that uses an enzyme linked to an antibody to detect a specific antigen. The further detection occurs by means of a secondary antibody that has linked an enzyme which reacts with a colorless substrate to give an end product that can be measured spectrophotometrically. Thus, it is an accurate method to quantify an antigen although it requires a proper selection of reagents and the adjustment of the volume and sample dilution to achieve a successful detection. In this thesis, we determined the levels of secreted $25(OH)D_3$ and $1,25(OH)_2D_3$ metabolites by osteoblastic cells cultured over UV-irradiated 7-DHC implants *(Paper I and II)*, confirming that these cells were able to produce the final vitamin D metabolite from the external

precursor. Furthermore, we determined the protein levels of MMP1 and TIMP1 in HGF *(Paper V)* in order to confirm the mRNA expression results.

❖ ***Alkaline phosphatase (ALP) activity***

ALP is an ectoenzyme attached to the osteoblast cell membrane whose expression is required for initiating bone mineralization (Golub et al., 1992). Determination of ALP activity is based on a colorimetric method that measures the hydrolization of p-Nitrogenyl phosphate (pNPP) through the formation of a yellow end product that is spectrophotometrically measured at 405 nm. ALP activity was measured as an estimation of bone differentiation in both *in vitro (Papers II, III and VI)* and *in vivo (Paper VI)* studies.

❖ ***Cell mineralization***

Inductively coupled atomic plasma emission spectroscopy (ICP-AES)

ICP-AES is a highly sensitive and precise analytical technique for quantifying a wide range of elements present in a solution through the emission of electromagnetic radiation at wavelengths characteristic of each particular element from excited atoms by inductively coupled plasma. Furthermore, ICP-AES has been used to measure elemental composition, such as determination of calcium content, in biological cells (Nomizu et al., 1994). Nevertheless, this method requires taking special care to avoid contamination of samples and materials with calcium from external sources. On this basis, we used ICP-AES to quantify the total calcium content extracted from cell monolayers *(Paper II)*. A standard curve using known calcium concentrations was performed. Thus, calcium content of each sample was calculated extrapolating the intensity of the emission from the standard curve.

Calcein Blue staining

Calcein Blue (also known as umbelliferone) is a fluorescent metal indicator that forms a highly fluorescent complex in the presence of alkaline metals such as Ca. Thus, the fluorescence of these complexes can be visualized with UV-irradiation. It has been used to label mineralized structures and, in comparison to other mineral staining such as alizarin red, calcein staining has several advantages: it is quicker, simpler and a more sensitive and inclusive method (Bauerlein, 2006). Given these properties, calcein blue is considered a useful method to monitor mineralized nodules formation in osteogenic cell cultures (Wang et al., 2006). Therefore, we determined bone-like nodule formation in hUC-MSCs *(Paper III)* by staining cells with calcein blue and further measuring fluorescence signal between 430 and 480 nm.

❖ ***Wound healing assay***

The wound healing assay is a simple and inexpensive method to study cell migration and repair *in vitro* (Rodriguez et al., 2005). It involves creating a “wound” in a cell monolayer and comparing the cellular events related to the wound-healing response. However, it entails some limitations compared to other available methods, such as a relatively longer time to perform and a larger amount of cells

and chemicals (Liang et al., 2007). Notwithstanding the above, the wound healing assay is commonly used due to its facility to set up. Therefore, with the aim of studying cell repair, we evaluated the gene expression of several typical HGF markers after the wound healing assay to evaluate the effect of the modified Ti surfaces on HGF response *(Paper V)*. First, cells were grown until confluence and then a scratch was created in the monolayer using a 10 µL tip. Cell monolayers were washed to remove cell debris and further allowed to close the scratch at standard cell culture conditions. Finally RNA was isolated as described before to study the mRNA levels of several markers.

3.3.3. Animal study

New Zealand White female rabbits were used for *in vivo* testing of the effect of UV-irradiated 7-DHC:VitE Ti implants on osseointegration. According to the 3 R's rule for good animal practice (http://oslovet.norecopa.no/3R), we used a limited number of animals. Thus, six female New Zealand White rabbits were used. Animals were kept in cages during the experimental period. The experiments were approved by the Norwegian Animal Research Authority (NARA) and the local ethical board.

The animal model used in this thesis is a standardized and validated model that was previously established for studying bone attachment to Ti implant surfaces (Rønold and Ellingsen, 2002). Furthermore, this rabbit model has been shown to predict well the effect on humans. The placement of coin-shaped implants in the cortical bone (Figure 3.8) does not represent the clinical condition but limits the number of parameters that may influence the result (Monjo et al., 2008; Monjo et al., 2012). Therefore, PTFE (polytetrafluoroethylene) caps were used to cover the back side of the implants to prevent bone formation around and on the back side of the implant, which would make the pull-out measurements irrelevant.

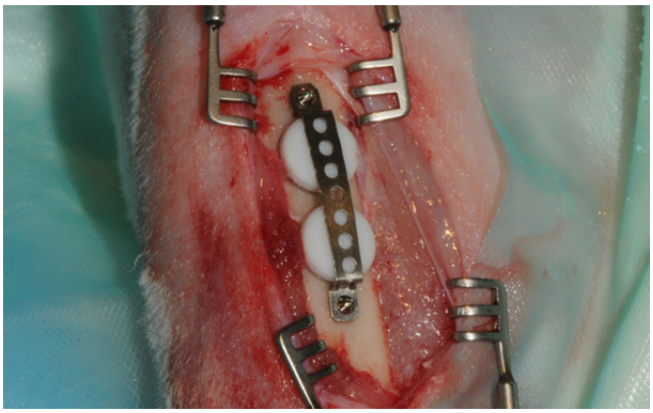

Figure 3.8. Placement of the modified Ti implants in the rabbit bone defect. PTFE caps cover the back side of the implants and Ti bond was used to avoid movements.

Four implants were placed in the tibia of each rabbit, two on the left side and two on the right side, according to the predetermined randomization protocol. The surgical procedure was previously standardized and validated by Rønold et al (Rønold and Ellingsen, 2002). After eight weeks of

healing, animals were sacrificed and the effect of the bioactive modified surfaces was evaluated by assessing the bone-to-implant attachment strength, wound fluid analyses (LDH activity, ALP activity and protein content) and bone tissue analysis (gene expression of bone markers using real time RT-PCR).

❖ **Bone tissue response**

Tensile removal force test

Evaluation of the strength needed to detach the implants from the bone was determined by using a tensile removal test (Figure 3.9). This test is simple, relatively inexpensive and fully standardized. However, its main disadvantage is to ensure the correct alignment of the specimen. In this thesis *(Paper VI)*, the detachment of the implants from the cortical bone was performed using a Lloyds LRX Materials testing machine (Lloyds Instruments Ltd, Segensworth, UK) fitted with a calibrated load-cell of 100 N. Cross-head sped range was set to 1.0 mm/min. Detailed information concerning this removal tensile test has been published elsewhere (Rønold and Ellingsen, 2002).

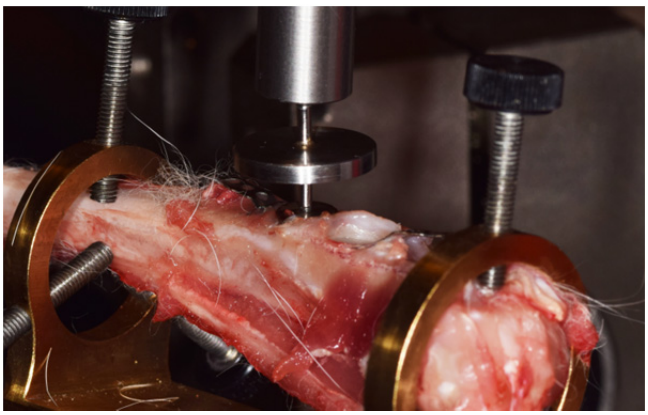

Figure 3.9. Ti implant attached to the cable during the tensile removal test.

Wound fluid analysis

Wound fluid was taken from the wound sites after coin removal for determination of the adverse tissue response upon implantation (LDH activity) and for assessing mineralization at the bone implant interface (ALP activity). Two sterile filter papers of the same size of the coins were applied for one min in each drilled hole to adsorb wound healing and then transferred to microcentrifuge tubes containing 200 µL of phosphate-buffered saline (PBS), and placed immediately on ice until LDH, ALP and protein analyses were performed as previously described in the 3.3.2. section.

Bone tissue analysis

Immediately after removal, implants were taken for further analysis of the peri-implant bone tissue attached to the Ti surfaces. RNA isolation and real-time RT-PCR were performed as previously described (Section 3.3.2).

3.4. Statistical analysis

For the data analysis Excel, GraphPad Prism and SPSS were used. Data were presented as mean values ± S.E.M. (standard deviation of the mean). Kolmogorov-Smirnov test was done to assume parametric or non-parametric distributions for the normality tests. Next, differences between groups were assessed by univariate analysis of variance (UNIANOVA) test followed by post-hoc pairwise comparisons using the minimum significance difference (DMS) test *(Paper III)*. When ANOVA test was not suitable for data *(Papers I, II, IV, V and VI)*, Mann-Whitney-test, Student t-test or paired t-test were run depending on the normal distribution of the data and the population conditions. Results were considered statistically significant at p-values ≤ 0.05.

Dose–response curves for 7-DHC were fitted with nonlinear regression analysis for sigmoid curves (GraphPad Prism), in order to evaluate the dose-response effect between the expression of the vitamin D hydroxylases and the secretion of the corresponding metabolites *(Paper I)*. Also a non-parametric correlation study was performed with Spearman's correlation to find eventual correlation between hydroxylase expression and vitamin D metabolite secretion. Strong correlation was considered when $0.5<|r|<1$. A positive |r| indicated a positive correlation.

In general, the number of replicates in each group was regarded sufficient to record significant difference when comparing the different surfaces *in vitro*. A higher number of samples may have been better for the study *in vivo* but the limitation of the use of animals in research was taken in consideration according to the 3R's rule.

4. Results

Paper I

UV-irradiated 7-Dehydrocholesterol coating on polystyrene surfaces is converted to active vitamin D by osteoblastic MC3T3-E1 cells

Satué M. ; Córdoba A. ; Ramis J.M. ; Monjo M.

Photochemical and Photobiological Sciences (2013), 12(6):1025-35.

Photochemical & Photobiological Sciences

RSC Publishing

PAPER

View Article Online
View Journal | View Issue

Cite this: *Photochem. Photobiol. Sci.*, 2013, **12**, 1025

UV-irradiated 7-dehydrocholesterol coating on polystyrene surfaces is converted to active vitamin D by osteoblastic MC3T3-E1 cells

María Satué, Alba Córdoba, Joana M. Ramis and Marta Monjo*

Received 29th January 2013,
Accepted 13th March 2013

DOI: 10.1039/c3pp50025j

www.rsc.org/pps

The aim of the present study was to determine the effects of UV irradiation on the conversion of 7-dehydrocholesterol (7-DHC), which has been coated onto a polystyrene surface, to cholecalciferol (D_3), and the resulting effect on the formation of vitamin D (1,25-D_3) by MC3T3-E1 cells. The changes in gene expression of the enzymes regulating its hydroxylation, *Cyp27b1* and *Cyp27a1*, were monitored as well as the net effect of the UV-treated 7-DHC coating on cell viability and osteoblast differentiation. MC3T3-E1 cells were found to express the enzymes required for synthesizing active 1,25-D_3, and we found a dose-dependent increase in the production of both 25-D_3 and 1,25-D_3 levels for UV-activated 7-DHC samples unlike UV-untreated ones. Cell viability revealed no cytotoxic effect for any of the treatments, but only for the highest dose of 7-DHC (20 nmol per well) that was UV-irradiated. Furthermore, osteoblast differentiation was increased in cells treated with some of the higher doses of 7-DHC when UV-irradiated, as shown by collagen-I, osterix and osteocalcin relative mRNA levels. The conversion of 7-DHC to preD_3 exogenously by UV irradiation and later to 25-D_3 by MC3T3-E1 cells was determined for the optimum 7-DHC dose (0.2 nmol per well), *i.e.* 8.6 ± 0.7% of UV-activated 7-DHC was converted to preD_3 and 6.7 ± 2.8% of preD_3 was finally converted to 25-D_3 under the conditions studied. In conclusion, we demonstrate that an exogenous coating of 7-DHC, when UV-irradiated, can be used to endogenously produce active vitamin D. We hereby provide the scientific basis for UV-activated 7-DHC coating as a feasible approach for implant therapeutics focused on bone regeneration.

1. Introduction

Among the numerous functions attributed to vitamin D, current evidence suggests that its primary function is to facilitate the processes that are essential for the maintenance of a healthy and mineralized skeleton. This hormone plays a key role in calcium and phosphate homeostasis and a deficiency would lead to resorption of bone, osteoporosis and reduced bone mineralization.[1,2] Thus, this vitamin has been linked to many bone diseases, such as osteoporotic hip fractures.[3] However, vitamin D status not only affects bone tissue, as it has been linked also to muscle decline and myopathy due to the inadequate level of the hormone.[4–6] Vitamin D supplementation has shown to improve bone mineralization in patients with chronic renal failure[7,8] and to enhance muscle strength and ability,[9] which is associated with fewer falls and fractures in elderly women.[10] Other benefits of vitamin D include anticancer[11] and immunomodulatory actions.[12]

It is well established that ultraviolet irradiation is the major source of vitamin D synthesis in the skin. 7-Dehydrocholesterol (7-DHC) is a photolabile cholesterol precursor that is converted to precholecalciferol (previtamin D_3) when exposed to ultraviolet B sunlight. The latter is transformed into cholecalciferol (D_3) and transported to the liver where it is hydroxylated at carbon 25 on the side chain by vitamin D_3 25-hydroxylase (CYP27A1) to form the major circulating intermediary, 25-hydroxyvitamin D_3 (25-D_3). Renal hydroxylation by 25-hydroxyvitamin D_3-1alpha-hydroxylase (CYP27B1) transforms the previous form into the biologically active steroid hormone, 1,25-dihydroxyvitamin D_3 (1,25-D_3) that is released into the circulation.[13–15] Nevertheless, while it is clear that circulating levels of 1,25-D_3 derive from kidney, there is evidence for extra renal synthesis of 1,25-D_3, including the skin,[16–18] liver[19] and a variety of haemopoietic cells and tissues.[20–22]

Local production of 1,25-D_3 in bone cells was first reported by Howard *et al.* in 1981.[23] They found that primary cultures of human bone cells incubated with 25-D_3 synthesized both 1,25-D_3 and 24,25-D_3, with specific activities similar in magnitude to those of the enzymes found in kidney cells.[23] Ichikawa *et al.* confirmed 1,25-D_3 conversion from 25-D_3 in mouse bone cells and reported the expression of the *Cyp27A1* mRNA in

Department of Fundamental Biology and Health Sciences, Research Institute on Health Sciences (IUNICS), University of Balearic Islands, Spain.
E-mail: marta.monjo@uib.es; Fax: +34 971 173184; Tel: +34 971 259960

mouse osteoblasts.[24] Lately, *Cyp27B1* mRNA expression in bone cells has been identified,[25,26] and the role in osteoblast differentiation and mineralization of locally produced 1,25-D_3 has been evidenced.[1,27,28] However, to the best of our knowledge, osteoblast production of active vitamin D (1,25-D_3) in response to exogenous 7-DHC coated on tissue culture plastic, with and without UV irradiation, has never been shown.

Taking into account that the full enzymatic machinery responsible for active vitamin D_3 synthesis is present in bone cells,[1,24] and given the described role of locally produced 1,25-D_3 in osteoblast differentiation and mineralization,[1,27,28] we hypothesized that UV-irradiated 7-DHC could be converted to active vitamin D by osteoblastic cells and could stimulate their differentiation. Hence, in the present study we have provided the scientific basis for the use of a UV-activated 7-DHC surface coating on a biomaterial surface, *e.g.* polystyrene, as a feasible and potential approach to be used in therapeutics focused on bone regeneration around titanium implants, *e.g.* coating bioactive titanium surfaces with the vitamin D precursor 7-DHC that is further UV-irradiated. A biomaterial surface that is previously coated with 7-DHC and UV-irradiated could be used to actively improve osseointegration in patients with reduced bone volume and quality or impaired bone healing. It is well known that current bone implant research is developing new strategies to produce more biocompatible materials and to improve the osseointegration process.

Therefore, we determined the effects of UV-irradiation in the conversion of a 7-DHC coating into previtamin D_3, and the resulting effect of the final 1,25-D_3 synthesis by MC3T3-E1 cells. Changes in gene expression of the key enzymes regulating its hydroxylation, *Cyp27b1* and *Cyp27a1*, were monitored and also the net effect of UV-treated 7-DHC on cell viability and osteoblast differentiation.

2. Experimental

2.1. Treatments with vitamin D metabolites

For the treatment with vitamin D metabolites, stock solutions of 2 mM 7-dehydrocholesterol (7-DHC, Sigma, St. Louis, MO, USA), 2 μM cholecalciferol (D_3, Sigma, St. Louis, MO, USA), and 2 μM 25-hydroxyvitamin D (25-D_3, Sigma, St. Louis, MO, USA) were prepared in absolute ethanol and filtered with a 0.22 mm pore size filter before use. Fourteen different groups were prepared; 8 were non-irradiated: 7-DHC at different doses (20 nmol, 2 nmol, 0.2 nmol, 2×10^{-2} nmol, and 2×10^{-3} nmol per well), 2×10^{-2} nmol D_3 per well, 2×10^{-2} nmol 25-D_3 per well and ethanol; and 6 were UV-irradiated: 7-DHC at the same different doses (20 nmol, 2 nmol, 0.2 nmol, 2×10^{-2} nmol and 2×10^{-3} nmol per well) and ethanol.

To treat polystyrene tissue culture plastic (TCP) wells, 10 μl of each dilution treatment were left on the TCP surfaces (30.68 mm^2 of surface area per well) and were allowed to air-dry for 15 min in the sterile flow bench. For UV-irradiation, a UV lamp of 302 nm was used at an intensity of irradiation of 6 mW cm^{-2} (UVP, Upland, CA, USA) during 30 minutes. Treated surfaces were immediately used for cell culture experiments.

2.2. Cell cultures

The mouse osteoblastic cell line MC3T3-E1 (DSMZ, Braunschweig, Germany) was selected as an *in vitro* model. Cells were routinely cultured at 37 °C in a humidified atmosphere of 5% CO_2, and maintained in α-MEM (PAA Laboratories GmbH, Pasching, Austria) supplemented with 10% fetal calf serum (FCS, PAA Laboratories GmbH, Pasching, Austria) and antibiotics (50 IU penicillin ml^{-1} and 50 μg streptomycin ml^{-1}, Sigma, St. Louis, MO, USA). Cells were subcultured 1 : 4 before reaching confluence using PBS and trypsin/EDTA. All experiments were performed after 8 passages of the MC3T3-E1 cells.

To test the effect of the different treatments onto the plastic wells, 96-well plates were used. Cells grown on untreated TCP were added as a control for all the experiments. Cells were seeded at a density of 30 000 cells cm^{-2} and were maintained in α-MEM supplemented with 10% FCS and antibiotics. Culture media were collected after 48 h, to test cytotoxicity and the production of the hydroxylated forms of vitamin D. Cells were harvested after 2 days of culture using Trizol reagent (Roche Diagnostics, Mannheim, Germany) to analyse early gene expression response of several osteoblast differentiation markers and enzymes involved in vitamin D synthesis using real-time RT-PCR.

MC3T3-E1 cells were also seeded on TCP without treatment and cultured up to 28 days to characterize the temporal gene expression profile of the enzymes involved in vitamin D synthesis. RT-PCR analyses were done after 1, 7, 14, 21 and 28 days of cell differentiation.

2.3. Determination of cell viability: LDH activity

Lactate dehydrogenase (LDH) activity in the culture media was used as an index of cell death. LDH activity was determined spectrophotometrically after 30 min incubation at 25 °C of 50 μl of culture and 50 μl of the reaction mixture by measuring the oxidation of NADH at 490 nm in the presence of pyruvate following the manufacturer's protocol (Cytotoxicity Detection Kit (LDH), Roche Diagnostics, Mannheim, Germany). Toxicity was presented relative to the LDH activity in the media of cells seeded on TCP without treatment (low control, 0% cell death) and on cells grown on TCP treated with 1% Triton X-100 (high control, 100% death), using the following equation:

$$\text{Cytotoxicity } (\%) = (\text{exp. value} - \text{low control})/(\text{high control} - \text{low control}) \times 100$$

2.4. Quantitative determination of 25(OH)D and 1,25$(OH)_2$D released to the culture media

25-D_3 and 1,25-D_3 released to the culture media after 2 days of treatment were analysed by enzyme-linked immunosorbent assay (ELISA). Aliquots from the culture media were centrifuged at 1800 rpm for 5 minutes at 4 °C and supernatants were used for 25-D_3 and 1,25-D_3 determination following the instructions described by the manufacturer (Immunodiagnostic Systems Ltd, Boldon, Tyne and Wear, UK).

Table 1 Primer sequences used for real time RT-PCR. The primer sequences for target and reference genes, product size and accession number are shown

Name	5′-Sequence-3′	Product size	Accession number
Alp	S: AAC CCA GAC ACA AGC ATT CC AS: GAG AGC GAA GGG TCA GTC AG	151 bp	X13409
Bmp-2	S: GCT CCA CAA ACG AGA AAA GC AS: AGC AAG GGG AAA AGG ACA CT	178 bp	NM_007553.2
Coll-I	S: AGA GCA TGA CCG ATG GAT TC AS: CCT TCT TGA GGT TGC CAG TC	177 bp	NM_007742.3
Cyp24a1	S: CTA TCG GGA CCA TCG CAA CGA AGC S: GCC CCA TAA AAT CAG CCA AGA CCT CA	158 bp	NM_009996.3
Cyp27a1	S: CGT CCT CTG CTG CCC TTT TGG AAG AS: GTG TGT TGG ATG TCG TGT CCA CCC	247 bp	NM_024264.4
Cyp27b1	S: TCC TGT GCC CAC CCC CAT GG AS: AGG GAG ACT AGC GTA TCT TGG GGA	167 bp	NM_010009.2
Il-6	S: ACT TCC ATC CAG TTG CCT TC AS: TTT CCA CGA TTT CCC AGA GA	171 bp	NM_031168.1
Oc	S: CCG GGA GCA GTG TGA GCT TA AS: TAG ATG CGT TTG TAG GCG GTC	81 bp	NM_007541
Opg	S: AGA CCA TGA GGT TCC TGC AC AS: AAA CAG CCC AGT GAC CAT TC	131 bp	NM_008764.3
Osx	S: ACT GGC TAG GTG GTG GTC AG AS: GGT AGG GAG CTG GGT TAA GG	135 bp	NM_007419
Rankl	S: GGC CAC AGC GCT TCT CAG AS: TGA CTT TAT GGG AAC CCG AT	141 bp	NM_011613
Gapdh	ACC CAG AAG ACT GTG GAT GG CAC ATT GGG GGT AGG AAC AC	171 bp	XM_132897
18S rRNA	S: GTA ACC CGT TGA ACC CCA TT AS: CCA TCC AAT CGG TAG TAG CG	151 bp	X00686

2.5. RNA isolation

RNA was isolated from cells using a monophasic solution of phenol and guanidine thiocyanate (Trizol, Roche Diagnostics, Mannheim, Germany) according to the manufacturer's protocol. RNA was quantified at 260 nm using a Nanodrop spectrophotometer (NanoDrop Technologies, Wilmington, DE, USA).

2.6. Real-time RT-PCR analysis

Total RNA previously isolated was reverse-transcribed to cDNA using a High Capacity RNA to cDNA kit (Applied Biosystems, Foster City, CA) according to the protocol of the supplier. The same amount of total RNA from each sample was converted into cDNA. Each cDNA was diluted 1/4 and aliquots were stored at −20 °C until PCR reactions were carried out.

Real-time RT-PCR was performed for two reference genes: 18S ribosomal RNA (*18S rRNA*) and glyceraldehyde-3-phosphate dehydrogenase (*Gapdh*), and 11 target genes: alkaline phosphatase (*Alp*), interleukin 6 (*Il-6*), collagen-type 1 (*Coll-1*), osteocalcin (*Oc*), bone morphogenetic protein 2 (*Bmp-2*), osterix (*Osx*), receptor activator of nuclear factor kappa-B ligand (*Rankl*), osteoprogesterin (*Opg*) and the genes involved in vitamin D synthesis such as vitamin D_3 25-hydroxylase (*Cyp27a1*), 25 hydroxyvitamin D_3-1-alpha hydroxylase (*Cyp27b1*) and 1,25-dihydroxyvitamin D_3 24-hydroxylase (*Cyp24a1*).

Real-time PCRs were performed in the Lightcycler 480® (Roche Diagnostics, Germany). Each reaction contained 5 µl of LightCycler-FastStart DNA Master^{PLUS} SYBR Green I (Roche Diagnostics, Mannheim, Germany), 0.5 µM of the sense and antisense specific primers (Table 1) and 3 µl of the diluted cDNA in a final volume of 10 µl. The normal amplification program consisted of a preincubation step for denaturation of the template cDNA (10 min, 95 °C), followed by 45 cycles consisting of a denaturation step (10 s 95 °C), an annealing step (10 s 60 °C, except for *Alp* that was 10 s at 65 °C, *Osx* with 10 s at 68 °C and *Cyp24a1* at 58 °C 10 s) and an extension step (10 s 72 °C). After each cycle, fluorescence was measured at 72 °C. Every run included a negative control without cDNA template. To confirm amplification specificity, PCR products were subjected to a melting curve analysis on the LightCycler and subsequently 2% agarose/TAE gel electrophoresis, T_m and amplicon size, respectively.

To allow relative quantification after PCR, real-time efficiencies were calculated from the given slopes in LightCycler 480 software (Roche Diagnostics, Mannheim, Germany) using serial dilutions. Relative quantification after PCR was calculated by normalizing the target gene concentration in each sample by the concentration mean of the two reference genes in a given sample using the "advanced relative quantification method" provided by LightCycler 480 analysis software.

2.7. Determination of the conversion of 7-DHC to preD$_3$ by HPLC

The amounts of 7-DHC and preD$_3$ present in the 0.2 nmol group plastic surfaces after 30 min of UV irradiation were quantified by HPLC. Results were compared with non-irradiated 7-DHC coated surfaces. Pure ethanol was used as the control. All solvents used were HPLC or analytical grade. Methanol (HPLC gradient grade), acetonitrile and tetrahydrofurane (both HPLC grade) were purchased from Fisher Scientific (Thermo Fisher Scientific, MA, USA). High purity deionized Milli-Q water was obtained from a Millipore system (Millipore Corporation, Billerica, MA, USA). Absolute ethanol was purchased from Scharlab (Barcelona, Spain). Individual stock

standard solutions of 7-DHC (250 μg ml^{-1}) and D_3 (10 mg ml^{-1}) were prepared in methanol and stored at −20 °C. Standard solutions of lower concentrations were obtained by dilution of stock solutions in methanol.

The coating of each surface was extracted by adding 100 μl of 'methanol–acetonitrile–tetrahydrofurane–water' (67 : 16 : 2 : 15, v : v) to each well and by shaking the plate for 2 min at 20 rpm. The content of three replicate wells was mixed to give a sample of ≈300 μl. An aliquot of 100 μl of the sample was injected into the HPLC system. Two replicate samples were prepared and analysed for each group.

The analysis was carried out using a Waters liquid chromatographic system (Milford, MA, USA), equipped with a refrigerated automatic injector WISP700 and a 600 pump system, connected to a Waters 996 photodiode array (PDA) detector. The software Empower was used for instrument control and data analysis. Detection was carried out at 282 nm.

A Nova Pak C18 column (Waters) was used to separate sample components before detection. The column temperature was set to 30 °C. Two solvents, A: 'methanol–acetonitrile–tetrahydrofurane–water' (67 : 16 : 2 : 15, v : v) and B: 'methanol–acetonitrile–tetrahydrofurane' (75 : 20 : 5, v : v), were used in the gradient elution mode as the mobile phase. Solvents A and B were vacuum-filtered through a nylon membrane (0.45 μm pore diameter) and degassed before use. The mobile phase flow rate was 1 ml min^{-1}. The binary gradient used was as follows: from 5% B to 90% B in 3 minutes, held for 9.5 min at 90% B, from 90% B to 5% B in 1 minute and equilibrated between injections at the initial conditions for 5 min (total run time = 15 min + 5 min equilibration between injections).

Quantification was performed by integration of the peak area of the corresponding analyte and interpolation of the peak area in 7-DHC or D_3 standard curves.

2.8. Statistics

All data are presented as mean values ± standard error of the mean (SEM). Dose–response curves for 7-DHC were fitted with nonlinear regression analysis for sigmoid curves, using GraphPad Prism version 5.00 for Windows (GraphPad Software, San Diego, California, USA). The Kolmogorov–Smirnov test was done to assume parametric or non-parametric distributions for the normality and correlation tests. Differences between groups were assessed by the Mann–Whitney-test or by the Student's *t*-test depending on their normal distribution. The Spearman's correlation coefficient was calculated to assess the correlation between hydroxylase expression and vitamin D metabolite secretion. The SPSS® program for Windows, version 17.0 (SPSS, Chicago, IL, USA), was used. The results were considered statistically significant at *p*-values ≤0.05.

3. Results

3.1. Effect of treatments on osteoblast viability

LDH activity was measured in the culture media after 48 h of culture as an index of toxicity (Fig. 1). All the non-UV-irradiated groups showed improved cell viability compared to the low control (cells seeded on the TCP surface without any treatment). Although significant differences were found when comparing the UV-irradiated 7-DHC groups *versus* their corresponding non-UV-irradiated 7-DHC groups or compared to the ethanol UV-irradiated group, only the higher dose of 7-DHC when UV exposed displayed a toxic effect (as compared to the low control).

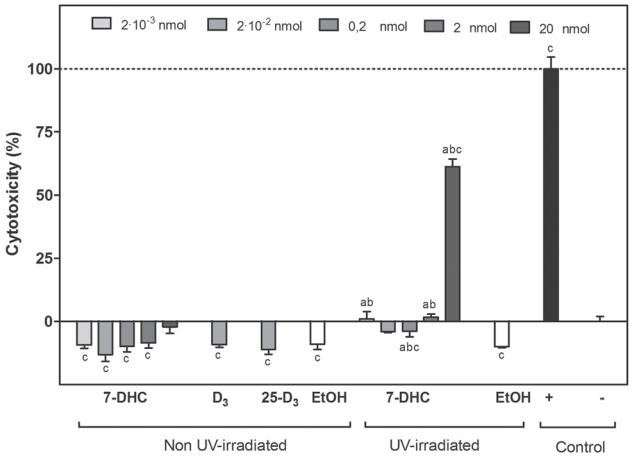

Fig. 1 LDH activity measured in culture media of MC3T3-E1 cells collected after 48 h of seeding. Positive control (+; 100% toxicity) was cell culture media from cells incubated with Triton X-100 at 1%. Negative control (–; 0% toxicity) was cell culture media from control cells. Values represent the mean ± SEM N = 6). Student's *t*-test ($p < 0.05$): [a]7-DHC UV-irradiated *vs.* the corresponding 7-DHC non-UV-irradiated; [b]treatment *vs.* the corresponding EtOH control and [c]treatment *vs.* the negative control.

3.2. Temporal gene expression of *Cyp27a1*, *Cyp27b1* and *Cyp24a1* in osteoblastic cells

In order to investigate the capability of osteoblasts to endogenously synthesize the active form of vitamin D, we first characterized temporal mRNA expression levels of different genes involved in vitamin D hydroxylation (*Cyp27a1* and *Cyp27b1*) and the gene involved in its degradation (*Cyp24a1*) at different timepoints (1, 7, 14, 21 and 28 days) by real-time RT-PCR (Fig. 2). We could confirm that the mouse osteoblastic cell line MC3T3-E1 expresses both activation genes. We found a differential expression profile between the enzymes. Thus, while *Cyp27a1* expression was upregulated over time, *Cyp27b1* gene kept a steady expression during osteoblast differentiation. As regards the enzyme responsible for 1,25-dihydroxyvitamin D_3 degradation, *Cyp24a1*, no constitutive gene expression could be detected in MC3T3-E1 cells at the different time points analysed.

3.3. Effect of treatments on gene expression of enzymes involved in vitamin D synthesis

Once we confirmed the constitutive expression of *Cyp27a1* and of *Cyp27b1* in MC3T3-E1 cells, we analysed the effect of treatments on its expression levels (Fig. 3A and B). A trend to high expression levels of *Cyp27a1* was found for the lower dose of 7-DHC treatment in both cases, when UV-irradiated and non-

UV-irradiated, although statistical significance was not reached. For the rest of 7-DHC UV-irradiated groups analysed a dose–response increase in *Cyp27a1* mRNA levels was found, showing significant differences compared to the non-UV-irradiated corresponding doses. It should also be noted that the EtOH UV-irradiated group also showed an increase in *Cyp27a1* mRNA levels. As regards *Cyp27b1*, an increase in mRNA levels was found for the higher concentrated 7-DHC samples which had been UV-irradiated, although significance was not reached.

Cyp24a1 was not constitutively expressed, but we investigated if its expression could be induced by any of the treatments. In fact, we found that *Cyp24a1* mRNA levels were only detected in cells treated with 25-D_3 (data not shown).

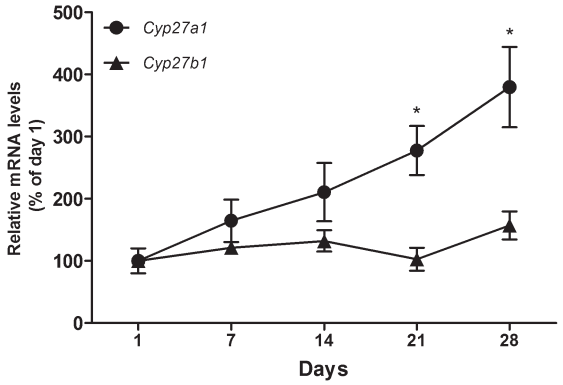

Fig. 2 Temporal gene expression profile of the enzymes responsible for vitamin D hydroxylation (*Cyp27a1*, *Cyp27b1*) in differentiating MC3T3-E1 cells. Data represent fold changes of target genes normalized to reference genes (*Gapdh*, *18S rRNA*), expressed relative to the first day that was set at 100%. Values represent the mean ± SEM ($N = 3$). Student's *t*-test ($p < 0.05$): **Cyp27a1* mRNA expression compared to the first day of cell culture.

3.4. Effect of treatment on the release of 25-D_3 and 1,25-D_3 into the cell culture media

To confirm the production of 25-D_3 and 1,25-D_3 by MC3T3-E1 cells, we quantified these metabolites in the cell culture media by ELISA after 48 h of treatment (Fig. 3C and D). In agreement with our hypothesis, when 7-DHC was activated by UV irradiation a dose–response was found for both, the production of 25-D_3 and of the final active vitamin D (1,25-D_3), while no dose–response was detected when 7-DHC was non-UV-irradiated. Therefore, UV-irradiation is required to yield

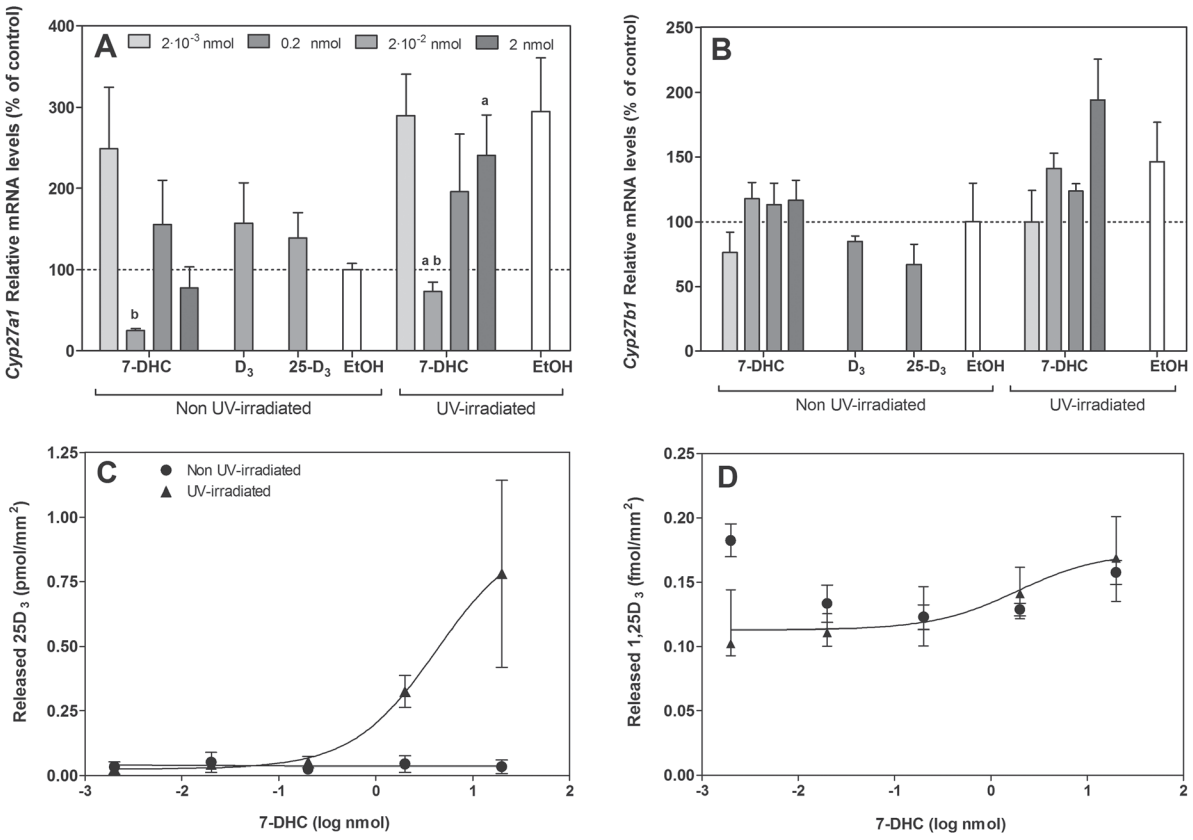

Fig. 3 Effect of the different treatments on the vitamin D hydroxylases gene expression and released intermediaries detection after 2 days of cell culture. (A) *Cyp27a1* and (B) *Cyp27b1* mRNA levels expressed as a percentage of the EtOH non-UV-irradiated group, which was set to 100%. Data represent fold changes of target genes normalized to reference genes (*Gapdh*, *18S rRNA*). Values represent the mean ± SEM ($N = 6$). Student's *t*-test ($p < 0.05$): [a]7-DHC UV-irradiated *vs*. the corresponding 7-DHC non-UV-irradiated and [b]treatment *vs*. the corresponding EtOH control. (C) Released 25-D_3 and (D) 1,25-D_3 intermediaries in response to different concentrations of 7-DHC (20, 2, 0.2, 2×10^{-2} and 2×10^{-3} nmol per well) UV-irradiated and non-UV-irradiated. Secretion data are related to TCP well surface area. Values represent the mean ± SEM ($N = 6$). Dose–response curves were fitted with nonlinear regression analysis. Only UV-irradiated 7-DHC revealed a dose–response curve of released 25-D_3 and 1,25-D_3.

active vitamin D production from 7-DHC. The D_3 and 25-D_3 groups were added to the experiment as controls. As expected, high concentrations of 25-D_3 were found for the 25-D_3 treated group, 2.37 ± 0.12 pmol mm^{-2} related to the TCP surface area were released to the culture media and 0.24 ± 0.02 fmol mm^{-2} of 1,25-D_3 were detected in the culture media. Cells treated with 2×10^{-2} nmol of D_3 showed 0.04 ± 0.02 pmol mm^{-2} and 0.10 ± 0.01 fmol mm^{-2} of 25-D_3 and of 1,25-D_3, respectively.

3.5. Effect of treatment on gene expression of several osteoblast markers

Several reports have demonstrated that vitamin D regulates osteoblast differentiation and mineralization. For this reason, real-time RT-PCR was performed to observe the effect of vitamin D treatments on several bone markers (Fig. 4 and 5). *Coll-1* showed increased mRNA levels in cells treated with 0.2 nmol 7-DHC UV-irradiated compared to the same treatment non-UV-irradiated (Fig. 4A). Higher expression levels of *Osx* were seen in all 7-DHC UV-irradiated groups compared to the non-irradiated ones, showing statistical significance in the 0.2 and 2 nmol groups (Fig. 4B). Higher *Alp* mRNA levels were found in cells treated with 2×10^{-3} nmol 7-DHC UV-irradiated compared to the same treatment non-UV-irradiated (Fig. 4C). As regards *Oc* mRNA levels (Fig. 4D), statistical differences were reached only for the 2 nmol 7-DHC UV-irradiated group compared to the same treatment non-UV-irradiated.

Bmp-2 mRNA levels (Fig. 5A) showed no important changes for the different groups of treatments. However, significantly lower levels were found for the 2×10^{-2} nmol 7-DHC UV-irradiated group compared to the non-irradiated one. No significant differences were found when comparing *Il-6* mRNA levels between the different 7-DHC doses when UV-irradiated and non-UV-irradiated, although the highest doses of UV-irradiated 7-DHC samples showed a trend to higher *Il-6* mRNA levels. Treatment with 2×10^{-2} nmol 25-D_3 induced significantly higher expression levels of this interleukin compared to the control (Fig. 5B). *Rankl* mRNA levels were lower in some of the 7-DHC non-UV-irradiated samples compared to their control (Fig. 5C). *Opg* mRNA levels showed no significant differences among the tested groups (Fig. 5D).

3.6. Quantification of the conversion of UV-irradiated 7-DHC to preD_3

HPLC analyses after 30 minutes of UV irradiation were performed on the dose of 0.2 nmol of 7-DHC added to the TCP

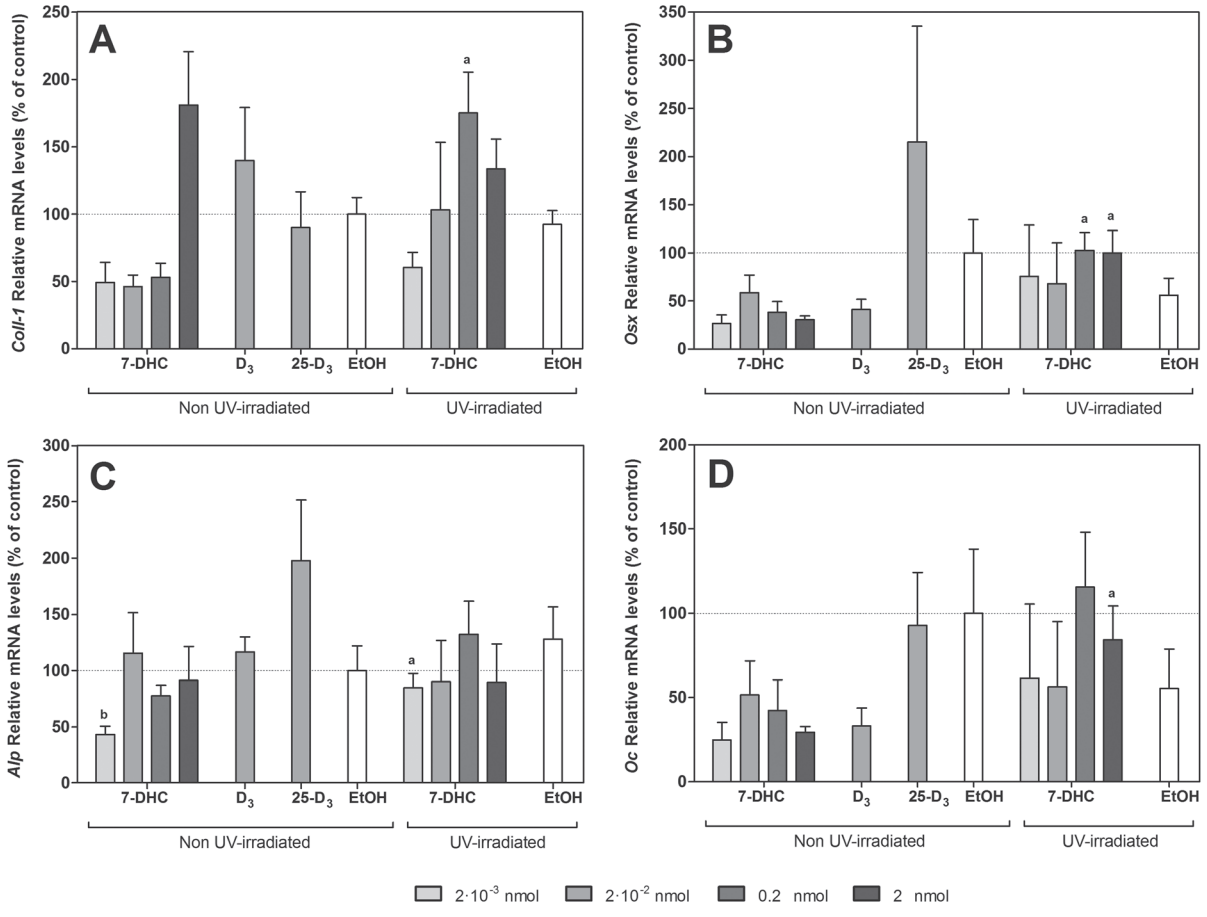

Fig. 4 Effect of the different treatments on gene expression levels of bone markers (*Coll-1*, *Osx*, *Alp* and *Oc*) in MC3T3-E1 cells cultured for 2 days. Data represent fold changes of target genes normalized to reference genes (*Gapdh* and *18S rRNA*), expressed as a percentage of the EtOH non-UV-irradiated group, which was set to 100%. Values represent the mean ± SEM ($N = 4$). Student's *t*-test ($p < 0.05$): [a]7-DHC UV-irradiated *vs*. the corresponding 7-DHC non-UV-irradiated and [b]treatment *vs*. the corresponding EtOH control.

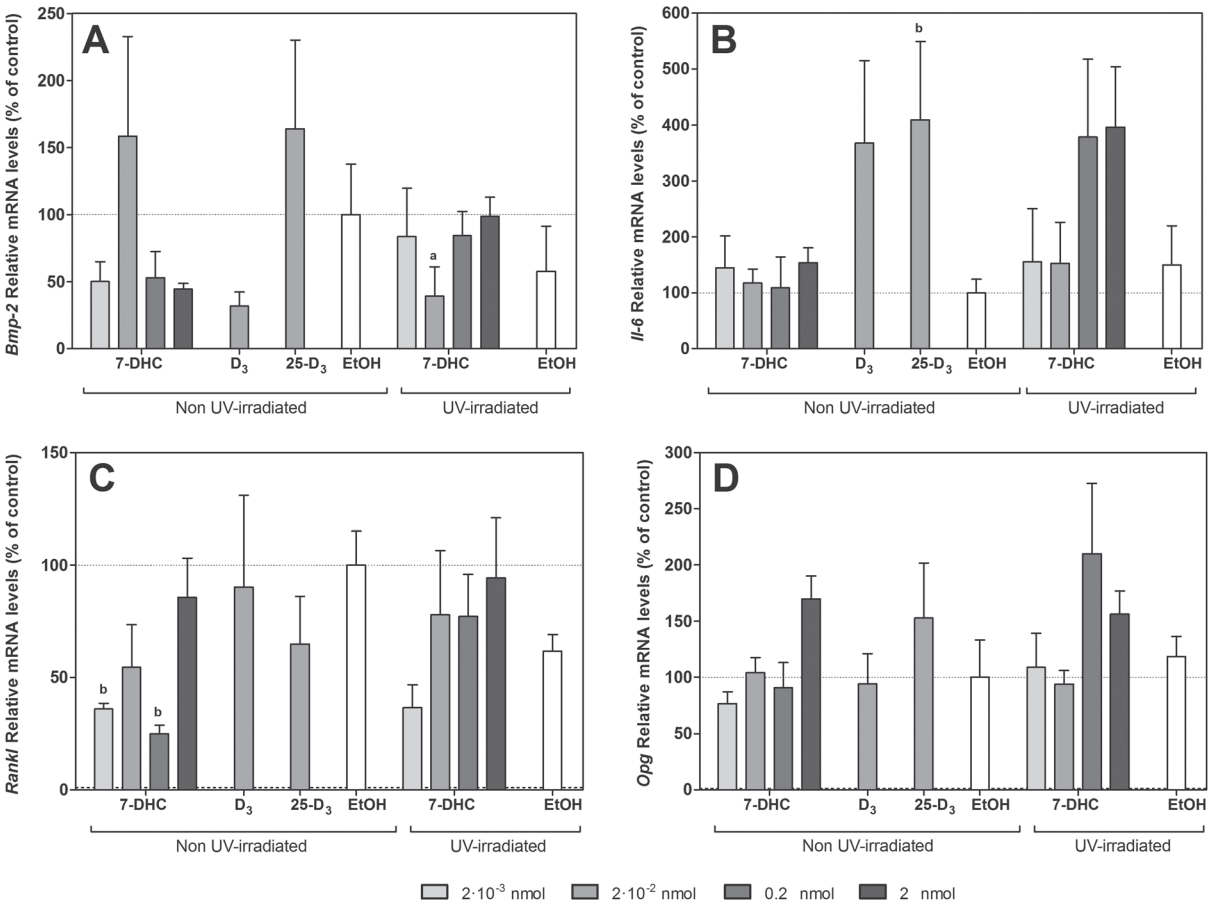

Fig. 5 Effect of the different treatments on gene expression levels of bone markers (*Bmp-2*, *Il-6*, *Rankl* and *Opg*) in MC3T3-E1 cells cultured for 2 days. Data were normalized to reference genes (*Gapdh* and *18S rRNA*). Values represent the mean ± SEM ($N = 4$). Student's *t*-test ($p < 0.05$): [a]7-DHC UV-irradiated *vs*. the corresponding 7-DHC non-UV-irradiated and [b]treatment *vs*. the corresponding EtOH control.

surface, as this amount was the one that presented lower toxicity and higher mRNA expression levels of different osteoblast related genes. Therefore, the conversion of 7-DHC to preD$_3$ on coated TCP plastic surfaces was quantified. In non-irradiated samples, only 7-DHC was detected, eluting at 13.2 min. The formation of preD$_3$ and other by-products such as lumisterol and tachysterol was observed for the UV-irradiated group, preD$_3$ eluted at 11.5 min, lumisterol eluted at 11.8 min and a small peak around 12.2 probably corresponded to the presence of tachysterol in the mixture. Quantification of peak areas showed that 0.77 ± 0.02 pmol mm^{-2} of preD$_3$ in relation to the TCP well surface area were produced when irradiating TCP surfaces coated with 9.01 ± 0.29 pmol mm^{-2} of 7-DHC, giving a 8.6 ± 0.7% conversion of 7-DHC to preD$_3$ after 30 min of UV exposure.

4. Discussion

There is growing evidence that osteoblasts are both sources and targets of 1,25-D$_3$ action,[1,24,27,29] and thus vitamin D may have multiple autocrine/paracrine actions in bone. In this way, it has been shown that vitamin D$_3$ treatment of osteoblasts inhibits cell proliferation and stimulates osteoblast differentiation, therefore promoting bone mineralization.[1,27–30] Here, we hypothesized that exogenously UV-irradiated 7-DHC could be converted into active vitamin D by osteoblasts and stimulate their differentiation.

Human skin cells exposed to ultraviolet B (UVB) radiation (spectral range 290–315 nm) convert 7-DHC into previtamin D$_3$ *in vivo*[31] and *in vitro*.[32] A UVB wavelength-dependent synthesis of vitamin D$_3$ was found in these cells, showing a maximum 1,25-D$_3$ ratio formation at 302 nm and no vitamin D$_3$ production when UV wavelengths >315 nm were used.[33,34] Here we report, for the first time, a similar process in osteoblastic cells with 7-DHC on plastic culture surfaces.

Our first goal was to check whether exogenously UV-irradiated 7-DHC had any cytotoxic effect. We found that although cells treated with UV-irradiated 7-DHC showed a decrease on cell viability compared to those non-UV-irradiated, only the highest 7-DHC dose used that was UV-irradiated was toxic to the cells. Probably, UV irradiation induced the generation of 7-DHC oxidation products that could affect negatively cell survival.[35] In fact, and in agreement with the LDH activity results, low levels of total RNA were obtained for this group and a proper normalization of the data could not be achieved with

the use of reference genes. Therefore the 20 nmol dose was excluded for gene expression analysis.

Our next goal was to investigate the regulation of the expression of the enzymes responsible for vitamin D_3 hydroxylation by the different treatments. Beforehand, we analysed their expression pattern during osteoblast differentiation from 1 to 28 days. We show for the first time that *Cyp27a1* expression is up-regulated over time, while *Cyp27b1* keeps a steady expression during osteoblast differentiation. In contrast, a previous report showed an activation of *Cyp27b1* expression over time in primary osteoblasts from femoral and tibial bone marrow.[30] These inconsistencies might be explained by the different cell model (cell line *versus* primary cells), and the different media compositions used in the different studies.

Our data showed a dose-dependent increase in *Cyp27a1* mRNA levels in response to UV-irradiated 7-DHC, suggesting a substrate induction of its expression. Moreover, this result agrees with the 25-D3 secreted levels measured for the UV-activated 7-DHC group, which revealed a 7-DHC dose–response curve. In fact, a significant Spearman's positive correlation (r = 0.703, p = 0.007) was observed between the *Cyp27a1* gene expression and the secretion of its product 25-D3. Interestingly, we have also found a trend to higher expression levels of *Cyp27a1* in cells cultured with the lower dose of 7-DHC and in the UV-irradiated EtOH group. This finding could be explained by the effect of new compounds formed on the TCP surface due to UV-treatment. In fact, it has been shown that washing with ethanol may leave C residues on the surfaces due to the formation of hydrogen bonds between the surface and the organic compound.[36,37]

High 25-D_3 doses have been shown to reduce *Cyp27b1* mRNA expression levels, suggesting the presence of a negative feedback in response to a new 1,25-D_3 product.[1] Actually, it has been found that there is an exponential relationship between 25-D_3 input and 1,25-D_3 output levels,[1] which likely reflects the fast degradation of 1,25-D_3 by *Cyp24a1* enzyme and the negative feedback previously described.[17,38] Our results revealed the highest 1,25-D_3 production for 25-D_3 treatment, but this performance does not appear in *Cyp27b1* mRNA levels for this treatment, suggesting that the product may induce a negative feedback. However, *Cyp27b1* mRNA expression in 25-D_3 treated samples was not statistically different. Possibly, with an earlier time point the induction of gene expression of these enzymes would have been clearer, as the production already showed differences after 48 h. As regards *Cyp24a1*, we could only detect its mRNA levels in 25-D_3 treated samples, which showed a higher 1,25-D_3 production. This finding is in accordance with previous studies revealing that 1,25-D_3 treatment upregulates *Cyp24a1* levels through a feedback system.[39]

Once we had established the effect of the different treatments on mRNA expression levels of the enzymes responsible for vitamin D_3 hydroxylation, we analysed the levels of 25-D_3 and 1,25-D_3 released to cell culture media after 48 h of treatment. Our data reveal a dose-dependent increase in both, the production of 25-D_3 and of 1,25-D_3 levels for UV-activated 7-DHC samples unlike UV-untreated ones. A previous study has demonstrated the generation of 25-D_3 and of 1,25-D_3 in a human skin equivalent model (fibroblasts co-cultured with keratinocytes in a collagen matrix) enriched with 7-DHC and irradiated with UVB.[33] In this study, the need for UV-irradiation was also demonstrated. In the present work, HPLC results showed a 8.6 ± 0.7% conversion of 7-DHC to preD_3 after 30 min of UV exposure, for the 0.2 nmol dose, which allowed us to calculate a conversion of preD_3 to 25-D_3 by the osteoblastic cells of 6.7 ± 2.8%.

Active vitamin D acts directly on osteoblasts and regulates osteoblast differentiation (reviewed in ref. 27). Therefore, we analysed the effect of the different treatments on the expression of different osteoblast related genes: *Coll-1*, an early marker which supports the cell proliferation stage,[40] *Osx*, a transcriptional factor involved in osteoblast differentiation,[41] and *Oc*, the most abundant non-collagenous protein in bone.[40] These genes showed increased mRNA levels in cells treated with some of the higher doses of UV-irradiated 7-DHC, pointing to an enhanced osteoblast differentiation in accordance with the effects observed by active vitamin D treatment previously reported.[42–45] Nonetheless, longer cell culture experiments could have shown higher differences among the groups.

Different effects have been found on the expression of *Il-6* by 1,25-D_3 treatment in osteoblasts. *Il-6* is a cytokine produced by cells of the osteoblast and osteoclast lineages that not only has a role in inflammation but also increases bone resorption and possibly bone remodeling.[46] In our study, 25-D_3 treatment induced higher mRNA expression levels of this interleukin compared to the control. In other studies, *Il-6* protein expression has been found to be down-regulated,[47] unchanged[48] and up-regulated[49] when murine osteoblasts were exposed to vitamin D treatments. Since this cytokine undergoes both transcriptional and translational regulation, Il-6 mRNA expression could be different from its secreted protein levels.

1,25-D_3 has been shown to induce osteoclast formation *via* up-regulation of RANKL and increasing the RANKL/OPG ratio in a number of reports,[50–55] although a decrease of the *Rankl*/*Opg* mRNA ratio[56] has also been shown, probably due to the fact that the studies were carried out at different moments of osteoblastic maturation with changes in the VDR expression.[56] Our results showed no remarkable effects as regards the *Rankl*/*Opg* relative expression.

In conclusion, our findings provide the feasibility of using UV irradiation to exogenously activate the vitamin D precursor 7-DHC for the endogenous synthesis of 1,25-D_3 by osteoblastic cells, as a proof-of-concept. In fact, the results found on osteoblast gene expression confirmed that treatment of MC3T3-E1 with UV-activated 7-DHC exerts a similar effect on osteoblast differentiation as 1,25-D_3 treatment. Furthermore, we have demonstrated that the enzymatic machinery for this pathway is present and is biologically active in bone cells. The authors do not envision that 7-DHC treatment and UV irradiation have to be performed directly in the patient, but as a pretreatment of biomaterial surfaces during implant production and always prior to their use *in vivo*, with the aim of improving

osseointegration in patients with reduced bone volume and quality or impaired bone healing. Further research is ongoing to study this clinical application.

Abbreviations

7-DHC	7-Dehydrocholesterol
D_3	Cholecalciferol
25-D_3	25-Hydroxyvitamin D_3
1,25-D_3	1,25-Dihydroxyvitamin D_3
Cyp27a1	Vitamin D_3 25-hydroxylase
Cyp27b1	25-Hydroxyvitamin D_3-1alpha-hydroxylase

Acknowledgements

This work was supported by the Ministerio de Ciencia e Innovación del Gobierno de España (Torres Quevedo contract to JMR, and Ramón y Cajal contract to MM) and Eureka-Eurostars Project Application E!5069 NewBone, Interempresas International Program (CIIP20101024) from the Centre for the Development of Industrial Technology (CDTI) and Technology Funds from Invest in Spain (C2_10_32).

References

1 G. J. Atkins, P. H. Anderson, D. M. Findlay, K. J. Welldon, C. Vincent, A. C. Zannettino, P. D. O'Loughlin and H. A. Morris, Metabolism of vitamin D3 in human osteoblasts: evidence for autocrine and paracrine activities of 1 alpha,25-dihydroxyvitamin D3, *Bone*, 2007, **40**, 1517–1528.
2 R. St-Arnaud, The direct role of vitamin D on bone homeostasis, *Arch. Biochem. Biophys.*, 2008, **473**, 225–230.
3 B. E. C. Nordin and H. A. Morris, Osteoporosis and vitamin D, *J. Cell. Biochem.*, 1992, **49**, 19–25.
4 D. Ayyar, F. Floyd, D. Barwick, P. Hudgson and D. Weightman, Myopathy in chronic renal failure, *Q. J. Med.*, 1974, **XLIII**, 509–524.
5 P. Irani, Electromyography in nutritional osteomalaic myopathy, *J. Neurol. Neurosurg. Psychiatry*, 1976, 686–693.
6 L. Ceglia, Vitamin D and skeletal muscle tissue and function, *Mol. Aspects Med.*, 2008, **29**, 407–414.
7 J. B. Eastwood, P. J. Bordier and E. M. Clarkson, The contrasting effects on bone histology of vitamin D and of calcium carbonate in the osteomalacia of chronic renal failure, *Clin. Sci. Mol. Med.*, 1974, **47**, 23–42.
8 J. B. Eastwood, T. C. B. Stamp and H. E. De Wardener, The effect of 25 hydroxy vitamin D3 in the osteomalacia of chronic renal failure, *Clin. Sci. Mol. Med.*, 1977, **52**, 499–508.
9 M. Samson, H. J. J. Verhaar, P. A. F. Jansen, P. L. de Vreede, J. W. Manten and S. A. Duursma, Muscle strength, functional mobility and vitamin D in older women, *Aging Clin. Exp. Res.*, 2000, **12**, 455–460.
10 M. Pfeifer, B. Begerow, H. W. Minne, C. Abrams, D. Nachtigall and C. Hansen, Effects of a short-term vitamin D and calcium supplementation on body sway and secondary hyperparathyroidism in elderly women, *J. Bone Miner. Res.*, 2000, **15**, 1113–1118.
11 M. F. Holick, Vitamin D: its role in cancer prevention and treatment, *Prog. Biophys. Mol. Biol.*, 2006, **92**, 49–59.
12 J. S. Adams and M. Hewison, Unexpected actions of vitamin D: new perspectives on the regulation of innate and adaptive immunity, *Nat. Clin. Pract. Endocrinol. Metab.*, 2008, **4**, 80–90.
13 J. L. Omdahl, H. A. Morris and B. K. May, Hydroxylase enzymes of the vitamin D pathway: expression, function, and regulation, *Annu. Rev. Nutr.*, 2002, **22**, 139–166.
14 P. H. Anderson, S. Iida, J. H. T. Tyson, A. G. Turner and H. A. Morris, Bone CYP27B1 gene expression is increased with high dietary calcium and in mineralising osteoblasts, *J. Steroid. Biochem. Mol. Biol.*, 2010, **121**, 71–75.
15 I. Aiba, T. Yamasaki, T. Shinki, S. Izumi, K. Yamamoto, S. Yamada, H. Terato, H. Ide and Y. Ohyama, Characterization of rat and human CYP2J enzymes as vitamin D 25-hydroxylases, *Steroids*, 2006, **71**, 849–856.
16 B. Lehmann and M. Meurer, Extrarenal sites of calcitriol synthesis: the particular role of the skin, *Recent Results Cancer Res.*, 2003, **164**, 135–145.
17 M. Schuessler, N. Astecker, G. Herzig, G. Vorisek and I. Schuster, Skin is an autonomous organ in synthesis, two-step activation and degradation of vitamin D3: CYP27 in epidermis completes the set of essential vitamin D3-hydroxylases, *Steroids*, 2001, **66**, 399–408.
18 D. D. Bikle, Vitamin D regulated keratinocyte differentiation, *J. Cell. Biochem.*, 2004, **92**, 436–444.
19 B. W. Hollis, 25-Hydroxyvitamin D3-1α-hydroxylase in porcine hepatic tissue: subcellular localization to both mitochondria and microsomes, *Proc. Natl. Acad. Sci. U. S. A.*, 1990, **87**, 6009–6013.
20 D. Zehnder, R. Bland, M. C. Williams, R. W. McNinch, A. J. Howie, P. M. Stewart and M. Hewison, Extrarenal expression of 25-hydroxyvitamin D3-1α-hydroxylase, *J. Clin. Endocrinol. Metab.*, 2001, **86**, 888–894.
21 M. Hewison, L. Freeman, S. V. Hughes, K. N. Evans, R. Bland, A. G. Eliopoulos, M. D. Kilby, P. A. H. Moss and R. Chakraverty, Differential regulation of vitamin D receptor and its ligand in human monocyte-derived dendritic cells, *J. Immunol.*, 2003, **170**, 5382–5390.
22 S. Hansdottir, M. M. Monick, S. L. Hinde, N. Lovan, D. C. Look and G. W. Hunninghake, Respiratory epithelial cells convert inactive vitamin D to its active form: potential effects on host defense, *J. Immunol.*, 2008, **181**, 7090–7099.
23 G. A. Howard, R. T. Turner, D. J. Sherrard and D. J. Baylink, Human bone cells in culture metabolize 25-hydroxyvitamin D3 to 1,25-dihydroxyvitamin D3 and 24,25-dihydroxyvitamin D3, *J. Biol. Chem.*, 1981, **256**, 7738–7740.
24 F. Ichikawa, K. Sato, M. Nanjo, Y. Nishii, T. Shinki, N. Takahashi and T. Suda, Mouse primary osteoblasts express vitamin D3 25-hydroxylase mRNA and convert

1α-hydroxyvitamin D3 into 1α,25-dihydroxyvitamin D3, *Bone*, 1995, **16**, 129–135.
25 D. K. Panda, S. A. Kawas, M. F. Seldin, G. N. Hendy and D. Goltzman, 25-Hydroxyvitamin D 1α-hydroxylase: structure of the mouse gene, chromosomal assignment, and developmental expression, *J. Bone Miner. Res.*, 2001, **16**, 46–56.
26 P. H. Anderson, P. D. O'Loughlin, B. K. May and H. A. Morris, Modulation of CYP27B1 and CYP24 mRNA expression in bone is independent of circulating 1,25(OH) 2D3 levels, *Bone*, 2005, **36**, 654–662.
27 M. Van Driel, H. A. P. Pols and J. P. T. M. Van Leeuwen, Osteoblast differentiation and control by vitamin D and vitamin D metabolites, *Curr. Pharm. Des.*, 2004, **10**, 2535–2555.
28 M. Van Driel, M. Koedam, C. J. Buurman, M. Hewison, H. Chiba, A. G. Uitterlinden, H. A. P. Pols and J. P. T. M. Van Leeuwen, Evidence for auto/paracrine actions of vitamin D in bone: 1α-Hydroxylase expression and activity in human bone cells, *FASEB J.*, 2006, **20**, E1811–E1819.
29 V. J. Woeckel, R. D. A. M. Alves, S. M. A. Swagemakers, M. Eijken, H. Chiba, B. C. J. Van Der Eerden and J. P. T. M. Van Leeuwen, 1α,25-(OH)2D3 acts in the early phase of osteoblast differentiation to enhance mineralization via accelerated production of mature matrix vesicles, *J. Cell. Physiol.*, 2010, **225**, 593–600.
30 P. H. Anderson, S. Iida, J. H. T. Tyson, A. G. Turner and H. A. Morris, Bone CYP27B1 gene expression is increased with high dietary calcium and in mineralising osteoblasts, *J. Steroid Biochem. Mol. Biol.*, 2010, **121**, 71–75.
31 M. F. Holick, J. A. MacLaughlin and M. B. Clark, Photosynthesis of previtamin D3 in human skin and the physiologic consequences, *Science*, 1980, **210**, 203–205.
32 M. K. Nemanic, J. Whitney and P. M. Elias, *In vitro* synthesis of vitamin D-3 by cultured human keratinocytes and fibroblasts: action spectrum and effect of AY-9944, *Biochim. Biophys. Acta, Gen. Subj.*, 1985, **841**, 267–277.
33 B. Lehmann, T. Genehr, P. Knuschke, J. Pietzsch and M. Meurer, UVB-induced conversion of 7-dehydrocholesterol to 1α,25- dihydroxyvitamin D3 in an *in vitro* human skin equivalent model, *J. Invest. Dermatol.*, 2001, **117**, 1179–1185.
34 J. A. MacLaughlin, R. R. Anderson and M. F. Holick, Spectral character of sunlight modulates photosynthesis of previtamin D3 and its photoisomers in human skin, *Science*, 1982, **216**, 1001–1003.
35 L. Xu, Z. Korade and N. A. Porter, Oxysterols from free radical chain oxidation of 7-dehydrocholesterol: product and mechanistic studies, *J. Am. Chem. Soc.*, 2010, **132**, 2222–2232.
36 D. E. MacDonald, B. E. Rapuano, N. Deo, M. Stranick, P. Somasundaran and A. L. Boskey, Thermal and chemical modification of titanium–aluminum–vanadium implant materials: effects on surface properties, glycoprotein adsorption, and MG63 cell attachment, *Biomaterials*, 2004, **25**, 3135–3146.
37 N. Håkan, Initial reactions of whole blood with hydrophilic and hydrophobic titanium surfaces, *Colloids Surf., B*, 1996, **6**, 329–333.
38 I. Schuster, H. Egger, D. Bikle, G. Herzig, G. S. Reddy, A. Stuetz, P. Stuetz and G. Vorisek, Selective inhibition of vitamin D hydroxylases in human keratinocytes, *Steroids*, 2001, **66**, 409–422.
39 P. Tarroni, I. Villa, E. Mrak, F. Zolezzi, M. Mattioli, C. Gattuso and A. Rubinacci, Microarray analysis of 1,25 (OH)2D3 regulated gene expression in human primary osteoblasts, *J. Cell. Biochem.*, 2011, 640–649.
40 G. S. Stein, J. B. Lian, J. L. Stein, A. J. Van Wijnen and M. Montecino, Transcriptional control of osteoblast growth and differentiation, *Physiol. Rev.*, 1996, **76**, 593–629.
41 A. Ulsamer, M. J. Ortuno, S. Ruiz, A. R. G. Susperregui, N. Osses, J. L. Rosa and F. Ventura, BMP-2 induces osterix expression through up-regulation of Dlx5 and its phosphorylation by p38, *J. Biol. Chem.*, 2008, **283**, 3816–3826.
42 T. L. Chen and D. Fry, Hormonal regulation of the osteoblastic phenotype expression in neonatal murine calvarial cells, *Calcif. Tissue Int.*, 1999, **64**, 304–309.
43 N. Kurihara, S. Ishizuka, M. Kiyoki, Y. Haketa, K. Ikeda and M. Kumegawa, Effects of 1,25-dihydroxyvitamin D3 on osteoblastic MC3T3-E1 cells, *Endocrinology*, 1986, **118**, 940–947.
44 Y. Maehata, S. Takamizawa, S. Ozawa, Y. Kato, S. Sato, E. Kubota and R. I. Hata, Both direct and collagen-mediated signals are required for active vitamin D3-elicited differentiation of human osteoblastic cells: roles of osterix, an osteoblast-related transcription factor, *Matrix Biol.*, 2006, **25**, 47–58.
45 T. Matsumoto, C. Igarashi, Y. Takeuchi, S. Harada, T. Kikuchi, H. Yamato and E. Ogata, Stimulation by 1,25-dihydroxyvitamin D3 of *in vitro* mineralization induced by osteoblast-like MC3T3-E1 cells, *Bone*, 1991, **12**, 27–32.
46 R. L. Jilka, G. Hangoc, G. Girasole, G. Passeri, D. C. Williams, J. S. Abrams, B. Boyce, H. Broxmeyer and S. C. Manolagas, Increased osteoclast development after estrogen loss: mediation by interleukin-6, *Science*, 1992, **257**, 88–91.
47 O. Kozawa, H. Tokuda, T. Kaida, H. Matsuno and T. Uematsu, Effect of vitamin D3 on interleukin-6 synthesis induced by prostaglandins in osteoblasts, *Prostaglandins, Leukotrienes Essent. Fatty Acids*, 1998, **58**, 119–123.
48 R. Gruber, G. Nothegger, G. M. Ho, M. Willheim and M. Peterlik, Differential stimulation by PGE2 and calcemic hormones of IL-6 in stromal/osteoblastic cells, *Biochem. Biophys. Res. Commun.*, 2000, **270**, 1080–1085.
49 J. M. Tran, C. R. Kleeman and J. Green, Production of interleukin-6 by osteoblastic cells is independent of medium inorganic phosphate, *Biochem. Mol. Med.*, 1995, **55**, 90–95.
50 M. Giner, M. A. Rios, M. A. Montoya, M. A. Vazquez, L. Naji and R. Perez-Cano, RANKL/OPG in primary cultures of osteoblasts from post-menopausal women. Differences between osteoporotic hip fractures and osteoarthritis, *J. Steroid Biochem. Mol. Biol.*, 2009, **113**, 46–51.

51 N. J. Horwood, J. Elliott, T. J. Martin and M. T. Gillespie, Osteotropic agents regulate the expression of osteoclast differentiation factor and osteoprotegerin in osteoblastic stromal cells, *Endocrinology*, 1998, **139**, 4743–4746.
52 T. Suda, E. Jimi, I. Nakamura and N. Takahashi, Role of 1 alpha,25-dihydroxyvitamin D3 in osteoclast differentiation and function, *Methods Enzymol.*, 1997, **282**, 223–235.
53 T. Suda, N. Takahashi, N. Udagawa, E. Jimi, M. T. Gillespie and T. J. Martin, Modulation of osteoclast differentiation and function by the new members of the tumor necrosis factor receptor and ligand families, *Endocr. Rev.*, 1999, **20**, 345–357.
54 G. P. Thomas, S. U. K. Baker, J. A. Eisman and E. M. Gardiner, Changing RANKL/OPG mRNA expression in differentiating murine primary osteoblasts, *J. Endocrinol.*, 2001, **170**, 451–460.
55 D. Zhang, Y. Q. Yang, X. T. Li and M. K. Fu, The expression of osteoprotegerin and the receptor activator of nuclear factor kappa B ligand in human periodontal ligament cells cultured with and without 1alpha,25-dihydroxyvitamin D3, *Arch. Oral Biol.*, 2004, **49**, 71–76.
56 P. A. Baldock, G. P. Thomas, J. M. Hodge, S. U. Baker, U. Dressel, P. D. O'Loughlin, G. C. Nicholson, K. H. Briffa, J. A. Eisman and E. M. Gardiner, Vitamin D action and regulation of bone remodeling: suppression of osteoclastogenesis by the mature osteoblast, *J. Bone Miner. Res.*, 2006, **21**, 1618–1626.

Paper II

UV photoactivation of 7-dehydrocholesterol on titanium implants enhances osteoblast differentiation and decreases Rankl gene expression

Satué M. ; Petzold C. ; Córdoba A. ; Ramis J.M. ; Monjo M.

Acta Biomaterialia (2013), 9(3):5759-70.

Acta Biomaterialia 9 (2013) 5759–5770

Contents lists available at SciVerse ScienceDirect

Acta Biomaterialia

journal homepage: www.elsevier.com/locate/actabiomat

UV photoactivation of 7-dehydrocholesterol on titanium implants enhances osteoblast differentiation and decreases *Rankl* gene expression

M. Satué [a], C. Petzold [b], A. Córdoba [a], J.M. Ramis [a], M. Monjo [a,*]

[a] Department of Fundamental Biology and Health Sciences, Research Institute on Health Sciences (IUNICS), University of Balearic Islands, Spain
[b] Department of Biomaterials, Institute for Clinical Dentistry, University of Oslo, Norway

ARTICLE INFO

Article history:
Received 9 July 2012
Received in revised form 8 October 2012
Accepted 13 November 2012
Available online 28 November 2012

Keywords:
Titanium implant
7-Dehydrocholesterol
Vitamin D
UV irradiation
Osteoblast differentiation

ABSTRACT

Vitamin D plays a central role in bone regeneration, and its insufficiency has been reported to have profound negative effects on implant osseointegration. The present study aimed to test the in vitro biological effect of titanium (Ti) implants coated with UV-activated 7-dehydrocholesterol (7-DHC), the precursor of vitamin D, on cytotoxicity and osteoblast differentiation. Fourier transform infrared spectroscopy confirmed the changes in chemical structure of 7-DHC after UV exposure. High-pressure liquid chromatography analysis determined a 16.5 ± 0.9% conversion of 7-DHC to previtamin D_3 after 15 min of UV exposure, and a 34.2 ± 4.8% of the preD_3 produced was finally converted to 25-hydroxyvitamin D_3 (25-D_3) by the osteoblastic cells. No cytotoxic effect was found for Ti implants treated with 7-DHC and UV-irradiated. Moreover, Ti implants treated with 7-DHC and UV-irradiated for 15 min showed increased 25-D_3 production, together with increased ALP activity and calcium content. Interestingly, *Rankl* gene expression was significantly reduced in osteoblasts cultured on 7-DHC-coated Ti surfaces when UV-irradiated for 15 and 30 min to 33.56 ± 15.28% and 28.21 ± 4.40%, respectively, compared with the control. In conclusion, these findings demonstrate that UV-activated 7-DHC is a biocompatible coating of Ti implants, which allows the osteoblastic cells to produce themselves active vitamin D, with demonstrated positive effects on osteoblast differentiation in vitro.

1. Introduction

Calcitriol (1,25-dihydroxyvitamin D_3, 1,25-D_3), the biologically active form of vitamin D_3, is produced by a hydroxylation cascade, which is preceded by photochemical activation. When provitamin D_3 (7-dehydrocholesterol, 7-DHC) is exposed to ultraviolet (UV) B irradiation, it is then converted to precholecalciferol (previtamin D_3). Afterwards, this molecule is transformed into cholecalciferol (D_3) and twice hydroxylated until 1,25-D_3 is formed and released to the circulation. This biological pathway starts in the skin, where 7-DHC is UV-activated, while the rest of the process continues in liver and kidney tissues through hydroxylation reactions [1]. 7-DHC is not normally detectable in tissues and fluids of human beings except in skin, and its synthesis is decreased in the skin with aging [2–4]. Moreover, extrarenal synthesis of 1,25-D_3 is possible and feasible in other tissues or cells, such as the skin [5–7], liver [8], lymph nodes [9], activated monocytes and macrophages [10,11] and dendritic cells [12].

Local production of 1,25-D_3 in bone cells from 25-D_3 was first reported by Howard et al. in 1981 [13]. They found that primary cultures of human bone cells incubated with 25-D_3 synthesized both 1,25-D_3 and 24,25-D_3, with specific activities similar in magnitude to those of the enzymes found in kidney cells [13]. Ichikawa et al. [14] confirmed 1,25-D_3 conversion from 25-D_3 in mouse bone cells and reported the expression of the vitamin D_3 25-hydroxylase CYP27A1 mRNA in mouse osteoblasts. Recently, 25-hydroxyvitamin D_3–1-alpha-hydroxylase CYP27B1 mRNA expression in bone cells has been identified [15,16], and the role in osteoblast differentiation and mineralization of locally produced 1,25-D_3 has been evidenced [17–19].

It was demonstrated recently that the vitamin D precursor 7-DHC can be used locally to produce active vitamin D by osteoblastic cells when 7-DHC is coating a tissue culture plastic (TCP) surface and is UV-irradiated before the cell culture [20]. Hence, UV-activated 7-DHC may be a feasible approach to be used in therapeutics focused on bone regeneration, e.g., functionalizing bioactive titanium (Ti) surfaces to enhance osseointegration in compromised patients. Recently, vitamin D has been suggested to play a central role in bone regeneration, and its insufficiency has been reported to have profound negative effects on implant osseointegration [21,22]. Also a high prevalence of vitamin D deficiency has been found across all age groups in different populations studied worldwide, which results from inadequate dietary intake, together with insufficient exposure to sunlight [23–25].

* Corresponding author. Tel.: +34 971 259960; fax: +34 971 173184.
E-mail address: marta.monjo@uib.es (M. Monjo).

1742-7061/$ - see front matter © 2012 Acta Materialia Inc. Published by Elsevier Ltd. All rights reserved.
http://dx.doi.org/10.1016/j.actbio.2012.11.021

Ti is the material most commonly used for bone implants, as it has outstanding physical and biological properties, such as low density, high mechanical strength and good corrosion resistance [22]. Current dental implant research aims to produce innovative surfaces able to promote a more favorable biological response to the implant material at the bone–implant interface and to accelerate osseointegration. Provitamin D_3 coating on Ti surfaces is suggested here to have a stimulatory effect on bone cells and accelerate bone regeneration as result of active vitamin D synthesis. This coating could show several advantages over using other hydroxylated forms of vitamin D, e.g., giving the vitamin D precursor 7-DHC directly to the cells would reduce the risk of vitamin D toxicity in the target cells, as its affinity for the vitamin D receptor is lower than the affinity of 1,25-D_3 [26]. Furthermore, 7-DHC is easily available and cheaper than the other forms of vitamin D_3, so this approach would entail a lower cost.

The aim of the study was to develop and optimize a bioactive coating of Ti implants with UV-activated 7-DHC. For that purpose, different UV time exposures were analyzed, and the one that achieved the highest 25-D3 synthesis and increased osteoblast differentiation in vitro was selected. Fourier transform infrared spectroscopy (FTIR) analysis and high-pressure liquid chromatography (HPLC) were used to characterize and quantify the conversion of 7-DHC to preD_3. Cytotoxicity, alkaline phosphatase (ALP) activity, calcium (Ca) content, 25-D_3 production, gene expression of bone markers and enzymes involved in vitamin D_3 synthesis were analyzed using MC3T3-E1 cells, as in an vitro model.

2. Materials and methods

2.1. Implants and treatments

Ti disks with diameter 6.25 mm and height 2 mm were machined from cp Ti rods (grade 2) and subsequently ground, polished and cleaned as described elsewhere [27]. For the surface modification of Ti implants, a stock solution of 2 mM 7-dehydrocholesterol (7-DHC; Sigma, St. Louis, MO, USA) were prepared in absolute ethanol and filtered with a 0.22 μm pore size filter before use.

To coat the implant surfaces, 10 μl of 7-DHC dilution (to have 0.2 nmol per Ti disk) or only ethanol were left on the surfaces and allowed to air-dry for 15 min in a sterile flow bench. UV-irradiation of implants was performed with a UV lamp emitting light at a wavelength of 302 nm with an intensity of ~6 mW cm^{-2}. In a previous pilot study, it was shown that 0.2 nmol was the optimal amount of 7-DHC to be used in polystyrene TCP (30.7 mm^2 of well surface area) under UV irradiation for the production of active vitamin D in MC3T3-E1 osteoblasts [20]. The same amount of 7-DHC was applied on the surface of Ti disks in the present study, as the culture plates containing the Ti disks had the same surface area as those previously used.

Thus, different groups were prepared: (1) non-irradiated samples, 7-DHC (0.2 nmol per Ti disk), D_3 and 25-D_3 (2×10^{-2} nmol per Ti disk) and ethanol (used as control for the non-irradiated group, EtOH); and (2) UV-irradiated samples, 7-DHC (0.2 nmol per Ti disk) and EtOH (used as control for the 7-DHC-irradiated group).

2.2. FTIR analysis of 7-DHC and D_3 coating on Ti surfaces

FTIR spectroscopy in reflective mode (DRIFT; Spectrum 100, Perkin Elmer, USA) was used to analyze the effect of UV irradiation on vitamin D conversion after 0, 15, 30 and 60 min of UV irradiation. Ti disks coated with 7-DHC or D_3 were UV-irradiated as described above. An equally irradiated but untreated Ti disk was used as a background for the FTIR measurements. The spectra obtained by FTIR spectroscopy were analyzed for typical absorbances connected to changes in chemical structure of 7-DHC and D_3 after UV exposure of the surface coatings. The spectra were smoothed and baseline corrected with the Spectrum program (version 6.3.2.0151, PerkinElmer, Inc., Waltham, USA). Typical peak areas were fitted and quantified with CasaXPS (version 2.3.15, Casa Software Ltd.) for comparison.

2.3. Quantitative determination of the conversion efficiency of 7-DHC to preD_3 by HPLC

The amounts of 7-DHC and preD_3 present in the 0.2 nmol 7-DHC surface coating after 15 min of UV irradiation were quantified by HPLC. Results were compared with non-irradiated 7-DHC-coated surfaces. Pure ethanol was used as control. All solvents used were HPLC or analytical grade. Methanol (HPLC gradient grade), acetonitrile and tetrahydrofurane (both HPLC grade) were purchased from Fisher Scientific (Thermo Fisher Scientific, MA, USA). High-purity deionized Milli-Q water was obtained from a Millipore system (Millipore Corporation, Billerica, MA, USA). Absolute ethanol was purchased from Scharlab (Barcelona, Spain). Individual stock standard solutions of 7-DHC (250 μg ml^{-1}) and D_3 (10 mg ml^{-1}) were prepared in methanol and stored at −20 °C. Standard solutions of lower concentrations were obtained by diluting stock solutions with methanol.

The coating of each surface was extracted by adding 100 μl of methanol/acetonitrile/tetrahydrofurane/water (67:16:2:15, v:v) to each well and shaking the plate for 2 min at 20 rpm. The content of three replicate wells was mixed to give a sample of ~300 μl. An aliquot of 100 μl of the sample was injected into the HPLC system. Two replicate samples were prepared and analyzed for each group.

The analysis were carried out using a Waters liquid chromatographic system (Milford, MA, USA), equipped with a refrigerated automatic injector WISP700 and a 600 pump system, connected to a Waters 996 photodiode array detector. The Empower software was used for instrument control and data analysis. Detection was carried out at 282 nm.

A Nova Pak C18 column (Waters) was used to separate sample components before detection. The column temperature was set to 30 °C. Two solvents were used in gradient elution mode as the mobile phase: A, methanol/acetonitrile/tetrahydrofurane/water (67:16:2:15, v:v); and B, methanol/acetonitrile/tetrahydrofurane (75:20:5, v:v). Solvents A and B were vacuum-filtered through a nylon membrane (0.45 μm pore diameter) and degassed before use. The mobile phase flow rate was 1 ml min^{-1}. The binary gradient used was as follows: from 5% B to 90% B in 3 min, held for 9.5 min at 90% B, from 90% B to 5% B in 1 min and equilibrated between injections at the initial conditions for 5 min (total run time = 15 + 5 min equilibration between injections).

Quantification was performed by integration of the peak area of the corresponding analyte and interpolation of the peak area in 7-DHC or D_3 standard curves.

2.4. Cell culture

The mouse osteoblastic cell line MC3T3-E1 (DSMZ, Braunschweig, Germany) was chosen as an in vitro model. Cells were routinely cultured in α-MEM (PAA Laboratories GmbH, Pasching, Austria), which contains ascorbic acid (45 μg ml^{-1}) and sodium dihydrogen phosphate (140 mg l^{-1}), and supplemented with 10% fetal bovine serum (PAA Laboratories GmbH, Pasching, Austria) and antibiotics (50 IU penicillin ml^{-1} and 50 μg streptomycin ml^{-1}) (Sigma, St. Louis, MO, USA) under standard cell culture conditions (at 37 °C in a humidified atmosphere of 5% CO_2). Under these conditions, these cells are able to differentiate and

mineralize. Cells were subcultured 1:4 before reaching confluence using phosphate buffered saline (PBS) and trypsin/EDTA. All experiments were carried out after eight passages of the MC3T3-E1 cells.

To test the effect of the surface modification, 96-well plates were used. Ti disks were placed in the wells, and then 7-DHC treatment was added. Once Ti surfaces were coated, UV-activation was performed there. Cells grown on untreated polystyrene TCP were added as a control for all experiments. Cells were seeded at a density of 30,000 cells cm^{-2}, and they were maintained in α-MEM supplemented with 10% FCS and antibiotics. Culture media were collected after 24 h to test cytotoxicity and after 48 h to determine the production of the hydroxylated form of vitamin D, 25-D_3. Cells were harvested after 2 days of culture using Trizol reagent (Roche Diagnostics, Mannheim, Germany), to analyze the gene expression of several osteoblast differentiation markers and enzymes involved in vitamin D synthesis using real-time reverse-transcription-polymerase chain reaction (RT-PCR). Cell number and morphology were also assessed after 48 h. Further, MC3T3-E1 cells were harvested after 21 days to measure ALP activity and after 28 days to measure the Ca content in the cell monolayer.

2.5. Quantitative determination of 25-D_3 released to the culture media

The 25-D_3 released to the culture media was analyzed by enzyme-linked immunosorbent assay (ELISA). Aliquots from the culture media (25 μl) were centrifuged at 1800 rpm for 5 min at 4 °C, and supernatants were used for 25-D_3 and determination following instructions described by the manufacturer (Immunodiagnostic Systems Ltd, Boldon, Tyne & Wear, UK).

2.6. Determination of cell viability: LDH activity

Lactate dehydrogenase (LDH) activity in the culture media was used as an index of cell death. LDH activity was determined spectrophotometrically after 30 min incubation at 25 °C of 50 μl of culture and 50 μl of the reaction mixture by measuring the oxidation of NADH at 490 nm in the presence of pyruvate, following the manufacturer's protocol (Cytotoxicity Detection Kit (LDH), Roche Diagnostics, Mannheim, Germany). Toxicity was presented relative to the LDH activity in the media of cells seeded on TCP without treatment (low control, 0% of cell death) and on cells grown on TCP treated with 1% Triton X-100 (high control, 100% of death), using the following equation: cytotoxicity (%) = (exp. value − low control)/(high control − low control) × 100.

2.7. Determination of number of cells

Cells growing on the different surfaces were lysed after 48 h of cell culture by a freeze–thaw method in deionized distilled water. Cell lysates were used for determining DNA quantity using Hoechst 33258 fluorescence assay. Samples were mixed with 20 μg ml^{-1} of Hoechst 33258 fluorescence stain (Sigma, St. Quentin Fallavier, France) in TNE buffer at pH 7.4 containing 10 mM Tris–HCl, 1 mM EDTA and 2 M NaCl. The intensity of fluorescence was measured at excitation and emission wavelengths of 356/465 nm using a multifunction microplate reader (Cary Eclipse fluorescence spectrophotometer, Agilent Technologies, Santa Clara, USA). Relative fluorescence units were correlated with the cell number using a linear standard curve.

2.8. Cell staining and cell morphology analysis

Confocal images of cells growing in the different treated surfaces at 48 h of cell culture were obtained. Cells were first fixed and then permeabilized and stained with Phalloidin-FITC (50 μg ml^{-1}; Sigma, St. Louis, MO, USA) to stain actin filaments. Finally, a drop of DAPI (Sigma, St. Louis, MO, USA) was added to stain the cell nucleus. Various images of each implant were taken with the confocal microscope (Leica DMI 4000B equipped with a Leica TCS SPE laser system) by measuring the fluorescence signal between 430 and 480 nm for DAPI and 500 and 525 nm for Phalloidin-FITC.

Images of cells were captured by scanning electron microscopy (SEM; Hitachi S-3400N, Hitachi High-Technologies Europe GmbH, Krefeld, Germany) at 48 h of cell culture (p = 40 Pa, V = 10 kV, analysis of backscattered electrons). In this case, cells were washed twice with PBS and fixed with glutaraldehyde 4% in PBS for 2 h. Then, the fixative solution was removed, and the cells were washed twice with distilled water. At 30 min intervals, the cells were dehydrated by the addition of 50%, 70%, 90% and 100% ethanol solutions and were subsequently air dried.

Quantitation of the percentage of Ti surface covered with MC3T3-E1cells was achieved by analyzing the previous images with ImageJ software (Rasband, W.S., ImageJ, US National Institutes of Health, Bethesda, MD, USA).

2.9. RNA isolation

RNA was isolated from cells using a monophasic solution of phenol and guanidine thiocyanate (Trizol, Roche Diagnostics, Mannheim, Germany) according to the manufacturer's protocol. RNA was quantified at 260 nm using a Nanodrop spectrophotometer (NanoDrop Technologies, Wilmington, DE, USA).

2.10. Real-time quantitative PCR analysis

Total RNA previously isolated was reverse-transcribed to cDNA using a High Capacity RNA to cDNA kit (Applied Biosystems, Foster City, CA) according to the protocol of the supplier. The same amount of total RNA from each sample was converted into cDNA. Each cDNA was diluted 1:4 and aliquots were stored at −20 °C until the PCR reactions were carried out.

Real-time RT-PCR was performed for two reference genes: 18S ribosomal RNA (*18S rRNA*), glyceraldehyde-3-phosphate dehydrogenase (*Gapdh*); and 10 target genes: alkaline phosphatase (*Alp*), Interleukin 6 (*Il-6*), collagen (*Coll-1*), Osteocalcin (*Oc*), bone morphogenetic protein 2 (*Bmp-2*), Osterix (*Osx*), receptor activator of nuclear factor kappa-B ligand (*Rankl*), osteoprotegerin (*Opg*) and genes involved in vitamin D synthesis such as vitamin D_3 25-hydroxylase (*Cyp27a1*) and 25 hydroxyvitamin D_3–1-alpha hydroxylase (*Cyp27b1*). Real-time PCR was performed in the Lightcycler 480® (Roche Diagnostics, Germany). Each reaction contained 5 μl of LightCycler-FastStart DNA Master^{PLUS} SYBR Green I (Roche Diagnostics, Mannheim, Germany), 0.5 μM of the sense and antisense specific primers (Table 1) and 3 μl of the cDNA dilution in a final volume of 10 μl. The normal amplification program consisted of a preincubation step for denaturation of the template cDNA (10 min, 95 °C), followed by 45 cycles consisting of a denaturation step (10 s, 95 °C), an annealing step (10 s, 60 °C, except for *Alp*, which was 10 s at 65 °C, and *Osx* with 10 s at 68 °C) and an extension step (10 s, 72 °C). After each cycle, fluorescence was measured at 72 °C. Every run included a negative control without cDNA template. To confirm amplification specificity, PCR products were subjected to a melting curve analysis on the LightCycler and, subsequently, 2% agarose/TAE gel electrophoresis, T_m and amplicon size, respectively.

To allow relative quantification after PCR, real-time efficiencies were calculated from the given slopes in the LightCycler 480 software (Roche Diagnostics, Mannheim, Germany) using serial dilutions. Relative quantification after PCR was calculated by normalizing target gene concentration in each sample by the concentration mean of the two reference genes in the given sample,

Table 1
Primer sequences used for real-time RT-PCR: product size and accession number are also indicated.

Name	5′-Sequence-3′	Product size	Accession number
Alp	S: AAC CCA GAC ACA AGC ATT CC AS: GAG AGC GAA GGG TCA GTC AG	151 bp	X13409
Bmp-2	S: GCT CCA CAA ACG AGA AAA GC AS: AGC AAG GGG AAA AGG ACA CT	178 bp	NM_007553.2
Coll-1	S: AGA GCA TGA CCG ATG GAT TC AS: CCT TCT TGA GGT TGC CAG TC	177 bp	NM_007742.3
Cyp27a1	S: CGT CCT CTG CTG CCC TTT TGG AAG AS: GTG TGT TGG ATG TCG TGT CCA CCC	247 bp	NM_024264.4
Cyp27b1	S: TCC TGT GCC CAC CCC CAT GG AS: AGG GAG ACT AGC GTA TCT TGG GGA	167 bp	NM_010009.2
Il-6	S: ACT TCC ATC CAG TTG CCT TC AS: TTT CCA CGA TTT CCC AGA GA	171 bp	NM_031168.1
Opg	AS: GGT AGG GAG CTG GGT TAA GG S: AGA CCA TGA GGT TCC TGC AC	131 bp	NM_008764.3
Oc	S: CCG GGA GCA GTG TGA GCT TA AS: TAG ATG CGT TTG TAG GCG GTC	81 bp	NM_007541
Osx	S: ACT GGC TAG GTG GTG GTC AG AS: AAA CAG CCC AGT GAC CAT TC	135 bp	NM_007419
Rankl	S: GGC CAC AGC GCT TCT CAG AS: TGA CTT TAT GGG AAC CCG AT	141 bp	NM_011613
Gapdh	S: ACC CAG AAG ACT GTG GAT GG AS: CAC ATT GGG GGT AGG AAC AC	171 bp	XM_132897
18*S rRNA*	S: GTA ACC CGT TGA ACC CCA TT AS: CCA TCC AAT CGG TAG TAG CG	151 bp	X00686

using the Advanced relative quantification method provided by the LightCycler 480 analysis software.

2.11. ALP activity, Ca content and total protein determination

Cell monolayers were collected at 21 cell differentiation days to determine ALP activity and total protein. In the same way, the Ca content was obtained from cell monolayers collected after 28 days of cell differentiation. In both cases, PBS containing 0.1% Triton X-100 was added to solubilize proteins. Cell lysates were put into freeze/thaw cycles (liquid nitrogen and a 37 °C water bath) to improve protein recovery. After centrifugation at 33,000*g* for 15 min at 4 °C, the supernatants were acquired and assayed for ALP activity, total protein and Ca content determination. ALP activity was calculated by measuring the cleavage of *p*-nitrophenyl phosphate (pNPP) (Sigma, St. Louis, MO, USA) in a soluble yellow end product, which absorbs at 405 nm. A volume of 100 μl of this substrate was used in combination with 25 μl of each sample supernatant or standard point. The standard curve was prepared from calf intestinal ALP (CIAP, 1 U μl^{-1}) (Promega, Madison, WI, USA) by mixing 1 μl from the stock CIAP with 5 ml of ALP buffer (1:5000 dilution), and then making 1:5 serial dilutions. Once the reaction was carried out, after 30 min in the dark at room temperature, it was stopped with the addition of 50 μl of 3 M sodium hydroxide. At this point, absorbance was read at 405 nm.

To determine the Ca content, samples were analyzed by inductively coupled plasma atomic emission spectrometry (ICP-AES; Optima 5300 DV, PerkinElmer, MA, USA). Cell supernatants were diluted 1:1 in 0.5 N HCl to extract Ca. Data were compared with the $CaCl_2$ standard curve included in the assay.

Total protein was determined using a BCA protein assay kit (Pierce, Rockford, IL, USA). For the analysis, cell supernatants were diluted 1:1 in PBS containing 0.1% Triton X-100. The standard curve and samples were analyzed as described by the manufacturer and reading the absorbance at 562 nm.

2.12. Statistics

All data are presented as mean values ± standard error of the mean (SEM). Statistical differences between groups were determined by Mann–Whitney test or by the Student *t*-test, depending on their normal distribution. The SPSS® program for Windows, version 17.0, was used. Results were considered statistically significant at *p*-values $\leqslant 0.05$.

3. Results

3.1. Changes in chemical structure of 7-DHC after UV exposure and D_3 on coated titanium implants

The FTIR absorbance spectra of 7-DHC changed with UV irradiation time (Table 2, Fig. 1), starting from short UV irradiation times of 15 min. From the absorbance spectra and the changes in peak areas measured (Table 2, Fig. 1), one can assume that no –OH groups were generated due to the irradiation, as the –OH stretch absorbance at 3300 cm^{-1} decreased slightly in area and also the absorbances of the –OH deformation vibration and –C–O stretch typical for phenolic compounds at 1360 cm^{-1} and 1220 cm^{-1} did not change in intensity (data not shown). A peak shift of the –OH stretching vibration towards higher wavenumbers for irradiated 7-DHC suggested the appearance of an additional peak at ~3470 cm^{-1} (Fig. 1) that can be assigned to –C=O stretching vibrations. Further, the –C=O stretching vibrations of ester and carboxylic groups at 1716 cm^{-1} increased clearly with irradiation time (Table 2) and may be caused by photo-oxidation processes. Peak fitting of the absorbance peak at 1850 cm^{-1} to 1550 cm^{-1} (Fig. 1) revealed the appearance of trans C=C bonds (1680 cm^{-1}) with an increasing peak area with irradiation time. The peak area of *cis* C=C double bonds (1650 cm^{-1}) increased as well, while the area of the C=C aromatic bonds (1625 cm^{-1}) remained stable (Table 2). In addition, changes in the region 970 cm^{-1} to ~500 cm^{-1} indicated changes in the ring substitution pattern, namely an increase for absorbances commonly assigned to 1,2,3 trisubstituted benzenes (960 cm^{-1}, 890 cm^{-1}, 800 cm^{-1}), and decreased absorbances for pentasubstituted benzenes (880 cm^{-1}) and 1,2,4,5 tetrasubstituted benzene (865 cm^{-1}) (Fig. 2). Thus, the FTIR spectra showed signs of changes in the ring structure, indicative of the ring opening reaction that converts 7-DHC to previtamin D_3.

Table 2
Quantification of the FTIR absorbance peak between 3800 cm^{-1} and 2700 cm^{-1} and of some absorbance peaks between 1850 cm^{-1} and 1550 cm^{-1}; the assigned molecular group with the approximate wavenumber of the maximum absorbance is given.

Substance	Peak area (A cm^{-1})					
	C=O 3470 cm^{-1}	OH 3300 cm^{-1}	C=O 1716 cm^{-1}	*trans* C=C 1680 cm^{-1}	*cis* C=C 1650 cm^{-1}	C=C aromatic 1625 cm^{-1}
Cholecalciferol	–	59.7	0.2	0.1	1.0	1.1
7-DHC	–	136.8	4.3	0.3	2.3	0.5
15 min UV	34.4	107.7	5.5	2.9	9.4	0.5
30 min UV	22.3	98.8	8.2	1.0	10.4	0.4
60 min UV	27.9	93.3	23.3	9.5	8.2	1.3

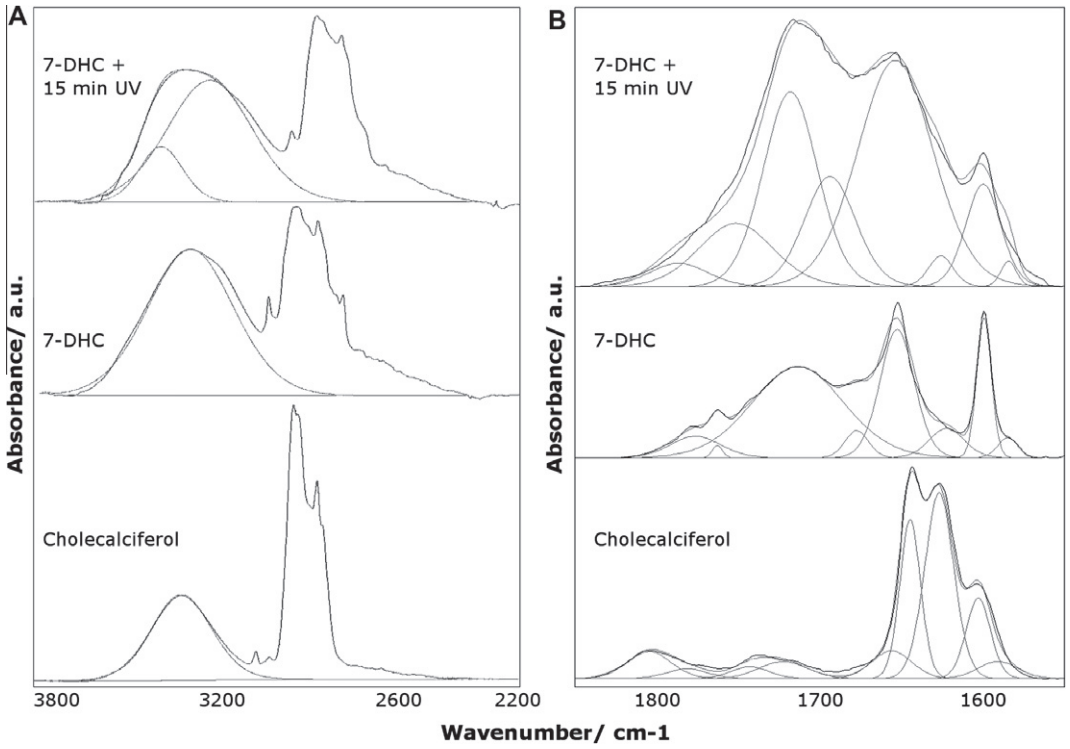

Fig. 1. Comparison of FTIR spectra for cholecalciferol (D_3), non-irradiated 7-DHC and 7-DHC irradiated for 15 min. The absorbances in the regions (A) 3800 cm^{-1} to 2200 cm^{-1} and (B) 1850 cm^{-1} to 1550 cm^{-1} are shown with the respective peaks fitted into the spectra.

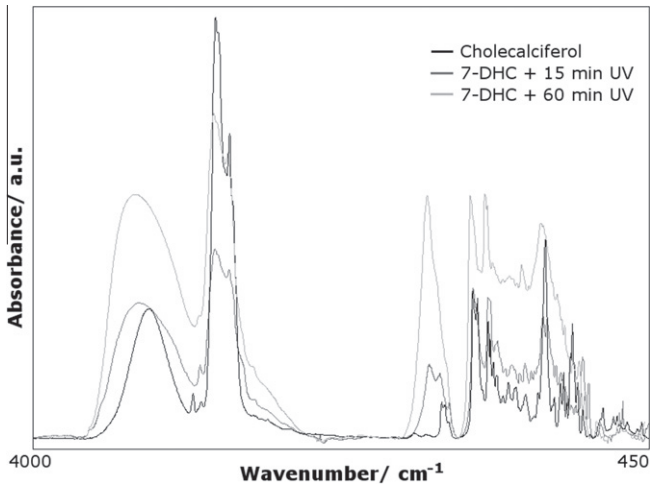

Fig. 2. Comparison of the FTIR absorbance spectra for cholecalciferol (D_3), 7-DHC after 15 min of UV irradiation, and 7-DHC after 60 min of UV irradiation for the entire wavenumber region measured (4000–450 cm^{-1}). The differences in the spectra were increasing with irradiation time.

3.2. Quantification of preD$_3$ production from UV irradiated 7-DHC-coated Ti implants and 25-D$_3$ secretion by MC3T3-E1 cells

Following the characterization of the chemical changes occurred in the 7-DHC after UV irradiation, the secretion of 25-D_3 from MC3T3-E1 cells to the cell culture media after 48 h was analyzed for the different UV irradiation time conditions (Fig. 3). As changes in the spectra indicating photo-oxidation increased with UV irradiation times, short irradiation times up to 30 min were chosen for further testing in vitro. Only 25-D_3 was analyzed in the samples because of its reported longer half-life and higher concentration than 1,25-D_3 [28]. As shown in Fig. 3, significant differences were detected between 7-DHC and ethanol-treated Ti samples when the UV exposure time was 15 min. Also significantly different was the amount of 25-D_3 released from 7-DHC UV-treated vs. UV-untreated. Surprisingly, UV irradiation of ethanol-treated Ti samples resulted in a time-dependent increase in the release of 25-D_3 by the cells, although this was not significant and to a lesser extent than 7-DHC-treated samples, except for the group UV irradiated for 30 min.

The conversion efficiency of 7-DHC to previtamin D_3 on 7-DHC-coated Ti surfaces was determined by HPLC after 15 min of irradiation, since the maximum 25-D_3 secretion was observed after

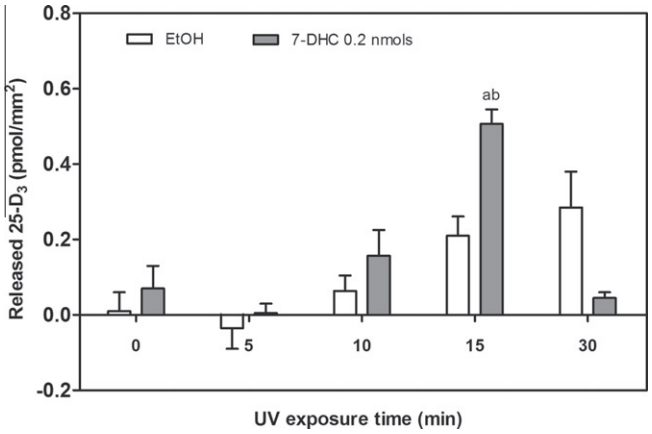

Fig. 3. Effect of UV time exposure of 7-DHC-coated Ti implants on 25-D_3 secretion (pmols secreted per Ti surface unit area) after 24 h of cell seeding. Values represent the mean ± SE ($n = 3$). Student's t-test ($p < 0.05$): [a]UV-treated vs. UV-untreated for 7-DHC and ethanol, respectively; [b]7-DHC treatment vs. the corresponding ethanol control at each UV irradiation time.

15 min of UV irradiation in 7-DHC samples (Fig. 3). Fig. 4 shows representative HPLC chromatograms of non-irradiated and irradiated 7-DHC samples. In non-irradiated samples, only 7-DHC was detected, eluting at 13.5 min. For the 15 min UV irradiated group, formation of preD_3 and other by-products like lumisterol and tachysterol was observed. preD_3 eluted at 11.7 min, lumisterol eluted at 12.1 min and a small peak around 12.4 min probably corresponded to the presence of tachysterol in the mixture. Quantification of peak areas showed that 1.49 ± 0.07 pmol mm^{-2} of preD_3 in relation to the Ti disk surface area were produced when irradiating Ti surfaces coated with 9.01 ± 0.29 pmol mm^{-2} of 7-DHC, giving a 16.5 ± 0.9% conversion of 7-DHC to preD_3 after 15 min of UV exposure.

Taking into account the HPLC results for the conversion of UV-activated 7-DHC to preD_3, the product yield of 25-D_3 from preD_3 was 34.2 ± 4.8% and 5.7 ± 0.8% of the initial amount of 7-DHC was finally converted to 25-D_3.

3.3. Effect of UV time exposure of 7-DHC-coated titanium implants on cell viability

Next, the effect of different UV irradiation times of 7-DHC-coated Ti implants on MC3T3-E1 cell viability after 24 h was investigated and compared with control surfaces (treated with ethanol only) under the same irradiation conditions. Cells were also cultured on TCP, as a reference surface, to have the positive and negative control for cytotoxicity. Fig. 5 shows that UV exposure decreased cytotoxicity for the ethanol treatment. Furthermore, lower cytotoxicity was found in the ethanol group from 0 to 15 min of UV irradiation compared with negative control (TCP), but also in 7-DHC samples previously UV-activated from 5 to 10 min. Significant differences were also observed for the 7-DHC group compared with their ethanol control group after 15 min of UV irradiation. D_3 and 25-D_3 treatments, which do not need UV activation, were also analyzed to compare their toxic levels with both 7-DHC groups. As expected, low cytotoxicity was observed in both treatments: −6.58 ± 1.42% and −10.03 ± 0.38%, respectively.

3.4. Effect of UV time exposure of 7-DHC-coated titanium implants on cell number and cell covered surface

Images obtained from confocal and SEM instruments show the cell morphology and the cell number for different UV-exposure

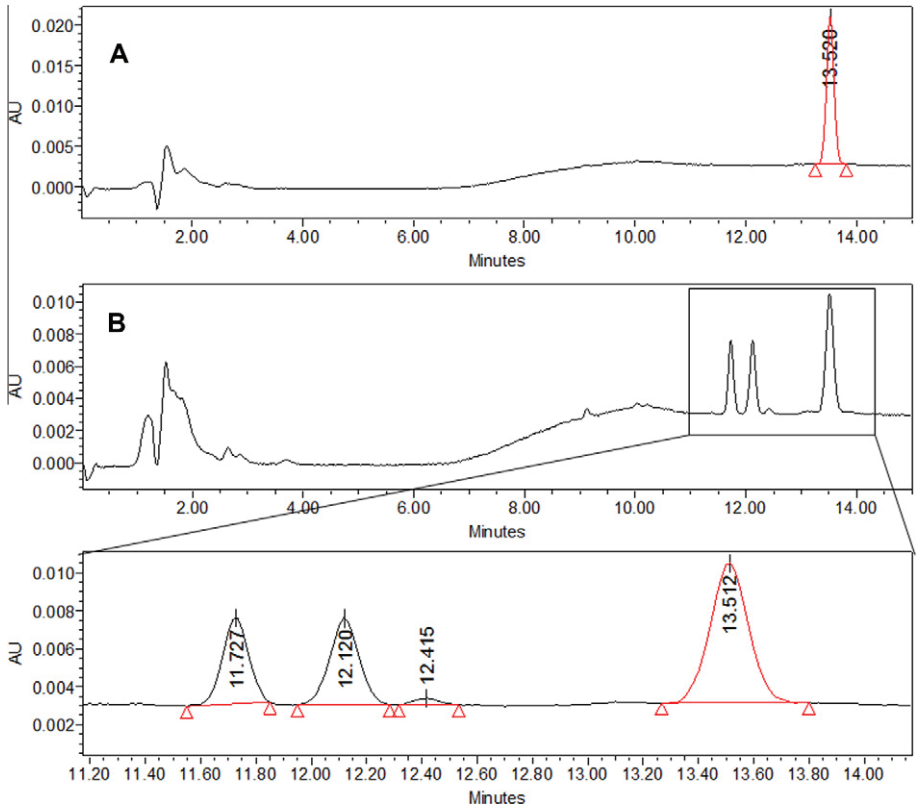

Fig. 4. Quantification of preD_3 production from UV irradiated 7-DHC. (a) HPLC chromatogram of a 7-DHC non-irradiated sample. Only 7-DHC is detected, eluting at 13.5 min retention time. (b) HPLC chromatogram of a 7-DHC irradiated sample (15 min irradiation time). Previtamin D_3 elutes at 11.7 min, lumisterol at 12.1 min and 7-DHC at 13.5 min. A small peak at 12.4 min is attributed to tachysterol.

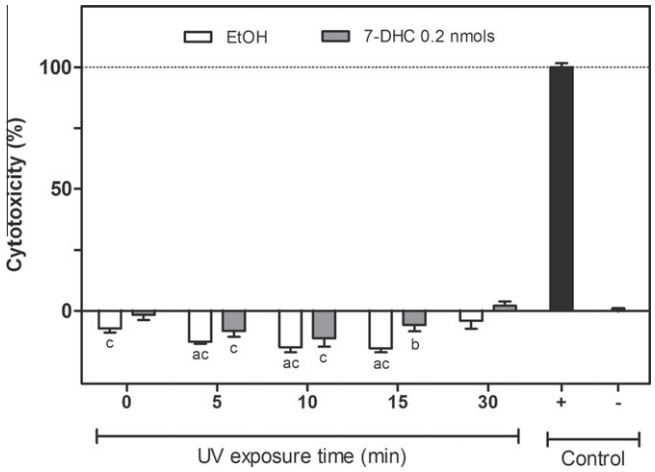

Fig. 5. Effect of UV time exposure of 7-DHC-coated implants on cell viability after 24 h of cell seeding. Positive control (+; 100% toxicity) was cell culture media from cells cultured on plastic wells (TCP) and incubated with Triton X-100 at 1%. Negative control (−; 0% toxicity) was cell culture media from untreated cells cultured on plastic wells (TCP). Values represent the mean ± SE ($n = 4$). Student's t-test ($p < 0.05$): [a]UV-treated vs. UV-untreated for 7-DHC and ethanol, respectively; [b]7-DHC treatment vs. the corresponding ethanol control at each UV irradiation time; and [c]treatments on Ti surfaces vs. the negative control (TCP).

times of 7-DHC and ethanol treatments on Ti surfaces (Fig. 6). More cells were present after 30 min of UV irradiation for both 7-DHC and ethanol groups. Data obtained from DNA content confirmed the significantly higher number of cells in these groups. In addition, on 7-DHC samples exposed to 30 min of UV irradiation, a significantly larger area of the Ti surfaces was covered with cells compared with non-irradiated 7-DHC surfaces. Together with the LDH activity results, the cell morphology and cell number confirmed the biocompatibility of the treatments and conditions used for the studies.

3.5. Effect of UV time exposure of 7-DHC-coated titanium implants on gene expression of hydroxylase enzymes

The gene expression of the hydroxylase *Cyp27a1* mRNA in 7-DHC samples (Fig. 7A) revealed a trend to be increased by the UV irradiation time, with a maximum at 15 min. Significant differences were found at 10 and 30 min of UV exposure compared with non-irradiated 7-DHC samples and at 30 min compared with ethanol-treated samples at the same UV-irradiation time. However, *Cyp27b1* gene expression was also upregulated with increasing UV exposure time in 7-DHC samples (Fig. 7B), with significant differences compared with UV-untreated 7-DHC samples at 15 and 30 min. Ethanol-treated samples kept a steady gene expression level, but with significant differences compared with non-irradiated ethanol samples at 5 and 15 min of UV irradiation.

3.6. Effect of UV time exposure of 7-DHC-coated titanium implants on osteoblast differentiation

Next, gene expression of several markers related to the proliferative stage of osteoblasts (collagen type-1), matrix maturation and differentiation (*Alp*, *Bmp-2*, *Osx*), mineralization (osteocalcin) and cytokines (*Il-6*, *Rankl*, *Opg*) was analyzed to investigate the effect of UV time exposure of 7-DHC-coated Ti implants on MC3T3-E1 osteoblasts (Fig. 8). *Coll-1* revealed a trend to decreased gene expression with UV exposure time in 7-DHC samples (Fig. 8A). Significant differences were found in 7-DHC samples exposed to UV irradiation for 15 and 30 min compared with ethanol-treated samples and non-irradiated 7-DHC samples. As regards *Alp* mRNA levels (Fig. 8B), statistical differences were found for the 30 min UV-exposed 7-DHC group compared with ethanol UV-exposed group. Moreover, all groups treated with 7-DHC and UV irradiation displayed higher *Alp* mRNA levels than their ethanol and UV-treated groups. *Osx* mRNA levels were very similar for all the groups (Fig. 8C), but significant differences were only found at 10 min of UV exposure. *Oc* gene expression was similar for different UV exposure times among the groups (Fig. 8D), although significant differences were found in the control group irradiated for 15 min compared with the non-irradiated one. A tendency to increased *Oc* mRNA levels in the 7-DHC UV-exposed for 15 min was observed. No statistical differences were observed for *Bmp-2* and *Il-6* mRNA levels when exposed to UV (Fig. 8E and F). Interestingly, *Rankl* mRNA levels revealed a statistically significant increase for the 10 min UV-exposed 7-DHC group compared with ethanol, but also a significant decrease for 15 and 30 min UV-exposed 7-DHC samples compared with ethanol and UV-untreated 7-DHC groups (Fig. 8G). Meanwhile, *Opg* mRNA levels kept a steady expression for the different UV exposure times (Fig. 8H), although a decrease was found for the 30 min UV-exposed 7-DHC samples.

3.7. Effect of UV time exposure of 7-DHC-coated titanium implants on Alp activity and mineralization

To investigate the effect of UV time exposure of 7-DHC-coated titanium implants on terminal osteoblast differentiation, ALP activity was measured in the cell monolayer on day 21 and Ca content on day 28 of cell culturing. UV-irradiated 7-DHC cells induced a significant higher ALP activity than the non-irradiated 7-DHC group (Fig. 9A). Additionally, non-irradiated 7-DHC and D_3 groups (44.75 ± 3.50% and 35.28 ± 4.23%, respectively) showed statistically lower ALP activity than the non-irradiated ethanol group, and the non-irradiated 25-D_3 group showed similar ALP activity (77.40 ± 13.40%) as the ethanol control. Ca levels were measured by ICP-AES. MC3T3-E1 cells showed a significant increase in the Ca content in UV-irradiated 7-DHC group compared with the non-irradiated and control groups (Fig. 9B). A trend to increase Ca levels was also observed for the 25-D_3 group, while it was in the same range for the D_3 and the non-irradiated 7-DHC groups (data not shown).

4. Discussion

Vitamin D deficiency has been reported to negatively affect bone regeneration, including fracture healing [29] and implant osseointegration [22]. Moreover, vitamin D supplementation has been proved to have a positive effect on cortical peri-implant bone formation in rats [21]. Overall, these investigations support the important role of vitamin D in controlling bone regeneration in healthy and osteoporotic bone. Ti and its alloys are the materials most frequently used as bone implants. An abundance of methods for surface modification to improve the performance of a Ti implant can be found, e.g., by changing the surface roughness or covering the surface with a layer of a bioactive substance, as reviewed in [30]. Recently, surface modification strategies have mostly been based on biological principles, which give the appropriate stimulus to the bone cells, thereby improving healing and integration responses after implantation [31,32]. This is important, especially for those suffering from bone deficiencies, e.g., diabetes or osteoporosis, which have increased drastically during the last century [33]. Here, the scientific basis is provided for a biocompatible coating of Ti implants with UV-activated 7-DHC, which is easy and cheap to produce, and allows the osteoblastic cells to produce themselves the active form of the vitamin D, with demonstrated positive effects on osteoblast differentiation in vitro.

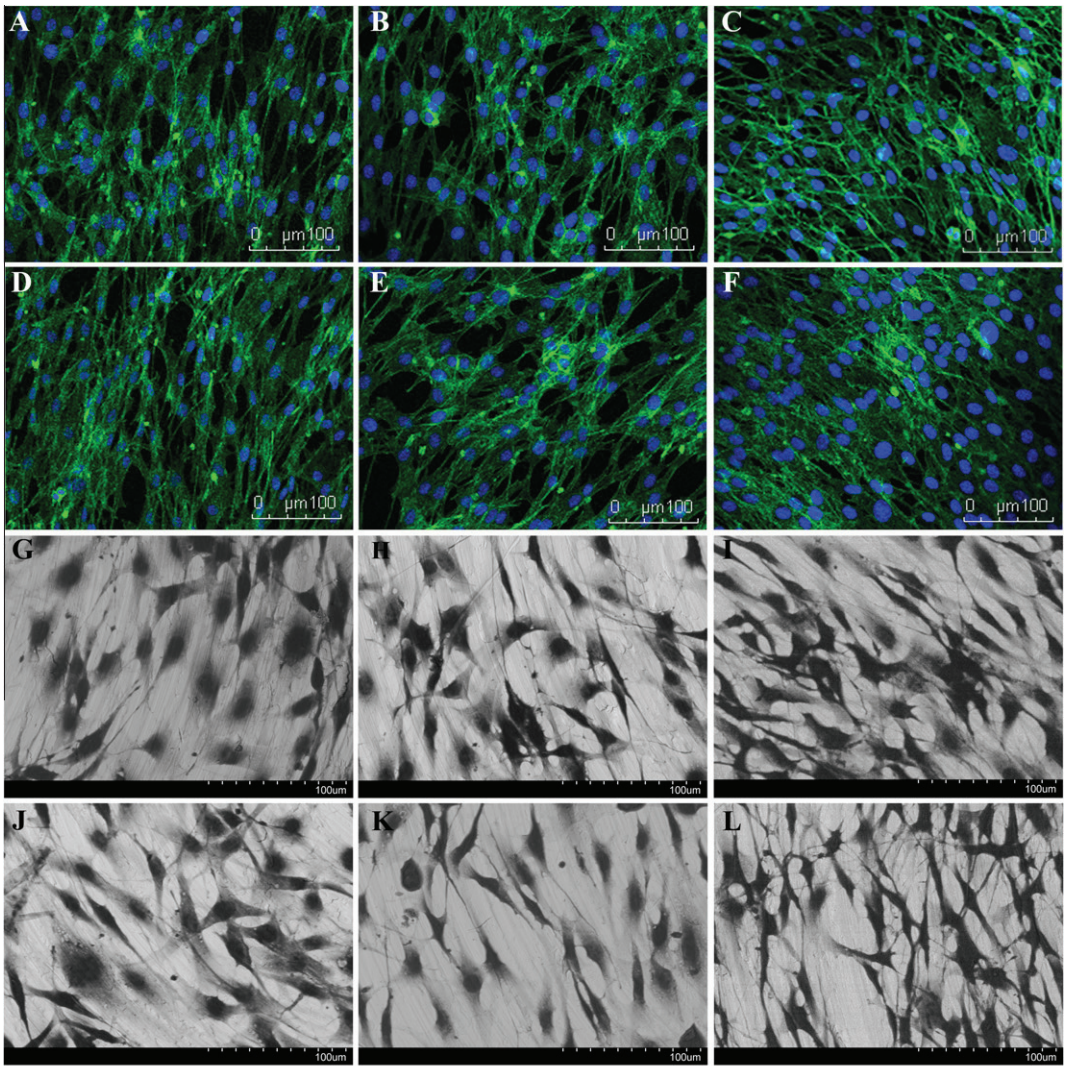

M

Coating	UV time exposure (min)	Cell number/implant (x 10^3)	% Implant surface covered with cells
7-DHC	0	18.9 ± 0.533	70.5 ± 2.15
	15	17.1 ± 0.546	76.3 ± 2.13
	30	21.6 ± 0.993[a]	78.3 ± 1.92[a]
Ethanol (Control)	0	18.3 ± 1.38	73.1 ± 2.06
	15	17.7 ± 1.07	70.9 ± 3.72
	30	21.8 ± 0.155[a]	80.0 ± 2.51

Fig. 6. Effect of UV time exposure of 7-DHC-coated Ti implants on cell number and cell morphology. Representative images obtained from confocal laser scanning microscope of MC3T3-E1 cells cultured for 48 h are shown. Cells were stained with phalloidin-FITC (stains actin filaments; green) and DAPI (stains nucleus, blue). 7-DHC treatment UV-exposed during (A) 0, (B) 15 and (C) 30 min, and ethanol (control) coating also UV-irradiated for (D) 0, (E) 15 and (F) 30 min. In the same way, representative SEM images after 48 h of cell culture. Both (G–I) 7-DHC and (J–L) ethanol coating for different long UV time exposures, (G, J) 0, (H, K) 15 and (I, L) 30 min. (M) Values represent the mean ± SE ($n = 5$) for total cell number per Ti implant and the percentage of Ti surface covered with MC3T3-E1 cells. Student's test ($p < 0.05$): [a]UV-treated vs. UV-untreated for 7-DHC and ethanol, respectively.

The first goal in the present investigation was to describe the conversion from 7-DHC to cholecalciferol with increasing UV irradiation times. As expected, none of the 7-DHC FTIR absorbance spectra after UV irradiation was completely similar to the absorbance spectrum of non-irradiated cholecalciferol, as it depends on the efficiency of the photochemical conversion and the appearance of several 7-DHC irradiation products. The FTIR spectra showed signs of changes in the ring structure, which are indicative of the ring opening reaction that converts 7-DHC to previtamin D_3 [34]. The appearance of –C=O groups indicated that other photo-oxidation products were also formed during UV irradiation, as reported earlier for oxidation of 7-DHC in benzene [35], but not for reactions in methanol [36]. As long irradiation times indicated photodegradation, short irradiation times up to 30 min were chosen for further testing in vitro. Irradiation times were carefully adjusted to enhance the formation of cholecalciferol using a UV source, but also to avoid the formation of degradation and/or undesired products from the UV-activated Ti surface. Ti is

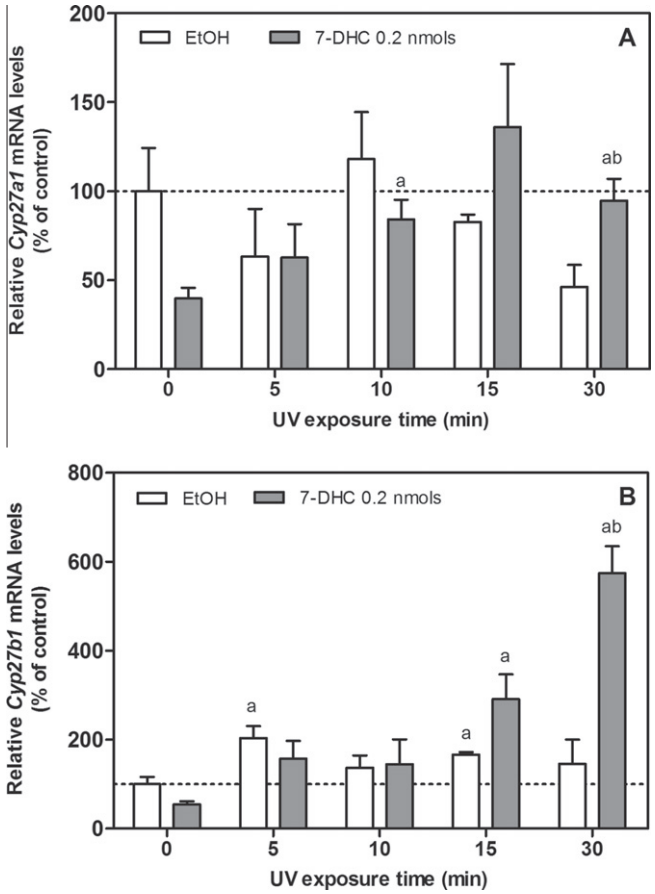

Fig. 7. Effect of UV time exposure of 7-DHC-coated Ti implants on gene expression of hydroxylase enzymes after 48 h of cell seeding. Data represent fold changes of target genes normalized to reference genes (*Gapdh*, *18S rRNA*), expressed as a percentage of the ethanol UV-untreated group, which was set to 100%. Values represent the mean ± SE ($n = 4$). Student's *t*-test ($p < 0.05$): [a]UV-treated vs. UV-untreated for 7-DHC and ethanol, respectively; [b]7-DHC treatment vs. the corresponding ethanol control at each UV irradiation time.

a well-known photocatalyst, and UV irradiation of Ti has been reported to result in surface sterilization and more biocompatible surfaces with increased wettability, as generation of electron–hole pairs leads to creation of reactive OH-groups on the surface, which then react with organic material [37]. HPLC analysis of UV irradiated 7-DHC-coated Ti surfaces confirmed the production of $preD_3$ with a 16.5 ± 0.9% product yield after 15 min of UV irradiation.

Several studies have reported conversion efficiencies of 7-DHC to previtamin D_3 and other photoproducts, under different irradiation and medium conditions. Few of the studies consulted reported also the final D_3 produced [38], which results from previtamin D_3 after thermal isomerization. Thus, Holick et al. [1] determined up to a 10% conversion of 7-DHC to previtamin D_3 when exposing 7-DHC ethanolic solutions to sunlight at various atmospheric conditions. MacLaughlin et al. [39] proposed an action spectrum for the conversion of 7-DHC to previtamin D_3 in the skin and reported up to a 65% conversion to previtamin D_3 at 295–300 nm irradiation wavelength. Norval et al. [40] calculated a 64% and 43% previtamin D_3 production in the photostationary state when irradiating 7-DHC at 300 nm or 305 nm, respectively [40].

Cytotoxicity was measured for the different conditions, and no toxic effect was found in any of them, demonstrating the biocompatibility of 7-DHC and UV-treated Ti surfaces in MC3T3-E1 osteoblasts. In fact, a higher cell number was observed after 30 min of UV irradiation, regardless of the coating, without differences in cell morphology. A tendency to increase cell proliferation with longer UV exposure time was reported earlier [36].

In addition, it was found that 25-D_3 release to the cell culture media was enhanced with UV-dose irradiation in the 7-DHC group, especially for 15 min of irradiation. At this time, 0.51 ± 0.07 pmol mm^{-2} of 25-D_3 in relation to the Ti surface area was released to the media after 48 h of cell culture. However, there was an important drop for samples irradiated for 30 min, which could probably be linked to the generation of photo-oxidation products. The gene expression profile of the hydroxylation enzymes Cyp27a1 and Cyp27b1 confirmed the effect of 7-DHC and UV irradiation with the resulting formation of 25-D_3. Thus, these results proved that the biological machinery to produce active vitamin D, which have been demonstrated previously on plastic TCP surfaces [20], is active in osteoblasts seeded on Ti surfaces. Moreover, 7-DHC treatment effect over time revealed the same expression pattern for the hydroxylase Cyp27a1 as for its product 25-D_3. The quantification by HPLC of $preD_3$ produced by 15 min irradiation of 7-DHC allowed calculation of a 34.2 ± 4.8% conversion of $preD_3$ to 25-D_3 by osteoblastic cells. Similar cellular conversion results were observed in an in vitro human skin equivalent model [41]. They found that cellular levels of D_3 and calcitriol after irradiation of culture media supplemented with 7-DHC at 297 nm and 16 h incubation at 37 °C were ~37% of the total amount of both D_3 and calcitriol formed in the original culture [41]. Thus, these results demonstrate that 15 min was a suitable UV exposure time to activate the vitamin D biosynthetic pathway on Ti disks under the conditions used.

Since vitamin D has been reported to increase osteoblast differentiation in vitro [17], the expression of several marker genes was analyzed. *Coll-1* decreased its expression when UV exposure time was increased in 7-DHC treated samples. This could be related to the progression of the cell towards differentiation, since this marker has been reported to decrease once the differentiation process starts [42]. This fact is also supported by the increase of relative *Alp* mRNA levels with increased UV exposure time in 7-DHC samples, which is linked to matrix maturation and differentiation processes [43]. However, although no significant differences were found for *Oc* and *Bmp-2* gene expression in the group treated with 7-DHC and UV irradiated for 15 min, a trend to increase their mRNA levels was observed. Moreover, after 21 days of cell culture, significantly higher ALP activity was found in this group compared with the control. Furthermore, Ca levels obtained from cell monolayer at 28 days of cell culture were the highest for this group with statistical differences compared with UV-untreated 7-DHC and control. Thus, with the evaluation of ALP activity and Ca content, it was possible to demonstrate an increased osteoblast differentiation in the UV-irradiated 7-DHC samples.

Bone resorption is stimulated by different factors, including 1,25-dihydroxyvitamin D_3 [44–46] and is controlled via osteoblastic cells [47,48]. Both Rankl and Opg have been proved to play a main role in osteoclastogenesis, and their ratio is a key factor for analysis in bone remodeling processes [49,50]. Data obtained from the present experiments revealed a significant and marked decrease of *Rankl* gene expression compared with control and UV-untreated 7-DHC groups, whereas *Opg* levels remained almost unchanged. This finding could point to an indirect regulation of osteoblasts decreasing osteoclastogenesis. Interestingly, a different response to vitamin D action has been suggested, depending on the osteoblastic differentiation stage. Hence, it has been reported that vitamin D decreases the Rankl/Opg ratio in mature osteoblasts, while it stimulates osteoclastogenesis through immature osteoblasts [48].

Although 1,25-dihydroxyvitamin D_3 is thought to be an important factor in osseointegration and fracture healing, there are not

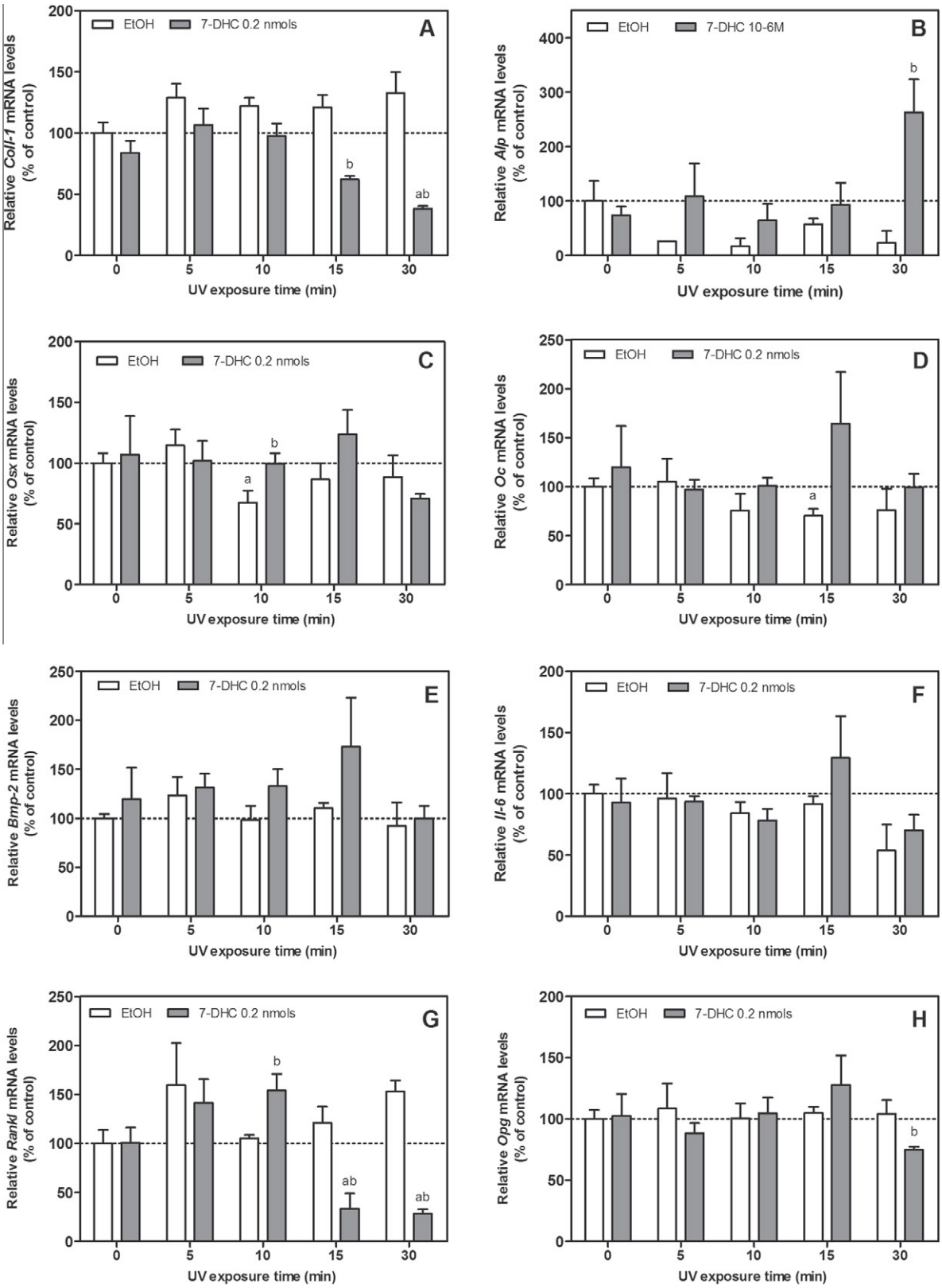

Fig. 8. Effect of UV time exposure of 7-DHC-coated Ti implants on osteoblast differentiation. Several bone markers (*Coll-1*, *Osx*, *Alp*, *Oc*, *Bmp-2*, *Il-6*, *Rankl* and *Opg*) were analyzed in MC3T3-E1 cells cultured for 48 h. Data represent fold changes of target genes normalized to reference genes (*Gapdh* and *18S rRNA*), expressed as a percentage of the EtOH UV-untreated group, which was set to 100%. Values represent the mean ± SE ($n = 4$). Student's *t*-test ($p < 0.05$): [a]UV-treated vs. UV-untreated for 7-DHC and ethanol, respectively; [b]7-DHC treatment vs. the corresponding ethanol control at each UV irradiation time.

many investigations into its mechanism of action. However, one study demonstrated that 1,25-dihydroxyvitamin D_3 was accumulated after fracture into the bony callus [51]. Recently, an ovariectomized rat model provided evidence that oral administration of

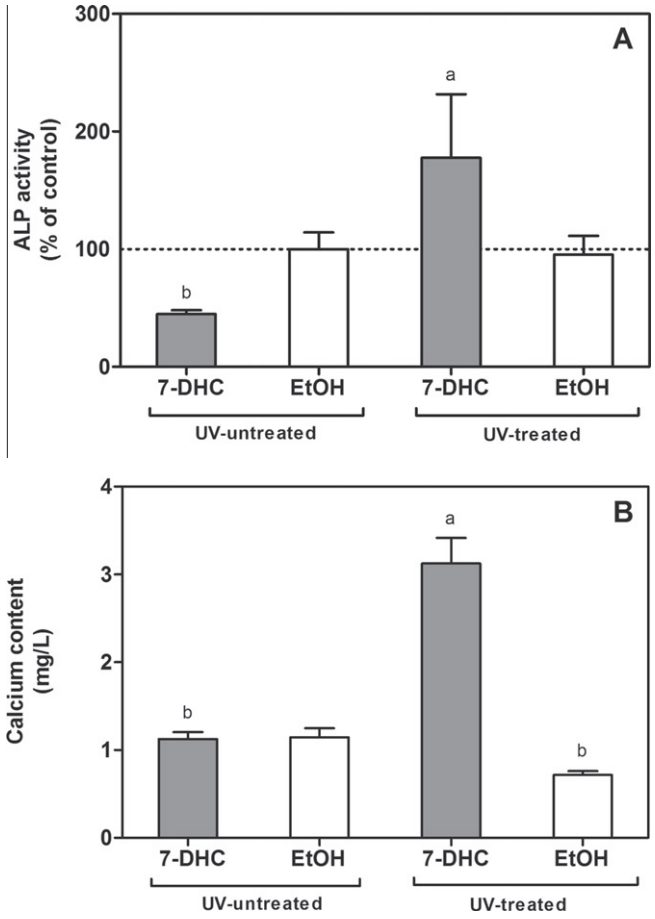

Fig. 9. Effect of 7-DHC and UV exposure of Ti implants on ALP activity and mineralization. (A) ALP activity measured at 21 days of MC3T3-E1 culture. Data were normalized to protein concentration and expressed as a percentage of the ethanol UV-untreated group, which was set to 100% ($n = 6$). (B) Ca content measured at 28 days of MC3T3-E1 culture. Values represent the mean ± SE ($n = 6$). Mann–Whitney test ($p < 0.05$): [a]UV-treated vs. UV-untreated for 7-DHC and ethanol, respectively; [b]7-DHC treatment vs. the corresponding ethanol control.

1,25-dihydroxyvitamin D_3 could increase the mechanical strength and microstructure of the fracture callus [52]. According to these results, some in vivo studies have revealed the relevant role of 1,25-dihydroxyvitamin D_3 on the osseointegration process. Indeed, vitamin D insufficiency in diet was reported to significantly impair the establishment of Ti6Al4V implant osseointegration in rat femur bones [22]. In addition, a later study performed in ovariectomized rats showed that the negative effect of vitamin D deficiency on cortical peri-implant bone formation could be compensated by vitamin D addition [21]. Since the results obtained in the present investigation describe only the in vitro osteoblastic cell response to Ti implants coated with UV-treated 7-DHC, no conclusions can be drawn regarding their potential in vivo performance. Thus, further research is ongoing to study their osseointegration in a validated animal model and its possible clinical application.

5. Conclusions

The present investigation showed for the first time the use of UV-activated 7-DHC to produce cholecalciferol locally at the surface of a titanium implant, which has been demonstrated to be a biocompatible and bioactive coating to increase differentiation of osteoblastic cells in vitro, as a result of endogenous cellular synthesis of the active form of vitamin D from cholecalciferol.

Disclosures

C.P and M.M. are inventors of a pending patent application based on some aspects of this work.

Acknowledgements

This work was supported by the the Ministerio de Ciencia e Innovación del Gobierno de España (Torres Quevedo contract to JMR, and Ramón y Cajal contract to MM) and Eureka-Eurostars Project Application E!5069 NewBone, Interempresas International Program (CIIP20101024) from the Centre for the Development of Industrial Technology (CDTI), Technology Funds from Invest in Spain (C2_10_32) and European Regional Development Fund (ERDF) from the European Union. Finally, the authors thank Mr. Ferran Hierro (University of the Balearic Islands) for his technical contribution with the scanning electron microscope.

Appendix A. Figures with essential colour discrimination

Certain figures in this article, particularly Figs. 4 and 6, is difficult to interpret in black and white. The full color images can be found in the on-line version, at http://dx.doi.org/10.1016/j.actbio.2012.11.021.

References

[1] Holick MF, Chen TC, Lu Z, Sauter E. Vitamin D and skin physiology: a D-lightful story. J Bone Miner Res 2007;22:V28–33.
[2] Kelley RI. Diagnosis of Smith–Lemli–Opitz syndrome by gas chromatography/mass spectrometry of 7-dehydrocholesterol in plasma, amniotic fluid and cultured skin fibroblasts. Clin Chim Acta 1995;236:45–58.
[3] MacLaughlin J, Holick MF. Aging decreases the capacity of human skin to produce vitamin D3. J Clin Invest 1985;76:1536–8.
[4] Tint GS, Irons M, Elias ER, Batta AK, Frieden R, Chen TS, et al. Defective cholesterol biosynthesis associated with the Smith–Lemli–Opitz syndrome. N Engl J Med 1994;330:107–13.
[5] Lehmann B, Meurer M. Extrarenal sites of calcitriol synthesis: the particular role of the skin. Recent Results Cancer Res 2003;164:135–45.
[6] Schuessler M, Astecker N, Herzig G, Vorisek G, Schuster I. Skin is an autonomous organ in synthesis, two-step activation and degradation of vitamin D3: CYP27 in epidermis completes the set of essential vitamin D3-hydroxylases. Steroids 2001;66:399–408.
[7] Bikle DD, Vitamin D. Regulated keratinocyte differentiation. J Cell Biochem 2004;92:436–44.
[8] Hollis BW. 25-Hydroxyvitamin D3–1α-hydroxylase in porcine hepatic tissue: subcellular localization to both mitochondria and microsomes. Proc Natl Acad Sci USA 1990;87:6009–13.
[9] Zehnder D, Bland R, Williams MC, McNinch RW, Howie AJ, Stewart PM, et al. Extrarenal expression of 25-hydroxyvitamin D3–1α-hydroxylase. J Clin Endocrinol Metab 2001;86:888–94.
[10] Adams JS, Beeker TG, Hongo T, Clemens TL. Constitutive expression of a vitamin D 1-hydroxylase in a myelomonocytic cell line: a model for studying 1,25-dihydroxyvitamin D production in vitro. J Bone Miner Res 1990;5:1265–9.
[11] Dusso AS, Finch J, Brown A, Ritter C, Delmez J, Schreiner G, et al. Extrarenal production of calcitriol in normal and uremic humans. J Clin Endocrinol Metab 1991;72:157–64.
[12] Hewison M, Freeman L, Hughes SV, Evans KN, Bland R, Eliopoulos AG, et al. Differential regulation of vitamin D receptor and its ligand in human monocyte-derived dendritic cells. J Immunol 2003;170:5382–90.
[13] Howard GA, Turner RT, Sherrard DJ, Baylink DJ. Human bone cells in culture metabolize 25-hydroxyvitamin D3 to 1,25-dihydroxyvitamin D3 and 24,25-dihydroxyvitamin D3. J Biol Chem 1981;256:7738–40.
[14] Ichikawa F, Sato K, Nanjo M, Nishii Y, Shinki T, Takahashi N, et al. Mouse primary osteoblasts express vitamin D3 25-hydroxylase mRNA and convert 1α-hydroxyvitamin D3 into 1α,25-dihydroxyvitamin D3. Bone 1995;16:129–35.
[15] Panda DK, Kawas SA, Seldin MF, Hendy GN, Goltzman D. 25-Hydroxyvitamin D 1α-hydroxylase: structure of the mouse gene, chromosomal assignment, and developmental expression. J Bone Miner Res 2001;16:46–56.
[16] Anderson PH, O'Loughlin PD, May BK, Morris HA. Modulation of CYP27B1 and CYP24 mRNA expression in bone is independent of circulating 1,25(OH)2D3 levels. Bone 2005;36:654–62.
[17] Van Driel M, Pols HAP, Van Leeuwen JPTM. Osteoblast differentiation and control by vitamin D and vitamin D metabolites. Curr Pharm Des 2004;10:2535–55.

[18] Van Driel M, Koedam M, Buurman CJ, Hewison M, Chiba H, Uitterlinden AG, et al. Evidence for auto/paracrine actions of vitamin D in bone: 1α-hydroxylase expression and activity in human bone cells. FASEB J 2006;20:E1811–9.
[19] Atkins GJ, Anderson PH, Findlay DM, Welldon KJ, Vincent C, Zannettino AC, et al. Metabolism of vitamin D3 in human osteoblasts: evidence for autocrine and paracrine activities of 1 alpha,25-dihydroxyvitamin D3. Bone 2007;40:1517–28.
[20] Satué M, Córdoba A, Ramis JM, Monjo M. UV-activated 7-dehydrocholesterol is converted to active vitamin D by osteoblastic MC3T3-E1 cells. Submitted for publication.
[21] Dvorak G, Fügl A, Watzek G, Tangl S, Pokorny P, Gruber R. Impact of dietary vitamin D on osseointegration in the ovariectomized rat. Clin Oral Implants Res 2011;23:1308–13.
[22] Kelly J, Lin A, Wang CJ, Park S, Nishimura I. Vitamin D and bone physiology: demonstration of vitamin D deficiency in an implant osseointegration rat model. J Prosthodont 2009;18:473–8.
[23] Glerup H, Mikkelsen K, Poulsen L, Hass E, Overbeck S, Thomsen J, et al. Commonly recommended daily intake of vitamin D is not sufficient if sunlight exposure is limited. J Intern Med 2000;247:260–8.
[24] Hall LM, Kimlin MG, Aronov PA, Hammock BD, Slusser JR, Woodhouse LR, et al. Vitamin D intake needed to maintain target serum 25-hydroxyvitamin D concentrations in participants with low sun exposure and dark skin pigmentation is substantially higher than current recommendations. J Nutr 2010;140:542–50.
[25] Macdonald HM, Mavroeidi A, Fraser WD, Darling AL, Black AJ, Aucott L, et al. Sunlight and dietary contributions to the seasonal vitamin D status of cohorts of healthy postmenopausal women living at northerly latitudes: a major cause for concern? Osteoporos Int 2011;22:2473–4.
[26] Chen TC, Persons KS, Lu Z, Mathieu JS, Holick MF. An evaluation of the biologic activity and vitamin D receptor binding affinity of the photoisomers of vitamin D3 and previtamin D3. J Nutr Biochem 2000;11:267–72.
[27] Lamolle SF, Monjo M, Rubert M, Haugen HJ, Lyngstadaas SP, Ellingsen JE. The effect of hydrofluoric acid treatment of titanium surface on nanostructural and chemical changes and the growth of MC3T3-E1 cells. Biomaterials 2009;30:736–42.
[28] Wootton AM. Improving the measurement of 25-hydroxyvitamin D. Clin Biochem Rev 2005;26:33–6.
[29] Brinker MR, O'Connor DP, Monla YT, Earthman TP. Metabolic and endocrine abnormalities in patients with nonunions. J Orthop Trauma 2007;21: 557–70.
[30] Palmquist A, Omar OM, Esposito M, Lausmaa J, Thomsen P. Titanium oral implants: surface characteristics, interface biology and clinical outcome. J R Soc Interface 2010;7:S515–27.
[31] Morra M, Cassinelli C, Cascardo G, Cahalan P, Cahalan L, Fini M, et al. Surface engineering of titanium by collagen immobilization. Surface characterization and in vitro and in vivo studies. Biomaterials 2003;24:4639–54.
[32] Ng JF, Weil T, Jaenicke S. Cationized bovine serum albumin with pendant RGD groups forms efficient biocoatings for cell adhesion. J Biomed Mater Res B Appl Biomater 2011;99B:282–90.
[33] Beikler T, Flemmig TF. Implants in the medically compromised patient. Crit Rev Oral Biol Med 2003;14:305–16.
[34] Socrates G. Infrared and raman characteristic group frequencies. 3rd ed. Chichester: John Wiley; 1999.
[35] Xu L, Korade Z, Porter NA. Oxysterols from free radical chain oxidation of 7-dehydrocholesterol: product and mechanistic studies. J Am Chem Soc 2010;132:2222–32.
[36] Anderson NA, Shiang JJ, Sension RJ. Subpicosecond ring opening of 7-dehydrochoiesterol studied by ultrafast spectroscopy. J Phys Chem A 1999;103:10730–6.
[37] Pacha-Olivenza MA, Gallardo-Moreno AM, Méndez-Vilas A, Bruque JM, González-Carrasco JL, González-Martín ML. Effect of UV irradiation on the surface Gibbs energy of Ti6Al4V and thermally oxidized Ti6Al4V. J Colloid Interface Sci 2008;320:117–24.
[38] Lehmann B, Knuschke P, Meurer M. UVB-induced conversion of 7-dehydrocholesterol to 1α,25-dihydroxyvitamin D3 (Calcitriol) in the human keratinocyte line HaCaT. Photochem Photobiol 2000;72:803–9.
[39] MacLaughlin JA, Anderson RR, Holick MF. Spectral character of sunlight modulates photosynthesis of previtamin D3 and its photoisomers in human skin. Science 1982;216:1001–3.
[40] Norval M, Bjorn LO, de Gruijl FR. Is the action spectrum for the UV-induced production of previtamin D-3 in human skin correct? Photochem Photobiol Sci 2010;9:11–7.
[41] Lehmann B, Genehr T, Knuschke P, Pietzsch J, Meurer M. UVB-induced conversion of 7-dehydrocholesterol to 1α,25-dihydroxyvitamin D3 in an in vitro human skin equivalent model. J Invest Dermatol 2001;117:1179–85.
[42] Stein GS, Lian JB, Stein JL, Van Wijnen AJ, Montecino M. Transcriptional control of osteoblast growth and differentiation. Physiol Rev 1996;76:593–629.
[43] Golub EE, Boesze-Battaglia K. The role of alkaline phosphatase in mineralization. Curr Opin Orthop 2007;18:444–8.
[44] Teti A, Volleth G, Carano A, Zambonin Zallone A. The effects of parathyroid hormone or 1,25-dihydroxyvitamin D3 on monocyte-osteoclast fusion. Calcif Tissue Int 1988;42:302–8.
[45] Flanagan AM, Stow MD, Kendall N, Brace W. The role of 1,25-dihydroxycholecalciferol and prostaglandin E2 in the regulation of human osteoclastic bone resorption in vitro. Int J Exp Pathol 1995;76:37–42.
[46] Suda T, Jimi E, Nakamura I, Takahashi N. Role of 1 alpha,25-dihydroxyvitamin D3 in osteoclast differentiation and function. Methods Enzymol 1997;282:223–35.
[47] Martin TJ, Ng KW. Mechanisms by which cells of the osteoblast lineage control osteoclast formation and activity. J Cell Biochem 1994;56:357–66.
[48] Baldock PA, Thomas GP, Hodge JM, Baker SU, Dressel U, O'Loughlin PD, et al. Vitamin D action and regulation of bone remodeling: suppression of osteoclastogenesis by the mature osteoblast. J Bone Miner Res 2006;21:1618–26.
[49] Horwood NJ, Elliott J, Martin TJ, Gillespie MT. Osteotropic agents regulate the expression of osteoclast differentiation factor and osteoprotegerin in osteoblastic stromal cells. Endocrinology 1998;139:4743–6.
[50] Suda T, Takahashi N, Udagawa N, Jimi E, Gillespie MT, Martin TJ. Modulation of osteoclast differentiation and function by the new members of the tumor necrosis factor receptor and ligand families. Endocr Rev 1999;20:345–57.
[51] Jingushi S, Iwaki A, Higuchi O, Azuma Y, Ohta T, Shida JI, et al. Serum 1α,25-dihydroxyvitamin D3 accumulates into the fracture callus during rat femoral fracture healing. Endocrinology 1998;139:1467–73.
[52] Fu L, Tang T, Miao Y, Hao Y, Dai K. Effect of 1,25-dihydroxy vitamin D3 on fracture healing and bone remodeling in ovariectomized rat femora. Bone 2009;44:893–8.

Paper III

UV-activated 7-dehydrocholesterol coated titanium implants promote differentiation of human umbilical cord mesenchymal stem cells into osteoblasts

Satué M. ; Ramis J.M. ; Monjo M.

Journal of Biomaterials Applications (2015), doi:10.1177/0885328215582324.

Functional biomaterials surfaces

JOURNAL OF
biomaterials
applications

Journal of Biomaterials Applications
0(0) 1–10

DOI: 10.1177/0885328215582324
jba.sagepub.com
SAGE

UV-activated 7-dehydrocholesterol-coated titanium implants promote differentiation of human umbilical cord mesenchymal stem cells into osteoblasts

María Satué, Joana M Ramis and Marta Monjo

Abstract

Vitamin D metabolites are essential for bone regeneration and mineral homeostasis. The vitamin D precursor 7-dehydrocholesterol can be used after UV irradiation to locally produce active vitamin D by osteoblastic cells. Furthermore, UV-irradiated 7-dehydrocholesterol is a biocompatible coating for titanium implants with positive effects on osteoblast differentiation. In this study, we examined the impact of titanium implants surfaces coated with UV-irradiated 7-dehydrocholesterol on the osteogenic differentiation of human umbilical cord mesenchymal stem cells. First, the synthesis of cholecalciferol (D_3) was achieved through the incubation of the UV-activated 7-dehydrocholesterol coating for 48 h at 23°C. Further, we investigated *in vitro* the biocompatibility of this coating in human umbilical cord mesenchymal stem cells and its potential to enhance their differentiation towards the osteogenic lineage. Human umbilical cord mesenchymal stem cells cultured onto UV-irradiated 7-dehydrocholesterol-coated titanium implants surfaces, combined with osteogenic supplements, upregulated the gene expression of several osteogenic markers and showed higher alkaline phosphatase activity and calcein blue staining, suggesting increased mineralization. Thus, our results show that the use of UV irradiation on 7-dehydrocholesterol -treated titanium implants surfaces generates a bioactive coating that promotes the osteogenic differentiation of human umbilical cord mesenchymal stem cells, with regenerative potential for improving osseointegration in titanium-based bone anchored implants.

Keywords

7-Dehydrocholesterol, UV irradiation, vitamin D, titanium implant, mesenchymal stem cells, osteogenic differentiation

Introduction

Numerous investigations endorse the extremely important role of vitamin D in maintaining a healthy and mineralized skeleton given its essential function in calcium and phosphate homeostasis and in promoting bone mineralization. Although the major source of vitamin D synthesis comes from the ultraviolet (UV) irradiation of 7-DHC, which is naturally found in our skin and further processed in the liver and kidney, there are evidences for extra renal synthesis of active vitamin D, 1,25-dihydroxyvitamin D_3 (1,25-D_3).[1–3] Indeed, we have demonstrated that 7-DHC can be used to locally produce active vitamin D by osteoblastic cells, when 7-DHC is coated onto a tissue culture plastic (TCP) surface and UV irradiated before the cell culture.[4] Furthermore, we have also developed a bioactive coating on titanium, based on UV-activated 7-DHC, which allows preosteoblastic cells to produce themselves active 1,25-D_3, with demonstrated positive effects on osteoblast differentiation *in vitro*.[5]

Human mesenchymal stem cells (hMSCs) have gained increasing interest in the past years for their therapeutic potential in regenerative medicine.

Department of Fundamental Biology and Health Sciences, Research Institute on Health Sciences (IUNICS), University of Balearic Islands, Palma de Mallorca, Spain; Instituto de Investigación Sanitaria de Palma, Palma de Mallorca, Spain

Corresponding author:
Marta Monjo, Research Institute on Health Sciences (IUNICS), University of Balearic Islands, Ctra. de Valldemossa, Palma de Mallorca 07122, Spain.
Email: marta.monjo@uib.es

These multipotent cells are able to self-renew and differentiate into a variety of cell types, such as osteoblasts, chondrocytes or adipocytes.[6–8] Interestingly, hMSCs have been described in virtually all post-natal tissues[9] and also in umbilical cord[10] and placenta.[11] Furthermore, their efficiency in different types of therapeutic strategies has been already demonstrated, including bone tissue regenerative approaches.[12–15] Although the mechanism by which these cells undergo commitment to one of the different mesenchymal lineages is not completely understood, it is believed to depend on the applied stimulus. Thus, several growth factors and hormones have been identified as specific lineage regulators, such as 1,25-D_3, which enhances both early and late stage markers of osteoblast differentiation in hMSCs.[16–18]

Since titanium implants (Ti) implants coated with UV-irradiated 7-DHC have already shown positive effects on preosteoblast differentiation *in vitro*,[5] we here hypothesized that these bioactive surfaces could also promote the osteogenic differentiation of hMSCs. Therefore, human umbilical cord-derived mesenchymal stem cells (hUC-MSCs) were used to evaluate the osteopromotive action of the UV-irradiated 7-DHC-coated implants. The biological response of hUC-MSCs to the bioactive surfaces was tested in terms of cytotoxicity, cell morphology, gene expression analysis of several makers related to osteoblast differentiation and finally, alkaline phosphatase (ALP) activity and staining of mineralized nodule, to examine osteoblast function.

Experimental

Treatment of titanium surfaces

Stock solutions of 7-DHC (Sigma, St. Louis, MO, USA) and cholecalciferol (D_3, Sigma, St. Louis, MO, USA) were prepared in absolute ethanol and filtered with a 0.22 μm pore size filter before use. Ti disks used were all made of grade 2 Ti with a diameter of 6.25 mm and a height of 1.95 mm. For the surface modification of Ti disks, 10 μl of 7-DHC (0.2 nmol/Ti disk) was dropped onto the Ti disks and UV irradiated using a UV lamp of 302 nm with an intensity of irradiation of 6 mW/cm^2 (UVP, Upland, CA, USA) for 15 min, as defined in a previous work.[4] Once irradiated, the Ti surfaces were incubated for 48 h at 23°C in the absence of light in order to stimulate the D_3 synthesis. Additionally, D_3 (75 pmol/Ti disk; expected equivalent dose of D_3 formed in UV-irradiated 7-DHC) and UV-irradiated ethanol were used as controls. Ti disks were processed to analyze their coating composition by HPLC or used for the *in vitro* experiments.

Determination of the D3 synthesis from UV-irradiated 7-DHC by HPLC

The amount of 7-DHC, preD_3 and D_3 on the surface was quantified by HPLC just after the UV irradiation and after 48 h of incubation post-irradiation as described elsewhere.[5]

All solvents used were of HPLC or analytical grade. Methanol (HPLC gradient grade), acetonitrile and tetrahydrofurane (both HPLC grade) were purchased from Fisher Scientific (Thermo Fisher Scientific, MA, USA). High-purity deionized Milli-Q water was obtained from a Millipore system (Millipore Corporation, Billerica, MA, USA). Absolute ethanol was purchased from Scharlab (Barcelona, Spain).

Isolation and culture of hUC-MSCs

hUC-MSCs were isolated from umbilical cords obtained in the process of human umbilical cord blood donation under the Concordia Cord Blood Donation Program. The samples were obtained after informed consent and with the approval of the Ethical Committee of Balearic Islands (CEIC-IB). Isolation of hUC-MSCs was performed as described in literature.[19]

Variables among different donors must be taken into account when using primary cells. For this reason and to improve validity of our data, we used two different donors. hUC-MSCs were seeded onto the modified implants at a density of 4.7×10^4 cell/cm^2 in a "growing media" consisting of DMEM/Glutamax/Low glucose, supplemented with penicillin (50 IU/ml), streptomycin (50 μg streptomycin/ml) and 20% fetal bovine serum (HyClone) under standard cell culture. Cells were also grown onto untreated TCP as a control. At confluence, "differentiation media" consisting of growing media supplemented with dexamethasone (10 nM), ascorbic acid (50 μg/ml) and β-glycerophosphate (10 mM) were used. Culture media were collected 48 h after cell seeding to test cytotoxicity. Cell morphology was also evaluated by confocal microscopy 48 h after seeding. Further, cells were harvested at days 5 and 14 of culture to analyze their gene expression levels of several osteogenic markers by real-time RT-PCR. Finally, hUC-MSCs cells were cultured for 21 days to analyze the ALP activity and stained with calcein blue to detect the formation of mineralized nodules.

Cell viability assay

Lactate dehydrogenase (LDH) activity in the culture media 48 h after cell seeding was used as an index of cell death. The LDH activity was estimated according to the manufacturer's kit instructions

(Roche Diagnostics, Mannheim, Germany) by assessing the rate of oxidation of NADH at 490 nm in the presence of pyruvate. Results were presented relative to the LDH activity in the media of cells seeded on TCP without treatment (negative control, 0% of cell death) and of cells grown on TCP treated with 1% Triton X-100 (positive control, 100% cell death). Eighteen samples were used for each group. The percentage of LDH activity was calculated using the following equation: Cytotoxicity (%) = (exp. value − negative control)/(positive control − negative control) × 100.

Cell morphology analysis

Confocal images of cells grown onto modified Ti disks were obtained after 48 h of cell culture. Cells were first fixed and then permeabilized and further stained with Phalloidin-FITC (50 $\mu g\,ml^{-1}$; Sigma, St. Louis, MO, USA) to stain actin filaments. Finally, a drop of Fluoroshield-DAPI (Sigma, St. Louis, MO, USA) was added to stain the cell nuclei. Various images of each implant were taken with the confocal microscope (Leica DMI 4000B equipped with a Leica TCS SPE laser system) by measuring the fluorescence signal between 430 and 480 nm for DAPI and 500 and 525 nm for Phalloidin-FITC.

RNA isolation and real-time RT-PCR analysis

RNA was isolated from cells using a monophasic solution of phenol and guanidine thiocyanate (Tripure, Roche Diagnostics, Mannheim, Germany) according to the manufacturer's protocol. RNA was quantified at 260 nm using a Nanodrop spectrophotometer (NanoDrop Technologies, Wilmington, DE, USA).

Total RNA previously isolated was reverse-transcribed to cDNA using High Capacity RNA to cDNA kit (Applied Biosystems, Foster City, CA) according to the protocol of the supplier. The same amount of total RNA from each sample was converted into cDNA.

Real-time RT-PCR was performed for two reference genes: beta-actin (β-ACTIN) and glyceraldehyde-3-phosphate dehydrogenase (GAPDH) and six osteogenic target genes: collagen type I (COLL-I), runt-related transcription factor (RUNX2), osteocalcin (OC), bone morphogenetic protein 2 (BMP2), osteonectin (SPARC) and osteopontin (SPP1). Nine samples for each group were used for the RT-PCR analyses after 5 days of cell culture while twelve samples per group were used for the RT-PCR analyses after 14 days of cell culture.

The reactions were performed in the Lightcycler 480® (Roche Diagnostics, Germany). Each reaction contained 500 nM of the corresponding oligonucleotide primers (Table 1), 5 µl of LightCycler-FastStart DNA MasterPLUS SYBR Green I (Roche Diagnostics, Mannheim, Germany) and 3 µl of the cDNA dilution in a final volume of 10 µl. The normal amplification program consisted of a pre-incubation step for denaturation of the template cDNA (10 min 95°C), followed by 45 cycles consisting of a denaturation step (10 s 95°C), an annealing step (10 s 60°C, except for OC, which was 10 s at 68°C) and an extension step (10 s 72°C). After each cycle, fluorescence was measured at 72°C. Every run included a negative control without cDNA template. To confirm amplification specificity, PCR products were subjected to a melting curve analysis on the LightCycler and subsequently 2% agarose/TAE gel electrophoresis, Tm and amplicon size, respectively.

Real-time efficiencies (E) were calculated from the given slopes in the LightCycler 480 software using serial dilutions, showing all the investigated transcripts high real-time PCR efficiency rates, and high linearity when different concentrations were used.

All samples were normalized by the geometric mean of the expression levels of *β-actin*, and *Gapdh* and fold

Table 1. Primer sequences used for real time RT-PCR.

Gene	Sequences	Product size	Accession number
BMP-2	S: CCT GAA ACA GAG ACC CAC CC AS: TCT CCG GGT TGT TTT CCC AC	208 bp	NM_001200.2
COLL-I	S: CCT GAC GCA CGG CCA AGA GG AS: GGC AGG GCT CGG GTT TCC AC	122 bp	NM_000088.3
OC	S: GAA GCC CAG CGG TGC A AS: CAC TAC CTC GCT GCC CTC C	70 bp	NM_199173
RUNX2	S: CTG TGC TCG GTG CTG CCC TC AS: CGT TAC CCG CCA TGA CAG TA	118 bp	NM_004348
SPARC	S: GCG GTC CTT CAG ACT GCC CG AS: CTT GCT GAG GGG CTG CCA AGG	138 bp	NM_003118
SPP1	S: ATG ATG GCC GAG GTG ATA GT AS: ACC ATT CAA CTC CTC GCT TT	134 bp	AF052124.1
β-ACTIN	S: CTG GAA CGG TGA AGG TGACA AS: AAG GGA CTT CCT GTA ACA A	140 bp	NM_001101
GAPDH	S: TGC ACC ACC AAC TGC TTA GC AS: GGC ATG GAC TGT GGT CAT GAG	87 bp	NM_002046

Note: Product size and accession number are also indicated.

changes were related to the control group using the mathematical model described by Pfaffl[20]: $\text{ratio} = E_{\text{target}}^{\Delta Cp \text{ target (mean control} - \text{sample)}} / E_{\text{reference}}^{\Delta Cp \text{ reference (mean control} - \text{sample)}}$, where Cp is the crossing point of the reaction amplification curve as determined by the LightCycler 480 software. Stability of reference genes was calculated using the BestKeeper tool.[21] A good consistence of the bestkeeper index was proved as its contributing reference genes were tightly correlated with it, with a significance level of $p = 0.001$ for all reference genes.

ALP activity analysis

Cell monolayers were collected at 21 days of cell culture in order to determine ALP activity. Proteins were solubilized by adding PBS containing 0.1% Triton X-100. Then, cell lysates were put into freeze/thaw cycles to improve protein recovery. After centrifugation at 33,000 *g* for 15 min at 4°C, supernatants were acquired and assayed for ALP activity. The method used measures the cleavage of p-nitrophenyl phosphate (pNPP; Sigma, St. Louis, MO, USA) in a soluble yellow end product which absorbs at 405 nm. A volume of 100 µl of this substrate was used in combination with 25 µl of each sample supernatant (10 samples for each group were used) or standard point. The standard curve was prepared from calf intestinal alkaline phosphatase (CIAP, 1 U/µl) (Promega, Madison, WI, USA) by mixing 1 µl from the stock CIAP with 5 ml of alkaline phosphatase buffer (1:5000 dilution), and then making 1:5 serial dilutions. Once the reaction was carried out, after 30 min in dark at room temperature, it was stopped with the addition of 50 µl of 3 M sodium hydroxide. Finally, absorbance was read at 405 nm.

Calcein blue staining

After 21 days of cell culture, bone-like nodule formation in hUC-MSCs was evaluated. To perform this assay, 10 mg of calcein blue was dissolved in 0.25 ml of KOH (1 M) and further 9.75 ml of distilled water was added to make up a 3.1×10^{-3} M calcein blue solution, as indicated in literature[22]; 15 µl of the solution was added to the culture media achieving a final concentration of calcein blue of 3.1×10^{-5} M and then incubated for 1 h at room temperature. Cells were washed with PBS and further fixed with 3.7% formaldehyde in PBS for 10 min. Cells were then washed with PBS and dried. Various images of each implant were taken using a confocal microscope (Leica DMI 4000B equipped with a Leica TCS SPE laser system) by measuring the fluorescence signal between 430 and 480 nm.

Statistics

All data are presented as mean values ± standard error of the mean (SEM). The Kolmogorov-Smirnov test was done to assume parametric or non-parametric distributions for the normality tests. Differences between groups were assessed by Mann-Whitney-test, Student's t-test or by paired t-test. The SPSS® program for Windows, version 17.0 (SPSS, Chicago, IL, US) was used. Results were considered statistically significant at p-values ≤ 0.05.

Results

D_3 production from UV-irradiated 7-DHC-coated Ti disks

We found that while preD_3 and lumisterol were formed immediately after UV irradiation (Figure 1(a)), D_3 was produced in sufficient amount (32.35 ± 4.16 pmol of D_3) after 48 h of incubation at 23°C (Figure 1(b)). In the case of D_3 control surfaces, HPLC analysis determined 48.68 ± 3.29 pmol of D_3 per Ti implant. Therefore, the mentioned surfaces previously coated with UV-irradiated 7-DHC and further incubated for 48 h at 23°C were analyzed for their osteopromotive potential in hUC-MSCs.

Cell viability and cell morphology

The effect of UV-irradiated 7-DHC-coated Ti disks on hUC-MSC cell cytotoxicity after 48 h was investigated and compared with control surfaces. Cells were also cultured on TCP to have the positive and negative control for cytotoxicity. Figure 2(a) shows that UV-irradiated 7-DHC coating increased the LDH activity in the culture media although values were relatively low, with 12.9 ± 2.9%. Indeed, at this time point, we also examined the cell morphology induced by each condition. As observed in Figure 2(b), hUC-MSCs seeded onto UV-irradiated 7-DHC-coated Ti disks showed their typical fibroblastic morphology as well as cells seeded onto EtOH and D_3 control surfaces. Thus, these findings confirmed that UV-irradiated 7-DHC-coated surfaces were biocompatible in hUC-MSCs.

mRNA levels of different osteogenic markers

The effect of UV-irradiated 7-DHC-coated Ti disks on mRNA levels of different markers was analyzed by real-time RT-PCR after 5 (Figure 3) and 14 days (Figure 4) of cell culture. Six different osteogenic markers were analyzed including COLL-I, RUNX2, OC, BMP2, SPARC and SPP1.

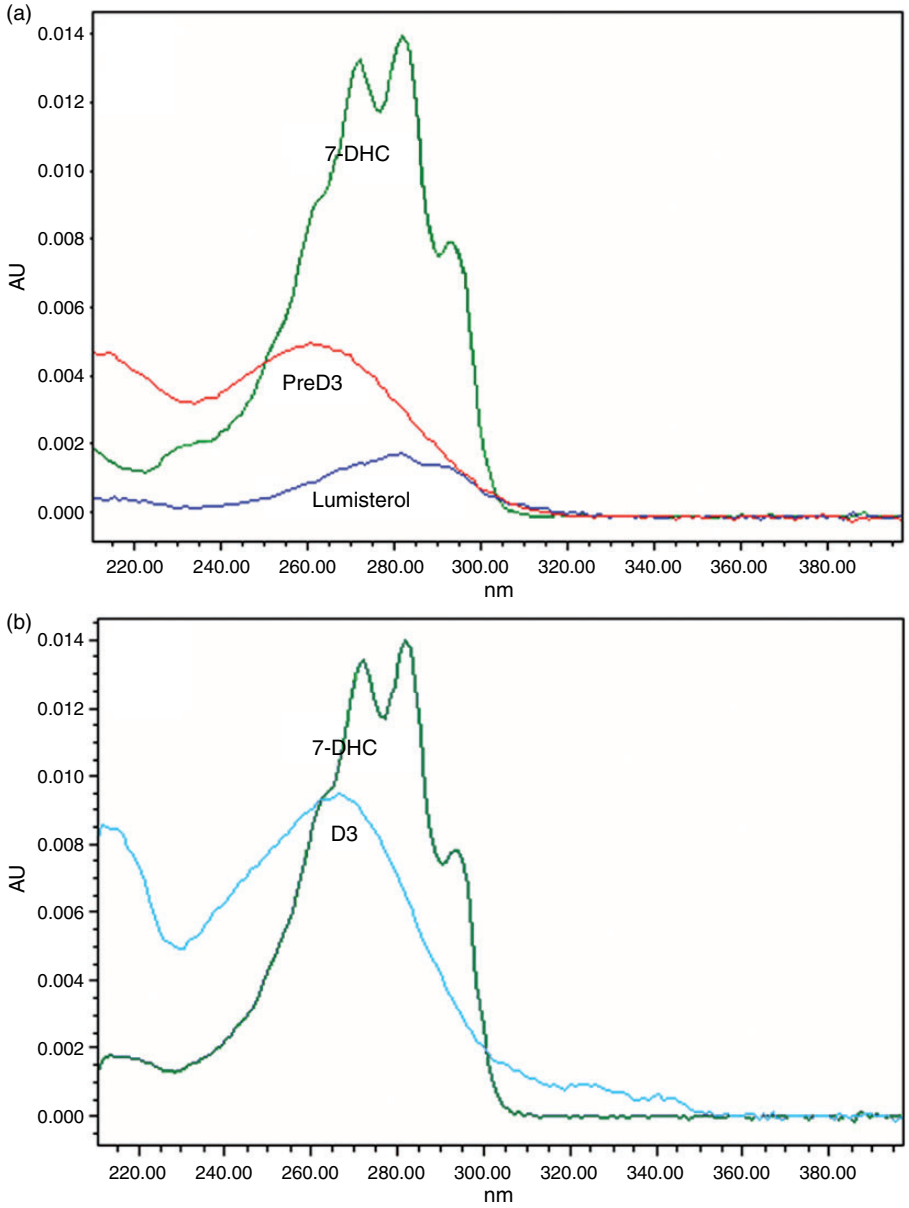

Figure 1. Quantification of the coating composition of UV-irradiated 7-DHC-coated Ti disks. (a) Absorption spectra of preD_3 (260.4 nm), lumisterol (280.6 nm) and 7-DHC (281.8 nm) immediately after UV activation of the 7-DHC coating. (b) Absorption spectra of D_3 (266.3 nm) and 7-DHC (281.8 nm) after previous UV irradiation and further incubation for 48 h at 23°C.

After five days of treatment (Figure 3), UV-irradiated 7-DHC-coated Ti disks induced higher COLL-1 mRNA expression levels than EtOH control, similar to D_3 control. In the same way, a trend to increase RUNX2 gene expression in UV-irradiated 7-DHC surfaces was found although it was only significantly enhanced in D_3 control. There was also a tendency to increase OC mRNA levels in both UV-irradiated 7-DHC and D_3-coated surfaces but statistical significance was not reached. Finally, the gene expression levels of BMP-2, SPARC and SPP1 in both UV-irradiated 7-DHC and D_3 surfaces were similar to EtOH control.

Interestingly, after 14 days of treatment (Figure 4), COLL-1, RUNX2, OC, BMP2 and SPARC mRNA levels were higher in cells cultured onto UV-irradiated 7-DHC and D_3-coated surfaces than cells cultured onto EtOH control surfaces. Also, a trend to increase the SPP1 mRNA levels was found in UV-irradiated 7-DHC and D_3-coated surfaces but significant differences were only found for UV-irradiated 7-DHC.

ALP activity and mineralization staining

To investigate the effect of UV-irradiated 7-DHC-coated Ti disks on terminal osteoblast differentiation,

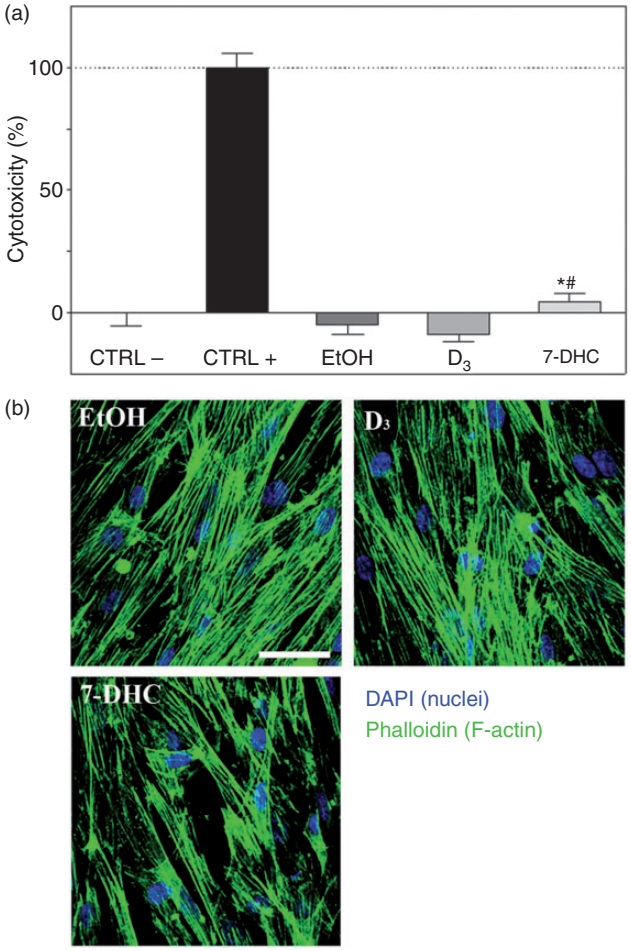

Figure 2. Effect of UV-activated 7-DHC-coated Ti disks on cell viability and morphology. (a) LDH activity measured from cell supernatants after 48 h of cell culture. Values were calculated using the following equation:
Cytotoxicity(%) = (exp.value−negative control)/(positive control−negative control) × 100. Positive control (100% cytotoxicity) was culture media from cells treated with 1% Triton X-100. Negative control (0% cytotoxicity) was culture media from control vehicle cells. Values represent the mean ± SEM (18 samples were used for each group). Differences between groups were assessed by Mann-Whitney test ($p < 0.05$): *7-DHC versus EtOH control; and # 7-DHC versus D_3. (b) Cell morphology of treated cells after 48 h of cell culture. Representative images were obtained using confocal laser scanning microscope.
Bar scale = 50 μm.

ALP activity was measured in the cell monolayer on day 21 of cell culture (Figure 5(a)). Results revealed that cells cultured onto UV-irradiated 7-DHC-coated Ti disks induced a significantly higher ALP activity than the EtOH control group. In the same way, D_3 control also showed higher ALP activity than EtOH.

Finally, matrix mineralization was qualitatively evaluated in order to confirm the previous findings after 21 days of cell culture using Calcein Blue fluorescent staining (Figure 5(b) to 5(d)). In agreement to the ALP activity results, more mineralization nodules were observed in cells seeded onto UV-irradiated 7-DHC and D_3 coatings than onto EtOH control surfaces, supporting a promotive action of these bioactive implants towards the osteogenic lineage in hUC-MSCs.

Discussion

There is a great interest in the extrarenal synthesis of vitamin D and its consequent biological potential, especially for the bone microenvironment.[3] Accordingly, we previously demonstrated that MC3T3-E1 osteoblasts were able to produce themselves final active vitamin D from UV-irradiated 7-DHC.[4] In the same way as osteoblastic cells, hMSCs are known to possess the necessary molecular machinery to both respond and form the active vitamin D metabolite, 1,25-D_3.[23] Thus, hMSCs express the VDR and vitamin D hydroxylases (CYP27A1, CYP27B1, CYP24A1 and CYP2R1) that regulate the concentration of final active 1,25-D_3.[24]

In the last years, a high prevalence of vitamin D deficiency has been found across all age groups worldwide, having a profound negative effect on osseointegration.[25,26] Although vitamin D supplementation is being used as a therapy to maintain bone mineral density,[27–29] giving cells the vitamin D precursor to locally synthesize themselves final active vitamin D could be more effective in the modulation of the osseointegrative properties of the implant. Therefore, we aimed at developing a biocompatible and bioactive coating using UV-irradiated 7-DHC for bone anchored implants, which could promote osteogenic differentiation of MSCs. Furthermore, this coating would lead to other important advantages than using other hydroxylated forms of vitamin D; for instance, it would be cheaper to produce, since 7-DHC is easily available and low-priced compared to 1,25-D_3.

The synthesis of 1,25-D_3 from 7-DHC involves a complex pathway. It starts when 7-DHC is UV-irradiated resulting in the formation of preD_3, which further isomerizes to D_3. This last reaction is time and temperature dependent.[30–32] According to these studies, we incubated the UV-activated 7-DHC-coated Ti disks at 23°C for 48 h in order to favor the formation of our target metabolite, D_3. Indeed, we managed to promote the conversion from preD_3 to D_3 when adding this incubation step, achieving a coating formed by 32.35 ± 4.16 pmol of D_3 per Ti implant.

UV-irradiated 7-DHC is a biocompatible coating for Ti disks with positive effects on MC3T3-E1 osteoblast differentiation *in vitro*,[5] but its effect on MSCs was

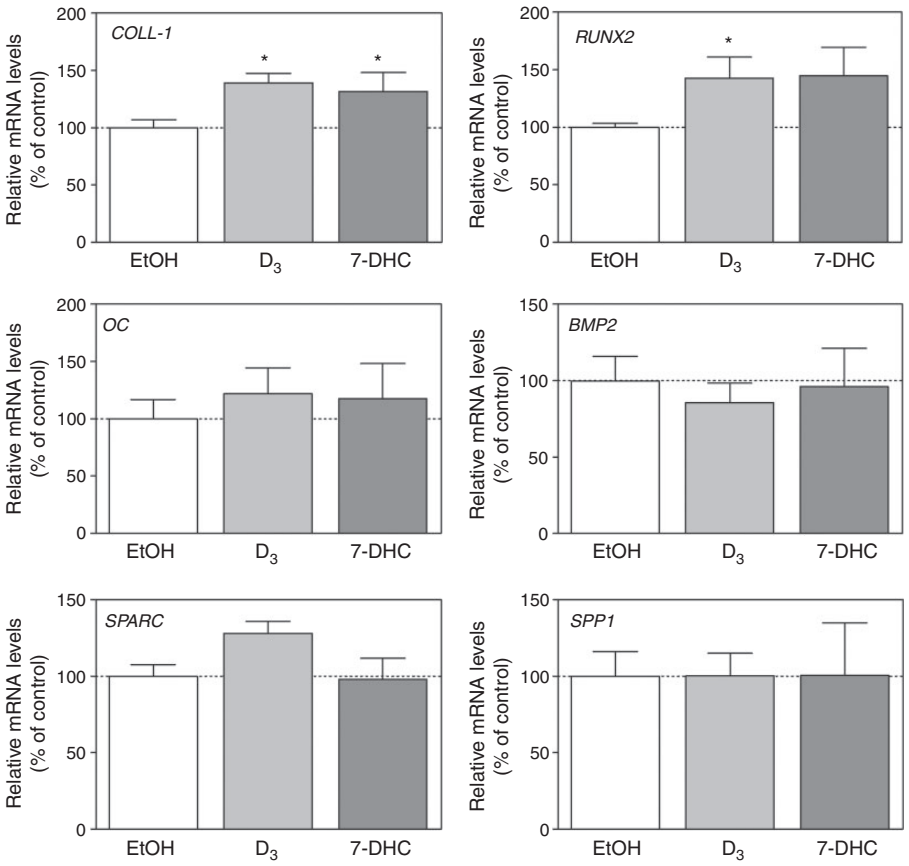

Figure 3. Effect of UV-activated 7-DHC-coated Ti disks on the mRNA expression levels of osteogenic markers in hUC-MSCs cultured for five days. Data were normalized to reference genes (*Gapdh* and *18 S rRNA*), expressed as percentage of control which was set to 100%. Values represent the mean ± SEM (9 samples were used for each group). Paired t-test was performed to assess differences between groups: $*p < 0.05$ treatment versus EtOH control.

unknown. These cells have huge potential and its appeal leads in the fact that MSCs are the main source of osteoprogenitor cells. Indeed, they are involved in normal skeletal homeostasis[33] and in bone reparative mechanisms.[34] Thus, hUC-MSCs provide a multipotent cell source capable to differentiate into osteoblasts when cultured with osteogenic supplements.[35] Also, vitamin D supplementation is known to promote osteoblast differentiation of hMSCs *in vitro*.[17,24,36–38] Indeed, all three metabolites (D_3, 25-D_3, and 1,25-D_3) have been suggested to stimulate *in vitro* osteoblastogenesis in hMSCs.[24] On the basis of that, we investigated the biological effect of D_3-coated implants, previously synthesized from UV-irradiated 7-DHC, on the osteogenic differentiation of hUC-MSCs.

First, we evaluated the cytotoxic effect of the surfaces and the cell morphology appearance after 48 h of cell culture. This coating showed higher LDH activity in hUC-MSCs but values were low with 12.9 ± 2.9%. In fact, the cell morphology observed in all treated surfaces corresponded to that which is typical of hUC-MSC, with thin fibroblastic cells. Thus, these findings confirmed the biocompatibility of Ti disks coated with UV-irradiated 7-DHC in these cells, in agreement with results obtained with MC3T3-E1 osteoblasts.[5]

Previous investigations demonstrate that vitamin D is required in human osteoblasts for their correct bone matrix mineralization.[39] Furthermore, 1,25-D_3 regulates the expression of other bone markers like COLL1, RUNX2 and OC,[40,41] reinforcing its role in the osteogenic differentiation. Experiments using human embryonic stem cells (hESCs) have shown that treatment with 1,25-D_3 increases COLL1, RUNX2, OC, SPARC and SPP1 when cells are cultured in an osteogenic induction medium.[42] In the same way, 1,25-D_3 also accelerates osteoblast differentiation of hMSCs, increasing COLL1, OC and SPP1.[43,44] With this aim, we evaluated the gene expression levels of several osteogenic markers (COLL1, RUNX2, OC, BMP2, SPARC and SPP1), ALP activity and nodule mineralization. In our study, we found that after 14 days of cell culture COLL1, RUNX2, BMP2, OC, SPARC and SPP1 were

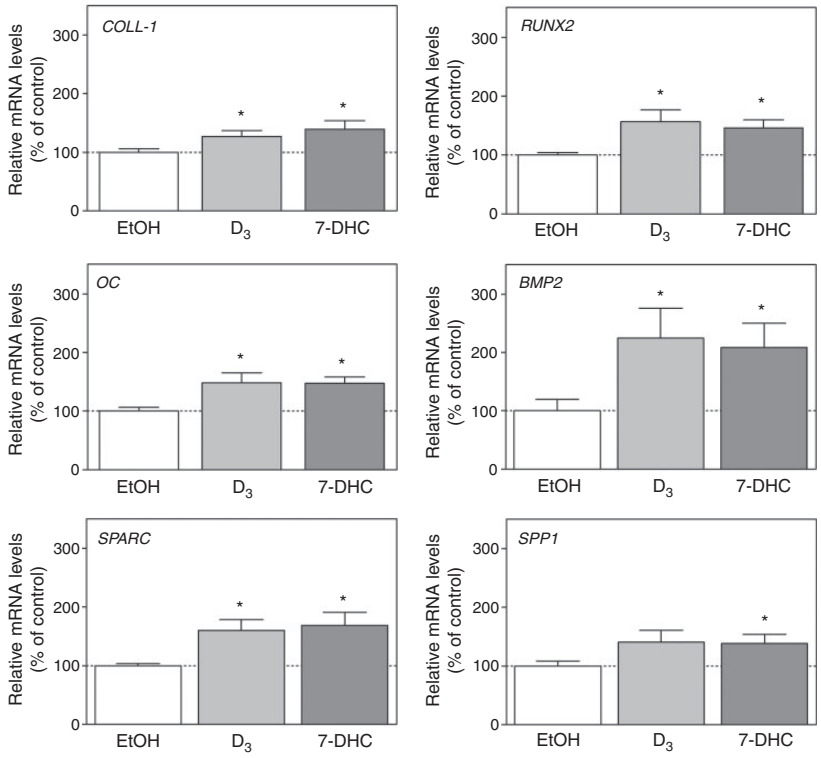

Figure 4. Effect of UV-activated 7-DHC-coated Ti disks on the mRNA expression levels of osteogenic markers in hUC-MSCs cultured for 14 days. Data were normalized to reference genes (*Gapdh* and 18S rRNA), expressed as percentage of control which was set to 100%. Values represent the mean ± SEM (12 samples were used for each group). Differences between groups were assessed by Student's t test: $*p < 0.05$ treatment versus EtOH control.

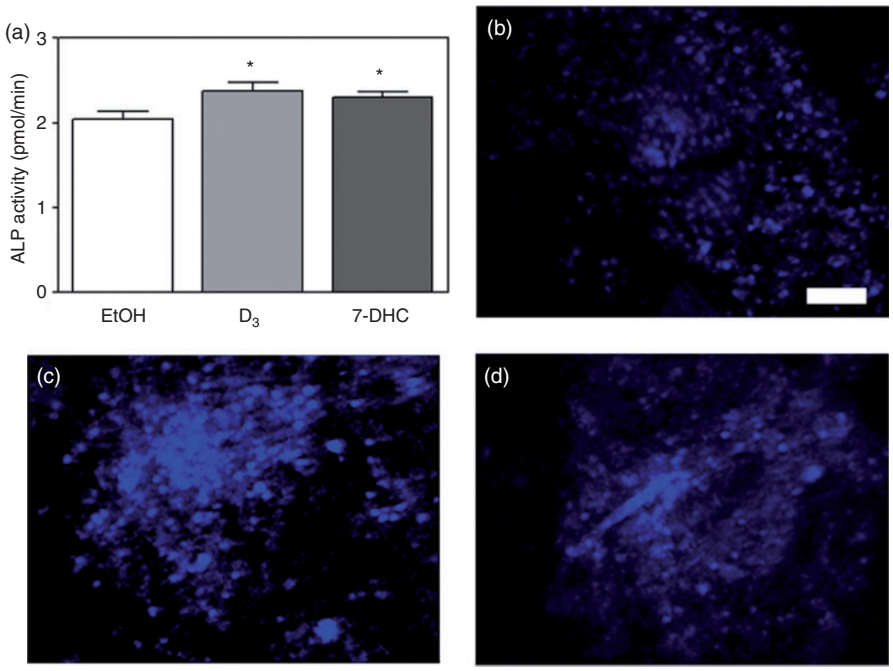

Figure 5. Effect of UV-activated 7-DHC-coated Ti disks on ALP activity and formation of mineralized nodules. (a) ALP activity measured after 21 days of hUC-MSC culture. Values represent the mean ± SEM (10 samples were used for each group). Differences between groups were assessed by Student́s t test: $*p < 0.05$ treatment versus EtOH control. Calcein Blue staining of bone-like nodules in hUC-MSC cultured for 21 days on EtOH (b), D3 (c) or UV-activated 7-DHC coated Ti disks (d). Representative images from confocal laser scanning are shown. Bar scale = 100 μm.

increased in UV-irradiated 7-DHC coatings and in control D_3 compared with control EtOH. These results are in accordance with the mentioned investigations and demonstrate that UV-irradiated 7-DHC coating has the same osteopromotive action than D_3 treatment in these cells. Furthermore, the high expression of these markers might be explained by the fact that several target genes, such as OC, RUNX2 and SPP1, seem to be regulated by the vitamin D response elements (VDREs) located in their gene promoters,[39,45–48] 1,25-D_3 also elevates ALP activity and increases matrix mineralization of both human osteoblasts and mesenchymal stem cells.[17,49,50] Accordingly, we found higher ALP activity in UV-irradiated 7-DHC-coated Ti disks, similar to D_3 control, when compared with EtOH. Moreover, mineralization images were also in agreement with the ALP results.

Conclusion

All in all, the present investigation shows for the first time the biological relevance of D_3-coated Ti disks, previously synthesized from UV-irradiated 7-DHC, in promoting hUC-MSC osteogenic differentiation. Regulating the fate of hMSC by hormones, such as 1,25-D_3, is critically relevant for the prevention of bone diseases and could be desirable in a bone tissue regenerative context, e.g. improving osseointegration in titanium-based bone anchored implants.

Acknowledgement

The authors thank Dr. Antoni Gayà and Dr. Javier Calvo for the isolation of hUC-MSCs.

Declaration of conflicting interests

None declared.

Funding

This work was supported by the Conselleria d'Educació, Cultura i Universitats del Govern de les Illes Balears and the European Social Fund (contract to JMR).

References

1. Lehmann B and Meurer M. Extrarenal sites of calcitriol synthesis: the particular role of the skin. *Recent Results Cancer Res* 2003; 164: 135–145.
2. Bikle DD. Vitamin D regulated keratinocyte differentiation. *J Cell Biochem* 2004; 92: 436–444.
3. Hewison M, Burke F, Evans KN, et al. Extra-renal 25-hydroxyvitamin D3-1alpha-hydroxylase in human health and disease. *J Steroid Biochem Mol Biol* 2007; 103: 316–321.
4. Satué M, Córdoba A, Ramis JM, et al. UV-irradiated 7-dehydrocholesterol coating on polystyrene surfaces is converted to active vitamin D by osteoblastic MC3T3-E1 cells. *Photochem Photobiol Sci* 2013; 12: 1025–1035.
5. Satué M, Petzold C, Córdoba A, et al. UV photoactivation of 7-dehydrocholesterol on titanium implants enhances osteoblast differentiation and decreases Rankl gene expression. *Acta Biomater* 2013; 9: 5759–5770.
6. Musina RA, Bekchanova ES, Belyavskii AV, et al. Differentiation potential of mesenchymal stem cells of different origin. *Bull Exp Biol Med* 2006; 141: 147–151.
7. Klingemann H, Matzilevich D and Marchand J. Mesenchymal stem cells – sources and clinical applications. *Transfus Med Hemother* 2008; 35: 272–277.
8. Salem HK and Thiemermann C. Mesenchymal Stromal Cells: current understanding and clinical Status. *Stem cells* 2010; 28: 585–596.
9. Da Silva Meirelles L, Chagastelles PC and Nardi NB. Mesenchymal stem cells reside in virtually all post-natal organs and tissues. *J Cell Sci* 2006; 119: 2204–2213.
10. Can A and Karahuseyinoglu S. Concise review: human umbilical cord stroma with regard to the source of fetus-derived stem cells. *Stem cells* 2007; 25: 2886–2895.
11. In't Anker PS, Scherjon S, a, Kleijburg-van der Keur C, et al. Isolation of mesenchymal stem cells of fetal or maternal origin from human placenta. *Stem cells* 2004; 22: 1338–1345.
12. Kon E, Muraglia A, Corsi A, et al. Autologous bone marrow stromal cells loaded onto porous hydroxyapatite ceramic accelerate bone repair in critical-size defects of sheep long bones. *J Biomed Mat Res A* 2000; 49: 328–337.
13. Bruder SP, Jaiswal N, Ricalton NS, et al. Mesenchymal stem cells in osteobiology and applied bone regeneration. *Clin Orthop Relat Res* 1998; 355(Suppl): S247–S256.
14. Horwitz EM, Gordon PL, Koo WK, et al. Isolated allogeneic bone marrow-derived mesenchymal cells engraft and stimulate growth in children with osteogenesis imperfecta: implications for cell therapy of bone. *Proc Natl Acad Sci USA* 2002; 99: 8932–8937.
15. Krampera M, Pizzolo G and Aprili GFM. Mesenchymal stem cells for bone, cartilage, tendon and skeletal muscle repair. *Bone* 2006; 39: 678–683.
16. Liu P, Oyajobi BO, Russell RG, et al. Regulation of osteogenic differentiation of human bone marrow stromal cells: interaction between transforming growth factor-beta and 1,25(OH)(2) vitamin D(3) in vitro. *Calcified Tissue Int* 1999; 65: 173–180.
17. Jørgensen NR, Henriksen Z, Sørensen OH, et al. Dexamethasone, BMP-2, and 1,25-dihydroxyvitamin D enhance a more differentiated osteoblast phenotype: validation of an in vitro model for human bone marrow-derived primary osteoblasts. *Steroids* 2004; 69: 219–226.
18. Beresford JN, Joyner CJ, Devlin C, et al. The effects of dexamethasone and 1,25-dihydroxyvitamin D3 on osteogenic differentiation of human marrow stromal cells in vitro. *Arch Oral Biol* 1994; 39: 941–947.
19. Ramis JM, Rubert M, Vondrasek J, et al. Effect of enamel matrix derivative and of proline-rich synthetic peptides on the differentiation of human mesenchymal stem cells toward the osteogenic lineage. *Tissue Eng Part A* 2012; 18: 1253–1263.
20. Pfaffl MW. A new mathematical model for relative quantification in real-time RT-PCR. *Nucleic Acids Res* 2001; 29: e45.

21. Pfaffl MW, Tichopad A, Prgomet C, et al. Determination of stable housekeeping genes, differentially regulated target genes and sample integrity: BestKeeper–Excel-based tool using pair-wise correlations. *Biotechnol Lett* 2004; 26: 509–515.
22. Goto T, Kajiwara H, Yoshinari M, et al. In vitro assay of mineralized-tissue formation on titanium using fluorescent staining with calcein blue. *Biomaterials* 2003; 24: 3885–3892.
23. Howard GA, Turner RT, Sherrard DJ, et al. Human bone cells in culture metabolize 25-hydroxyvitamin D3 to 1,25-dihydroxyvitamin D3 and 24,25-dihydroxyvitamin D3. *J Biol Chem* 1981; 256: 7738–7740.
24. Geng S, Zhou S, Bi Z, et al. Vitamin D metabolism in human bone marrow stromal (mesenchymal stem) cells. *Metab Clin Exp* 2013; 62: 768–777.
25. Kelly J, Lin A, Wang CJ, et al. Vitamin D and bone physiology: demonstration of vitamin D deficiency in an implant osseointegration rat model. *J Prosthodont* 2009; 18: 473–478.
26. Dvorak G, Fügl A, Watzek G, et al. Impact of dietary vitamin D on osseointegration in the ovariectomized rat. *Clin Oral Implants Res* 2012; 23: 1308–1313.
27. Passeri G, Vescovini R, Sansoni P, et al. Calcium metabolism and vitamin D in the extreme longevity. *Exp Gerontol* 2008; 43: 79–87.
28. Zhou W, Langsetmo L, Berger C, et al. Longitudinal changes in calcium and vitamin D intakes and relationship to bone mineral density in a prospective population-based study: the Canadian multicentre osteoporosis study (CaMos). *J Musculoskelet Neuronal Interact* 2013; 13: 470–479.
29. Gaffney-Stomberg E, Lutz LJ, Rood JC, et al. Calcium and vitamin D supplementation maintains parathyroid hormone and improves bone density during initial military training: a randomized, double-blind, placebo controlled trial. *Bone* 2014; 68: 46–56.
30. MacLaughlin JA, Anderson RR and Holick MF. Spectral character of sunlight modulates photosynthesis of previtamin D3 and its photoisomers in human skin. *Science* 1982; 216: 1001–1003.
31. Holick MF. The cutaneous photosynthesis of previtamin D3: a unique photoendocrine system. *J Invest Dermatol* 1981; 77: 51–58.
32. Holick MF. *Vitamin D: physiology, molecular biology, and clinical applications*. New York, NY: Humana Press, 2010.
33. Deschaseaux F, Sensébé L and Heymann D. Mechanisms of bone repair and regeneration. *Trends Mol Med* 2009; 15: 417–429.
34. Bielby R, Jones E and McGonagle D. The role of mesenchymal stem cells in maintenance and repair of bone. *Injury* 2007; 38(Suppl 1): S26–S32.
35. Jaiswal N, Haynesworth SE, Caplan AI, et al. Osteogenic differentiation of purified, culture-expanded human mesenchymal stem cells in vitro. *J Cell Biochem* 1997; 64: 295–312.
36. Liu P, Oyajobi BO, Russell RG, et al. Regulation of osteogenic differentiation of human bone marrow stromal cells: interaction between transforming growth factor-beta and 1,25(OH)(2) vitamin D(3) In vitro. *Calcified Tissue Int* 1999; 65: 173–180.
37. Piek E, Sleumer LS, van Someren EP, et al. Osteo-transcriptomics of human mesenchymal stem cells: accelerated gene expression and osteoblast differentiation induced by vitamin D reveals c-MYC as an enhancer of BMP2-induced osteogenesis. *Bone* 2010; 46: 613–627.
38. Zhou S, Glowacki J, Kim SW, et al. Clinical characteristics influence in vitro action of 1,25-Dihydroxyvitamin D3 in human marrow stromal cells. *Connect Tissue Res* 2012; 27: 1992–2000.
39. Mansell JP and Blackburn J. Lysophosphatidic acid, human osteoblast formation, maturation and the role of 1α,25-Dihydroxyvitamin D3 (calcitriol). *Biochim Biophys Acta* 2013; 1831: 105–108.
40. Jurutka PW, Bartik L, Whitfield GK, et al. Vitamin D receptor: key roles in bone mineral pathophysiology, molecular mechanism of action, and novel nutritional ligands. *J Bone Miner Res* 2007; 22(Suppl 2): V2–V10.
41. Paredes R, Arriagada G, Cruzat F, et al. Bone-specific transcription factor Runx2 interacts with the 1alpha,25-dihydroxyvitamin D3 receptor to up-regulate rat osteocalcin gene expression in osteoblastic cells. *Mol Cell Biol* 2004; 24: 8847–8861.
42. Zur Nieden NI, Kempka G and Ahr HJ. In vitro differentiation of embryonic stem cells into mineralized osteoblasts. *Differentiation* 2003; 71: 18–27.
43. D'Ippolito G, Schiller PC, Perez-stable C, et al. Cooperative actions of hepatocyte growth factor and 1,25-dihydroxyvitamin D3 in osteoblastic differentiation of human vertebral bone marrow stromal cells. *Bone* 2002; 31: 269–275.
44. Chen K, Perez-Stable C, D'Ippolito G, et al. Human bone marrow-derived stem cell proliferation is inhibited by hepatocyte growth factor via increasing the cell cycle inhibitors p53, p21 and p27. *Bone* 2011; 49: 1194–1204.
45. Kraichely DM and MacDonald PN. Transcriptional activation through the vitamin D receptor in osteoblasts. *Front Biosci* 1998; 3: d821–d833.
46. Olivares-Navarrete R, Sutha K, Hyzy SL, et al. Osteogenic differentiation of stem cells alters vitamin D receptor expression. *Stem Cells Dev* 2012; 21: 1726–1735.
47. Li JJ, Kim RH, Zhang Q, et al. Characteristics of vitamin D3 receptor (VDR) binding to the vitamin D response element (VDRE) in rat bone sialoprotein gene promoter. *Eur J Oral Sci* 1998; 106(Suppl): 408–417.
48. Shen Q and Christakos S. The vitamin D receptor, Runx2, and the Notch signaling pathway cooperate in the transcriptional regulation of osteopontin. *J Biol Chem* 2005; 280: 40589–40598.
49. Beresford JN, Joyner CJ, Devlin C, et al. The effects of dexamethasone and 1,25-dihydroxyvitamin D3 on osteogenic differentiation of human marrow stromal cells in vitro. *Arch Oral Biol* 1994; 39: 941–947.
50. Van Driel M, Koedam M, Buurman CJ, et al. Evidence that both 1alpha, 25-dihydroxyvitamin D3 and 24-hydroxylated D3 enhance human osteoblast differentiation and mineralization. *J Cell Biochem* 2006; 99: 922–935.

Paper IV

Cholecalciferol synthesized after UV-activation of 7-dehdydrocholesterol onto titanium implants inhibits osteoclastogenesis in vitro

Satué M.; Ramis J.M. ; Monjo M

Journal of Biomedical Materials Research: Part A (2014), doi: 10.1002/jbm.a.35364.

Society For Biomaterials

Cholecalciferol synthesized after UV-activation of 7-dehydrocholesterol onto titanium implants inhibits osteoclastogenesis *in vitro*

María Satué, Joana M. Ramis, Marta Monjo

Department of Fundamental Biology and Health Sciences, Research Institute on Health Sciences (IUNICS), University of Balearic Islands, Palma de Mallorca, Spain

Received 25 June 2014; revised 8 October 2014; accepted 22 October 2014
Published online 00 Month 2014 in Wiley Online Library (wileyonlinelibrary.com). DOI: 10.1002/jbm.a.35364

Abstract: UV-activated 7-dehydrocholesterol (7-DHC) has been successfully used as a biocompatible coating for titanium (Ti) implants producing active vitamin D with positive effect on osteoblast differentiation. Since an osseointegrating implant must promote bone formation while delay resorption, here we determine the effect of this coating on the pre-osteoclast cell line RAW 264.7. Moreover, D_3 synthesis was optimized by (1) the supplementation with VitE of the 7-DHC coating to reduce 7-DHC oxidation and (2) the addition of an incubation step (48 h at 23°C) after UV-irradiation to favor isomerization. *In vitro* results with RAW264.7 cells showed no cytotoxic effect of the coatings and a significant decrease of osteoclastogenesis. Indeed, TRAP immunostaining suggested an inhibition of Trap-positive multinucleated cells and the mRNA levels of different phenotypic, fusion, and activity markers were reduced, particularly with 7-DHC:VitE. In conclusion, we demonstrate an improvement of the D_3 synthesis from UV-activated 7-DHC when combined with VitE and show that these implants inhibit osteoclastogenesis *in vitro*.

Key Words: 7-dehydrocholesterol, cholecalciferol, α-tocopherol, titanium implant, osteoclastogenesis

How to cite this article: Satué M, Ramis JM, Monjo M 2014. Cholecalciferol synthesized after UV-activation of 7-dehydrocholesterol onto titanium implants inhibits osteoclastogenesis *in vitro*. J Biomed Mater Res Part A 2014:00A:000–000.

INTRODUCTION

Current dental implant research aims at producing innovative surfaces via modifying the implant surface with biologically active substances to improve the biological response to the implant material and to accelerate the osseointegration process. We have previously proved that ultraviolet (UV)-activated 7-dehydrocholesterol (7-DHC) is a biocompatible and bioactive coating that allows osteoblasts to produce themselves active vitamin D_3, with positive effects on their differentiation *in vitro*.[1] Indeed, multiple research studies have demonstrated the essential role of vitamin D_3 in maintaining a healthy and mineralized skeleton. Not only that, but also its deficiency leads to bone resorption, osteoporosis, reduced bone mineralization, and poor implant osseointegration.[2,3]

The synthesis of vitamin D_3 from the 7-DHC precursor is a complex pathway. UVB-irradiation of 7-DHC produces a ring opening that results in the formation of previtamin D_3 ($preD_3$), an unstable metabolite which further isomerizes via heat to cholecalciferol (D_3),[4] as seen in Figure 1. However, $preD_3$ not only isomerizes to D_3, but also to the secondary products lumisterol, tachysterol, and toxisterols.[5,6] UVB irradiation at the optimal wavelength and during the right time is an important factor for the synthesis of $preD_3$. Indeed, the use of long irradiation periods or long UV wavelengths can lead to the synthesis of irreversible or undesired products.[7] In human skin cells, for instance, the UVB spectral range 290–315 converts 7-DHC into $preD_3$, with a maximum at 302 nm, and there is no production when UV wavelengths $>$ 315 nm are used.[8] In line with this, we previously screened the time of UV exposure at 302 nm and an optimal production of $preD_3$ was found when 7-DHC was UV exposed for 15 min.[1] However, once $preD_3$ is synthesized, it undergoes a thermal isomerization to D_3 that is time and temperature dependent.[9,10] In our previous studies, implants were characterized immediately after UV irradiation, but, in the light of the above, in the present study we have incubated the 7-DHC coating after UV irradiation and evaluated the effect of time and temperature during this incubation on the yield of D_3 synthesis. Thus, we first aimed at optimizing the 7-DHC coating for the synthesis of D_3 by testing different incubation times and temperatures. Second, we combined this coating with increasing concentrations of α-tocopherol (VitE) to protect 7-DHC from oxidation after UV-irradiation.

To achieve greater peri-implant bone formation, an implant surface must promote osteogenesis while delay bone resorption, ultimately producing more bone before the start of the remodeling process.[11] Since in a previous study we showed that Ti implants coated with UV-irradiated 7-

Correspondence to: M. Monjo; e-mail: marta.monjo@uib.es

DHC have positive effects on osteoblast differentiation *in vitro,*[1] in the present study we aimed to determine the effect of the optimized coating on osteoclastogenesis. To this end, we determined the *in vitro* response of RAW264.7 cells to the modified implants by analyzing cytotoxicity, TRAP and actin immunostaining, and the gene expression of osteoclast phenotypic, fusion, and activity markers.

EXPERIMENTAL

Treatment of polystyrene and titanium surfaces

Stock solutions of 7-DHC (Sigma, St. Louis, MO) and VitE (Sigma, St. Louis, MO) were prepared in absolute ethanol and filtered with a 0.22 mm pore size filter before use. Four different groups were prepared by adding 0.2 n*M* 7-DHC per well or 0.2 n*M* 7-DHC per well supplemented with VitE (20:1, 5:1, 1:1) on a mass-to-mass (m:m) basis. To treat tissue culture plastic wells, 10 μL of 7-DHC:VitE (20:1, m:m) were left on the TCP surfaces (30.68 mm^2 of surface area per well) and after UV-irradiated using a UV lamp of 302 nm with an intensity of irradiation of 6 mW/cm^2 (UVP, Upland, CA) during 15 min, as defined in a previous study.[1] Once UV-irradiated, coating composition was analyzed by HPLC at this point of time and after incubation up to 96 h at −20°C, 4°C, or 23°C in absence of light.

Ti implants used were all made of grade 2 with a diameter of 6.25 mm and a height of 1.95 mm. All disks were machined from cp Ti rods and subsequently ground, polished, and cleaned as described elsewhere.[12] For the surface modification of Ti implants, 10 μL of 7-DHC:VitE (20:1, 5:1, 1:1; m:m) were left on the surfaces. Additionally, only ethanol, VitE (0.18 pmol/Ti disk) or 7-DHC (0.2 n*M* /Ti disk) were considered as controls for the *in vitro* experiments. Once the surfaces were coated, UV irradiation was performed as described earlier. Ti implants were immediately processed to analyze their coating composition by HPLC or directly used for the *in vitro* experiments.

Determination of the conversion of 7-DHC to D_3 by HPLC

The amount of 7-DHC, preD_3, and D_3 present in the surface coating after 15 min of UV irradiation and after different incubation times was quantified by HPLC.

All solvents used were HPLC or analytical grade. Methanol (HPLC gradient grade), acetonitrile, and tetrahydrofurane (both HPLC grade) were purchased from Fisher Scientific (Thermo Fisher Scientific, MA). High-purity deionized Milli-Q water was obtained from a Millipore system (Millipore Corporation, Billerica, MA). Absolute ethanol was purchased from Scharlab (Barcelona, Spain). The coating of each surface was extracted and analyzed as described elsewhere.[1]

Cell culture

The transformed murine monocytic cell line RAW 264.7 was obtained from ATCC (Manassas, VA). Cells were cultured at 37°C in 5% CO_2 atmosphere in Dulbecco modified Eagles medium (DMEM) supplemented with 10% FBS and antibiotics (50 IU penicillin/mL and 50 μg streptomycin/mL).

To test the effect of the surface modification, cells were seeded at a density of 3.0×10^4 cells/cm^2 and, after an overnight period, the culture medium was replaced with medium containing 4 ng/mL RANKL (R&D Systems, Minneapolis, MN). Medium was changed every 48 h over the course of 5 days.

Determination of cytotoxicity

The LDH activity in the culture medium was estimated according to the manufacturer's kit instructions (Roche Diagnostics, Mannheim, Germany), by assessing the rate of oxidation of NADH at 490 nm in presence of piruvate. Results were presented relative to the LDH activity in the medium of cells seeded on tissue culture plastic (TCP) without treatment (low control, 0% of cell death) and of cells grown on TCP treated with 1% Triton X-100 (high control, 100% cell death). The percentage of LDH activity was calculated using the following equation:

$$\text{Cytotoxicity}(\%) = (\text{exp.value} - \text{low control}) / (\text{high control} - \text{low control}) \times 100.$$

TRAP immunostaining

To confirm the generation of multinucleated osteoclast-like cells, TRAP positive multinucleated (three or more nuclei) osteoclasts were visualized by confocal microscopy. Confocal images of cells growing in the different coated implants were obtained after 5 days of cell culture. Cells were first fixed for 15 min with 2% formaldehyde in PBS and then permeabilized for 10 min with 0.1% Triton X-100 in PBS. Cells were immunostained with anti-Trap antibody (1:100; Thermo Fisher Scientific, MA) for 1 h at 37°C followed by 1.5 h of incubation at room temperature with Cy3 (1:200; Thermo Fisher Scientific, MA). Cells were then incubated with Phalloidin-FITC (5 μg/mL; Sigma, St. Louis, MO) to stain actin rings. Finally, a drop of Fluoroshield-DAPI (Sigma, St. Louis, MO) was added to stain cell nuclei. Two implants for each group were used to perform the experiment and six images of each implant were taken with the confocal microscope (Leica DMI 4000B equipped with Leica TCS SPE laser system).

RNA isolation and real-time RT-PCR analysis

RNA was isolated from cells using a monophasic solution of phenol and guanidine thiocyanate (Trizol, Roche Diagnostics, Mannheim, Germany) according to the manufacturer's protocol. RNA was quantified at 260 nm using a Nanodrop spectrophotometer (NanoDrop Technologies, Wilmington, DE).

Total RNA previously isolated was reverse-transcribed to cDNA using High Capacity RNA to cDNA kit (Applied Biosystems, Foster City, CA) according to the protocol of the supplier. The same amount of total RNA from each sample was converted into cDNA. Each cDNA was diluted 1/4 and aliquots were stored at −20°C until the PCR reactions were carried out.

Real-time RT-PCR was performed for two reference genes: 18S ribosomal RNA (*18S rRNA*), glyceraldehyde-3-phosphate dehydrogenase (*Gapdh*), and 10 target genes: tartrate resistant acid phosphatase (*Trap*), calcitonin receptor

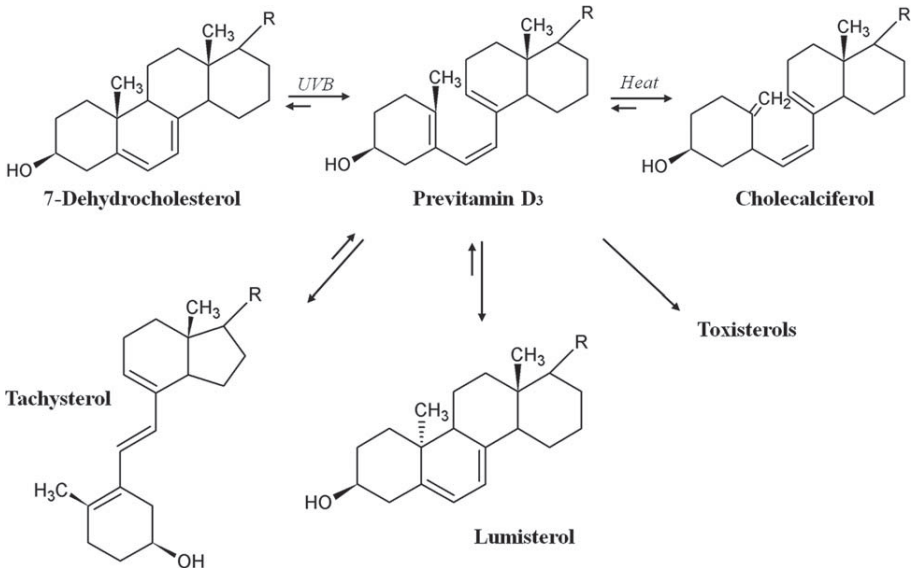

FIGURE 1. Scheme of the vitamin D_3 photosynthesis from 7-DHC. UVB irradiation produces previtamin D_3 formation, which further undergoes a temperature-dependent isomerization to the thermally stable cholecalciferol. However, UVB exposure also results in the photoisomerization of preD_3 to tachysterol, lumisterol, and toxisterols.

(CalcR), integrin alpha-V *(Itgav),* integrin beta-3 *(Itgb3)*, a disintegrin, and metalloproteinase domain-containing protein 8 *(Adam8)*, dendritic cell-specific transmembrane protein *(Dc-Stamp)*, vacuolar-type H^+ ATPase (subunit Atp6v0d2) (*H^+-ATPase*), carbonic anhydrase II *(Car2)*, cathepsin K (*CtsK*) and metalloproteinase-9 (*Mmp9*).

The reactions were performed in the Lightcycler 480® (Roche Diagnostics, Germany). Each reaction contained 500 n*M* of the corresponding oligonucleotide primers (18s rRNA-F: 5′-GTAACCCGTTGAACCCCATT-3′; 18s rRNA-R: 5′-CCATCCA ATCGGTAGTAGCG-3′; *Gapdh*-F: 5′-ACCCAGAAGACTGTG-GATG G-3′; *Gapdh*-R: 5′-CACATTGGG-GGTAGGAACAC-3′ *Trap*-F: 5′-G CGACCATTGTTAGCCACATACG-3′; *Trap*-R: 5′-CGTTGATGTCGCA CAGAGGGAT-3′; *CalcR*-F: 5′-TGGTGCGGCGGGATCCTATAAGT-3′: *CalcR*-R: 5′-AGCGTAGGCGTTGCTCGTCG-3′; *Itgav*-F: 5′-TCGTTT CTATCCCACCGCAG-3′; *Itgav*-R: 5′-GAAGACCAGCGAGCAGTTGA-3′; *Itgb3*-F: 5′-AGGGGAGATGTGTTCCGGCCA-3′; *Itgb3*-R: 5′-AC ACACAGCTGCCGCACTCG-3′; *Adam8*-F: 5′-GCCTCTGGCTGCTCA GCGTCTTA-3′; Adam8-R: 5′-CCCAGCAGGTCCCTGTTCTTTCG-3′; *Dc-Stamp*-F: 5′-GGCTGACGGGAAACCGAGCC-3′; *Dc-Stamp*-R: 5′-ACAGAAGCAGCAGTTGGCCCAG-3′; *Ctsk*-F: 5′-AGCAGAACGGA GGCATTGACTC-3′; *Ctsk*-R: 5′-TTTAGCTGCCTTTGCCGTGGC-3′; *Mmp*9-F: 5′-GCTGACTACGATAAGGACGGCA-3′; *Mmp*9-R: 5′-GC GGCCCTCAAAGATGAACGG-3′); *H+ATPase*-F: 5′-ACGGTGATGTC ACAGCAGACGT-3′; *H+ATPase*-R: 5′-CCTCTGGATAGAGCCTGCC GCA-3′; *Car2*-F: 5′-CTCTGCTGGAATGTGTGACCTG-3′ and *Car2*-R: 5′-CTGAGCTGGACGCCAGTTGTC-3′). 5 μL of LightCycler-FastStart DNA MasterPLUS SYBR Green I (Roche Diagnostics, Mannheim, Germany) and 3 μL of the cDNA dilution in a final volume of 10 μL. The normal amplification program consisted of a preincubation step for denaturation of the template cDNA (10 min 95°C), followed by 45 cycles consisting of a denaturation step (10 s 95°C), an annealing step (10 s 60°C), and an extension step (10 s 72°C). After each cycle, fluorescence was measured at 72°C. Every run included a negative control without cDNA template. To confirm amplification specificity, PCR products were subjected to a melting curve analysis on the LightCycler and subsequently 2% agarose/TAE gel electrophoresis, Tm and amplicon size, respectively.

Real-time efficiencies (*E*) were calculated from the given slopes in the LightCycler 480 software using serial dilutions, showing all the investigated transcripts high real-time PCR efficiency rates, and high linearity when different concentrations were used.

All samples were normalized by the geometric mean of the expression levels of 18S rRNA and *Gapdh* and fold changes were related to the control group using the mathematical model described by Pfaffl[13]:

$$\text{ratio} = E_{\text{target}}^{\text{DCp target (mean control}-\text{sample)}} / E_{\text{reference}}^{\text{DCp reference (mean control}-\text{sample)}}$$

where Cp is the is the crossing point of the reaction amplification curve as determined by the LightCycler 480 software. Stability of reference genes was calculated using the Best-Keeper tool.[14] A good consistence of the bestkeeper index was proved as its contributing reference genes were tightly correlated with it, with a significance level of $p = 0.001$ for all reference genes.

Statistics

All data are presented as mean values ± standard error of the mean (SEM). The Kolmogorov-Smirnov test was done to assume parametric or non-parametric distributions for the normality tests. The effect of time on the coating composition was assessed by the univariate analysis of variance

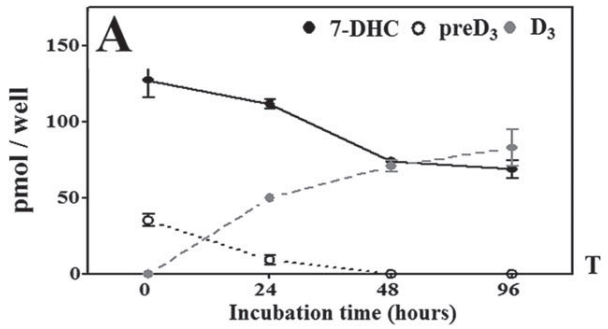

	0 vs. 24h	0 vs. 48h	0 vs. 96h	24 vs. 48h	24 vs. 96h	48 vs. 96h
7-DHC	0.161	**0.002**	**0.001**	**0.013**	**0.004**	0.642
$preD_3$	**0.000**	**0.000**	**0.000**	**0.032**	**0.032**	1.000
D_3	**0.001**	**0.000**	**0.000**	0.083	**0.009**	0.283

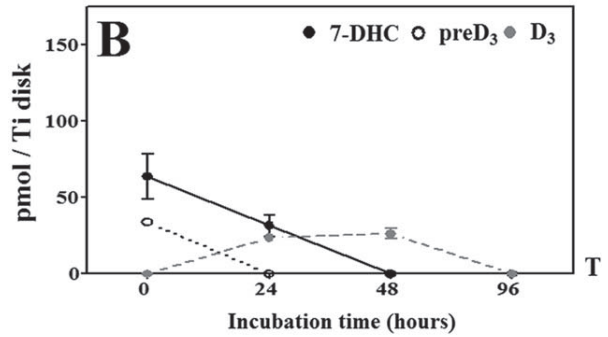

	0 vs. 24h	0 vs. 48h	0 vs. 96h	24 vs. 48h	24 vs. 96h	48 vs. 96h
7-DHC	**0.015**	**0.000**	**0.000**	**0.011**	**0.011**	1.000
$preD_3$	**0.037**#	**0.037**#	**0.037**#	1.000 #	1.000 #	1.000 #
D_3	**0.000**	**0.000**	1.000	0.330	**0.000**	**0.000**

FIGURE 2. Coating composition of UV-irradiated 7-DHC:VitE (20:1;m:m) in polystyrene and Ti surfaces after different incubation times at 23°C. The remainder of 7-DHC and the formed $preD_3$ and D_3 in polystyrene (A) and Ti (B) surfaces were quantified by HPLC. Values represent the mean ± SEM ($N = 6$). The effect of time (T) was assessed by UNIANOVA test: p-values obtained from post-hoc analyses (DMS test), in bold when statistically significant. No ANOVA test could be performed for $preD_3$ composition in Ti surfaces, so p-values were calculated by Mann-Whitney-test.#

(UNIANOVA) test followed by post-hoc pairwise comparisons using the minimum significance difference (DMS) test. When ANOVA test was not suitable for data, Mann-Whitney-test or Student t-test were run depending on the normal distribution of the data. The SPSS® program for Windows, version 17.0 (SPSS, Chicago, IL) was used. Results were considered statistically significant at the p-values ≤ 0.05.

RESULTS

Effect of incubation time on the composition of the 7-DHC:VitE (20:1; m:m) coatings after UV-irradiation

In polystyrene surfaces. The coating composition in polystyrene was dependent on the incubation time. $PreD_3$ was detected just after UV-irradiation of 7-DHC:VitE (20:1; m:m) coatings in polystyrene surfaces, and its amount decreased over time. D_3 was detected after 24 h of incubation at 23°C [Fig. 2(A)], increasing its amount after 96 h of incubation at 23°C. The amount of 7-DHC decreased over time. In addition, we found that polystyrene surfaces incubated for 24 h at 4°C or −20°C showed only 7-DHC and $preD_3$, similar to that found immediately after irradiation (data not shown).

In Ti surfaces. The coating composition in Ti surfaces was dependent on the incubation time, except for $preD_3$. Ti surfaces coated with 7-DHC:VitE (20:1; m:m) and incubated at 23°C after UV-irradiation [Fig. 2(B)] showed similar amount of D_3 after 24 and after 48 h of incubation, but the amount of D_3 measured in titanium was much lower than

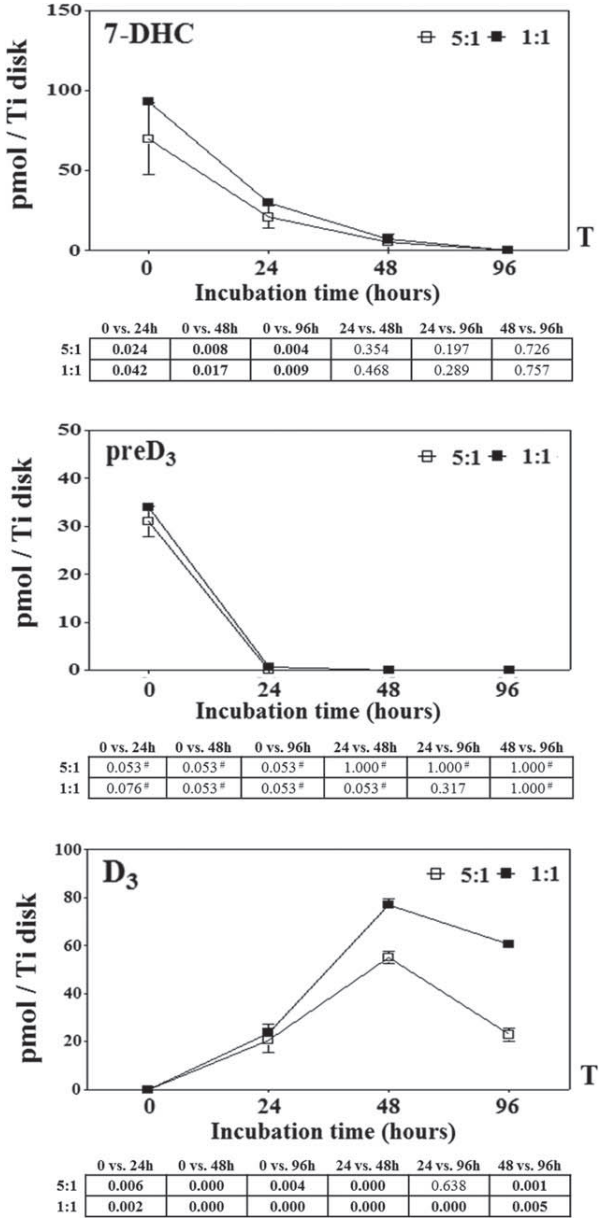

	0 vs. 24h	0 vs. 48h	0 vs. 96h	24 vs. 48h	24 vs. 96h	48 vs. 96h
5:1	**0.024**	**0.008**	**0.004**	0.354	0.197	0.726
1:1	**0.042**	**0.017**	**0.009**	0.468	0.289	0.757

	0 vs. 24h	0 vs. 48h	0 vs. 96h	24 vs. 48h	24 vs. 96h	48 vs. 96h
5:1	0.053#	0.053#	0.053#	1.000#	1.000#	1.000#
1:1	0.076#	0.053#	0.053#	0.053#	0.317	1.000#

	0 vs. 24h	0 vs. 48h	0 vs. 96h	24 vs. 48h	24 vs. 96h	48 vs. 96h
5:1	**0.006**	**0.000**	**0.004**	**0.000**	0.638	**0.001**
1:1	**0.002**	**0.000**	**0.000**	**0.000**	**0.000**	**0.005**

FIGURE 3. Coating composition of UV-irradiated 7-DHC:VitE (5:1, 1:1; m:m) in Ti surfaces after different incubation times at 23°C. The remainder of 7-DHC and the formed $preD_3$ and D_3 were quantified by HPLC. Values represent the mean ± SEM ($N = 6$). The effect of time (T) was assessed by UNIANOVA test: p-values obtained from post-hoc analyses (DMS test), in bold when statistically significant. No ANOVA test could be performed for $preD_3$ composition in Ti surfaces, so p-values were calculated by Mann-Whitney-test.#

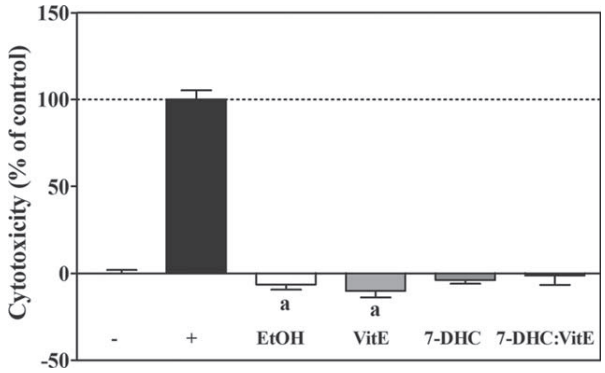

FIGURE 4. Effect of UV-irradiated 7-DHC:VitE (1:1; m:m) coated Ti on cell viability after 24 h of RAW264.7 cell seeding. High control (100% cytotoxicity) was culture medium from cells cultured on tissue culture plastic (TCP) treated with 1% Triton X-100. Low control (0% cytotoxicity) was culture medium from control vehicle cells cultured on TCP. The percentage of LDH activity was calculated using the following equation: Cytotoxicity (%) = (exp.value − low control)/(high control − low control) × 100. Values represent the mean ± SEM ($N = 6$). Differences between groups were assessed by Mann-Whitney test: a $p < 0.05$ treatment versus control.

in polystyrene surfaces. Furthermore, the amount of 7-DHC considerably decreased over the first 48 h whereas no $preD_3$ was detected after 48 h of incubation. Finally, no metabolites were detected after 96 h of incubation at 23°C.

Effect of the VitE dose and incubation time on the composition of the 7-DHC:VitE coatings in Ti surfaces after UV-irradiation

Figure 3 shows the amount of 7-DHC, $preD_3$, and D_3 detected on the Ti surfaces coated with different VitE doses (5:1 and 1:1; 7-DHC:VitE; m:m) and incubated over time after UV-irradiation at 23°C. 7-DHC and D_3 composition was dependent on the incubation time for both doses of 7-DHC:VitE. Indeed, after 24 h of incubation at 23°C there was synthesis of D_3 in both cases but the highest amount of D_3 was found after 48 h of incubation at 23°C, especially with the maximum dose of VitE used. Thus, the highest synthesis of D_3 was found when 7-DHC:VitE (1:1; m:m) was incubated for 48 h at 23°C, in which 75.6 ± 3.5 pmol/Ti implant of D_3 were measured. Then, this condition was selected to perform the *in vitro* experiments in RAW264.7 cells.

In vitro response of RAW264.7 cells to UV-activated 7-DHC:VitE (1:1;m:m) coated Ti surfaces

Effect on cytotoxicity. We evaluated the toxic effect of the UV-activated 7-DHC:VitE (1:1; m:m) coated Ti implants on RAW264.7 cells by measuring LDH activity in the culture medium after 24 h of cell culture. As seen in Figure 4, UV exposure increased cell viability in OCL cultured on UV-irradiated EtOH and VitE coated implants, whereas also a trend to protect cell viability was observed in the 7-DHC and the 7-DHC:VitE groups but without significant differences.

Effect on osteoclastogenesis. For the investigation of OCL formation, cells were immunostained for actin filaments, nuclei, and TRAP protein (Fig. 5). TRAP-positive multinucleated osteoclast-like cells (OCL) were found in control (UV-irradiated EtOH) Ti surfaces [Fig. 5(A,B)]. A lower number of OCL was found in Ti disks when coated with VitE [Fig. 5(C,D)], 7-DHC [Fig. 5(E,F)] and especially with 7-DHC:VitE [Fig. 5(G,H)]. We also assessed the gene expression levels of key phenotypic and functional OCL markers. Our findings show that *Trap* and *CalcR* mRNA expression levels were decreased in cells seeded on Ti surfaces coated with VitE, 7-DHC and especially with 7-DHC:VitE

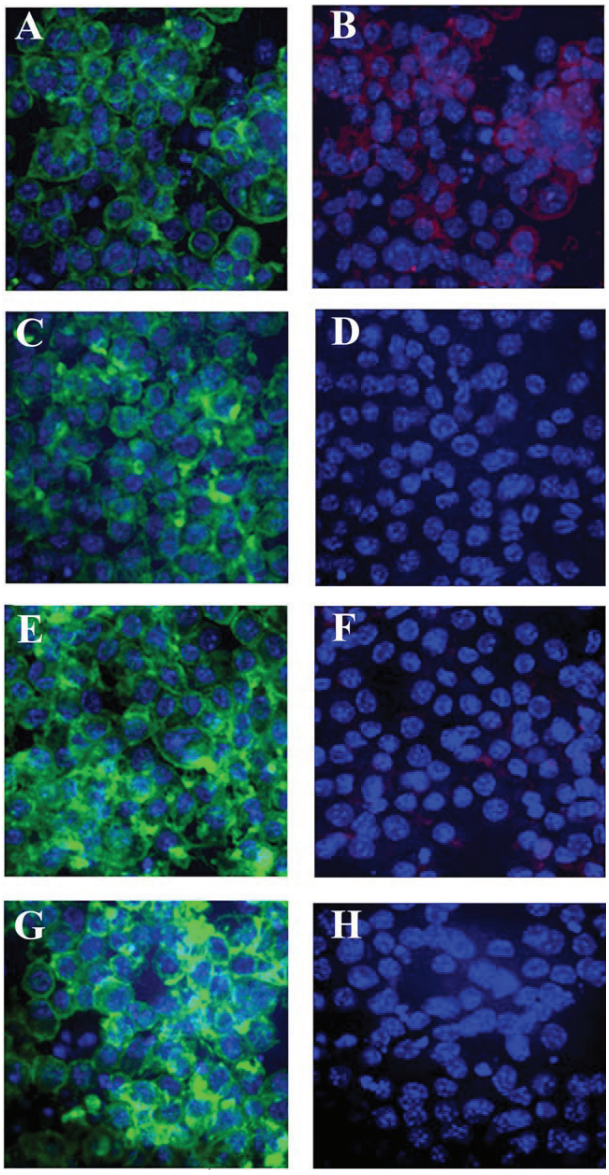

FIGURE 5. Effect of UV-irradiated 7-DHC:VitE (1:1; m:m) coated implants on the generation of multinucleated TRAP-positive cells (OCL). Cells were seeded over UV-irradiated EtOH (A-B), VitE (C-D), 7-DHC (E-F), or 7-DHC:VitE (G-H) coated Ti and dosed with 4 ng/mL RANKL for 5 days. Cells were then stained with Phalloidin-FITC (actin filaments; green), Fluoroshield-DAPI (nucleous; blue) and anti-Trap labeled with Cy3 (Trap protein, red). Representative images from confocal laser scanning are shown. Bar scale = 50 μm. [Color figure can be viewed in the online issue, which is available at wileyonlinelibrary.com.]

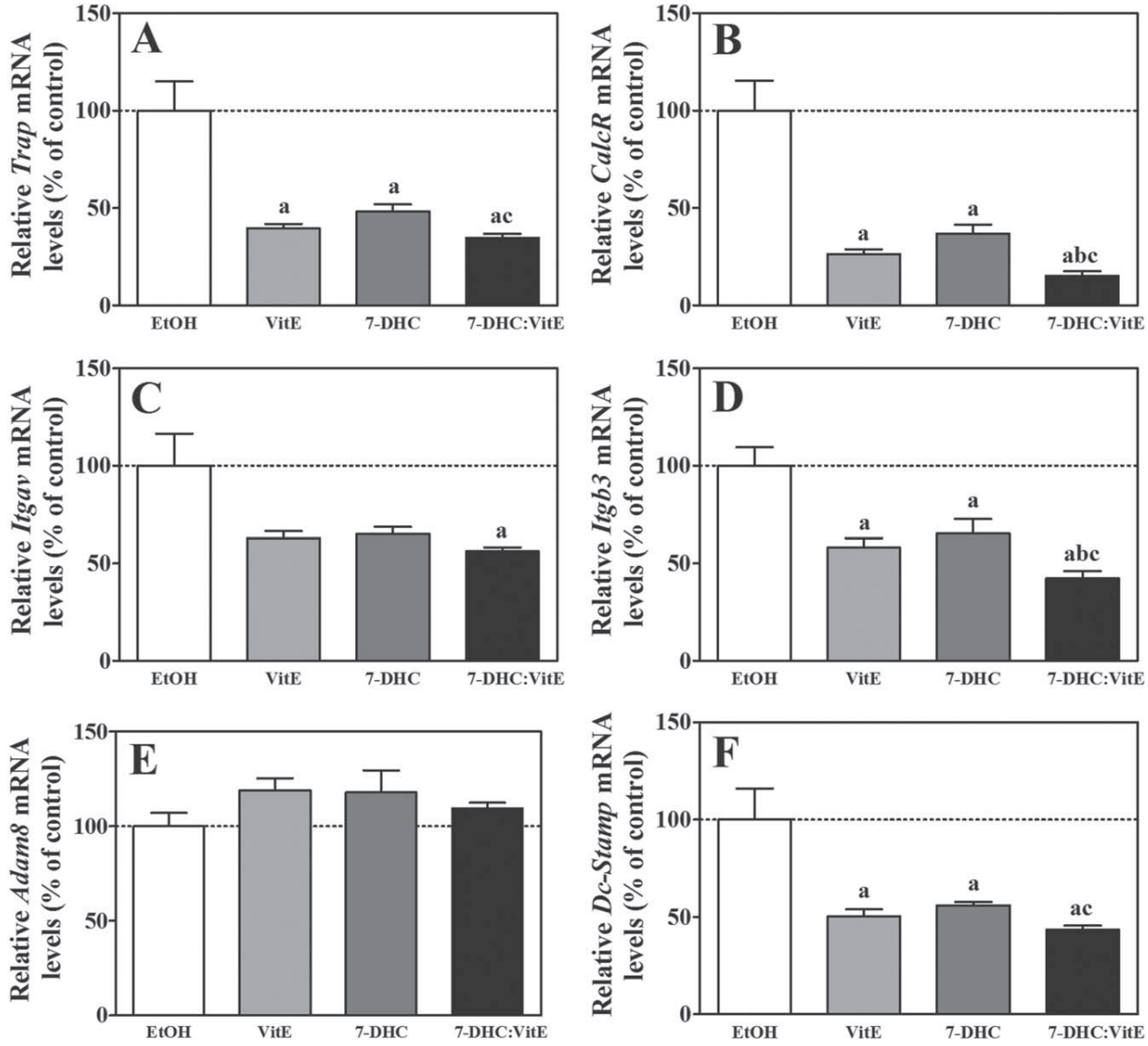

FIGURE 6. Effect of UV-irradiated 7-DHC:VitE (1:1; m:m) coated implants on the mRNA expression levels of phenotypic and fusion markers of RAW 264.7 cells. Cells were cultured over the treated surfaces and dosed with 4 ng/mL RANKL for 5 days. (A) *Trap*; (B) *CalcR*; (C) *Itgab*; (D) *Itgb3*; (E) *Adam8*; and (F) *Dc-Stamp* mRNA levels of RANKL-stimulated cells seeded over Ti surfaces coated with UV-irradiated 7-DHC:VitE (1:1; m:m). Data were normalized to reference genes (*Gapdh* and *18S rRNA*), expressed as percentage of control which was set to 100%. Values represent the mean ± SEM ($N = 6$). Differences between groups were assessed by Student's *t* test: [a] $p < 0.05$ treatment versus EtOH control; [b] $p < 0.05$ 7-DHC:VitE versus VitE control; and [c] $p < 0.05$ 7-DHC:VitE versus 7-DHC control.

[Fig. 6(A,B)], in agreement with the TRAP staining results (Fig. 5). Regarding the fusion markers, 7-DHC:VitE decreased *Itgav* [Fig. 6(C)] while the three coatings down-regulated *Itgb3* [Fig. 6(D)], mainly the 7-DHC:VitE one. No differences were achieved for *Adam8* [Fig. 6(E)] but *Dc-Stamp* was inhibited in all treatments, especially in 7-DHC:VitE [Fig. 6(F)].

The functional markers *Car2* [Fig. 7(A)], *Ctsk* and *Mmp9* [Fig. 7(C,D)] were down-regulated in cells cultured in all coated surfaces, particularly the 7-DHC:VitE one, although no statistical differences were reached for *Car2* in 7-DHC surfaces. No statistical differences were found for H^+*ATPase* [Fig. 7(B)] in any coating, although expression levels tended to be lower than control for all the coatings.

DISCUSSION

In this study, we show that the yield of D_3 synthesis from UV-irradiated 7-DHC can be improved on titanium implant surfaces by adding vitamin E and an incubation step after irradiation with appropriate time and temperature conditions. We previously showed that polystyrene surfaces coated with 7-DHC and UV-irradiated for 30 min produced 8.6% of $preD_3$[15] and that Ti surfaces coated with 7-DHC produced 16.5% of $preD_3$ when UV-irradiated for 15 min.[1] In our previous studies, implants were characterized immediately after UV irradiation. However, since published studies support that the $preD_3$-D_3 isomerization occurs via heat,[4,9,10] we decided to incubate our coatings after UV-

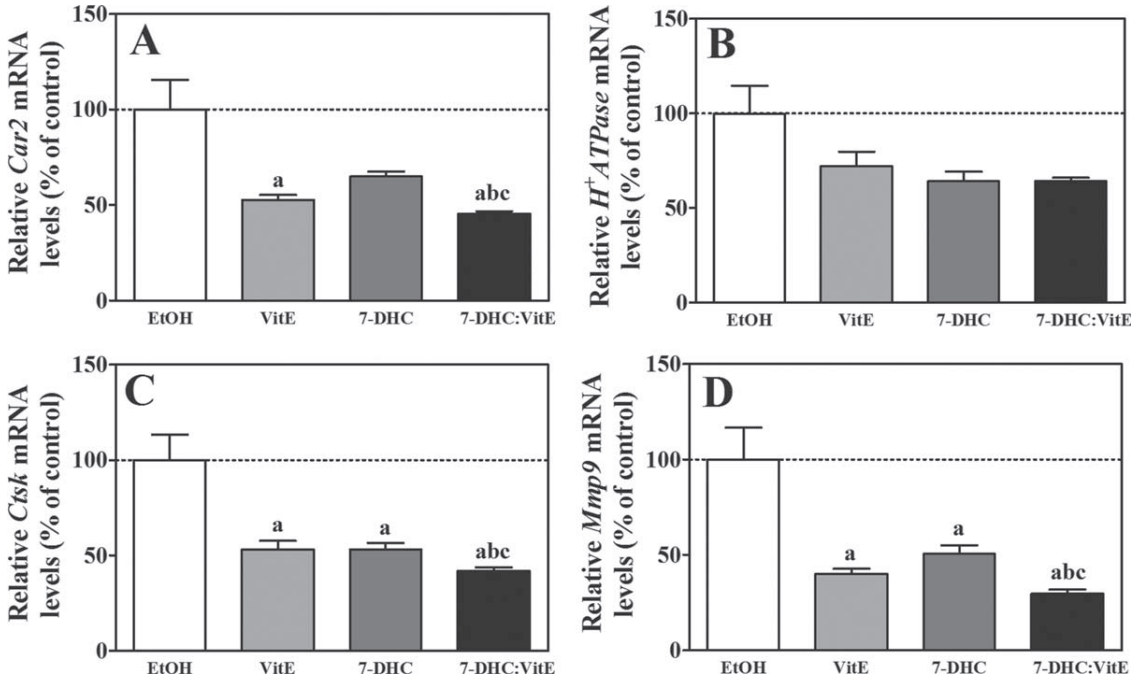

FIGURE 7. Effect of UV-irradiated 7-DHC:VitE (1:1; m:m) coated implants on the mRNA expression levels of functional makers of RAW264.7 cells. Cells were cultured over the treated surfaces and dosed with 4 ng/mL RANKL for 5 days. (A) *Car-2;* (B) *H^+ATPase;* (C) *Ctsk;* and (D) *Car-2* mRNA levels of RANKL-stimulated cells seeded over Ti surfaces coated with UV-irradiated 7-DHC:VitE (1:1; m:m). Data were normalized to reference genes (*Gapdh* and *18S rRNA*), expressed as percentage of control which was set to 100%. Values represent the mean ± SEM ($N = 6$). Differences between groups were assessed by Student's *t* test: [a]$p < 0.05$ treatment versus EtOH control; [b]$p < 0.05$ 7-DHC:VitE versus VitE control; and [c]$p < 0.05$ 7-DHC:VitE versus 7-DHC control.

irradiation and to evaluate the effect of time and temperature of this incubation on the yield of D_3 synthesis.

Our first results were discouraging, since we could not detect either 7-DHC or its photoproducts (data not shown). These lack of detection could be the result of a rapid degradation of the compounds, since 7-DHC and its photoproducts are sensitive to light, heat, and oxygen. In particular, 7-DHC is the most reactive lipid known to maintain a peroxidative free radical chain reaction.[16,17] Therefore, we hypothesized that the supplementation with an antioxidant agent could preserve 7-DHC and its photoproducts stability. VitE was selected as a lipid soluble antioxidant[18] with positive effects on bone. VitE suppresses the production of certain cytokines involved in increased bone loss[19] and prevents bone resorption as oxygen-free radicals are linked to osteoclast formation and activation.[20]

The addition of VitE to the 7-DHC coating (20:1; m:m) increased the percentage of preD_3 production without further incubation in both, polystyrene (14.5%) and Ti surfaces (29.0%). In agreement with this result, a recent study demonstrated that VitE supplementation decreased the oxysterols levels derived from 7-DHC in cultured human SLOS fibroblasts,[21] reinforcing its antioxidant action in preserving 7-DHC stability.

Our next step was to evaluate the effect of time and temperature on 7-DHC:VitE (20:1; m:m) coatings after irradiation in polystyrene surfaces. We determined that, in polystyrene surfaces, the optimal incubation conditions that promote the thermal conversion to cholecalciferol were 48 h at 23°C. Furthermore, incubation at 4°C and at −20°C stopped the thermal isomerization and maintained the initial composition of the UV-photoactivated 7-DHC; whereas incubation at 37°C yielded no metabolites (data not shown), probably due to their degradation. This discrepancy at 37°C with previous research[4,9,22–24] might be explained by the fact that the thermal isomerization, here, is done onto Ti surfaces in dry conditions, rather than in aqueous solutions.

Then, we evaluated the effect of time on the synthesis of D_3 when 7-DHC:VitE (20:1; m:m) coatings were incubated at 23°C after UV irradiation on Ti implants. Surprisingly, we found that D_3 synthesis in Ti surfaces was inferior to that in polystyrene, and that no metabolite could be detected after 96 h of incubation. This result can be explained by the different material composition. UV treatment of Ti surfaces improves the hydrophilicity and removes hydrocarbons from the Ti surface.[25,26] In fact, Ti implants have an outer layer of titanium dioxide (TiO_2) that produces high levels of reactive oxygen species (ROS), such as hydroxyl radicals, super-oxide anions, hydrogen peroxide and single oxygen, when UV-irradiated.[27–30] However, ROS cause oxidative damage to organic compounds, such as the 7-DHC coating, what results in a lower synthesis of D_3. In the case of the polystyrene surfaces, UV irradiation may form species of lower oxidation states maintaining better the stability of 7-DHC. As a result, the difference in the degree of oxidation in Ti and polystyrene leads to a different composition of the coatings after UV irradiation.

To solve this problem in Ti surfaces, we evaluated increasing VitE doses (5:1 and 1:1; 7-DHC:VitE; m:m) to avoid the oxidation of 7-DHC and its photoproducts and, in consequence, increase the formation of D_3. And indeed, we found that using the higher dose of VitE (1:1; 7-DHC:VitE; m:m), the function of preventing 7-DHC degradation was completely fulfilled, leading to a higher synthesis of D_3 when incubated for 48 h at 23°C (75.6 ± 3.5 pmol/Ti implant of D_3).

Successful osseointegration of an implant requires equilibrium between the action of both osteoblasts and osteoclasts. Reducing osteoclastogenesis in the peri-implant region is then an effective strategy to improve bone-implant integration and its further maintenance. Given the positive results obtained in osteoblastic cells,[1] we investigated the *in vitro* response of 7-DHC:VitE (1:1; m:m) coated Ti surfaces in the murine pre-osteoclastic cell line RAW264.7. As osteoblastic cells, RAW264.7 cells express the enzymatic machinery required to synthesize final active vitamin D.[31] Initially, vitamin D was thought to be a bone resorption inductor.[32,33] Indeed, 1,25(OH)D_3 induced OCL formation from bone marrow cells.[34,35] Nevertheless, active vitamin D compounds are used as therapeutic drugs to treat osteoporosis. These compounds improve bone mineral density, reduce bone resorption and bone fracture frequency by inhibiting osteoclastogenesis.[36,37] Various *in vivo* studies confirm the effect of vitamin D metabolites on suppressing osteoclast activity.[38–41] These vitamin D compounds are believed to improve the bone remodeling process by changing the bone microenvironment.[42] The *in vitro* inhibitory action of vitamin D metabolites on osteoclastogenesis is said to work through the suppression of the c-Fos transcription factor[43] and the induction of interferon β.[44] According to these findings, we aimed at evaluating if there was a reduction in osteoclastogenesis through the biological action of UV-activated 7-DHC:VitE coated implants.

We demonstrate the biocompatibility of the coating in RAW264.7 cells and the inhibition of the osteoclastogenesis *in vitro*. RAW264.7 cells are in a pre-osteoclast state that responds to RANKL stimulation *in vitro* to develop mature OCL through the monocyte fusion. Mature OCLs contain multiple nuclei and are surrounded by a stabilizing ring of actin filaments. Furthermore, OCL highly express TRAP, a sensitive and specific indicator of osteoclast functionality[45,46] and several fusion markers involved in the formation of the multinucleated OCL.[47–49] But besides TRAP and the fusion factors, an active OCL express markers that participate in the bone resorption process, via acidifying the bone microenvironment and digesting the organic matrix. Interestingly, several studies link the gene expression levels of these markers to the resorptive effect of mature OCL.[50–53] Therefore, our results show that our optimized surface impaired both osteoclastogenesis and bone resorption *in vitro*.

In summary, we have optimized D_3 synthesis in our implants by supplementing 7-DHC with VitE and by adding an incubation step of 48 h at 23°C after UV-irradiation. The optimized implants have shown a strong effect inhibiting osteoclastogenesis. Therefore, this approach can be considered as a novel implant therapy aiming at reducing osteoclast resorption and increasing bone formation.

ACKNOWLEDGMENT

This work was supported by the Ministerio de Ciencia e Innovación del Gobierno de España (Ramón y Cajal contract to M.M.).

REFERENCES

1. Satué M, Petzold C, Cordoba A, Ramis JM, Monjo M. UV photoactivation of 7-dehydrocholesterol on titanium implants enhances osteoblast differentiation and decreases Rankl gene expression. Acta Biomater 2013;9:5759–5770.
2. Kelly J, Lin A, Wang CJ, Park S, Nishimura I. Vitamin D and bone physiology: Demonstration of vitamin D deficiency in an implant osseointegration rat model. J Prosthodont 2009;18:473–478.
3. Dvorak G, Fugl A, Watzek G, Tangl S, Pokorny P, Gruber R. Impact of dietary vitamin D on osseointegration in the ovariectomized rat. Clin Oral Implants Res 2012;23:1308–1313.
4. MacLaughlin JA, Anderson RR, Holick MF. Spectral character of sunlight modulates photosynthesis of previtamin D3 and its photoisomers in human skin. Science 1982;216:1001–1003.
5. Terenetskaya I. Spectral monitoring of biologically active solar UVB radiation using an *in vitro* model of vitamin D synthesis. Talanta 2000;53:195–203.
6. Grigoryan ZL, Martiryan AI, Nersesyan LA, Markaryan SA. Photochemical transformations of 7-dehydrocholesterol. Russ J Appl Chem 2009;82:509–511.
7. Braun M, Fuß W, Kompa KL, Wolfrum J. Improved photosynthesis of previtamin D by wavelengths of 280–300 nm. J Photoch Phothobio A 1991;61:15–26.
8. Lehmann B, Genehr T, Knuschke P, Pietzsch J, Meurer M. UVB-induced conversion of 7-dehydrocholesterol to 1alpha,25-dihydroxyvitamin D3 in an *in vitro* human skin equivalent model. J Invest Dermatol 2001;117:1179–1185.
9. Holick MF. The cutaneous photosynthesis of previtamin D3: A unique photoendocrine system. J Invest Dermatol 1981;77(1):51–8.
10. Holick MF. Vitamin D: Physiology, Molecular Biology, and Clinical Applications (Nutrition and Health), 2nd ed. New York, NY: Humana Press; 2010.
11. Palmquist A, Omar OM, Esposito M, Lausmaa J, Thomsen P. Titanium oral implants: Surface characteristics, interface biology and clinical outcome. J R Soc Interface 2010;7 (Suppl 5):S515–S527.
12. Lamolle SF, Monjo M, Rubert M, Haugen HJ, Lyngstadaas SP, Ellingsen JE. The effect of hydrofluoric acid treatment of titanium surface on nanostructural and chemical changes and the growth of MC3T3-E1 cells. Biomaterials 2009;30:736–742.
13. Pfaffl MW. A new mathematical model for relative quantification in real-time RT-PCR. Nucleic Acids Res 2001;29.
14. Pfaffl MW, Tichopad A, Prgomet C, Neuvians TP. Determination of stable housekeeping genes, differentially regulated target genes and sample integrity: BestKeeper–Excel-based tool using pair-wise correlations. Biotechnol Lett 2004;26:509–515.
15. Satué M, Cordoba A, Ramis JM, Monjo M. UV-irradiated 7-dehydrocholesterol coating on polystyrene surfaces is converted to active vitamin D by osteoblastic MC3T3-E1 cells. Photochem Photobiol Sci 2013;12:1025–1035.
16. Xu L, Davis TA, Porter NA. Rate constants for peroxidation of polyunsaturated fatty acids and sterols in solution and in liposomes. J Am Chem Soc 2009;131:13037–13044.
17. Porter NA. A Perspective on free radical autoxidation: The physical organic chemistry of polyunsaturated fatty acid and sterol peroxidation. J Org Chem 2013;78:3511–3524.
18. Wang X, Quinn PJ. Vitamin E and its function in membranes. Prog Lipid Res 1999;38:309–336.
19. Nazrun AS, Norazlina M, Norliza M, Nirwana SI. The anti-inflammatory role of vitamin e in prevention of osteoporosis. Adv Pharmacol Sci 2012:(142702);7.
20. Lee NK, Choi YG, Baik JY, Han SY, Jeong DW, Bae YS, Kim N, Lee SY. A crucial role for reactive oxygen species in RANKL-induced osteoclast differentiation. Blood 2005;106:852–859.

21. Korade Z, Xu L, Harrison FE, Ahsen R, Hart SE, Folkes OM, Mirnics K, Porter NA. Antioxidant supplementation ameliorates molecular deficits in Smith-Lemli-Opitz syndrome. Biol Psychiatry 2014;75:215–222.
22. Lehmann B, Meurer M. Vitamin D metabolism. Dermatol Ther 2010;23:2–12.
23. Norval M, Bjorn LO, de Gruijl FR. Is the action spectrum for the UV-induced production of previtamin D3 in human skin correct? Photochem Photobiol Sci 2010;9:11–17.
24. Olds WJ, McKinley AR, Moore MR, Kimlin MG. *In vitro* model of vitamin D3 (cholecalciferol) synthesis by UV radiation: Dose-response relationships. J Photochem Photobiol B 2008;93:88–93.
25. Gao Y, Liu Y, Zhou L, Guo Z, Rong M, Liu X, Lai C, Ding X. The effects of different wavelength UV photofunctionalization on micro-arc oxidized titanium. PLoS ONE 2013;8:e68086.
26. Ogawa T. Ultraviolet photofunctionalization of titanium implants. Int J Oral Maxillofac Implants 2014;29.
27. Fujishima A, Rao TN, Tryk DA. Titanium dioxide photocatalysis. J Photoch Photobio C 2000;1:1–21.
28. Konaka R, Kasahara E, Dunlap WC, Yamamoto Y, Chien KC, Inoue M. Irradiation of titanium dioxide generates both singlet oxygen and superoxide anion. Free Radic Biol Med 1999;27:294–300.
29. Konaka R, Kasahara E, Dunlap WC, Yamamoto Y, Chien KC, Inoue M. Ultraviolet irradiation of titanium dioxide in aqueous dispersion generates singlet oxygen. Redox Rep 2001;6:319–325.
30. Reeves JF, Davies SJ, Dodd NJF, Jha AN. Hydroxyl radicals (OH) are associated with titanium dioxide (TiO2) nanoparticle-induced cytotoxicity and oxidative DNA damage in fish cells. Mutat Res-Fund Mol 2008;640:113–122.
31. van Driel MKM, Buurman CJ, Hewison M, Chiba H, Uitterlinden AG, Pols HA, van Leeuwen JP. Evidence for auto/paracrine actions of vitamin D in bone: 1Alpha-hydroxylase expression and activity in human bone cells. FASEB J 2006;20:2417–2419.
32. Carlsson A. Tracer experiments on the effect of vitamin D on the skeletal metabolism of calcium and phosphorus. Acta Physiol Scand 1952;26:212–220.
33. Bauer GC. Bone salt metabolism in bone growth and bone repair studied in rats by means of Ca45, P32, and Na22. Acta Orthop Scand 1954;23:247–253.
34. Roodman GD, Ibbotson KJ, MacDonald BR, Kuehl TJ, Mundy GR. 1,25-Dihydroxyvitamin D3 causes formation of multinucleated cells with several osteoclast characteristics in cultures of primate marrow. Proc Natl Acad Sci USA 1985;82:8213–8217.
35. Takahashi N, Yamana H, Yoshiki S, Roodman GD, Mundy GR, Jones SJ, Boyde A, Suda T. Osteoclast-like cell formation and its regulation by osteotropic hormones in mouse bone marrow cultures. Endocrinology 1988;122:1373–1382.
36. Sairanen S, Karkkainen M, Tahtela R, Laitinen K, Makela P, Lamberg-Allardt C, Valimaki MJ. Bone mass and markers of bone and calcium metabolism in postmenopausal women treated with 1,25-dihydroxyvitamin D (Calcitriol) for four years. Calcif Tissue Int 2000;67:122–127.
37. Aloia JF, Vaswani A, Yeh JK, Ellis K, Yasumura S, Cohn SH. Calcitriol in the treatment of postmenopausal osteoporosis. Am J Med 1988;84 (3 Part 1):401–408.
38. de Freitas PH, Hasegawa T, Takeda S, Sasaki M, Tabata C, Oda K, Li M, Saito H, Amizuka N. Eldecalcitol, a second-generation vitamin D analog, drives bone minimodeling and reduces osteoclastic number in trabecular bone of ovariectomized rats. Bone 2011;49: 335–342.
39. Gardiner EM, Baldock PA, Thomas GP, Sims NA, Henderson NK, Hollis B, White CP, Sunn KL, Morrison NA, Walsh WR. Increased formation and decreased resorption of bone in mice with elevated vitamin D receptor in mature cells of the osteoblastic lineage. FASEB J 2000;14:1908–1916.
40. Shiraishi A, Takeda S, Masaki T, Higuchi Y, Uchiyama Y, Kubodera N, Sato K, Ikeda K, Nakamura T, Matsumoto T. Alfacalcidol inhibits bone resorption and stimulates formation in an ovariectomized rat model of osteoporosis: Distinct actions from estrogen. J Bone Miner Res 2000;15:770–779.
41. Uchiyama Y, Higuchi Y, Takeda S, Masaki T, Shira-Ishi A, Sato K, Kubodera N, Ikeda K, Ogata E. ED-71, a vitamin D analog, is a more potent inhibitor of bone resorption than alfacalcidol in an estrogen-deficient rat model of osteoporosis. Bone 2002;30:582–588.
42. Takahashi N, Udagawa N, Suda T. Vitamin D endocrine system and osteoclasts. Bonekey Rep 2014;3.
43. Takasu H, Sugita A, Uchiyama Y, Katagiri N, Okazaki M, Ogata E, Ikeda K. c-Fos protein as a target of anti-osteoclastogenic action of vitamin D, and synthesis of new analogs. J Clin Invest 2006; 116:528–535.
44. Suda T, Jimi E, Nakamura I, Takahashi N. Role of 1 alpha,25-dihydroxyvitamin D3 in osteoclast differentiation and function. Methods Enzymol 1997;282:223–235.
45. Kirstein B, Chambers TJ, Fuller K. Secretion of tartrate-resistant acid phosphatase by osteoclasts correlates with resorptive behavior. J Cell Biochem 2006;98:1085–1094.
46. Seol J, Lee H, Kim N, Park S. Tartrate-resistant acid phosphatase as a diagnostic factor for arthritis. Int J Mol Med 2009;24:57–62.
47. Ishizuka H, Garcia-Palacios V, Lu G, Subler MA, Zhang H, Boykin CS, Choi SJ, Zhao L, Patrene K, Galson DL. ADAM8 enhances osteoclast precursor fusion and osteoclast formation *in vitro* and *in vivo*. J Bone Miner Res 2011;26:169–181.
48. Yagi M, Miyamoto T, Sawatani Y, Iwamoto K, Hosogane N, Fujita N, Morita K, Ninomiya K, Suzuki T, Miyamoto K. DC-STAMP is essential for cell-cell fusion in osteoclasts and foreign body giant cells. J Exp Med 2005;202:345–351.
49. Nakamura I, Pilkington MF, Lakkakorpi PT, Lipfert L, Sims SM, Dixon SJ, Rodan GA, Duong LT. Role of alpha(v)beta(3) integrin in osteoclast migration and formation of the sealing zone. J Cell Sci 1999;112 (Part 22):3985–3993.
50. Tong H-S, Sakai DD, Sims SM, Dixon JS, Yamin M, Goldring SR, Snead ML, Minkin C. Murine osteoclasts and spleen cell polykaryons are distinguished by mRNA phenotyping. J Bone Miner Res 1994;9:577–584.
51. Asotra S, Gupta AK, Sodek J, Aubin JE, Heersche JN. Carbonic anhydrase II mRNA expression in individual osteoclasts under "resorbing" and "nonresorbing" conditions. J Bone Miner Res 1994;9:1115–1122.
52. Wesolowski G, Duong LT, Lakkakorpi PT, Nagy RM, Tezuka K-I, Tanaka H, Rodan GA, Rodan SB. Isolation and Characterization of highly enriched, prefusion mouse osteoclastic cells. Exp Cell Res 1995;219:679–686.
53. Wucherpfennig AL, Li YP, Stetler-Stevenson WG, Rosenberg AE, Stashenko P. Expression of 92 kD type IV collagenase/gelatinase B in human osteoclasts. J Bone Miner Res 1994;9:549–556.

Paper V

Improved human gingival fibroblast response to titanium implants coated with UV-irradiated vitamin D precursor and vitamin E

Satué M. ; Gómez-Florit M. ; Monjo M. ; Ramis J.M.

Manuscript (2015).

Improved human gingival fibroblast response to titanium implants coated with UV-irradiated vitamin D precursor and vitamin E

María Satué[1,2†], Manuel Gómez-Florit [1,2†] Marta Monjo[1,2*] and Joana M. Ramis[1,2*]

[1]*Department of Fundamental Biology and Health Sciences, Research Institute on Health Sciences (IUNICS), University of Balearic Islands, Spain*

[2]*Instituto de Investigación Sanitaria de Palma, 07010 Palma, España.*

Running title: Gingival cell response to modified Ti implants

[†] Both authors contributed equally to the work.

* Corresponding author:

Research Institute on Health Sciences (IUNICS). University of Balearic Islands, Ctra. de Valldemossa, km 7.5 (E-07122). Palma de Mallorca, Spain. Phone: +34-971259960. Fax: +34971173184 ; E-mail: joana.ramis@uib.es, marta.monjo@uib.es

ABSTRACT

Background and Objective. UV-irradiated 7-dehydrocholesterol (7-DHC) and vitamin E (VitE) coated titanium (Ti) implants have a beneficial effect on bone cells. Human gingival fibroblasts (HGFs) are the most abundant cells in periodontal tissues and they are involved in the wound healing repair. The objective of this study was to evaluate the response of HGFs to Ti implants coated with UV-irradiated 7-DHC and VitE, for improved soft tissue integration of dental implants.

Methods. Ti surfaces were coated with 7-DHC and VitE, UV-irradiated and incubated for 48 hours at 23ºC to allow cholecalciferol (D_3) synthesis from 7-DHC onto the Ti surface. HGFs were cultured on the modified surfaces and the influence of the coating in these cells was evaluated through the analysis of (i) biocompatibility, (ii) mRNA levels of genes involved in the extracellular matrix composition and turnover, inflammatory response, periodontal bone resorption and wound healing, and (iii) protein levels of matrix metalloproteinase-1 (MMP1) and metallopeptidase inhibitor-1 (TIMP1).

Results. We found a beneficial effect of UV-irradiated 7-DHC:VitE coated Ti implants on HGFs. Besides being biocompatible with HGFs, our coating increased collagen III α1 and fibronectin whilst decreased interleukin-8 mRNA levels. TIMP1 was increased at both mRNA and protein levels in HGFs cultured on UV-irradiated 7-DHC:VitE coated Ti implants. Finally, our coating decreased RANKL mRNA levels in HGFs.

Conclusion. UV-irradiated 7-DHC:VitE coated Ti implants have a positive effect on HGFs *in vitro* by reducing the inflammatory response and ECM breakdown.

Keywords

7-Dehydrocholesterol, vitamin D, soft tissue integration, dental implant.

1. INTRODUCTION

The biological relevance of vitamin D in the bone metabolism is widely recognized (1). However, non-skeletal functions of vitamin D are currently gaining notoriety since several evidences link this hormone to autoimmune diseases, cancers and periodontal health (2). The synthesis of vitamin D starts in our body when its precursor, 7-dehydrocholesterol (7-DHC), is UV-irradiated and further twice hydroxylated in the liver and kidney until forming the final active metabolite, 1-25-dihydroxyvitamin D_3 (1,25-D_3). Interestingly, recent investigations have revealed extra-renal sites of vitamin D production, such as macrophages (3), skin (4), bone (5,6) and periodontal tissues (7–9).

A successful dental implant requires its integration with hard (bone) and soft (gingiva) tissues. Although there are numerous strategies aiming at improving osseointegration of dental materials, recent studies are also focusing on the soft tissue integration (10–12). Gingival fibroblasts (HGFs) are the most abundant cells in the gingiva and they are responsible for the synthesis of extracellular matrix (ECM) and for the wound healing repair and regeneration after the dental implant installation (13,14). HGFs are able to produce final active vitamin D since they express the required enzymatic machinery to synthesize 1,25-D_3 (15), as the osteoblastic cells do (5). In previous studies we proved that UV-irradiated 7-DHC coated titanium (Ti) implants allow pre-osteoblastic (16) and mesenchymal stem cells (17) to produce themselves active vitamin D with positive effects on their osteogenic differentiation. Furthermore, these modified surfaces inhibit osteoclastogenesis, especially when combining 7-DHC with the antioxidant α-tocopherol (VitE), as it allows the achievement of higher levels of vitamin D synthesis (6). Therefore, given the promising results of UV-irradiated 7-DHC:VitE coated Ti implants on bone cells, it was of our great interest to determine their biological effect on HGF.

To this purpose, we assessed the effect of UV-irradiated 7-DHC:VitE coated Ti implants on HGF cell viability, morphology, gene expression and protein levels of specific markers involved in the ECM turnover and wound healing.

2. MATERIALS AND METHODS

2.1. Implants and treatments

Stock solutions of 7-DHC and VitE (Sigma, St. Louis, MO, USA) were prepared in absolute ethanol and filtered with a 0.22 µm pore size filter before use. Ti implants used were all made of grade 4 with a diameter of 6.2 mm and a height of 2 mm (Implantmedia, Lloseta, Spain). All disks were machined from cp Ti rods and subsequently cleaned as described elsewhere (18). For the surface modification of Ti implants, 10 µL of 0.2 nM 7-DHC supplemented with VitE on a mass-to-mass basis (1:1; m:m) were left on the surfaces. Additionally, only ethanol, VitE (0.18 pmol/Ti disk) or 7-DHC (0.2 nmols/Ti disk) were considered as controls for *in vitro* experiments. Once the surfaces were coated, UV irradiation was performed as described elsewhere (16), UV-irradiation produces a ring opening of 7-DHC that results in the formation of preD_3. Ti surfaces were then incubated for 48 hours at 23 ºC in absence of light in order to favor the

$preD_3$-D_3 isomerization. Finally, modified surfaces were processed to analyze their coating composition by HPLC or directly used for *in vitro* experiments.

2.2. Determination of the conversion of 7-DHC to D_3 by HPLC

The amount of 7-DHC, $preD_3$ and D_3 on the surface was quantified by HPLC just after the UV-irradiation and after 48 hours of incubation post-irradiation as described in a previous study (16).

2.3. Cell culture

Three different donors of primary HGF (Provitro GmbH, Berlin, Germany) were used (range 19-47 years; male:female ratio 2:1). Provitro assured that cells were obtained ethically and legally and that all donors provided written informed consent. HGFs were cultured at 37˚C/5% CO_2 and maintained in fibroblast growth medium (Provitro GmbH) supplemented with 10% fetal calf serum, 50 ng amphotericin/mL and 50 µg gentamicin/mL (Provitro GmbH). Experiments were performed with HGFs between passages 7 and 8 after isolation.

To test the effect of the surface modification, cells were seeded at a density of $2.3x10^4$ cells/cm^2. Culture media were changed every other day with 100 µM ascorbic acid addition in order to promote collagen deposition. Cytotoxicity, cell morphology, gene expression, protein quantification, wound healing assay and inflammatory response were evaluated after 3 days of culture and gene expression and protein quantification after 14 days of culture.

2.4. Cytotoxicity analysis

Lactate dehydrogenase (LDH) activity in the culture media 3 d after cell seeding was used as an index of cell death. The LDH activity was estimated according to the manufacturer's kit instructions (Roche Diagnostics, Mannheim, Germany) by assessing the rate of oxidation of NADH at 490nm in presence of pyruvate. Results were presented relative to the LDH activity in the media of cells seeded on tissue culture plastic (TCP) without treatment (low control, 0% of cell death) and of cells grown on TCP treated with 1% Triton X-100 (high control, 100% cell death). The percentage of LDH activity was calculated using the following equation: Cytotoxicity (%) = (exp.value – low control)/ (high control – low control) x 100.

2.5. Cell morphology analysis

Confocal images of cells grown onto modified Ti disks were obtained after 3 d of cell culture. Cells were first fixed and then permeabilized and further stained with Phalloidin-FITC (50 µg/mL; Sigma) to stain actin filaments. Finally, a drop of Fluoroshield-DAPI (Sigma) was added to stain the cell nuclei. Various images of each implant were taken with the confocal microscope (Leica DMI 4000B with Leica TCS SPE laser system) by measuring the fluorescence signal between 430 and 480 nm for DAPI and 500 and 525 nm for Phalloidin-FITC.

2.6. RNA isolation and real-time RT-PCR analysis

Total RNA was isolated using Tripure® (Roche Diagnostics) and total RNA was quantified at 260 nm using a Nanodrop spectrophotometer (NanoDrop Technologies, Wilmington, DE, USA). The same amount of RNA was reverse transcribed to cDNA at 42 ºC for 60 min using

High Capacity RNA-to-cDNA kit (Applied Biosystems, Foster City, CA, USA), according to the protocol of the supplier. Aliquots of each cDNA were frozen (-20 °C) until the PCR reactions were carried out.

Real-time PCR was performed for two reference genes, glyceraldehyde-3-phosphate dehydrogenase (GAPDH) and beta-actin (ACTBL2), and several target genes (Table 1). Real-time PCR was performed in the Lightcycler 480® (Roche Diagnostics) using SYBR green detection. Each reaction contained 7 µL Lightcycler-FastStart DNA MasterPLUS SYBR Green I (containing Fast Start Taq polymerase, reaction buffer, dNTPs mix, SYBR Green I dye and $MgCl_2$), 0.5 µM of each, the sense and the antisense specific primers (Table 1) and 3 µL of the cDNA dilution in a final volume of 10 µL. The amplification program consisted of a pre-incubation step for denaturation of the template cDNA (5 min 95 °C), followed by 45 cycles consisting of a denaturation step (10 s 95 °C), an annealing step (10 s 60 °C) and an extension step (10 s 72 °C). After each cycle, fluorescence was measured at 72 °C. A negative control without a cDNA template was run in each assay. Real-time efficiencies (E) were calculated from the given slopes in the LightCycler 480 software using serial dilutions, showing all the investigated transcripts high real-time PCR efficiency rates, and high linearity when different concentrations were used. PCR products were subjected to a melting curve analysis on the LightCycler and subsequently 2% agarose/ TAE gel electrophoresis to confirm amplification specificity, Tm and amplicon size, respectively.

All samples were normalized by the geometric mean of the expression levels of ACTBL2 and GAPDH and fold changes were related to the control groups using the following equation (19): ratio = $E_{target}^{\Delta Cp\ target\ (mean\ control\ -\ sample)}$ / $E_{reference}^{\Delta Cp\ reference\ (mean\ control\ -\ sample)}$, where Cp is the is the crossing point of the reaction amplification curve amd E is the efficiency from the given slopes using serial dilutions, as determined by the LightCycler 480 software. Stability of reference genes was calculated using the BestKeeper tool (20).

2.7. Enzyme-linked immunosorbent assays (ELISA)

The detection of TIMP1 and MMP1 was performed from cell culture media after 3 and 14 d of cell culture by commercially available ELISA kits (Sigma) according to kit instructions. Absorbance values were measured with a microplate reader at 450 nm.

2.8. Wound healing assay

Wound healing assay was performed on confluent monolayers (after 3 d of cell culture) grown on the modified Ti surfaces. HGF cells were scraped with 10 µl sterile pipette tips in a straight line to create a scratch. HGF cells grown on TCP were used as control to determine confluence. Then, cell monolayers were washed once with growth medium to remove cell debris and detached cells. HGF cells were allowed to close the scratch for 2 days at standard cell culture conditions. At this point of time, culture medium was removed and RNA was isolated as described before to study gene expression of MMP1, ACTA2, EDN1 and TGFB1.

2.9. Statistical analysis

All data are presented as mean values ± standard error of the mean (S.E.M.). The Kolmogorov–Smirnov test was done to assume parametric or non-parametric distributions.

Differences between groups were assessed by Mann-Whitney-test, Student t-test or by paired t-test. The SPSS® program for Windows, version 17.0 (SPSS, Chicago, IL, US) was used. Results were considered statistically significant at the p-values ≤ 0.05.

3. RESULTS

3.1. D_3 production from UV-irradiated 7-DHC coated Ti disks

We analyzed the coating composition of the different modified Ti disks after 48 h of incubation at 23 ºC. HPLC analyses determined 61.82 ± 9.96 pmol and 31.34 ± 5.10 pmol of D_3 per Ti disk for 7-DHC:VitE and 7-DHC surfaces, respectively.

3.2. Effect of UV-irradiated 7-DHC:VitE coated Ti surfaces on cell viability and morphology in HGFs

We first evaluated the effect of these modified surfaces on cell viability and morphology. LDH activity, an index of cytotoxicity, showed that 7-DHC coated Ti surfaces produced a higher LDH release (8.44 ± 3.15 %) compared with EtOH control (1.48 ± 5.45 %). Otherwise, no differences were found in 7-DHC:VitE coated Ti surfaces (2.70 ± 2.71 %) and in VitE coated Ti surfaces (6.31 ± 2.50 %) when compared with EtOH control. Furthermore, cell morphology visualization (not shown) indicated that cells maintained their typical fibroblastic morphology in all the coated surfaces.

3.3. Effect of UV-irradiated 7-DHC:VitE coated Ti surfaces on gene expression in HGFs

We analysed the mRNA levels of HGF cells cultured on the modified Ti surfaces after 3 and 14 days of culture (Figure 1). 7-DHC:VitE up-regulated COL3A1 and FN1 expression compared with 7-DHC control at day 14 (37% and 55% increase respectively). Also 7-DHC and 7-DHC:VitE increased almost a 20% FN1 expression at day 3 compared with EtOH control. Regarding MMP1, cells cultured on 7-DHC:VitE showed a 40% higher mRNA expression levels compared with EtOH control at day 3, although the same group showed a significantly lower expression levels at day 14 when compared with VitE and 7-DHC controls (20% and 30% decrease respectively). TIMP1 gene expression at day 3 increased a 10% in cells cultured onto 7-DHC:VitE compared with EtOH control and VitE .

In evaluating the cytokines, no differences were found in IL6 gene expression but 7-DHC:VitE significantly decreased the mRNA levels of IL8 after 14 days of cell culture when compared with the three controls (up to 3-fold decrease). After 3 days, VitE increased IL10 whilst 7-DHC decreased its expression compared with EtOH control. Also a lower expression of IL10 was found in 7-DHC:VitE when compared with VitE after 3 and 14 days of culture. Finally, RANKL expression was down-regulated in cells cultured for 3 days on 7-DHC compared with EtOH control and in cells cultured on 7-DHC:VitE surfaces compared with EtOH and VitE controls (40% and 60% decrease respectively). Furthermore, OPG increased a 20% in 7-DHC:VitE group when compared with VitE control. RANKL and OPG mRNA levels after 14 days of cell culture could not be determined due to their low expression levels.

3.4. Effect of UV-irradiated 7-DHC:VitE coated Ti surfaces on MMP1 and TIMP1 production in HGFs

We quantified MMP1 and TIMP1 protein levels after 3 and 14 days of cell culture (Figure 2). Production of MMP1 was similar in all modified surfaces but TIMP1 significantly increased in cells cultured for 14 days on 7-DHC:VitE surfaces compared with VitE control.

3.5. Effect of UV-irradiated 7-DHC:VitE coated Ti surfaces on wound healing in HGFs

We analysed the effect of UV-irradiated 7-DHC:VitE coating on gene expression after wound healing (Figure 3). No differences were found for ACTA2, TGFB1 and EDN mRNA levels but cells cultured on 7-DHC showed a lower mRNA expression of MMP1 compared with EtOH and VitE controls.

4. DISCUSSION

Most of the dental implant studies have only focused on osseointegration although their success depends on both hard and soft tissue integration. Indeed, an ideal dental implant should: (i) promote peri-implant bone healing and osseointegration, and (ii) promote soft tissue healing around the implant forming a biological seal between the oral cavity and the bone (21). Thus, an optimal soft tissue healing would prevent bacterial penetration, reduce inflammation and induce gingival fibroblast proliferation to aid in the tissue regeneration process. However, if fibroblasts fail to repair the wound between the implant and the surrounding tissue, the generated inflammatory reaction to bacterial invasion could lead to implant loss via peri-implantitis.

Although rough/micro-rough surfaces are required for optimal osseointegration of implant fixtures in contact to the jawbone, most implant systems use machined surface topographies for implant abutments (22,23), which are in contact with the soft tissue. In fact, several in vitro studies show that fibroblasts prefer smooth surfaces, and especially machined micro-grooved surfaces, rather than rough surfaces (24–27) while in vivo studies show that surface roughness does not affect soft tissue dimensions (21). Furthermore, micro-grooved surfaces can inhibit epithelial downgrowth (24). For these reasons, we selected machined micro-grooved surfaces for this study.

Vitamin D has a positive role in implant osseointegration (28–31). In previous studies, we proved that UV-irradiated 7-DHC coated Ti implants allowed vitamin D in-cell biosynthesis, promoting osteoblast differentiation (16) and inhibiting osteoclastogenesis especially when supplemented with VitE (6). Furthermore, on one hand, vitamin D supplementation has been suggested to have a beneficial effect on the oral health (2), on the other hand, HGFs were able to produce final active vitamin D (15), thus, we hypothesized that UV-irradiated 7-DHC:VitE coated Ti implants would have a positive effect on soft tissue integration. Our results show that the UV-irradiated 7-DHC:VitE coated Ti surfaces are biocompatible with HGFs, up-regulate FN1, COL3A1 and down-regulate IL8 and RANKL mRNA levels. Furthermore, this coating increases TIMP1 mRNA and protein levels, suggesting a beneficial effect on soft tissue integration.

Excessive inflammation levels after an implant placement are related to decreased wound healing, leading to limited soft tissue integration. In the present study, we show that UV-

irradiated 7-DHC:VitE coated Ti surfaces significantly downregulated IL8 mRNA levels, an important proinflamatory cytokine closely related to peri-implantitis (32). Similarly, human periodontal ligament cells decreased IL8 when stimulated with vitamin D (33), suggesting its potential to inhibit gingival inflammation. Another important event during inflammation is the induction of MMPs that leads to increased collagen destruction (13) which is regulated by their inhibitors, TIMPs (34). Therefore, the increase in TIMP1 production found on our coating might damp down the excessive collagen breakdown caused by inflammation.

HGFs are responsible for forming a collagen-rich ECM and for repairing wound (14,35). Besides its anti-inflammatory activity, our coating increases FN1 and COL3A1 mRNA levels. On one hand, FN1 is involved in cell adhesion (36) so a higher FN1 expression may be related to an increased cell adhesion onto 7-DHC:VitE coated Ti. However, cell adhesion studies should be performed to confirm this result. On the other, COL3A1 is increased in HGF maturation (37) and scarless wound healing (38) so an increase in their mRNA levels may also be beneficial for soft tissue integration. In addition, healing process can produce either a scarred tissue or a functional regenerated tissue, depending on the expression of fibrotic markers (39). No differences were found in the mRNA levels of these markers after the wound healing among the different surfaces. Thus, this steady expression suggests a more regenerative response rather than a more scarring effect.

HGFs can produce osteoclast-stimulating or inhibiting cytokines that are involved in bone resorption in periodontitis (40,41). These include RANKL, which activates osteoclastogenesis, and its decoy OPG that prevents osteoclast formation. Indeed, clinical investigations showed that RANKL is upregulated while OPG is downregulated in periodontitis, leading to a higher bone resorption (42,43). In this study, we found that UV-irradiated 7-DHC:VitE coated Ti surfaces decreased RANKL mRNA levels at short term, which could be beneficial to avoid peri-implant bone resorption. However, Liu et al. (8) found that $25D_3$ and $1,25D_3$ addition up-regulated RANKL mRNA in HGF. This discrepancy may be explained by the vitamin D metabolite dose used to stimulate cells. Here, according to previous studies using this coating (16), a lower $25D_3$ and $1,25D_3$ cell production is expected when compared with the concentrations used by Liu et al. (8).

5. CONCLUSIONS

In this study we show for the first time the biological potential of UV-irradiated 7-DHC:VitE coated Ti implants on gingival fibroblasts. We demonstrate that these modified surfaces are biocompatible with HGFs, decrease IL8 and increase FN1 and COL3A1 mRNA levels, suggesting a positive action in the inflammatory response and in the ECM maturation. Also, UV-irradiated 7-DHC:VitE coated Ti increases TIMP1 at both mRNA and protein levels, suggesting therefore a decrease in the MMP-related ECM breakdown. Additionally, our coating decreases RANKL mRNA levels, which may imply an indirect inhibition of bone resorption. All in all, these findings show that UV-irradiated 7-DHC:VitE coated Ti implants may have a beneficial effect for soft tissue integration and implant success. Nevertheless, we acknowledge that *in vivo* studies are required to confirm the results here presented and to settle the clinical potential of the coating here proposed.

6. ACKNOWLEDGEMENT

This work was supported by the Ministerio de Ciencia e Innovación del Gobierno de España (Torres Quevedo contract to MGF and Ramón y Cajal contract to MM).

REFERENCES

1. St-Arnaud R. The direct role of vitamin D on bone homeostasis. *Arch Biochem Biophys* 2008;**473**:225–30.

2. Stein SH, Livada R, Tipton D a. Re-evaluating the role of vitamin D in the periodontium. *J Periodontal Res* 2013;**49**:545–53.

3. Adams JS, Beeker TG, Hongo T, Clemens TL. Constitutive expression of a vitamin D 1-hydroxylase in a myelomonocytic cell line: a model for studying 1,25-dihydroxyvitamin D production in vitro. *J Bone Min Res* 1990;**5**:1265–9.

4. Lehmann B, Meurer M. Extrarenal sites of calcitriol synthesis: the particular role of the skin. *Recent Results Cancer Res* 2003;**164**:135–45.

5. Satué M, Córdoba A, Ramis JM, Monjo M. UV-irradiated 7-dehydrocholesterol coating on polystyrene surfaces is converted to active vitamin D by osteoblastic MC3T3-E1 cells. *Photochem Photobiol Sci* 2013;**12**:1025–35.

6. Satué M, Ramis JM, Monjo M. Cholecalciferol synthesized after UV-activation of 7-dehydrocholesterol onto titanium implants inhibits osteoclastogenesis in vitro. *J Biomed Mater Res A* 2014:1–9.

7. Liu K, Meng H, Hou J. Activity of 25-Hydroxylase in Human Gingival Fibroblasts and Periodontal Ligament Cells. *PLoS One* 2012;**7**:e52053.

8. Liu K, Meng H, Hou J. Characterization of the autocrine/paracrine function of vitamin D in human gingival fibroblasts and periodontal ligament cells. *PLoS One* 2012;**7**:e39878.

9. Amano Y, Komiyama K, Makishima M. Vitamin D and periodontal disease. *J Oral Sci* 2009;**51**:11–20.

10. Van Brakel R, Cune MS, van Winkelhoff AJ, de Putter C, Verhoeven JW, van der Reijden W. Early bacterial colonization and soft tissue health around zirconia and titanium abutments: an in vivo study in man. *Clin Oral Implant Res* 2011;**22**:571–7.

11. Nisapakultorn K, Suphanantachat S, Silkosessak O, Rattanamongkolgul S. Factors affecting soft tissue level around anterior maxillary single-tooth implants. *Clin Oral Implant Res* 2010;**21**:662–70.

12. Esposito M, Maghaireh H, Grusovin MG, Ziounas I, Worthington H V. Soft tissue management for dental implants: what are the most effective techniques? A Cochrane systematic review. *Eur J Oral Implant* 2012;**5**:221–38.

13. Bartold PM, Walsh LJ, Narayanan AS. Molecular and cell biology of the gingiva. *Periodontol 2000* 2000;**24**:28–55.

14. Abiko Y, Hiratsuka K, Kiyama-Kishikawa M, Tsushima K, Ohta M, Sasahara H. Profiling of differentially expressed genes in human gingival epithelial cells and fibroblasts by DNA microarray. *J Oral Sci* 2004;**46**:19–24.

15. Liu K, Meng H, Hou J. Activity of 25-Hydroxylase in Human Gingival Fibroblasts and Periodontal Ligament Cells. *PLoS One* 2012;**7**:e52053.

16. Satué M, Petzold C, Córdoba A, Ramis JM, Monjo M. UV photoactivation of 7-dehydrocholesterol on titanium implants enhances osteoblast differentiation and decreases Rankl gene expression. *Acta Biomater* 2013;**9**:5759–70.

17. Satué M, Ramis JM, Monjo M. UV-activated 7-dehydrocholesterol coated titanium implants promote differentiation of human umbilical cord mesenchymal stem cells into osteoblasts. *J Biomater Appl* 2015.

18. Lamolle SF, Monjo M, Rubert M, Haugen HJ, Lyngstadaas SP, Ellingsen JE. The effect of hydrofluoric acid treatment of titanium surface on nanostructural and chemical changes and the growth of MC3T3-E1 cells. *Biomaterials* 2009;**30**:736–42.

19. Pfaffl MW. A new mathematical model for relative quantification in real-time RT-PCR. *Nucleic Acids Res* 2001;**29**:e45.

20. Pfaffl MW, Tichopad A, Prgomet C, Neuvians TP. Determination of stable housekeeping genes, differentially regulated target genes and sample integrity: BestKeeper--Excel-based tool using pair-wise correlations. *Biotechnol Lett* 2004;**26**:509–15.

21. Sculean A, Gruber R, Bosshardt DD. Soft tissue wound healing around teeth and dental implants. *J Clin Periodontol* 2014;**41 Suppl 1**:S6–22.

22. Schwarz F, Herten M, Sager M, Wieland M, Dard M, Becker J. Histological and immunohistochemical analysis of initial and early subepithelial connective tissue attachment at chemically modified and conventional SLA titanium implants. A pilot study in dogs. *Clin Oral Investig* 2007;**11**:245–55.

23. Kloss FR, Steinmüller-Nethl D, Stigler RG, Ennemoser T, Rasse M, Hächl O. In vivo investigation on connective tissue healing to polished surfaces with different surface wettability. *Clin Oral Implants Res* 2011;**22**:699–705.

24. Rompen E, Domken O, Degidi M, Pontes AEF, Piattelli A. The effect of material characteristics, of surface topography and of implant components and connections on soft tissue integration: a literature review. *Clin Oral Implants Res* 2006;**17 Suppl 2**:55–67.

25. Wieland M, Chehroudi B, Textor M, Brunette DM. Use of Ti-coated replicas to investigate the effects on fibroblast shape of surfaces with varying roughness and constant chemical composition. *J Biomed Mater Res* 2002;**60**:434–44.

26. Guillem-Marti J, Delgado L, Godoy-Gallardo M, Pegueroles M, Herrero M, Gil FJ. Fibroblast adhesion and activation onto micro-machined titanium surfaces. *Clin Oral Implants Res* 2013;**24**:770–80.

27. Gomez-Florit M, Xing R, Ramis JM, Taxt-Lamolle S, Haugen HJ, Lyngstadaas SP, et al. Human gingival fibroblasts function is stimulated on machined hydrided titanium zirconium dental implants. *J Dent* 2014;**42**:30–8.

28. Zhou C, Li Y, Wang X, Shui X, Hu J. 1,25Dihydroxy vitamin D(3) improves titanium implant osseointegration in osteoporotic rats. *Oral Surg Oral Med Oral Pathol Oral Radiol* 2012;**114**:S174–8.

29. Naito Y, Jimbo R, Bryington MS, Vandeweghe S, Chrcanovic BR, Tovar N, et al. The influence of 1α.25-dihydroxyvitamin d3 coating on implant osseointegration in the rabbit tibia. *J Oral Maxillofac Res* 2014;**5**:e3.

30. Kelly J, Lin A, Wang CJ, Park S, Nishimura I. Vitamin D and bone physiology: demonstration of vitamin D deficiency in an implant osseointegration rat model. *J Prosthodont* 2009;**18**:473–8.

31. Dvorak G, Fügl A, Watzek G, Tangl S, Pokorny P, Gruber R. Impact of dietary vitamin D on osseointegration in the ovariectomized rat. *Clin Oral Implant Res* 2012;**23**:1308–13.

32. PetkoviĆ AB, MatiĆ SM, StamatoviĆ N V, VojvodiĆ D V, TodoroviĆ TM, LaziĆ ZR, et al. Proinflammatory cytokines (IL-1beta and TNF-alpha) and chemokines (IL-8 and MIP-1alpha) as markers of peri-implant tissue condition. *Int J Oral Maxillofac Surg* 2010;**39**:478–85.

33. Tang X, Pan Y, Zhao Y. Vitamin D inhibits the expression of interleukin-8 in human periodontal ligament cells stimulated with Porphyromonas gingivalis. *Arch Oral Biol* 2013;**58**:397–407.

34. Sakagami G, Sato E, Sugita Y, Kosaka T, Kubo K, Maeda H, et al. Effects of nifedipine and interleukin-1alpha on the expression of collagen, matrix metalloproteinase-1, and tissue inhibitor of metalloproteinase-1 in human gingival fibroblasts. *J Periodontal Res* 2006;**41**:266–72.

35. Bartold PM, Narayanan a S. Molecular and cell biology of healthy and diseased periodontal tissues. *Periodontol 2000* 2006;**40**:29–49.

36. Van der Pauw MT, Van den Bos T, Everts V, Beertsen W. Phagocytosis of fibronectin and collagens type I, III, and V by human gingival and periodontal ligament fibroblasts in vitro. *J Periodontol* 2001;**72**:1340–7.

37. Gómez-Florit M, Ramis JM, Xing R, Taxt-Lamolle S, Haugen HJ, Lyngstadaas SP, et al. Differential response of human gingival fibroblasts to titanium- and titanium-zirconium-modified surfaces. *J Periodontal Res* 2014;**49**:425–36.

38. Satish L, Kathju S. Cellular and Molecular Characteristics of Scarless versus Fibrotic Wound Healing. *Dermatol Res Pr* 2010;**2010**:790234.

39. Lin N-H, Gronthos S, Bartold PM. Stem cells and periodontal regeneration. *Aust Dent J* 2008;**53**:108–21.

40. Teng Y-TA. Protective and destructive immunity in the periodontium: Part 1--innate and humoral immunity and the periodontium. *J Dent Res* 2006;**85**:198–208.

41. Lerner UH. Inflammation-induced bone remodeling in periodontal disease and the influence of post-menopausal osteoporosis. *J Dent Res* 2006;**85**:596–607.

42. Belibasakis GN, Bostanci N, Hashim A, Johansson A, Aduse-Opoku J, Curtis M a, et al. Regulation of RANKL and OPG gene expression in human gingival fibroblasts and periodontal ligament cells by Porphyromonas gingivalis: a putative role of the Arg-gingipains. *Microb Pathog* 2007;**43**:46–53.

43. Yucel-Lindberg T, Båge T. Inflammatory mediators in the pathogenesis of periodontitis. *Expert Rev Mol Med* 2013;**15**:e7.

TABLES

Table 1. Sense (S) and antisense (A) primers used in the real-time PCR of reference and target genes.

Related function	Gene	Primer sequence (5´- 3´)	Product size (bp)	GeneBank Accession Number
ECM component	Collagen III α1 (COL3A1)	S: GGCCTACTGGGCCTGGTGGT A: CCACGTTCACCAGGGGCACC	190	NM_000090.3
ECM turnover	Matrix metalloproteinase-1 (MMP1)	S: TGTCAGGGGAGATCATCGGGACA A: TGGCCGAGTTCATGAGCTGCA	177	NM_002421.3
ECM turnover	Metallopeptidase inhibitor 1 (TIMP1)	S: TTCCGACCTCGTCATCAGGG A: TAGACGAACCGGATGTCAGC	144	NM_003254.2
ECM component / cell adhesion	Fibronectin (FN1)	S: CGGAGAGACAGGAGGAAATAGCCCT A: TTGCTGCTTGCGGGGCTGTC	150	NM_212482.1
Anti-inflammatory cytokine	Interleukin-10 (IL10)	S: TTA TCT TGT CTC TGG GCT TGG A: ATG AAG TGG TTG GGG AAT GA	139	NM_000572.2
Pro-inflamatory cytokine	Interleukin-6 (IL6)	S: AGGAGACTTGCCTGGTGAAA A: GCATTTGTGGTTGGGTCAG	196	NM_000600.3
Pro-inflamatory cytokine	Interleukin-8 (IL8)	S: GGTGCAGTTTTGCCAAGGAG A: TTCCTTGGGGTCCAGACAGA	183	NM_000584.3
Periodontal bone resorption	Osteoprotegerin (OPG)	S: AGGCGATACTTCCTGTTGCC A: GATGTCCAGAAACACGAGCG	163	NM_002546.3
Periodontal bone resorption	Receptor Activator of NF-κB Ligand (RANKL)	S: CAGAGCGCAGATGGATCCTAA A: TCCTTTTGCACAGCTCCTTGA	180	NM_003701.3
Wound healing	α-smooth muscle actin (ACTA2)	S: TAAGACGGGAATCCTGTGAAGC A: TGTCCCATTCCCACCATCAC	184	NM_001141945.1
Wound healing	Endothelin-1 (EDN1)	S: ACGGCGGGGAGAAACCCACT A: ACGGAACAACGTGCTCGGGA	147	NM_001955.4
Wound healing	Transforming growth factor-β1 (TGFB1)	S: TGTCACCGGAGTTGTGCGGC A: GGCCGGTAGTGAACCCGTTG	131	NM_000660.4
Reference gene	Beta-actin (ACTBL2)	S: CTGGAACGGTGAAGGTGACA A: AAGGGACTTCCTGTAACAATGCA	136	NM_001101.3
Reference gene	Glyceraldehyde 3-phosphate dehydrogenase (GAPDH)	S: TGCACCACCAACTGCTTAGC A: GGCATGGACTGTGGTCATGAG	87	NM_002046.3

ECM: extracellular matrix

FIGURES

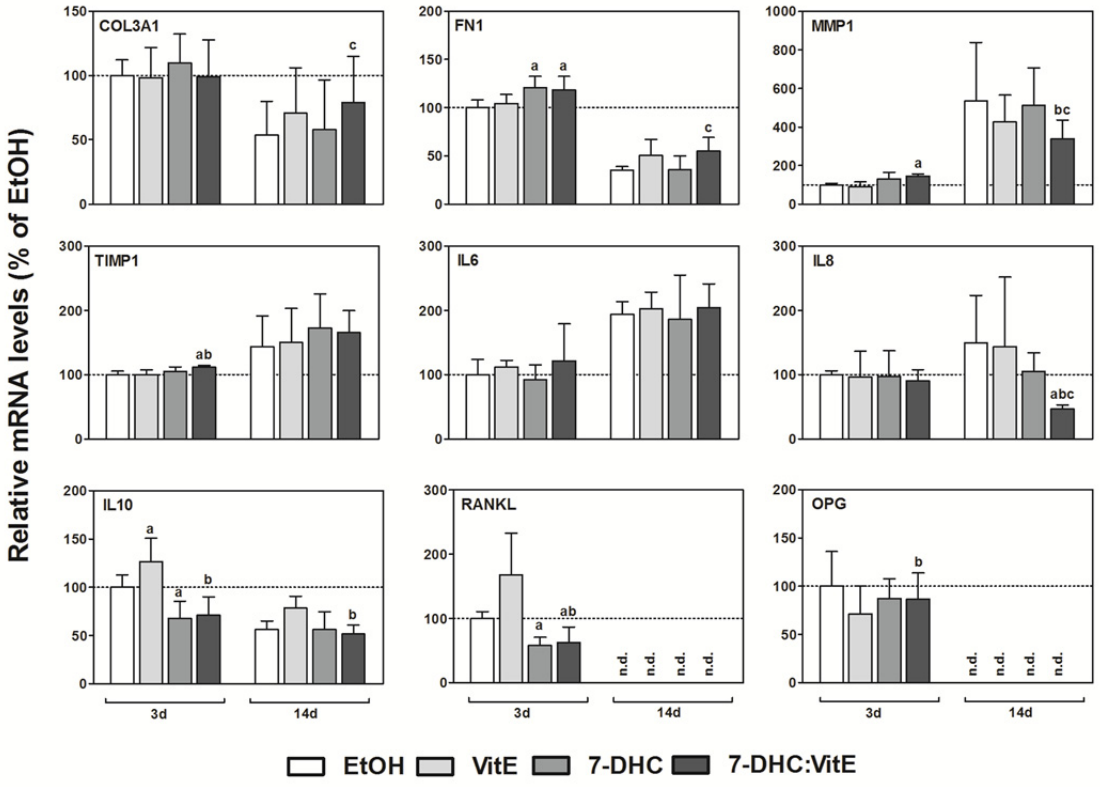

Figure 1. Effect of UV-irradiated 7-DHC:VitE coated Ti disks on gene expression levels of HGF grown for 3 and 14 d. Data represent fold changes of target genes normalized to beta-actin and GAPDH (reference genes) expressed relative to EtOH control (3 d or 14 d) that was set at 100%. Values represent the mean ± S.E.M. (N=6; 3 donors). Significant differences were assessed by paired t t-test: [a] treatment versus the corresponding EtOH control for each time point; [b] treatment versus the corresponding VitE control for each time point; [c] treatment versus the corresponding 7-DHC control for each time point.

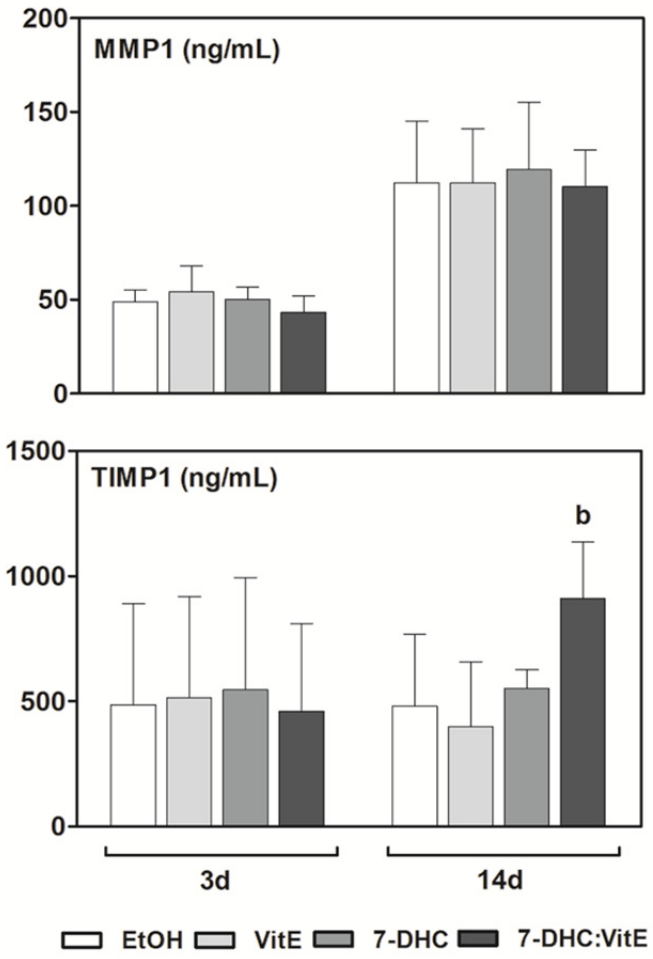

Figure 2. Effect of UV-irradiated 7-DHC:VitE coated Ti disks on MMP1 and TIMP1 protein levels and their ratio after 3 and 14 d of cell culture. Values represent the mean ± S.E.M. (N=6; 3 donors). Significant differences were assessed by paired t-test: [b] treatment versus the corresponding VitE control for each time point.

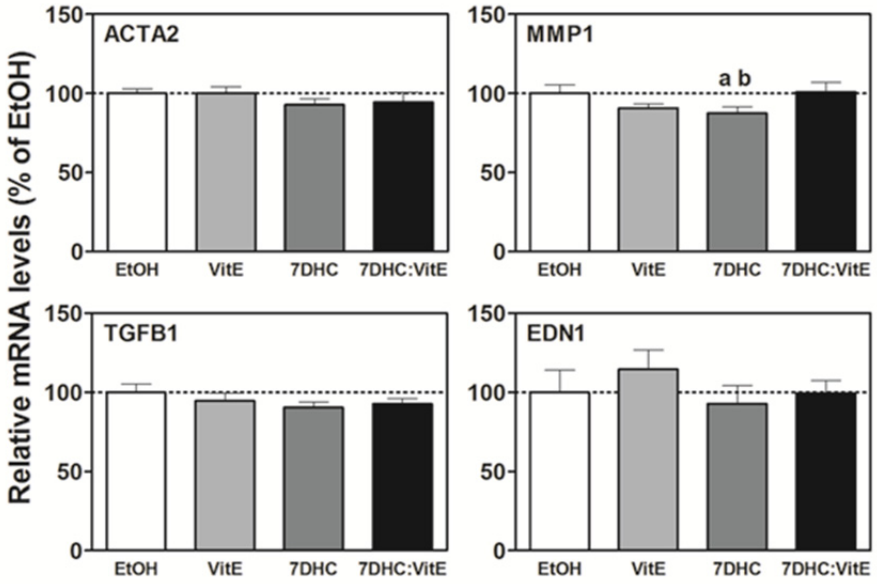

Figure 3. Effect of UV-irradiated 7-DHC:VitE coated Ti disks on wound healing. Gene expression levels 48 h after scratching HGF monolayers of MMP1, ACTA2, EDN1 and TGFB1 of HGF cells seeded on to the different modified Ti surfaces. Data represent fold changes of target genes normalized to beta-actin and GAPDH (reference genes) expressed relative to EtOH control that was set at 100%. Values represent the mean ± S.E.M. (N=6, 1 donor). Significant differences were assessed by Student t- test ($p < 0.05$): [a] treatment versus EtOH control; [b] treatment versus VitE control.

Paper VI

Titanium implants coated with UV irradiated vitamin D precursor and vitamin E: in vivo performance and coating stability

Satué M. ; Monjo M. ; Ronold H.J. ; Lyngstadaas S.P. ; Ramis J.M.

Manuscript (2015).

Titanium implants coated with UV irradiated vitamin D precursor and vitamin E: in vivo performance and coating stability

María Satué[1,2], Marta Monjo[1,2*], Hans Jacob Ronold[3], Staale Petter Lyngstadaas[4], and Joana M. Ramis[1,2*]

[1]*Department of Fundamental Biology and Health Sciences, Research Institute on Health Sciences (IUNICS), University of Balearic Islands, Spain*

[2]*Instituto de Investigación Sanitaria de Palma, Spain*

[3]*Department of Prosthetics an Oral Function, Institute for Clinical Dentistry, University of Oslo, Norway*

[4]*Department of Biomaterials, Institute for Clinical Dentistry, University of Oslo, Norway*

Running title: *In vivo* performance of vitamin D precursor coated implants

* Corresponding author:

Research Institute on Health Sciences (IUNICS). University of Balearic Islands, Ctra. de Valldemossa, km 7.5 (E-07122). Palma de Mallorca, Spain. Phone: +34-971259607. Fax: +34971173184 ; E-mail: joana.ramis@uib.es, marta.monjo@uib.es

ABSTRACT

Objectives. This study aimed at evaluating the biological response of titanium implants coated with UV-irradiated 7-dehydrocholesterol (7-DHC) and vitamin E (VitE) *in vivo* and analyzing the effects of ageing on their stability and bioactivity *in vitro*.

Materials and Methods. Titanium surfaces were coated with 7-DHC and VitE, UV-irradiated and incubated for 48 hours at 23ºC to allow cholecalciferol synthesis. The *in vivo* biological response was tested using a rabbit tibial model after 8 weeks of healing by analyzing the wound fluid and the mRNA levels of several markers at the bone-implant interface. The stability of the coating after storage up to 12 weeks was determined using HPLC analysis and the bioactivity of the stored modified implants was studied by an *in vitro* study with MC3T3-E1 cells.

Results. A significant increase in gene expression levels of osteocalcin was found in the bone tissue attached to implants coated with the low dose of 7-DHC and VitE, together with a higher ALP activity in the wound fluid. Implants treated with the high dose of 7-DHC and vitE showed increased tissue necrosis and inflammation. Regarding the ageing effects, coated implants were stable and bioactive up to 12 weeks when stored at 4ºC and avoiding oxygen, light and moisture.

Conclusion. The present work demonstrates that Ti implants coated with UV-irradiated 7-DHC and VitE promote in vivo gene expression of bone formation markers and ALP activity, while they keep their osteopromotive potential *in vitro* and composition when stored up to 12 weeks at 4ºC.

Keywords

7-Dehydrocholesterol, vitamin D, vitamin E, dental implant, titanium, bone formation, in vivo, coating stability

1. INTRODUCTION

Vitamin D deficiency leads to bone resorption, osteoporosis and reduced bone mineralization (Holick et al., 2005; Mata-Granados et al., 2013; Lips and Van Schoor, 2011). Thus, patients with bone diseases, such as the case of osteoporosis, are supplemented with vitamin D (Amin et al., 1999; Lips and Van Schoor, 2011; Nordin and Morris, 1992). Although the major source of vitamin D comes from the 7-dehydrocholesterol (7-DHC), which is present in our skin and subsequently processed in the liver and kidney, extra renal synthesis of vitamin D is also possible (Lehmann and Meurer, 2003; Bikle, 2004; Hewison et al., 2007). UV-irradiated 7-DHC can be used to locally produce active vitamin D by osteoblastic cells (Satué, Córdoba, et al., 2013) and as a biocompatible coating for Ti implants allowing both osteoblastic (Satué, Petzold, et al., 2013) and mesenchymal stem cells (Satué et al., 2015) to produce active vitamin D, with positive effects on their osteogenic differentiation *in vitro*. Interestingly, not just a beneficial effect of these modified implants on stimulating osteoblast differentiation has been proved but also an inhibition of osteoclastogenesis and bone resorption has been suggested *in vitro*, especially when combining 7-DHC with the antioxidant α-tocopherol (VitE) (Satué et al., 2014).

The modern implants were introduced by Brånemark who demonstrated that titanium embedded in rabbit bone was completely attached and difficult to remove (Brånemark et al., 1969). Since then, implant research has evolved; improving the survival rate and longevity. Current implants show high success rates but there is still ongoing research to improve the clinical performance in more challenging conditions. Thus, there is an urgent need for improving dental implants in patients with compromised skeletal structures, with poor bone quality or quantity (Simon and Watson, 2002). Furthermore, the increase of life expectancy in the current society increases age-related bone diseases (Kloss and Gassner, 2006). Given the fact that Ti implants coated with the vitamin D precursor promote osteoblast differentiation and inhibit osteoclastogenesis *in vitro*, we hypothesized that this strategy could improve osseointegration in a validated animal model. Another important factor to consider in dental implant research is the maintenance of the bioactivity of the implant for a certain period of time. Thus, orthopedic and dental implants are sold as storable medical devices but the ageing effects on them have barely been addressed (Att et al., 2009). Although Ti is the most commonly used material for bone implants due to its outstanding properties (Palmquist et al., 2010), the addition of bioactive molecules to the implant surface makes them more difficult to handle and store than unmodified ones, which could limit their clinical use (Ferraris et al., 2012). Thereby, developing a bioactive coating with good stability and able to maintain its bioactivity during storage is of high interest for future clinical use.

The purpose of this study was to evaluate the biological response of UV-activated 7-DHC:VitE coated Ti implants *in vivo*. The secondary aim was to analyze the effect of ageing on the stability and bioactivity of the coating. A rabbit tibial model of bone peri-implant bone healing was used to confirm its biological activity *in vivo* whilst MC3T3-E1 murine pre-osteoblast cells were used to assess their stability and bioactivity *in vitro* after storage up to 12 weeks.

2. MATERIALS AND METHODS

2.1. Sample preparation

This study employed Ti disks with a diameter of 6.25 mm and a height of 2 mm, machined from cp Ti rods (grade 2). For the *in vivo* study, surfaces were subsequently blasted with titanium dioxide (TiO_2) particles with grain size between 90-110 μm. The distance from the implants to the jets was approximately 20 mm during blasting procedure and the TiO_2 particle stream hit the surface with an angle of 90º. The air pressure used for blasting was set to 0.5 MPa. All implants were cleaned with trichloroethylene followed by rising with 100% ethanol and subsequently by ethanol in an ultrasonic bath. A final rinse with deionized water and neutral pH was performed to ensure clean surface.

Stock solutions of 7-dehydrocholesterol and α-tocopherol (7-DHC and VitE; Sigma St. Louis, MO, USA) were prepared in absolute ethanol and filtered with a 0.22 μm pore size filter before use. For the surface coating, two doses of 7-DHC were used in the *in vivo* study: 0.2 nmol per Ti disk (Low dose; LD) and 2 nmol per Ti disk (High dose; HD); both supplemented with VitE (1:1) on a mass-to-mass (m:m) basis. Only the LD of the *in vivo* study (0.2 nmols 7-DHC /Ti disk) supplemented with VitE (1:1) on a mass-to-mass (m:m) basis was used for the *in vitro* analyses. Thus, 10 μl of each treatment were left on the surfaces and further UV-irradiated and incubated for 48 hours at 23ºC as described in previous studies (Satué et al., 2014). Ethanol (EtOH) coating was used for the control group, which was also UV-irradiated and incubated for 48 hours at 23ºC.
Ti disks were processed to analyze their coating composition by HPLC. Implants for *in vivo* analysis were stored in cold, dry and dark conditions until the animal study was performed. Similarly, implants for *in vitro* analysis were packaged in dark and dry conditions and further stored at -20, 4 and 23ºC, for 3, 6 and 12 weeks.

2.2. Determination of the D_3 synthesis from UV-irradiated 7-DHC by HPLC

The coating composition of the different surfaces, both *in vivo* and *in vitro*, was quantified by HPLC as previously described (Satué, Petzold, et al., 2013). All solvents used were HPLC or analytical grade. Methanol (HPLC gradient grade), acetonitrile and tetrahydrofurane (both HPLC grade) were purchased from Fisher Scientific (Thermo Fisher Scientific, MA, USA). High-purity deionized Milli-Q water was obtained from a Millipore system (Millipore Corporation, Billerica, MA, USA). Absolute ethanol was purchased from Scharlab (Barcelona, Spain).

2.3. *In vivo* study

Six New Zealand White female rabbits (ESF Produkter Estuna AB, Norrtälje, Sweden) were used for *in vivo* testing of the effect of UV-irradiated 7-DHC:VitE Ti implants on osseointegration. During the experimental period, the animals were kept in at standardized room temperature, humidity and diet. The experiments were approved by the Norwegian Animal Research Authority (NARA) and registered by this authority. The procedures have thus been conducted in accordance with the Animal Welfare Act of June 01st 2010, No. 94 and Regulation on Animal Experimentation of January 15th 1996. Sedation and anesthesia and all surgical procedures were done as described by Rønold et al (Rønold and Ellingsen, 2002). After eight

weeks of healing, animals were sacrificed and the effect of the bioactive modified surfaces was evaluated by assessing the bone-to-implant attachment strength, wound fluid analyses (LDH activity, ALP activity and protein content) and bone tissue analyses (mRNA levels of bone markers using real-time RT-PCR). After removing the implants, photographs of the implantation sites were taken. These pictures were evaluated to assess the blood presence on the implantation site.

Evaluation of the strength needed to detach the implants from the bone was determined by using a tensile removal test. The detachment of the implants from the cortical bone was performed using a Lloyds LRX Materials testing machine (Lloyds Instruments Ltd, Segensworth, UK) fitted with a calibrated load-cell of 100 N. Cross-head sped range was set to 1.0 mm/min. Detailed information concerning this removal tensile test have been published elsewhere (Rønold and Ellingsen, 2002).

After implant detachment, wound fluid sampling and analysis of LDH activity, ALP activity and total protein were performed as previously detailed (Haugen et al., 2013; Monjo et al., 2010). Total RNA was isolated from peri-implant bone tissue attached to the extracted implants using TRIzol® reagent (Invitrogen Life Technologies, Carlsbad, CA, USA) according to the manufacturer's protocol and quantified at 260 nm using a Nanodrop spectrophotometer (NanoDrop Technologies, Wilmington, DE, USA). The same amount of RNA (450 ng) of the total RNA isolated was reverse transcribed to cDNA using RevertAid First Strand cDNA Synthesis kit (Thermo Scientific, USA) that contains both oligo(dT) and random hexamers. Each cDNA was diluted 1/6 and aliquots were frozen (-20^{o}C) until the PCR reactions were carried out. Real-time PCR was performed in the CFX96 Real-time PCR system (Bio-Rad, Hercules, CA) using SYBR green detection. Real-time PCR was done for three reference genes: 18S ribosomal RNA (18S rRNA), glyceraldehyde-3-phosphate dehydrogenase (GAPDH) and β-actin, and thirteen target genes: collagen type I (COLL-I), bone morphogenetic protein 2 (BMP-2), runt-related transcription factor 2 (RUNX2), osteocalcin (OC), tartrate-resistant acid phosphatase (TRAP), calcitonin receptor (CALCR), vacuolar type proton ATPase (H^{+}ATPase), receptor activator of nuclear factor-kappaB ligand (RANKL), tumor necrosis factor-α (TNF-α), interleukin-6 (IL-6), interleukin-10 (IL-10), vitamin D 25-hydroxylase (CYP27A1) and vitamin D receptor (VDR). The primer sequences used are detailed in Table 1. The concentration of PCR reaction components, amplification program and quantification were performed as documented earlier (Monjo et al., 2008).

2.4. *In vitro* study

The mouse osteoblastic cell line MC3T3-E1 (DSMZ, Braunschweig, Germany) was chosen as the *in vitro* model to evaluate the bioactivity of the modified surfaces after storage. Cells were routinely cultured in α-MEM (PAA Laboratories GmbH, Pasching, Austria), supplemented with 10% fetal bovine serum (PAA Laboratories GmbH, Pasching, Austria) and antibiotics (50 IU penicillin mL^{-1} and 50 µg streptomycin mL^{-1}) (Sigma, St. Louis, MO, USA) under standard cell culture conditions (at 37 ºC in a humidified atmosphere of 5% CO_2). Cells were seeded at a density of 30,000 cells cm^{-2}. After 48 h of cell culture, supernatants were collected to test cytotoxicity and metabolic activity, and further cells were harvested to analyze the mRNA levels of several osteoblast differentiation markers using real-time reverse-transcription-polymerase

chain reaction (RT-PCR). Further, MC3T3-E1 cells were harvested after 5 days of cell culture to measure ALP activity and total protein content.

Cytotoxicity and metabolic activity analyses from the culture media were carried out using the Cytotoxicity Detection kit (Roche Diagnostics, Mannheim, Germany) and Presto Blue reagent (Life Technologies, Carlsbad, CA), according to each supplier's protocol.

RNA was isolated from cells using Tripure (Roche Diagnostics, Mannheim, Germany) following the instructions of the manufacturer. RNA was quantified at 260 nm using a Nanodrop spectrophotometer (NanoDrop Technologies, Wilmington, DE, USA). Total RNA previously isolated was reverse-transcribed to cDNA using High Capacity RNA to cDNA kit (Applied Biosystems, Foster City, CA) according to the protocol of the supplier. Real-time PCR was performed for two reference genes: 18S ribosomal RNA (*18S rRNA*), glyceraldehyde-3-phosphate dehydrogenase (*Gapdh*), and four target genes: Collagen (*Coll-1*), Bone morphogenetic protein 2 (*Bmp-2*), Osteocalcin (*Oc*) and Osterix (*Osx*). The primer sequences, the concentration of PCR reaction components, amplification programs and quantification methods have been previously reported (Satué, Petzold, et al., 2013). Finally, ALP activity and protein content analyses were performed as documented earlier (Satué, Petzold, et al., 2013).

2.5. Statistics

All data are presented as mean values ± standard error of the mean (S.E.M.). The Kolmogorov-Smirnov test was done to assume parametric or non-parametric distributions. Differences between groups were assessed by Mann-Whitney-test or by Student t-test depending on their normal distribution. The SPSS® program for version 17.0 (SPSS, Chicago, IL, US) and GraphPad Prism® version 5.0 (GraphPad Software Inc., San Diego, CA, USA) were used. Results were considered statistically significant at the p-values ≤ 0.05.

3. RESULTS

3.1. Quantification of the D_3 production from UV-irradiated 7-DHC:VitE coated Ti implants

We analyzed the coating composition of the modified blasted Ti implants used for the *in vivo* analyses. Once coated with 7-DHC:VitE, these surfaces were further UV-irradiated and incubated for 48 h at 23ºC. HPLC analyses determined 771.3 ± 6.3 pmol and 61.4 ± 4.2 pmol of D_3 per Ti implant produced after UV irradiation for 2 and 0.2 nmol 7-DHC:VitE (1:1; m:m) coated surfaces, respectively.

Similarly, modified Ti implants used for the *in vitro* study were analyzed by HPLC to determine their composition after different conditions. First, UV-irradiated coated Ti implants (0.2 nmol 7-DHC:VitE (1:1; m:m)), once incubated for 48 h at 23ºC, were then stored at different temperatures (-20, 4 and 23ºC) for up to 3 weeks in order to assess their shelf-life stability. After the 3-week storage, similar results in the coating composition were observed when stored at -20 and 4ºC (66.49 ± 1.66 and 73.35 ± 0.72 pmol D_3 per Ti implant respectively), but a decrease in the D_3 composition was found when stored at 23ºC (49.88 ± 0.35 pmol D_3 per Ti implant). Given these results, we selected 4ºC for the 12-week storage and further bioactivity analyses. As

expected, no relevant changes were found in the coating composition of the 4ºC-stored UV-activated 7-DHC:VitE Ti implants (73.8 ± 2.4; 75.7 ± 1.8 and 72.9 ± 2.3 pmol D_3 per Ti implant were measured after 3, 6 and 12-week storage at 4ºC, respectively) when compared with the non-stored ones.

3.2. *In vivo* biomechanical evaluation, wound fluid analyses and macroscopic observation of the implant site

The biomechanical evaluation of the implants using the tensile test showed that the pull-out force applied until loosening implants was similar in the control group and in both groups treated with low and high vitamin D doses (Fig. 1A). However, the LDH activity present in the wound fluid collected from the implant site was higher in the VitD-HD group when compared with the Ti control (Fig. 1B). The ALP activity, which was corrected for total protein content in the wound fluid to calculate the specific ALP activity, was increased in VitD-LD coated Ti implants although only significantly when compared with VitD-HD (Fig. 1C). A visual inspection of the implant site was also performed. Thus, representative pictures of the cortical bone defects hosting the different Ti implants were selected to illustrate the visible amount of blood clot remaining at the interface (Fig. 1D). The VitD-HD group showed a higher amount of blood remaining at the interface compared with the control, while the VitD-LD group showed the lowest amount of blood.

3.3. *In vivo* gene expression analyses from peri-implant cortical bone tissue

Changes in the relative mRNA levels of target genes related to bone formation (COLL-1, BMP-2, RUNX2 and OC), bone resorption (TRAP, CALCR, H^+ATPase and RANKL), inflammation (TNF-α, IL6 and IL10) and vitamin D metabolism (CYP27A1 and VDR) were evaluated in the peri-implant bone tissue (Fig. 2). Although without significant differences, VitD-LD and VitD-HD showed lower COLL-1 mRNA levels compared with control (Fig. 2A). Levels of BMP-2, RUNX2 and OC were increased in the VitD-LD group, and OC was significantly higher in VitD-LD coated implants (Fig. 2A). Regarding the indicators of bone resorption (Fig. 2B), TRAP levels were significantly decreased in VitD-HD coated samples compared with the control group. Nevertheless, no significant differences were observed in the mRNA levels of CALCR and H^+ATPase. A trend to increase RANKL levels was found in VitD-LD coated samples. In addition, mRNA levels of pro-inflammatory (TNF-α and IL6) cytokines showed that VitD-HD significantly increased TNF-α levels (Fig. 2C). However, the levels of the anti-inflammatory (IL10) cytokine remained unchanged for the different groups (Fig. 2C). Finally, vitamin D 25-hydroxylase (CYP27A1) and vitamin D receptor (VDR) mRNA levels tended to be increased in implants coated with VitD-LD (Fig. 2D).

3.4. *In vitro* bioactivity analyses of UV-irradiated 7-DHC:VitE coated Ti implants.

Since we observed that the coating composition of UV-activated 7-DHC:VitE was stable up to 12 weeks of storage at 4ºC, we assessed whether the bioactivity of these surfaces using MC3T3-E1 cells was also maintained. First, we analyzed the cell viability of these cells seeded onto modified Ti surfaces that had been previously stored for 3, 6 and 12 weeks at 4ºC (Fig. 3A). EtOH-treated surfaces were used as control for each storage time and also fresh treatments (EtOH and UV-activated 7-DHC:VitE that were not stored (NS)) were ran in every

experiment as controls. Although 3-week stored UV-activated 7-DHC:VitE showed a lower LDH activity than non-stored UV-activated 7-DHC:VitE, no differences were found for the rest of the stored treatments. Furthermore, metabolic activity of cells cultured onto non-stored UV-activated 7-DHC:VitE and stored UV-activated 7-DHC:VitE coated Ti implants revealed no differences among the groups (data not shown).

In order to determine whether the stored implants were bioactive after the storage or not, we analyzed the mRNA levels of several markers related to proliferation, matrix maturation and mineralization (Fig. 3B-E). Thus, *Coll-1* was up-regulated in 3 week-stored UV-irradiated 7-DHC:VitE and 6 week-stored EtOH control when compared with the non-stored ones. Interestingly, *Bmp-2*, *Osx* and *Oc* levels were significantly increased in all UV-irradiated 7-DHC:VitE coated Ti implants, both non-stored and stored samples. Furthermore, *Bmp-2* and *Osx* were also upregulated in 3 week-stored EtOH compared with the non-stored EtOH. UV-irradiated 7-DHC:VitE coated Ti implants stored after 3 and 6 weeks increased *Osx* mRNA levels compared with the non-stored control. Also, *Oc* was upregulated in UV-irradiated 7-DHC:VitE coated Ti implants after 3-week storage compared with the non-stored control and EtOH control stored for 12 weeks was increased when compared with the non-stored EtOH. Finally, to investigate the effect of ageing on the terminal osteoblast differentiation induced by UV-irradiated 7-DHC:VitE coated Ti implants, ALP activity was measured in the cell monolayer on day 7 of cell culturing (Fig. 3F). In agreement with the gene expression findings, ALP activity was statistically increased in both stored and non-stored UV-irradiated 7-DHC:VitE coated Ti implants compared with EtOH control, although a lower ALP activity was observed in the EtOH control group at 6 and 12 weeks of storage.

4. DISCUSSION

The present study shows that UV-irradiated 7-DHC:VitE coated Ti implants promote the gene expression of the late bone formation marker osteocalcin in the peri-implant bone, increased ALP activity in the wound fluid and maintain their stability and bioactivity properties after 12-week storage *in vitro*.

Recently, several investigations have confirmed the importance of vitamin D action in the osseointegration process; with impaired implant osseointegration in vitamin D deficiency cases (Cho et al., 2011; Dvorak et al., 2012; Wu et al., 2013; Naito et al., 2014; Liu et al., 2014) and promoted peri-implant bone formation in vitamin D supplementation treatments (Kelly et al., 2009; Mengatto et al., 2011; Dvorak et al., 2012). However, to the best of our knowledge, the present study shows for the first time the effect of the UV-irradiated vitamin D precursor coated implants, supplemented with VitE, in the *in vivo* bone response. Thus, in order to study the osseointegration process of UV-irradiated 7-DHC:VitE coated Ti implants, we used standardized coin-shaped Ti implants that were placed in cortical bone defects in the rabbit tibia. This model is close to the clinical situation for implant osseointegration and can be considered as a valid model in humans (Monjo et al., 2008; Rønold and Ellingsen, 2002). Furthermore, it enables to analyze the bone-implant retention, the visual inspection of the healing defect as well as sampling of the bone tissue attached to the extracted implants to

evaluate specific biological markers related to bone formation, bone resorption, inflammation and vitamin D metabolism.

After the implant placement, a series of bone modeling and remodeling steps take place (Stanford, 2010). First, a blood clot is formed at the implant surface (Slaets et al., 2006) which further influences the osteogenic response (Hong et al., 1999; Hong et al., 2005). Chemistry and topography of the implant surface influence interactions with blood components (Gorbet and Sefton, 2004; Baker et al., 2008) as well as the further recruitment of osteogenic cells (Kloss et al., 2013; Wennerberg et al., 1996). Furthermore, cessation of circulation at the broken ends causes necrosis in the peri-implant bone tissue (Davies, 2003). In the present study, visual observation of the bone defects after implant detachment revealed a denser blood clot in the VitD-HD samples whilst the less dense blood clot was found in the VitD-LD group. A possible explanation of these results is that the VitD-HD increased necrosis in the peri-implant tissue, as suggested by the LDH activity results, and also implied a higher expression of pro-inflammatory cytokines such as TNF-α. Accordingly, several animal and clinical studies have identified suppressive effects of high dose vitamin D supplementation on bone formation (Yamaguchi and Weitzmann, 2012). However, the lower presence of blood observed in the interface after removal of VitD-LD coated implants suggested that this coating accelerates the formation of the coagulum and its further replacement with granulation tissue and osteoid. Indeed, the ALP activity results revealed a higher degree of matrix mineralization for VitD-LD coated implants. Furthermore, VitD-LD coated implants showed the most suitable balance in mRNA levels of markers involved in bone formation and bone resorption in the bone-implant interface. Thus, a trend to decrease COLL-1 whilst to increase BMP-2 and RUNX2 mRNA levels were found in VitD-LD samples, which then significantly increased OC levels. Also, lower TRAP mRNA levels were observed, in line with the inhibition of the osteoclastogenesis *in vitro* (Satué et al., 2014). The mRNA levels of cytokines expressed by monocytes and macrophages in the peri-implant bone tissue revealed that VitD-LD coated implants may trigger the most appropriate inflammatory response during healing. Finally, peri-implant bone tissue in contact with VitD-LD coated surfaces tended to up-regulate CYP27A1 and VDR mRNA levels, suggesting an increased vitamin D synthesis in the peri-implant bone tissue. Similarly, systemic administration of vitamin D in different animal models has resulted in the improvement of the implants osseointegration (Dvorak et al., 2012; Wu et al., 2013; Liu et al., 2014) but also the action of implants treated with vitamin D locally has been investigated *in vivo*. Thus, Cho et al. (Cho et al., 2011) demonstrated that PLGA/1,25$(OH)_2D_3$ coating stimulated bone formation adjacent to the surface of implants and later, Naito el at. (Naito et al., 2014) observed possible dose dependent effects of 1,25$(OH)_2D_3$ coated implants on the peri-implant bone response although without statistical differences. Therefore, differences in the bone response depend on the vitamin D dose used. Indeed, a different response was found in the present study depending on the dose of the coating used, with a negative effect on bone (higher inflammation and necrosis) when a higher dose of VitD was used.

It is well known that current innovative biomaterials use biologically active molecules to improve their functions in regenerating or repairing target tissues (Healy et al., 1999; Rice et al., 2013; Joddar and Ito, 2011). But their packaging and storage may involve difficulties for their further clinical application. Furthermore, the shelf life of common titanium materials designed for

the clinical practice rarely has been recorded; very few investigations have studied the effects of storage methods and time-related bioactivity of these biomaterials. But due to its clinical relevance, there is increasing awareness and interest in this issue (Suzuki et al., 2009; Ferraris et al., 2012; Lu et al., 2012; Guillot et al., 2013; Wang et al., 2013; Ueno et al., 2012). For instance, it has been proved that the biological potential of an old Ti implant is lower than a new one as it is exposed to air adsorbing unavoidably contaminations, changing the surface composition (Lu et al., 2012). Thus, UV treatment of Ti surfaces is an example of strategy overcoming time-related degrading bioactivity (Suzuki et al., 2009). Also changes in the temperature, moisture and other storage conditions influence the final bioactivity of the biomaterial (Ferraris et al., 2012; Guillot et al., 2013; Tian et al., 2002; Scharnweber et al., 2010). Biological molecules usually present low stability under environmental conditions since they tend to denature in activity due to humidity and heat (Ferraris et al., 2012). Indeed, several investigations confirm the effect of storage temperatures on the stability of different drugs (Tian et al., 2002; Mohl and Winter, 2006; Dong et al., 2006). Vitamin D stability depends on temperature but also on other specific conditions, such as oxygen, light and moisture which cause its degradation (Kaushik et al., 2014; Haham et al., 2012). Accordingly, we protected the modified coatings from light, oxygen and moisture and further evaluated how temperature affected the coating composition. In this research, we proved that our coating was stable up to 12 weeks when stored in a refrigerator (4ºC), under nitrogen packaging and in absence of light. Moreover, *in vitro* studies demonstrated its bioactivity after 12-week storage at the mentioned conditions, in the same way that the previous study performed with UV-irradiated 7-DHC coated implants (Satué, Petzold, et al., 2013).

5. CONCLUSION

The present work demonstrates that Ti implants coated with UV-irradiated 7-DHC and VitE promote in vivo gene expression of bone formation markers and keep their osteopromotive potential in vitro and composition when stored up to 12 weeks at 4ºC and avoiding light, oxygen and moisture. Developing a coating for dental implants with potential to improve the biological response in skeletal compromised structures and with minimum shelf-life stability and bioactivity is critically relevant for its further clinical application.

6. ACKNOWLEDGEMENT

This work was supported by the Conselleria d'Educació, Cultura i Universitats del Govern de les Illes Balears and the European Social Fund (contract to JMR) and NILS Science and Sustainability Programme (ES07 EEA Grants; 013-Abel-CM-2013).

REFERENCES

Amin, S., LaValley, M.P., Simms R.W. & Felson, D.T. (1999) The role of vitamin D in corticosteroid-induced osteoporosis: a meta-analytic approach. *Arthritis & Rheumatism* **42**:1740–51.

Att, W., Hori, N., Takeuchi, M., Ouyang, J., Yang, Y., Anpo, M. et al. (2009) Time-dependent degradation of titanium osteoconductivity: An implication of biological aging of implant materials. *Biomaterials* **30**:5352–5363.

Baker, S.E., Sawvel, A.M., Fan, J., Shi, Q., Strandwitz, N. & Stucky, G.D. (2008) Blood clot initiation by mesocellular foams: dependence on nanopore size and enzyme immobilization. *Langmuir* **24**:14254–60.

Bikle, D.D. (2004) Vitamin D regulated keratinocyte differentiation. *Journal of Cellular Biochemistry* **92**:436–44.

Brånemark, P.I., Adell, R., Breine, U., Hansson, B.O., Lindström, J. & Ohlsson, A. (1969) Intra-osseous anchorage of dental prostheses. I. Experimental studies. *Scandinavian Journal of Plastic and Reconstructive Surgery* **3**:81–100.

Cho, Y.J., Heo, S.J., Koak, J.Y., Kim, S.K., Lee, S.J. & Lee, J.H. (2011) Promotion of osseointegration of anodized titanium implants with a 1α,25-dihydroxyvitamin D3 submicron particle coating. *International Journal of Oral and Maxillofacial Implants* **26**:1225–32.

Davies, J.E. (2003) Understanding Peri-Implant Endosseous Healing. *Journal of Dental Education* **67**:932–949.

Dong, W.Y., Körber, M., López Esguerra, V. & Bodmeier, R. (2006) Stability of poly(D,L-lactide-co-glycolide) and leuprolide acetate in in-situ forming drug delivery systems. *Journal of Controlled Release* **115**:158–67.

Dvorak, G., Fügl, A., Watzek, G., Tangl, S., Pokorny, P. & Gruber, R. (2012) Impact of dietary vitamin D on osseointegration in the ovariectomized rat. *Clinical Oral Implants Research* **23**:1308–1313.

Ferraris, S., Pan, G., Cassinelli, C., Mazzucco, L., Vernè, E. & Spriano, S. (2012) Effects of sterilization and storage on the properties of ALP-grafted biomaterials for prosthetic and bone tissue engineering applications. *Biomedical Materials* **7**:054102.

Gorbet, M.B. & Sefton, M.V. (2004) Biomaterial-associated thrombosis: roles of coagulation factors, complement, platelets and leukocytes. *Biomaterials* **25**:5681–703.

Guillot, R., Gilde, F., Becquart, P., Sailhan, F., Lapeyrere, A., Logeart-Avramoglou, D. et al. (2013) The stability of BMP loaded polyelectrolyte multilayer coatings on titanium. *Biomaterials* **34**:5737–46.

Haham, M., Ish-Shalom, S., Nodelman, M., Duek, I., Segal, E., Kustanovich, M. et al. (2012) Stability and bioavailability of vitamin D nanoencapsulated in casein micelles. *Food & Function* **3**:737–44.

Haugen, H.J., Monjo, M., Rubert, M., Verket, A., Lyngstadaas, S.P., Ellingsen, J.E. et al. (2013) Porous ceramic titanium dioxide scaffolds promote bone formation in rabbit peri-implant cortical defect model. *Acta Biomaterialia* **9**:5390–5399.

Healy, K.E., Rezania, A. & Stile, R.A. (1999) Designing Biomaterials to Direct Biological Responses. *Annals of the New York Academy of Sciences* **875**:24–35.

Hewison, M., Burke, F., Evans, K.N., Lammas, D.A., Sansom, D.M., Liu, P. et al. (2007) Extra-renal 25-hydroxyvitamin D3-1alpha-hydroxylase in human health and disease. *Journal of Steroid Biochemistry and Molecular Biology* **103**:316–21.

Holick, M.F., Siris, E.S., Binkley, N., Beard, M.K., Khan, A., Katzer, J.T. et al. (2005) Prevalence of Vitamin D inadequacy among postmenopausal North American women receiving osteoporosis therapy. *The Journal of Clinical Endocrinology and Metabolism* **90**:3215–24.

Hong, J., Andersson, J., Ekdahl, K.N., Elgue, G., Axén, N., Larsson, R. et al. (1999) Titanium is a highly thrombogenic biomaterial: possible implications for osteogenesis. *Thrombosis and Haemostasis* **82**:58–64.

Hong, J., Azens, A., Ekdahl, K.N., Granqvist, C.G. & Nilsson, B. (2005) Material-specific thrombin generation following contact between metal surfaces and whole blood. *Biomaterials* **26**:1397–403.

Joddar, B. & Ito, Y. (2011) Biological modifications of materials surfaces with proteins for regenerative medicine. *Journal of Materials Chemistry* **21**:13737.

Kaushik, R., Sachdeva, B. & Arora, S. (2014) Vitamin D2 stability in milk during processing, packaging and storage. *LWT - Food Science and Technology* **56**:421–426.

Kelly, J., Lin, A., Wang, C.J., Park, S. & Nishimura, I. (2009) Vitamin D and bone physiology: Demonstration of vitamin D deficiency in an implant osseointegration rat model. *Journal of Prosthodontics* **18**:473–478.

Kloss, F.R. & Gassner, R. (2006) Bone and aging: effects on the maxillofacial skeleton. *Experimental Gerontology* **41**:123–9.

Kloss, F.R., Singh, S., Hächl, O., Rentenberger, J., Auberger, T., Kraft, A. et al. (2013) BMP-2 immobilized on nanocrystalline diamond-coated titanium screws; demonstration of osteoinductive properties in irradiated bone. *Head and Neck* **35**:235–41.

Lehmann, B. & Meurer, M. (2003) Extrarenal sites of calcitriol synthesis: the particular role of the skin. *Recent Results in Cancer Research* **164**:135–45.

Lips, P. & Van Schoor, N.M. (2011) The effect of vitamin D on bone and osteoporosis. *Best Practice & Research: Clinical Endocrinology and Metabolism* **25**:585–91.

Liu, W., Zhang, S., Zhao, D., Zou, H., Sun, N., Liang, X. et al. (2014) Vitamin D supplementation enhances the fixation of titanium implants in chronic kidney disease mice. *PLoS One* **9**:3–8.

Lu, H., Zhou, L., Wan, L., Li, S., Rong, M. & Guo, Z. (2012) Effects of storage methods on time-related changes of titanium surface properties and cellular response. *Biomedical Materials* **7**:055002.

Mata-Granados, J.M., Cuenca-Acevedo, J.R., Luque de Castro, M.D., Holick, M.F. & Quesada-Gómez, J.M. (2013) Vitamin D insufficiency together with high serum levels of vitamin A increases the risk for osteoporosis in postmenopausal women. *Archives of Osteoporosis* **8**:124.

Mengatto, C.M., Mussano, F., Honda, Y., Colwell, C.S. & Nishimura, I. (2011) Circadian rhythm and cartilage extracellular matrix genes in osseointegration: A genome-wide screening of implant failure by vitamin D deficiency. *PLoS One* **6**: e15848.

Mohl, S. & Winter, G. (2006) Continuous release of Rh-interferon (alpha-2a from triglyceride implants: storage stability of the dosage forms. *Pharmacaeutical Development and Technology* **11**:103–10.

Monjo, M., Lamolle, S.F., Lyngstadaas, S.P., Rønold, H.J. & Ellingsen, J.E. (2008) In vivo expression of osteogenic markers and bone mineral density at the surface of fluoride-modified titanium implants. *Biomaterials* **29**:3771–80.

Monjo, M., Rubert, M., Wohlfahrt, J.C., Rønold, H.J., Ellingsen, J.E. & Lyngstadaas, S.P. (2010) In vivo performance of absorbable collagen sponges with rosuvastatin in critical-size cortical bone defects. *Acta Biomaterialia* **6**:1405–1412.

Naito, Y., Jimbo, R., Bryington, M.S., Vandeweghe, S., Chrcanovic, B.R., Tovar, N. et al. (2014) The Influence of 1α.25-Dihydroxyvitamin D3 Coating on Implant Osseointegration in the Rabbit Tibia. *Journal of Oral & Maxillofacial Research* **5**:1–8.

Nordin, B.E. & Morris, H.A. (1992) Osteoporosis and vitamin D. *Journal of Cellular Biochemistry* **49**:19–25.

Palmquist, A., Omar, O.M., Esposito, M., Lausmaa, J. & Thomsen, P. (2010) Titanium oral implants: surface characteristics, interface biology and clinical outcome. *Journal of the Royal Society Interface* **7**:S515–27.

Rice, J.J., Martino, M.M., De Laporte, L., Tortelli, F., Briquez, P.S. & Hubbell, J. (2013) Engineering the regenerative microenvironment with biomaterials. *Advanced Health Materials* **2**:57–71.

Rønold, H.J. & Ellingsen, J.E. (2002) The use of a coin shaped implant for direct in situ measurement of attachment strength for osseointegrating biomaterial surfaces. *Biomaterials* **23**:2201–2209.

Satué, M., Córdoba, A., Ramis, J.M. & Monjo, M. (2013) UV-irradiated 7-dehydrocholesterol coating on polystyrene surfaces is converted to active vitamin D by osteoblastic MC3T3-E1 cells. *Photochemical & Photobiological Sciences* **12**:1025–35.

Satué, M., Petzold, C., Córdoba, A., Ramis, J.M. & Monjo, M. (2013) UV photoactivation of 7-dehydrocholesterol on titanium implants enhances osteoblast differentiation and decreases Rankl gene expression. *Acta biomaterialia* **9**:5759–70.

Satué, M., Ramis, J.M. & Monjo, M. (2014) Cholecalciferol synthesized after UV-activation of 7-dehydrocholesterol onto titanium implants inhibits osteoclastogenesis in vitro. *Journal of Biomedical Materials Research: Part A*. DOI: 10.1002/jbm.a.35364

Satué, M., Ramis, J.M. & Monjo, M. (2015) UV-activated 7-dehydrocholesterol coated titanium implants promote differentiation of human umbilical cord mesenchymal stem cells into osteoblasts. *Journal of Biomaterials Applications.* DOI: 10.1177/0885328215582324.

Scharnweber, D., Schlottig, F., Oswald, S., Becker, K. & Worch, H. (2010) How is wettability of titanium surfaces influenced by their preparation and storage conditions? *Journal of Materials Science - Materials in Medicine* **21**:525–32.

Simon, Z. & Watson, P.A. (2002) Biomimetic dental implants--new ways to enhance osseointegration. *Journal of the Canadian Dental Association* **68**:286–8.

Slaets, E., Carmeliet, G., Naert, I. & Duyck, J. (2006) Early cellular responses in cortical bone healing around unloaded titanium implants: an animal study. *Journal of Periodontology* **77**:1015–24.

Stanford, C.M. (2010) Surface modification of biomedical and dental implants and the processes of inflammation, wound healing and bone formation. *International Journal of Molecular Sciences* **11**:354–369.

Suzuki, T., Hori, N., Att, W., Kubo, K., Iwasa, F., Ueno, T. et al. (2009) Ultraviolet treatment overcomes time-related degrading bioactivity of titanium. *Tissue Engineering: Part A* **15**:3679–88.

Tian, Y., Li, L., Gao, X., Deng, J., Stephens, D., Robinson, D. et al. (2002) The effect of storage temperatures on the in vitro properties of a polyanhydride implant containing gentamicin. *Drug Development and Industrial Pharmacy* **28**:897–903.

Ueno, T., Takeuchi, M., Hori, N., Iwasa, F., Minamikawa, H., Igarashi, Y. et al. (2012) Gamma ray treatment enhances bioactivity and osseointegration capability of titanium. *Journal of Biomedical Materials Research Part B: Applied Biomaterials* **100**:2279–87.

Wang, H., Shang, R., Guan, Y., Wang, Y. & Teng, W. (2013) Bioactivity of ultraviolet ray-treated titanium surface in nitrogen storing environment. *Zhonghua Kou Qiang Yi Xue Za Zhi* **48**:294–8.

Wennerberg, A., Albrektsson, T., Johansson, C. & Andersson, B. (1996) Experimental study of turned and grit-blasted screw-shaped implants with special emphasis on effects of blasting material and surface topography. *Biomaterials* **17**:15–22.

Wu, Y., Yu, T., Yang, X., Li, F., Ma, L., Yang, Y. et al. (2013) Vitamin D3 and insulin combined treatment promotes titanium implant osseointegration in diabetes mellitus rats. *Bone* **52**:1–8.

Yamaguchi, M. & Weitzmann, M.N. (2012) High dose 1,25(OH)2D3 inhibits osteoblast mineralization in vitro. *International Journal of Molecular Medicine* **29**:934–8.

TABLES

Table 1. Oligonucleotide sequences of sense (S) and antisense (A) primers used in the real-time PCR of target and reference genes and amplicon size of the resulting products.

Gene	Primer sequence	Product size (bp)
BMP2	S 5′- ATG GGT TTG TGG TGG AAG TG-3′ A 5′- GCT GTT TGT GTT TCG CTT GA -3′	195
CALCR	S 5′- CAA ATG ACA CCC ATC CAA CA -3′ A 5′- ACA TCC ATC CAT CCC AGG TC -3′	162
COLL1	S 5′- AGA GCA TGA CCG ATG GAT TC-3′ A 5′- CCT TCT TGA GGT TGC CAG TC-3′	177
CYP27A1	S 5′- CGC GTC CTC TGC TGC CCT TT-3′ A 5′- ACC CGG ACT CCA TCT GGC CC-3′	139
H^+ATPase	S 5′ -CCG AAA CCT CCT GAA GAA AA-3′ A 5′- ATA GCC GTG GTG CTG AAG TC-3′	165
IL10	S 5′- CCT TTG GCA GGG TGA AGA CT -3′ A 5′- ATG GCT GGA CTC TGG TTC TC -3	175
IL6	S 5′- TAA TGA GAC CTG CCT GCT GA -3′ A 5′- GCT TGA GGG TGG CTT CTT C -3′	191
OC	S 5′- GAA GCC CAG CGG TGC A -3′ A 5′- CAC TAC CTC GCT GCC CTC C -3′	70
RANKL	S 5’- CAG AGC GCA GAT GGA TCC TAA -3′ A 5′- TCC TTT TGC ACA GCT CCT TGA -3′	180
RUNX2	S 5′- GCC TTC AAG GTG GTA GCC C -3′ A 5′- CGT TAC CCG CCA TGA CAG TA -3′	67
TNF-α	S 5′- TCC GTG AAA ACA GAG CAG AA -3′ A 5′- GAG CAG AGG TTC GGT GAT GT -3′	160
TRAP	S 5′- CCT GGG CGA CAA CTT TTA CT -3′ A 5′- TTG GAG ACC TTG GAA TAG GC -3′	180
VDR	S 5′- GGGAGATGATCCTGAAGCGG -3′ A 5′- GGAACTGAGGTGGTCTGAGC -3′	254
β-ACTIN	S 5′- GCG ACC TCA CCG ACT ACC T -3′ A 5′- GCC ATC TCG TTC TCG AAG TC -3′	136
GAPDH	S 5′- TGC ACC ACC AAC TGC TTA GC -3′ A 5′- GGC ATG GAC TGT GGT CAT GAG -3′	87
18S rRNA	S 5′- GTA ACC CGT TGA ACC CCA TT -3′ A 5′- CCA TCC AAT CGG TAG TAG CG -3′	151

FIGURES

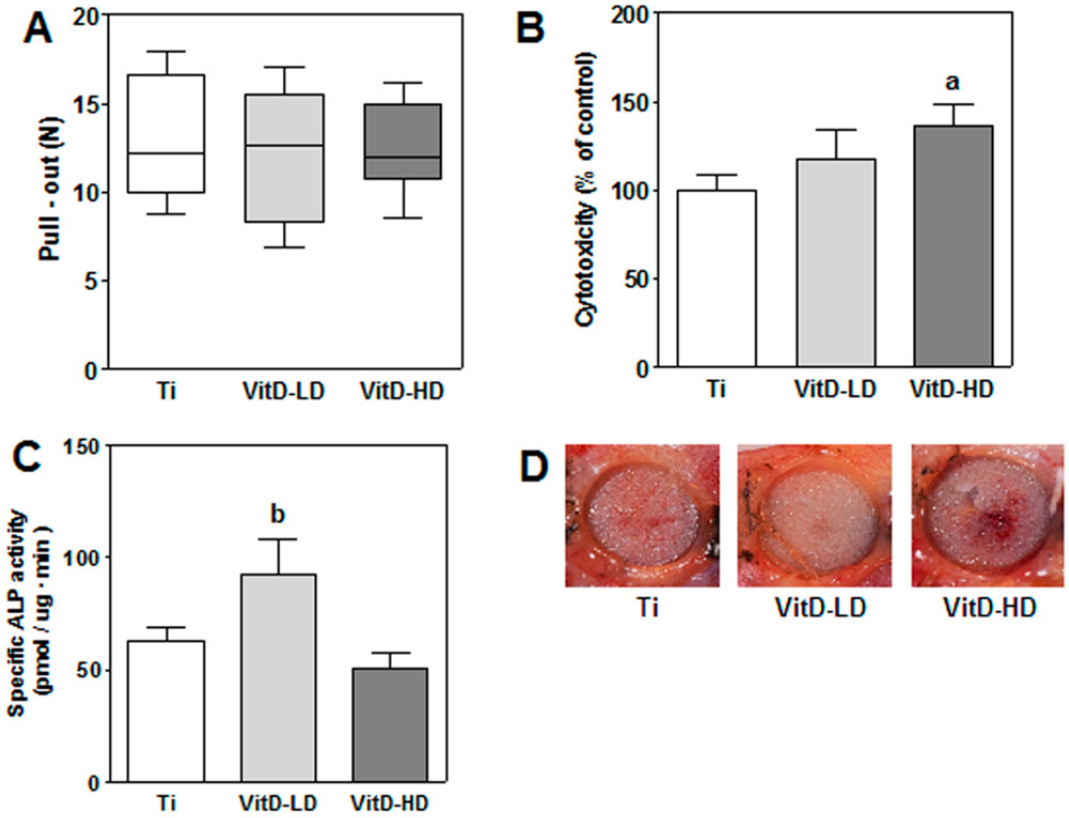

Figure 1. In vivo analysis of wound fluid from implantation sites after implant removal. (A) Median values, interquartile ranges, and minima and maxima for forces needed to pull out the implants after 8 weeks of implantation. (B) LDH activity from the wound fluid collected from the implant site was expressed as a percentage of Ti control, which was set to 100%. (C) ALP activity corrected for total protein in the wound fluid. Values represent the mean ± S.E.M. (N=8). Differences between groups were assessed by Student's t-test ($p < 0.05$): [a] treatment versus Ti; [b] VitD-LD versus VitD-HD. (D) Representative pictures of the bone defects after implant removal.

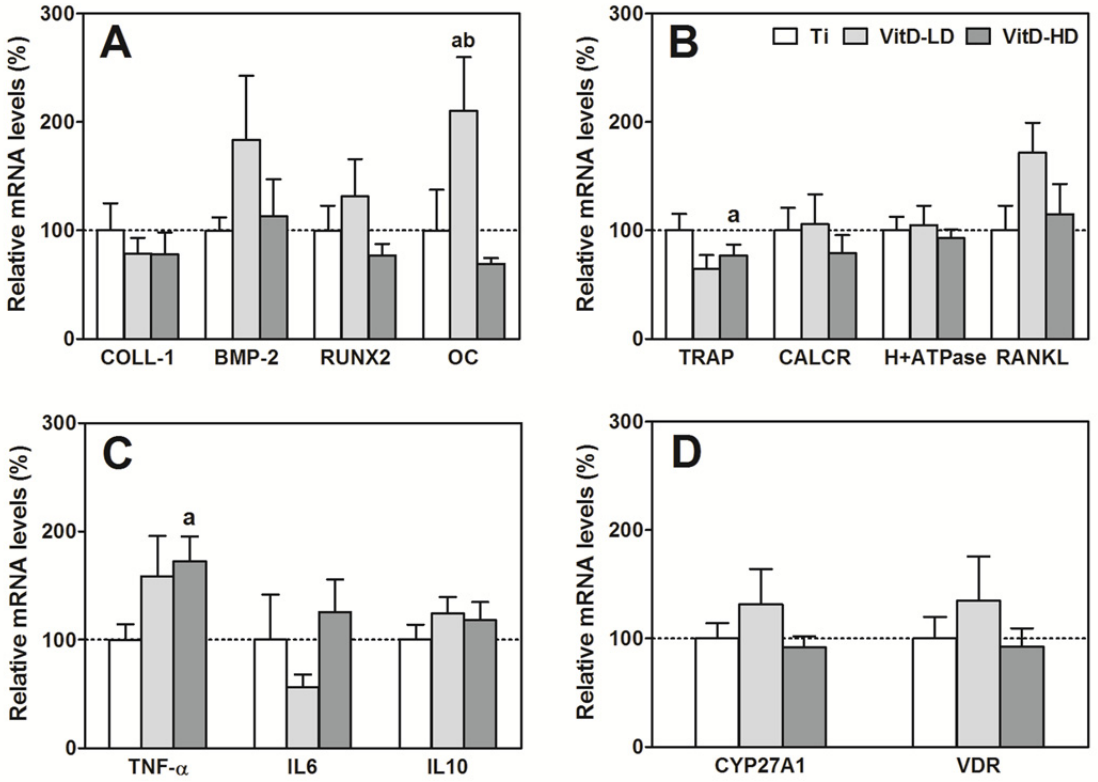

Figure 2. In vivo mRNA levels of bone formation markers COLL-1, BMP-2, RUNX2 and OC (A), bone resorption markers TRAP, CALCR, H^+ATPase and RANKL (B), inflammation markers TNF-α, IL6 and IL10 (C) and vitamin D related markers CYP27A1 and VDR (D) at the bone implant interface after 8 weeks of healing. Data represent fold changes of target genes normalized to reference genes (GAPDH, β-actin and 18S rRNA), expressed relative to Ti surfaces which were set at 100%. Values represent the mean ± S.E.M. (N=8). Significant differences were assessed by Student's t-test ($p< 0.05$): [a] treatment versus Ti; [b] VitD-LD versus VitD-HD.

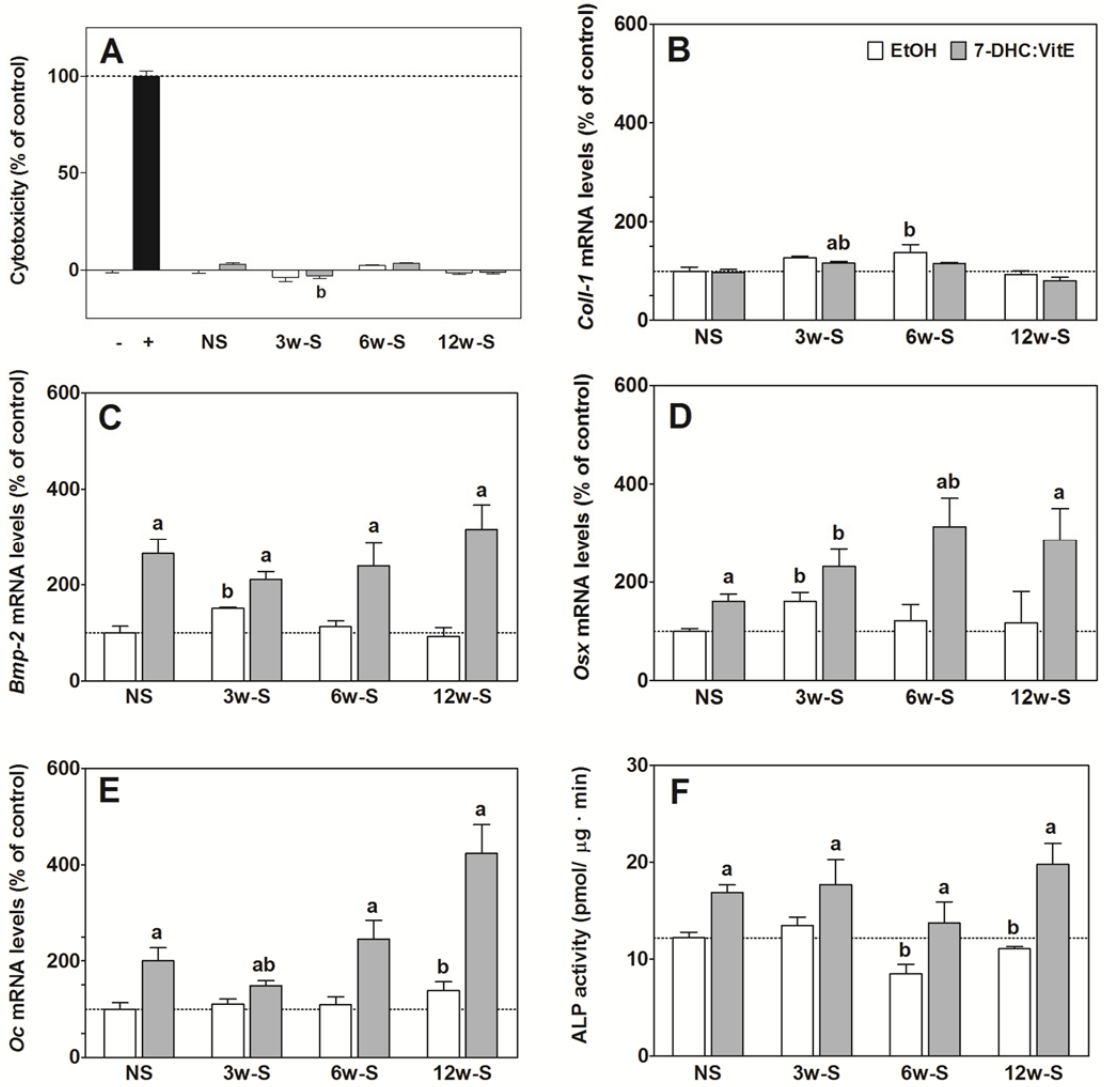

Figure 3. In vitro cell study confirming the bioactivity of UV-irradiated 7-DHC:VitE coated Ti implants. (A) LDH activity measured from culture media of MC3T3-E1 cells. Positive control (100%) was cell culture media from cells incubated with Triton X-100 at 1%. Negative control (0%) was cell culture media from cells seeded without any treatment. (B-E) mRNA levels of osteoblast differentiation markers *Coll-1* (B), *Bmp-2* (C), *Osx* (D) and *Oc* (E) in MC3T3-E1 cells. Data represent fold changes of target genes normalized to reference genes (GAPDH and 18S rRNA), expressed as percentage of control which was set to 100%. (D) ALP activity corrected for total protein in culture media of MC3T3-E1 cells. Values represent the mean ± S.E.M. (N=6). Significant differences were assessed by Student's t-test ($p < 0.05$): [a] 7-DHC:VitE versus EtOH for each storage time; [b] treatment of each storage time versus the same NS treatment.

5. General discussion & Future perspectives

5. General discussion & Future perspectives

The ultimate goal of current implant research is the development of new strategies in order to include patients that nowadays are excluded from dental implant therapies, being implant surface modifications among the strategies developed (Le Guéhennec et al., 2007; Novaes et al., 2010). This challenge is related to the increasing number of patients with compromised skeletal health what is partly due to the ageing of the population (Geetha et al., 2009). On one hand, it should be noted that one of the most important factors to avoid bone loss is the maintenance of adequate vitamin D status. Indeed, vitamin D deficiency leads to decreased bone mineral density and increases the risk of fractures (Lips and Van Schoor, 2011; Atkins et al., 2007; St-Arnaud, 2008) whilst its supplementation has shown beneficial effects on bone (Plum and DeLuca, 2010; Kubodera, 2009; Nishii, 2002; Tilyard et al., 1992). Interestingly, vitamin D has also a positive effect on oral health since it seems to lower the risk of periodontal diseases (Garcia, 2014; Martelli et al., 2014; Amano et al., 2009). On the other hand, it is important to consider that osteoporosis and related fractures are increasing considerably due to the increasing life expectancy and ageing of the population. Furthermore, vitamin D levels decline with increasing age (Feldman et al., 2013), which enhances the risk for bone loss and periodontal disease prevalence. Therefore, it is evident the crucial importance of vitamin D in maintaining a healthy skeleton and its application in challenging skeletal structures with impaired hard or soft tissue regeneration.

An ideal implant should promote peri-implant bone healing and osseointegration, whilst enhance soft tissue healing around the implant. Current dental implant surface modifications aim at improving these processes, especially in compromised skeletal structures, to further achieve successful long-term implant integration and stability. Thus, the research of this thesis aimed at developing a novel bioactive coating using the UV-irradiated vitamin D precursor 7-DHC to enhance hard and soft tissue regeneration. First, we aimed at investigating whereas osteoblastic cells could produce final active vitamin D from external UV-irradiated 7-DHC *in vitro*. Once it was demonstrated *(Paper I)*, the use of UV-irradiated 7-DHC as a bioactive coating for Ti implants to promote osteoblast differentiation as well as the biological action of this coating on other cells related to the skeletal tissue were further evaluated *(Papers II to V)*. Finally, the modified surfaces were tested *in vivo* using a rabbit animal study and the ageing effects on their composition and bioactivity were studied *in vitro (Paper VI)*.

The role of vitamin D in controlling bone mineralization is widely recognized (St-Arnaud, 2008) as well as its natural synthesis. It starts when human skin is exposed to sunlight which photoactivates 7-DHC and forms D_3 that is further twice hydroxylated in the liver and in the kidney until forming the active metabolite. Interestingly, extrarenal tissues and cells, including bone and gingival cells, express the enzymatic machinery required for synthesizing active vitamin D (Bikle, 2009). Furthermore, the use of the vitamin D precursor could entail several benefits when compared with the active metabolite, including lower cell toxicity, since the affinity of the non-hydroxylated forms for the vitamin D receptor is lower than the affinity of $1,25(OH)_2D_3$ (Chen et al., 2000). Also, 7-DHC is easily available and lower priced than the other forms of vitamin D_3, so this approach would entail a cheaper production. In the present doctoral thesis, UV-irradiated 7-DHC was used for the first time to locally produce vitamin D in bone and gingival cells and the resulting biological response was further evaluated. Results concluded

that UV-irradiated 7-DHC can be used as a bioactive coating for Ti implants to promote peri-implant tissue healing. Indeed, in accordance with numerous studies using vitamin D metabolites to maintain bone mineralization and reduce bone resorption (Atkins et al., 2007; Plum and DeLuca, 2010; Duncan, 2013), UV-irradiated 7-DHC coating involved higher osteoblast differentiation and mineralization whilst decreased osteoclast formation *in vitro*, especially when supplemented with vitamin E (VitE). The addition of an antioxidant to the coating was necessary for maintaining 7-DHC stability as well as for avoiding the oxidation of the vitamin D metabolites. For this purpose, VitE was the ideal candidate since it is a lipid soluble antioxidant with positive effects on bone. It prevents bone resorption (Nazrun et al., 2012) and preserves 7-DHC stability through its antioxidant properties (Korade et al., 2014). On the other hand, isomerization of preD_3 into D_3 is known to be a time and temperature dependent reaction (Holick, 2010). Accordingly, a controlled time and temperature incubation step was included in the coating preparation in order to favour the D_3 synthesis onto the Ti surface. Thus, the antioxidant addition and the incubation step after the UV-irradiation process increased the yield of the D_3 conversion obtained from the 7-DHC coating on the Ti surfaces.

The coating proposed in this doctoral thesis is based on the synthesis of D_3 on the Ti implant, which is further metabolized to its active form by the cells. Therefore, it would be expected that our coating has a similar mechanism of action than that found when 1,25$(OH)_2D_3$ is added. However, although the positive action of active vitamin D in maintaining a healthy skeleton is well-known, the fully biological pathway in which it is involved is not completely clear. Numerous investigations have suggested that vitamin D induces osteoblast differentiation and mineralization through the activation of the VDREs located in their gene promoters, such as COLL1, SPP1, OC, etc (Pike et al., 2012). Similarly, 1,25$(OH)_2D_3$ stimulates in the same manner the osteogenic differentiation from human mesenchymal stem/stromal cells (Zhou et al., 2006; Prince et al., 2001; Jørgensen et al., 2004; Zhou et al., 2012) by promoting the expression of similar bone markers (D'Ippolito et al., 2002; Chen et al., 2011). Additionally, 1,25$(OH)_2D_3$ elevates ALP activity and matrix mineralization of both human osteoblasts and mesenchymal stem cells (Van Driel and Van Leeuwen, 2014). In accordance with these studies, we proved that UV-irradiated 7-DHC coated implants promoted both *in vitro* differentiation of osteoblasts *(Paper II)* and MSCs *(Paper III)*, demonstrating its potential for the improvement on the osseointegration process of the implants. From these results, it can be considered that these modified implants are osteoconductive, since they support bone cell growth over its surface. However, in addition to being osteoconductive, an implant surface should be osteoinductive, in other words, it should be able to stimulate undifferentiated and pluripotent cells into bone forming cells. However, with the studies we have performed in this thesis we can not confirm the osteoinductive properties of our coating. In order to determine its osteoinductive capacity, MSCs should have been seeded on the modified surfaces without the supplementation of osteogenic factors and analyse if cells differentiate into the osteogenic lineage.

Besides the bone-forming cells, osteoclasts perform a relevant function in the bone remodelling process and their role at the bone-implant interface should be considered when evaluating dental implants. Interestingly, 1,25$(OH)_2D_3$ is thought to be involved in the suppression of bone resorption in an autocrine/paracrine manner (Takahashi et al., 2014). Thus, vitamin D may alter the bone microenvironment as well as affect the differentiation of MSCs into osteoblasts, modifying the RANKL expression. RANKL is expressed by most osteoblast-lineage cells and its levels decrease during

osteoblast maturation (Atkins et al., 2003). Vitamin D may directly affect osteoblasts to suppress bone resorption in a site-specific manner, by modulating RANKL expression. In fact, in this thesis we found that our coating inhibited RANKL mRNA levels in osteoblastic cells *in vitro (Paper II)*. But also a direct action of vitamin D on osteoclast activity has been considered (Takahashi et al., 2014), regulating the c-Fos transcription factor (Takasu et al., 2006) and the interferon β (Sakai et al., 2009), which are involved in osteoclastogenesis. These findings could explain the results found in this thesis when our coating was evaluated in osteoclastic cells, demonstrating its inhibitory action in osteoclastogenesis *in vitro (Paper IV)*.

On the other hand, since endosseous implants are in contact with both hard and soft tissues, it was of our interest to determine the biological potential of our coating in gingival cells. $1,25(OH)_2D_3$ has been suggested to have a beneficial effect on oral health (Garcia et al., 2011; Bashutski et al., 2011) and HGFs are able to produce the final active vitamin D (Liu et al., 2012). In line with this, we found that our coating showed a beneficial impact on HGFs through its anti-inflammatory properties *(Paper V)*. Similarly, previous literature suggested a favourable anti-inflammatory response in periodontal ligament cells when treated with $1,25(OH)_2D_3$ (Tang et al., 2013). Furthermore, results showed that our coating decreased MMP-related ECM breakdown and increased collagen synthesis, what would lead to the improvement of the soft tissue integration and the implant success. However, despite the positive results found in our study regarding the gingival fibroblast response to our modified implants, more in-depth studies would be required to elucidate the biochemical mechanisms involved in the cell response to the modified surfaces and the in vivo response of the soft tissue. Also, recent investigations have highlighted the anti-inflammatory potential of vitamin D as well as its anti-microbial activity (Amano et al., 2009; Stein et al., 2013; Martelli et al., 2014). Developing a bioactive surface coating capable of reducing possible bacterial infections and painful inflammatory processes would provide a key strategy in the dental implant field. Therefore, it would be very interesting to carry out future studies investigating the potential of UV-irradiated 7-DHC:VitE coated Ti implants in combating inflammation and bacterial colonization.

In vivo, two doses of 7-DHC were evaluated, the optimal *in vitro* dose and a 10 times higher dose. This experimental design was set in order to overcome the difficulty of the extrapolation of *in vitro* data to the *in vivo* situation. Moreover, it is known that the dose of vitamin D applied influences its effect. A different action of the modified implants was found in the *in vivo* experiment when using the low and the high doses of treatment. We found higher OC mRNA levels in the peri-implant bone tissue in the low dose studied, suggesting a more mature stage of the differentiation process *(Paper VI)*. Indeed, OC is considered one of the best predictive markers for osseointegration of Ti implants (Monjo et al., 2012). While the low dose of UV-irradiated 7-DHC:VitE revealed a positive effect on bone formation, a more toxic and inflammatory response was observed when using the high dose. This finding is in agreement with other studies which have identified suppressive effects of high dose of vitamin D supplementation on bone formation (Yamaguchi and Weitzmann, 2012). Further experiments could be performed using an animal model with poor bone quality or reduced bone quantity, e.g. an osteoporotic rat model which resembles human osteoporosis. In fact, several studies have used ovariectomized rats when studying the effect of vitamin D levels on the osseointegration of Ti implants (Kelly et al., 2009; Dvorak et al., 2012; Zhou et al., 2012). In any case, it is important to

consider the limitation of animal models and consequently we can not draw conclusions on the success or failure of a modified implant through the data collected by animal models used alone.

Another important issue considered in the present doctoral thesis was the ageing effect on the bioactive modified implants. Thus, although not many works describe the shelf-life stability of implantable medical devices, it is of great interest to determine how long these materials remain bioactive as well as the possible changes in their surface composition. Indeed, it is believed that one of the major limitations of implant surfaces modified with biological molecules is their shelf-life stability during storage and after their sterilization. In this thesis we demonstrated that UV-irradiated 7-DHC:VitE coated implants maintain their composition and their osteopromotive potential when stored up to 12 weeks at 4ºC and avoiding light, oxygen and moisture exposure *(Paper VI)*. However, further studies analyzing the ageing effects on the coating after storage at longer-term as well as the influence of the sterilization process in the stability and bioactivity of the coating would be greatly useful to consider its further clinical application. Thus, the sterilization of biomaterials is challenging due to the physicochemical changes and possible toxic residues obtained with the commonly used sterilization techniques (Türker et al., 2014). However, gamma radiation does not have any toxic residue and seems to be the best method to sterilize surface modified implants in future studies.

All in all, the work derived from this thesis has proved the feasibility of using the UV-irradiated vitamin D precursor, 7-DHC, to produce active vitamin D in cells involved in both hard and soft tissues. Furthermore, this finding has resulted in the development of a novel bioactive coating for Ti implants, using UV-irradiated 7-DHC, which may represent a potential strategy to improve both hard and soft tissue integration of dental implants.

6. Conclusions

6. Conclusions

I. Osteoblastic cells have the whole enzymatic machinery required to synthesize the final active vitamin D metabolite and are able to produce $1,25(OH)_2D_3$ from external UV-irradiated 7-DHC coated onto polystyrene surfaces. Furthermore, UV-irradiated 7-DHC can be used to produce D_3 locally at the surface of a Ti implant, which is a biocompatible and bioactive coating that increases differentiation of osteoblastic cells. Similarly, Ti implants coated with UV-irradiated 7-DHC promote hUC-MSC osteogenic differentiation *in vitro*.

II. The addition of an antioxidant agent, such as vitamin E, to the 7-DHC coating prior to UV-irradiation preserves the stability of the coating increasing the yield of $preD_3$ synthesis. Furthermore, D_3 formation from $preD_3$ is improved by including an incubation step at 23ºC for 48 hours after the UV-irradiation of the coated implant.

III. UV-irradiated 7-DHC : VitE coated Ti implants decrease *in vitro* osteoclastogenesis, reducing the number of Trap-positive multinucleated cells and the expression of different phenotypic, fusion and activity markers.

IV. A beneficial biological response was observed when UV-irradiated 7-DHC : VitE coated Ti implants were tested in HGFs *in vitro*. The coating shows a positive action in the inflammatory response and in the ECM maturation/breakdown.

V. *In vivo*, UV-irradiated 7-DHC : VitE coated Ti implants promote the gene expression of the late bone formation marker OC in the peri-implant bone and increase ALP activity in the wound fluid. Additionally, this coating maintains its composition and its bioactivity properties when stored up to 12 weeks at 4ºC, avoiding light, oxygen and moisture exposure.

VI. All in all, UV-irradiated 7-DHC : VitE coating can be considered in future dental implant therapies aiming at improving both, peri-implant hard and soft tissue healing.

7. References

7. References

Abiko Y, Hiratsuka K, Kiyama-Kishikawa M, Tsushima K, Ohta M, Sasahara H (2004). Profiling of differentially expressed genes in human gingival epithelial cells and fibroblasts by DNA microarray. *J Oral Sci,* 46:19–24.

Acton QA (2012). Osteoblasts—Advances in Research and Application. Atlanta, Georgia: ScholarlyEditions.

Albrektsson T, Johansson C (2001). Osteoinduction, osteoconduction and osseointegration. *Eur Spine J,* 10:96–101.

Amano Y, Komiyama K, Makishima M (2009). Vitamin D and periodontal disease. *J Oral Sci,* 51:11–20.

Anil S, Anand PS, Alghamdi H, Jansen J a (2005). Dental Implant Surface Enhancement and Osseointegration. Implant Dentistry - A Rapidly Evolving Practice. Rijeka, Croatia: InTech.

Arriagada G, Henriquez B, Moena D, Merino P, Ruiz-Tagle C, Lian JB, et al. (2010). Recruitment and subnuclear distribution of the regulatory machinery during 1alpha,25-dihydroxy vitamin D3-mediated transcriptional upregulation in osteoblasts. *J Steroid Biochem Mol Biol,* 121:156–8.

Ashcroft GS, Dodsworth J, van Boxtel E, Tarnuzzer RW, Horan MA, Schultz GS, et al. (1997). Estrogen accelerates cutaneous wound healing associated with an increase in TGF-beta1 levels. *Nat Med,* 3:1209–15.

Atkins GJ, Anderson PH, Findlay DM, Welldon KJ, Vincent C, Zannettino ACW, et al. (2007). Metabolism of vitamin D3 in human osteoblasts: evidence for autocrine and paracrine activities of 1 alpha,25-dihydroxyvitamin D3. *Bone* 40:1517–28.

Atkins GJ, Kostakis P, Pan B, Farrugia A, Gronthos S, Evdokiou A, et al. (2003). RANKL expression is related to the differentiation state of human osteoblasts. *J Bone Miner Res,* 18:1088–98.

Ballanti P, Minisola S, Pacitti MT, Scarnecchia L, Rosso R, Mazzuoli GF, et al. (1997). Tartrate-resistant acid phosphate activity as osteoclastic marker: sensitivity of cytochemical assessment and serum assay in comparison with standardized osteoclast histomorphometry. *Osteoporos Int,* 7:39–43.

Baron R (2003). Anatomy and biology of bone matrix and cellular elements. Primer on the metabolic bone diseases and disorders of mineral metabolism. Washington, DC, USA: John Wiley & Sons.

Barrère F, van der Valk CM, Meijer G, Dalmeijer RAJ, de Groot K, Layrolle P (2003). Osteointegration of biomimetic apatite coating applied onto dense and porous metal implants in femurs of goats. *J Biomed Mater Res B Appl Biomater*, 67:655–65.

Bartold PM, Haynes DR (1991). Interleukin-6 production by human gingival fibroblasts. *J Periodontal Res,* 26:339–45.

Bartold PM, Narayanan a S (2006). Molecular and cell biology of healthy and diseased periodontal tissues. *Periodontol 2000,* 40:29–49.

Bartold PM, Walsh LJ, Narayanan AS (2000). Molecular and cell biology of the gingiva. *Periodontol 2000,* 24:28–55.

Bashutski JD, Eber RM, Kinney JS, Benavides E, Maitra S, Braun TM, et al. (2011). The impact of vitamin D status on periodontal surgery outcomes. *J Dent Res,* 90:1007–12.

Bauer S, Schmuki P, von der Mark K, Park J (2013). Engineering biocompatible implant surfaces. *Prog Mater Sci,* 58:261–326.

Bauerlein E (2006). Biomineralization: Progress in Biology, Molecular Biology and Application. Weinheim, Germany: John Wiley & Sons.

Bellido T, Plotkin LI, Bruzzaniti A, Dimeglio LA, Imel EA, Weaver CM, et al. (2014). Bone cells. Basic and Applied Bone Biology. San Diego, CA, USA: Academic Press.

Bikle DD (2009). Extra renal synthesis of 1,25-dihydroxyvitamin D and its health implications. *Clin Rev Bone Miner Metab,* 7:114–125.

Bikle DD (2004). Vitamin D regulated keratinocyte differentiation. *J Cell Biochem,* 92:436–44.

Boskey A., Gadaleta S, Gundberg C, Doty S., Ducy P, Karsenty G (1998). Fourier transform infrared microspectroscopic analysis of bones of osteocalcin-deficient mice provides insight into the function of osteocalcin. *Bone,* 23:187–196.

Brånemark PI (1977). Osseointegrated implants in the treatment of the edentulous jaw. Experience from a 10-year period. Scand. *J Plast Reconstr Surg,* 16:1–132.

Brånemark PI, Adell R, Breine U, Hansson BO, Lindström J, Ohlsson A (1969). Intra-osseous anchorage of dental prostheses. I. Experimental studies. *Scand J Plast Reconstr Surg,* 3:81–100.

Braun M, Fuß W, Kompa KL, Wolfrum J (1991). Improved photosynthesis of previtamin D by wavelengths of 280–300 nm. *J Photochem Photobiol A Chem,* 61:15–26.

Buckwalter JA, Glimcher MJ, Cooper RR, Recker R (1995). Bone Biology. *J Bone Joint Surg Am,* 77-A:1256–1275.

Bustin SA (2000). Absolute quantification of mRNA using real-time reverse transcription polymerase chain reaction assays. *J Mol Endocrinol,* 25:169–93.

Bustin SA, Benes V, Garson JA, Hellemans J, Huggett J, Kubista M, et al. (2009). The MIQE guidelines: minimum information for publication of quantitative real-time PCR experiments. *Clin Chem,* 55:611–22.

Carano RA, Filvaroff EH (2003). Angiogenesis and bone repair. *Drug Discov Today,* 8:980–989.

Chen K, Perez-Stable C, D'Ippolito G, Schiller PC, Roos BA, Howard GA (2011). Human bone marrow-derived stem cell proliferation is inhibited by hepatocyte growth factor via increasing the cell cycle inhibitors p53, p21 and p27. *Bone,* 49:1194–204.

Chen TC, Persons KS, Lu Z, Mathieu JS, Holick MF (2000). An evaluation of the biologic activity and vitamin D receptor binding affinity of the photoisomers of vitamin D3 and previtamin D3. *J Nutr Biochem,* 11:267–272.

Chittur KK (1998). FTIR/ATR for protein adsorption to biomaterial surfaces. *Biomaterials* 19:357–69.

Cho Y-J, Heo S-J, Koak J-Y, Kim S-K, Lee S-J, Lee J-H (2011). Promotion of osseointegration of anodized titanium implants with a 1,25-dihydroxyvitamin D3 submicron particle coating. *Int J Oral Maxillofac Implant,* 26:1225–32.

Christakos S (2004). Vitamin D Gene Regulation. Principles of bone biology. San Diego, CA, USA: Academic Press.

Clarke B (2008). Normal bone anatomy and physiology. *Clin J Am Soc Nephrol,* 3:131–139.

Cochran D, Froum S (2013). Peri-implant mucositis and peri-implantitis: a current understanding of their diagnoses and clinical implications. *J. Periodontol,* 84:436–43.

Collin-Osdoby P, Osdoby P (2012). RANKL-mediated osteoclast formation from murine RAW 264.7 cells. *Methods Mol Biol,* 816:187–202.

Corle TR, Kino GS (1996). Confocal Scanning Optical Microscopy and Related Imaging Systems. San Diego, CA, USA: Academic Press.

Cunningham BW, Orbegoso CM, Dmitriev AE, Hallab NJ, Sefter JC, Asdourian P, et al. (2003). The effect of spinal instrumentation particulate wear debris. *Spine J,* 3:19–32.

Cury PR, Araújo VC, Canavez F, Furuse C, Araújo NS (2007). Hydrocortisone Affects the Expression of Matrix Metalloproteinases (MMP-1, -2, -3, -7, and -11) and Tissue Inhibitor of Matrix Metalloproteinases (TIMP-1) in Human Gingival Fibroblasts. *J Periodontol,* 78:1309–1315.

Czekanska EM, Stoddart MJ, Richards RG, Hayes JS (2012). In search of an osteoblast cell model for in vitro research. *Eur Cell Mater,* 24:1–17.

D'Ippolito G, Schiller PC, Perez-stable C, Balkan W, Roos BA, Howard GA (2002). Cooperative actions of hepatocyte growth factor and 1,25-dihydroxyvitamin D3 in osteoblastic differentiation of human vertebral bone marrow stromal cells. *Bone,* 31:269–75.

Davies CA, Jeziorska M, Freemont AJ, Herrick AL (2006). Expression of osteonectin and matrix Gla protein in scleroderma patients with and without calcinosis. *Rheumatology (Oxford),* 45:1349–55.

Davila JC, Rodriguez RJ, Melchert RB, Acosta D (1998). Predictive value of in vitro model systems in toxicology. *Annu Rev Pharmacol Toxicol,* 38:63–96.

Dawes KE, Cambrey AD, Campa JS, Bishop JE, McAnulty RJ, Peacock AJ, et al. (1996). Changes in collagen metabolism in response to endothelin-1: evidence for fibroblast heterogeneity. *Int J Biochem Cell Biol,* 28:229–38.

DeLuca HF (2004). Overview of general physiologic features and functions of vitamin D. *Am J Clin Nutr,* 80:1689S–96S.

DeLuca HF, Clagett-Dame M (2013). Vitamin D. Encyclopedia of Biological Chemistry. San Diego, CA, USA: Academic Press.

Deschaseaux F, Sensébé L, Heymann D (2009). Mechanisms of bone repair and regeneration. *Trends Mol Med,*15:417–29.

Dimitriou R, Jones E, McGonagle D, Giannoudis P V (2011). Bone regeneration: current concepts and future directions. *BMC Med,* 9:66.

Domeij H, Yucel-Lindberg T, Modeer T (2002). Signal pathways involved in the production of MMP-1 and MMP-3 in human gingival fibroblasts. *Eur J Oral Sci,* 110:302–306.

Dominici M, Le Blanc K, Mueller I, Slaper-Cortenbach I, Marini F, Krause D, et al. (2006). Minimal criteria for defining multipotent mesenchymal stromal cells. The International Society for Cellular Therapy position statement. *Cytotherapy* 8:315–7.

Duncan WE (2013). Osteomalacia, rickets and vitamin D insufficiency. Endocrine secrets. Philadelphia, PA, USA: Elsevier Inc.

Dunlevy JR, Couchman JR (1995). Interleukin-8 induces motile behavior and loss of focal adhesions in primary fibroblasts. *J Cell Sci,* 108:311–321.

Dvorak G, Fügl A, Watzek G, Tangl S, Pokorny P, Gruber R (2012). Impact of dietary vitamin D on osseointegration in the ovariectomized rat. *Clin Oral Implant Res,* 23:1308–13.

Elias CN, Lima JHC, Valiev R, Meyers M a. (2008). Biomedical applications of titanium and its alloys. *Jom,* 60:46–49.

Engleman VW, Nickols GA, Ross FP, Horton MA, Griggs DW, Settle SL, et al. (1997). A peptidomimetic antagonist of the alpha(v)beta3 integrin inhibits bone resorption in vitro and prevents osteoporosis in vivo. *J Clin Invest,* 99:2284–92.

Everts V, Delaissé JM, Korper W, Jansen DC, Tigchelaar-Gutter W, Saftig P, et al. (2002). The bone lining cell: its role in cleaning Howship's lacunae and initiating bone formation. *J Bone Miner Res,* 17:77–90.

Farina C, Gagliardi S (2002). Selective inhibition of osteoclast vacuolar H(+)-ATPase. *Curr Pharm Des,* 8:2033–2048.

Feldman D, Krishnan A V., Swami S (2013). Vitamin D. Biology, Actions, and Clinical Implications. Osteoporosis. Waltham, MA, USA: Academic Press.

Fernández-Tresguerres-Hernández-Gil I, Alobera-Gracia MA, del-Canto-Pingarrón M, Blanco-Jerez L (2006). Physiological bases of bone regeneration II. The remodeling process. *Med oral, Patol oral Cir bucal,* 11:151–157.

Fiorito S, Magrini L, Goalard C (2003). Pro-inflammatory and anti-inflammatory circulating cytokines and periprosthetic osteolysis. *J Bone Joint Surg Br,* 85:1202–6.

Fleisch H (2000). Bone and mineral metabolism. Biphosphonates in bone disease. From the Laboratory to the Patient. San Diego, CA, USA: Academic press.

Franceschi RT LY (2011). Vitamin D regulation of osteoblast function. Vitamin D. San Diego, CA, USA: Academic Press.

García AJ, Schwarzbauer JE, Boettiger D (2002). Distinct Activation States of $\alpha 5\beta 1$ Integrin Show Differential Binding to RGD and Synergy Domains of Fibronectin. *Biochemistry* 41:9063–9069.

Garcia MN (2014). Vitamin D May Reduce Periodontal Disease Prevalence in Older Men. *J Evid Based Dent Pract,* 14:39–41.

Garcia MN, Hildebolt CF, Miley DD, Dixon D a, Couture R a, Spearie CLA, et al. (2011). One-year effects of vitamin D and calcium supplementation on chronic periodontitis. *J Periodontol,* 82:25–32.

Geetha M, Singh a. K, Asokamani R, Gogia a. K (2009). Ti based biomaterials, the ultimate choice for orthopaedic implants - A review. *Prog Mater Sci,* 54:397–425.

Geissler U, Hempel U, Wolf C, Scharnweber D, Worch H, Wenzel K (2000). Collagen type I-coating of Ti6Al4V promotes adhesion of osteoblasts. *J Biomed Mater Res,* 51:752–60.

Gittens R a., Olivares-Navarrete R, Schwartz Z, Boyan BD (2014). Implant osseointegration and the role of microroughness and nanostructures: Lessons for spine implants. *Acta Biomater,* 10:3363–3371.

Golub EE, Harrison G, Taylor AG, Camper S, Shapiro IM (1992). The role of alkaline phosphatase in cartilage mineralization. *Bone Miner,* 17:273–8.

Gómez-Florit M, Ramis JM, Xing R, Taxt-Lamolle S, Haugen HJ, Lyngstadaas SP, et al. (2014). Differential response of human gingival fibroblasts to titanium- and titanium-zirconium-modified surfaces. *J Periodontal Res,* 49:425–36.

Gruber R, Bosshardt DD (2015). Dental Implantology and Implants: Basic Aspects and Tissue Interface. Stem Cell Biology and Tissue Engineering in Dental Sciences. San Diego, CA, USA: Academic Press.

Guillem-Marti J, Delgado L, Godoy-Gallardo M, Pegueroles M, Herrero M, Gil FJ (2013). Fibroblast adhesion and activation onto micro-machined titanium surfaces. *Clin Oral Implants Res,* 24:770–80.

Hadjidakis DJ, Androulakis II (2006). Bone remodeling. *Ann N Y Acad Sci,* 1092:385–96.

Hansdottir S, Monick MM, Hinde SL, Lovan N, Look DC, Hunninghake GW (2008). Respiratory epithelial cells convert inactive vitamin D to its active form: potential effects on host defense. *J Immunol,* 181:7090–9.

Hayman a R, Bune a J, Bradley JR, Rashbass J, Cox TM (2000). Osteoclastic tartrate-resistant acid phosphatase (Acp 5): its localization to dendritic cells and diverse murine tissues. *J Histochem Cytochem,* 48:219–228.

Heaney RP, Recker RR, Grote J, Horst RL, Armas LAG (2011). Vitamin D(3) is more potent than vitamin D(2) in humans. *J Clin Endocrinol Metab,* 96:E447–52.

Henriksen K, Neutzsky-Wulff A V., Bonewald LF, Karsdal M a. (2009). Local communication on and within bone controls bone remodeling. *Bone,* 44:1026–1033.

Hewison M, Freeman L, Hughes S V, Evans KN, Bland R, Eliopoulos AG, et al. (2003). Differential regulation of vitamin D receptor and its ligand in human monocyte-derived dendritic cells. *J Immunol,* 170:5382–5390.

Hinsley EE, Kumar S, Hunter KD, Whawell SA, Lambert DW (2012). Endothelin-1 stimulates oral fibroblasts to promote oral cancer invasion. *Life Sci,* 91:557–61.

Holick MF (1981). The cutaneous photosynthesis of previtamin D3: a unique photoendocrine system. *J Invest Dermatol,* 77:51–58.

Holick MF (2005). Vitamin D. Modern Nutrition in Health and Disease. Baltimore, Maryland, USA: Lippincott Williams & Wilkins.

Holick MF (2010). Vitamin D. Physiology, Molecular Biology, and Clinical Applications. New York, NY, USA: Humana Press.

Horne WC, Baron R (2000). Regulating Bone Resorption : Targeting Integrins , Calcitonin Receptor , and Cathepsin K. Principles of bone biology. San Diego, CA, USA: Academic Press.

Hsu YC, Chen MJ, Yu YM, Ko SY, Chang CC (2010). Suppression of TGF-β1/SMAD pathway and extracellular matrix production in primary keloid fibroblasts by curcuminoids: Its potential therapeutic use in the chemoprevention of keloid. *Arch Dermatol Res,* 302:717–724.

Hugh L. J. Makin DJHT (1984). Measurements of Vitamin D and its Metabolites by Gas Chromatography-Mass Spectrometry. Vitamin D. Boston, MA: Springer US.

Imai Y, Youn M-Y, Inoue K, Takada I, Kouzmenko A, Kato S (2013). Nuclear receptors in bone physiology and diseases. *Physiol Rev,* 93:481–523.

Inoue S (2005). Postmenopausal osteoporosis. *Nihon Naika Gakkai Zasshi,* 94:626–631.

Ishizuka H, García-Palacios V, Lu G, Subler MA, Zhang H, Boykin CS, et al. (2011). ADAM8 enhances osteoclast precursor fusion and osteoclast formation in vitro and in vivo. *J Bone Miner Res,* 26:169–81.

Jaiswal N, Haynesworth SE, Caplan AI, Bruder SP (1997). Osteogenic differentiation of purified, culture-expanded human mesenchymal stem cells in vitro. *J Cell Biochem,* 64:295–312.

Jensen ED, Gopalakrishnan R, Westendorf JJ (2010). Regulation of gene expression in osteoblasts. *BioFactors,* 36:25–32.

Jimi E, Hirata S, Osawa K, Terashita M, Kitamura C, Fukushima H (2012). The current and future therapies of bone regeneration to repair bone defects. *Int J Dent,* 2012:1–8.

Jones G (2008). Pharmacokinetics of vitamin D toxicity. *Am J Clin Nutr,* 88:582S–586S.

Jones G, Prosser DE (2011). The activating enzymes of vitamin D metabolism (25- and 1α-hydroxylases). Vitamin D. San Diego, CA, USA: Academic Press.

Jørgensen NR, Henriksen Z, Sørensen OH, Civitelli R (2004). Dexamethasone, BMP-2, and 1,25-dihydroxyvitamin D enhance a more differentiated osteoblast phenotype: validation of an in vitro model for human bone marrow-derived primary osteoblasts. *Steroids,* 69:219–26.

Josse S, Faucheux C, Soueidan A, Grimandi G, Massiot D, Alonso B, et al. (2004). Chemically Modified Calcium Phosphates as Novel Materials for Bisphosphonate Delivery *Adv Mater*, 16:1423–1427.

Kärkkäinen M, Tuppurainen M, Salovaara K, Sandini L, Rikkonen T, Sirola J, et al. (2010). Effect of calcium and vitamin D supplementation on bone mineral density in women aged 65-71 years: a 3-year randomized population-based trial (OSTPRE-FPS). *Osteoporos Int,* 21:2047–55.

Katagiri T, Takahashi N (2002). Regulatory mechanisms of osteoblast and osteoclast differentiation. *Oral Dis,* 8:147–59.

Kelly J, Lin A, Wang CJ, Park S, Nishimura I (2009). Vitamin D and bone physiology: demonstration of vitamin D deficiency in an implant osseointegration rat model. *J Prosthodont,* 18:473–8.

Keselowsky BG, Collard DM, García AJ (2003). Surface chemistry modulates fibronectin conformation and directs integrin binding and specificity to control cell adhesion. *J Biomed Mater Res A,* 66:247–59.

Kikuchi K, Kadono T, Furue M, Tamaki K (1997). Tissue inhibitor of metalloproteinase 1 (TIMP-1) may be an autocrine growth factor in scleroderma fibroblasts. *J Invest Dermatol,* 108:281–284.

Kini U, Nandeesh BN (2012). Physiology of Bone Formation, Remodelling, and Metabolism. Radionuclide and Hybrid Bone Imaging. Hybrid Bone Imaging. Springer Berlin Heidelberg.

Komori T, Yagi H, Nomura S, Yamaguchi A, Sasaki K, Deguchi K, et al. (1997). Targeted disruption of Cbfa1 results in a complete lack of bone formation owing to maturational arrest of osteoblasts. *Cell,* 89:755–64.

Korade Z, Xu L, Harrison FE, Ahsen R, Hart SE, Folkes OM, et al. (2014). Antioxidant supplementation ameliorates molecular deficits in Smith-Lemli-Opitz syndrome. *Biol Psychiatry,* 75:215–22.

Kubodera N (2009). D-hormone derivatives for the treatment of osteoporosis: from alfacalcidol to eldecalcitol. *Mini Rev Med Chem,* 9:1416–22.

Lai C-F, Cheng S-L (2005). Alphavbeta integrins play an essential role in BMP-2 induction of osteoblast differentiation. *J Bone Miner Res,* 20:330–40.

Le Guéhennec L, Soueidan a, Layrolle P, Amouriq Y (2007). Surface treatments of titanium dental implants for rapid osseointegration. *Dent Mater,* 23:844–54.

Lee AMC, Sawyer RK, Moore AJ, Morris HA, O'Loughlin PD, Anderson PH (2014). Adequate dietary vitamin D and calcium are both required to reduce bone turnover and increased bone mineral volume. *J Steroid Biochem Mol Biol,* 144 Pt A:159–62.

Lee NK (2005). A crucial role for reactive oxygen species in RANKL-induced osteoclast differentiation. *Blood,* 106:852–859.

Lehenkari P, Hentunen T a, Laitala-Leinonen T, Tuukkanen J, Väänänen HK (1998). Carbonic anhydrase II plays a major role in osteoclast differentiation and bone resorption by effecting the steady state intracellular pH and Ca2+. *Exp Cell Res,* 242:128–137.

Lehmann B, Genehr T, Knuschke P, Pietzsch J, Meurer M (2001). UVB-induced conversion of 7-dehydrocholesterol to 1alpha,25-dihydroxyvitamin D3 in an in vitro human skin equivalent model. *J Invest Dermatol,* 117:1179–1185.

Lensmeyer GL, Wiebe DA, Binkley N, Drezner MK (2006). HPLC method for 25-hydroxyvitamin D measurement: comparison with contemporary assays. *Clin Chem,* 52:1120–6.

Lian JB, Stein GS, Montecino M, Stein JL van WA (2011). Genetic and epigenetic control of the regulatory machinary for skeletal develpment and bone formation: contributions of vitamin D3. Vitamin D. San Diego: Elsevier/Academic Press.

Liang C-C, Park AY, Guan J-L (2007). In vitro scratch assay: a convenient and inexpensive method for analysis of cell migration in vitro. *Nat Protoc,* 2:329–33.

Lin S, Sangaj N, Razafiarison T, Zhang C, Varghese S (2011). Influence of physical properties of biomaterials on cellular behavior. *Pharm Res,* 28:1422–30.

Lips P, Van Schoor NM (2011). The effect of vitamin D on bone and osteoporosis. *Best Pr Res Clin Endocrinol Metab,* 25:585–91.

Liu K, Meng H, Hou J (2012). Activity of 25-Hydroxylase in Human Gingival Fibroblasts and Periodontal Ligament Cells AT Slominski, editor. *PLoS One,* 7:e52053.

Liu W, Zhang S, Zhao D, Zou H, Sun N, Liang X, et al. (2014). Vitamin D supplementation enhances the fixation of titanium implants in chronic kidney disease mice. *PLoS One,* 9:3–8.

Liu X, Chu PK, Ding C (2010). Surface nano-functionalization of biomaterials. *Mater Sci Eng R Reports,* 70:275–302.

Mackiewicz Z, Niklińska WE, Kowalewska J, Chyczewski L (2011). Bone as a source of organism vitality and regeneration. *Folia Histochem Cytobiol,* 49:558–569.

Martelli FS, Martelli M, Rosati C, Fanti E (2014). Vitamin D: relevance in dental practice. *Clin Cases Miner Bone Metab,* 11:15–19.

Mavrogenis a. F, Dimitriou R, Parvizi J, Babis GC (2009). Biology of implant osseointegration. *J Musculoskelet Neuronal Interact,* 9:61–71.

McHugh KP, Hodivala-Dilke K, Zheng MH, Namba N, Lam J, Novack D, et al. (2000). Mice lacking beta3 integrins are osteosclerotic because of dysfunctional osteoclasts. *J Clin Invest,* 105:433–40.

McNamara LE, McMurray RJ, Biggs MJP, Kantawong F, Oreffo ROC, Dalby MJ (2010). Nanotopographical control of stem cell differentiation. *J Tissue Eng,* 2010:120623.

Mendonça G, Mendonça DBS, Aragão FJL, Cooper LF (2008). Advancing dental implant surface technology - From micron- to nanotopography. *Biomaterials* 29:3822–3835.

Monjo M, Lamolle SF, Lyngstadaas SP, Rønold HJ, Ellingsen JE (2008). In vivo expression of osteogenic markers and bone mineral density at the surface of fluoride-modified titanium implants. *Biomaterials,* 29:3771–80.

Monjo M, Ramis JM, Rønold HJ, Taxt-Lamolle SF, Ellingsen JE, Lyngstadaas SP (2012). Correlation between molecular signals and bone bonding to titanium implants. *Clin Oral Implants Res,* 24:1035–43.

Morandini ACDF, Sipert CR, Ramos-Junior ES, Brozoski DT, Santos CF (2011). Periodontal ligament and gingival fibroblasts participate in the production of TGF-β, interleukin (IL)-8 and IL-10. *Braz Oral Res,* 25:157–162.

Naito Y, Jimbo R, Bryington MS, Vandeweghe S, Chrcanovic BR, Tovar N, et al. (2014). The influence of 1α.25-dihydroxyvitamin d3 coating on implant osseointegration in the rabbit tibia. *J Oral Maxillofac Res,* 5:e3.

Nakamura I, Pilkington MF, Lakkakorpi PT, Lipfert L, Sims SM, Dixon SJ, et al. (1999). Role of alpha(v)beta(3) integrin in osteoclast migration and formation of the sealing zone. *J Cell Sci,* 112:3985–3993.

Nardi, N. Beyer; da Silva Meirelles L (2006). Mesenchymal Stem Cells: Isolation, In Vitro Expansion and Characterization. *Handb Exp Pharmacol*, 174:249–82.

Navarro M, Michiardi a, Castaño O, Planell J a (2008). Biomaterials in orthopaedics. *J R Soc Interface,* 5:1137–58.

Nazrun a S, Norazlina M, Norliza M, Nirwana SI (2012). The anti-inflammatory role of vitamin e in prevention of osteoporosis. *Adv Pharmacol Sci,* 2012:142702.

Niinomi M (2003). Recent research and development in titanium alloys for biomedical applications and healthcare goods. *Sci Technol Adv Mater,* 4:445–454.

Nishii Y (2002). Active vitamin D and its analogs as drugs for the treatment of osteoporosis: advantages and problems. *J Bone Miner Metab,* 20:57–65.

Noda M, Denhardt DT (2008). Osteopontin. Principles of Bone Biology. San Diego, CA, USA: Academic Press.

Nomizu T, Kaneco S, Tanaka T, Ito D, Kawaguchi H, Vallee BT (1994). Determination of Calcium Content in Individual Biological Cells by Inductively Coupled Plasma Atomic Emission Spectrometry. *Anal Chem,* 66:3000–3004.

Norman A (2012). Vitamin D. The calcium homeostatic steroid hormone. New York, NY, USA: Academic Press.

Novaes AB, de Souza SLS, de Barros RRM, Pereira KKY, Iezzi G, Piattelli A (2010). Influence of implant surfaces on osseointegration. *Braz Dent J,* 21:471–481.

Nyan M, Miyahara T, Noritake K, Hao J, Rodriguez R, Kuroda S, et al. (2010). Molecular and tissue responses in the healing of rat calvarial defects after local application of simvastatin combined with alpha tricalcium phosphate. *J Biomed Mater Res B Appl Biomater,* 93:65–73.

Omdahl JL, Morris HA, May BK (2002). Hydroxylase enzymes of the vitamin D pathway: expression, function, and regulation. *Annu Rev Nutr,* 22:139–66.

Ouchi A, Ishikura M, Konishi K, Nagaoka S-I, Mukai K (2009). Kinetic study of the prooxidant effect of alpha-tocopherol. Hydrogen abstraction from lipids by alpha-tocopheroxyl radical. *Lipids,* 44:935–43.

Palaiologou AA, Yukna RA, Moses R, Lallier TE (2001). Gingival, dermal, and periodontal ligament fibroblasts express different extracellular matrix receptors. *J Periodontol,* 72:798–807.

Palmquist A, Omar OM, Esposito M, Lausmaa J, Thomsen P (2010). Titanium oral implants: surface characteristics, interface biology and clinical outcome. *J R Soc Interface,* 7:S515–27.

Peterson WJ, Tachiki KH, Yamaguchi DT (2004). Serial passage of MC3T3-E1 cells down-regulates proliferation during osteogenesis in vitro. *Cell Prolif,* 37:325–36.

Pfaffl MW (2001). A new mathematical model for relative quantification in real-time RT-PCR. *Nucleic Acids Res,* 29:e45.

Pfaffl MW, Tichopad A, Prgomet C, Neuvians TP (2004). Determination of stable housekeeping genes, differentially regulated target genes and sample integrity: BestKeeper--Excel-based tool using pair-wise correlations. *Biotechnol Lett,* 26:509–15.

Pike JW, Meyer MB, Bishop K a (2012). Regulation of target gene expression by the vitamin D receptor - an update on mechanisms. *Rev Endocr Metab Disord,* 13:45–55.

Plum LA, DeLuca HF (2010). Vitamin D, disease and therapeutic opportunities. *Nat Rev Drug Discov,* 9:941–955.

Porter NA (2013). A Perspective on Free Radical Autoxidation: The Physical Organic Chemistry of Polyunsaturated Fatty Acid and Sterol Peroxidation. *J Org Chem,* 78:3511–3524.

Priemel M, von Domarus C, Klatte TO, Kessler S, Schlie J, Meier S, et al. (2010). Bone mineralization defects and vitamin D deficiency: histomorphometric analysis of iliac crest bone biopsies and circulating 25-hydroxyvitamin D in 675 patients. *J Bone Miner Res,* 25:305–12.

Prince M, Banerjee C, Javed A, Green J, Lian JB, Stein GS, et al. (2001). Expression and regulation of Runx2/Cbfa1 and osteoblast phenotypic markers during the growth and differentiation of human osteoblasts. *J Cell Biochem,* 80:424–40.

Quent VMC, Loessner D, Friis T, Reichert JC, Hutmacher DW (2010). Discrepancies between metabolic activity and DNA content as tool to assess cell proliferation in cancer research. *J Cell Mol Med,* 14:1003–13.

Raggatt LJ, Partridge NC (2010). Cellular and molecular mechanisms of bone remodeling. *J Biol Chem,* 285:25103–25108.

Rao J, Otto WR (1992). Fluorimetric DNA assay for cell growth estimation. *Anal Biochem,* 207:186–92.

Reichrath J (2007). Vitamin D and the skin: an ancient friend, revisited. *Exp Dermatol,* 16:618–25.

Robey PG (2008). Non-collagenous Bone Matrix Proteins. Principles of bone biology. San Diego, CA, USA: Academic Press.

Robling AG, Castillo AB, Turner CH (2006). Biomechanical and molecular regulation of bone remodeling. *Annu Rev Biomed Eng,* 8:455–98.

Rockey DC, Weymouth N, Shi Z (2013). Smooth muscle α actin (Acta2) and myofibroblast function during hepatic wound healing. *PLoS One,* 8:e77166.

Rodriguez LG, Wu X, Guan J-L (2005). Wound-healing assay. *Methods Mol Biol,* 294:23–29.

Rønold HJ, Ellingsen JE (2002). The use of a coin shaped implant for direct in situ measurement of attachment strength for osseointegrating biomaterial surfaces. *Biomaterials* 23:2201–2209.

Sairanen S, Kärkkäinen M, Tähtelä R, Laitinen K, Mäkelä P, Lamberg-Allardt C, et al. (2000). Bone mass and markers of bone and calcium metabolism in postmenopausal women treated with 1,25-dihydroxyvitamin D (Calcitriol) for four years. *Calcif Tissue Int,* 67:122–7.

Sakai S, Takaishi H, Matsuzaki K, Kaneko H, Furukawa M, Miyauchi Y, et al. (2009). 1-Alpha, 25-dihydroxy vitamin D3 inhibits osteoclastogenesis through IFN-beta-dependent NFATc1 suppression. *J Bone Miner Metab,* 27:643–52.

Salgado AJ, Coutinho OP, Reis RL (2004). Bone tissue engineering: State of the art and future trends. *Macromol Biosci,* 4:743–765.

Sase SP, Ganu J V, Nagane N (2012). Osteopontin : A Novel Protein Molecule. *Ind Med Gaz,* 2012:62–66.

Satish L, Kathju S (2010). Cellular and molecular characteristics of scarless versus fibrotic wound healing. *Dermatol Res Pr,* 2010.

Sculean A, Gruber R, Bosshardt DD (2014). Soft tissue wound healing around teeth and dental implants. *J Clin Periodontol,* 41:S6–22.

Seeman E (2008). Basic Principles. Modeling and remodeling: The cellular machinery responsible for the gain and loss of bone's material and structural strength. Principles of bone biology. San Diego, CA, USA: Academic Press.

Shea JE, Miller SC (2005). Skeletal function and structure: implications for tissue-targeted therapeutics. *Adv Drug Deliv Rev,* 57:945–57.

Shrivats AR, Alvarez P, Schutte L, Hollinger JO (2014). Bone Regeneration. Principles of Tissue Engineering. Elsevier.

Silva MJ (2012). Skeletal Aging and Osteoporosis: Biomechanics and Mechanobiology. Springer-Verlag Berlin Heidelberg.

Sims N a., Gooi JH (2008). Bone remodeling: Multiple cellular interactions required for coupling of bone formation and resorption. *Semin Cell Dev Biol,* 19:444–451.

Smith BC (2011). Fundamentals of Fourier Transform Infrared Spectroscopy. CRC Press.

Souberbielle JC, Body JJ, Lappe JM, Plebani M, Shoenfeld Y, Wang TJ, et al. (2010). Vitamin D and musculoskeletal health, cardiovascular disease, autoimmunity and cancer: Recommendations for clinical practice. *Autoimmun Rev,* 9:709–15.

Souza W De (2007). Electron Microscopy Visualization of the Cell Surface of Trypanosomatids. Modern Research and Educational Topics on Microscopy. Badajoz, Spain: Formatex.

Soysa NS, Alles N, Aoki K, Ohya K (2012). Osteoclast formation and differentiation: An overview. *J Med Dent Sci,* 59:65–74.

St-Arnaud R (2008). The direct role of vitamin D on bone homeostasis. *Arch Biochem Biophys,* 473:225–230.

Stein GS, Lian JB, Stein JL, Van Wijnen AJ, Montecino M (1996). Transcriptional control of osteoblast growth and differentiation. *Physiol Rev,* 76:593–629.

Stein SH, Livada R, Tipton D a (2013). Re-evaluating the role of vitamin D in the periodontium. *J Periodontal Res,* 49:545–53.

Suda T, Takahashi N, Udagawa N, Jimi E, Gillespie MT, Martin TJ (1999). Modulation of osteoclast differentiation and function by the new members of the tumor necrosis factor receptor and ligand families. *Endocr Rev,* 20:345–57.

Sudo H, Kodama HA, Amagai Y, Yamamoto S, Kasai S (1983). In vitro differentiation and calcification in a new clonal osteogenic cell line derived from newborn mouse calvaria. *J Cell Biol,* 96:191–8.

Sul Y-T, Johansson C, Wennerberg A, Cho L-R, Chang B-S, Albrektsson T (2005). Optimum surface properties of oxidized implants for reinforcement of osseointegration: surface chemistry, oxide thickness, porosity, roughness, and crystal structure. *Int J Oral Maxillofac Implants,* 20:349–359.

Sundaram K, Nishimura R, Senn J, Youssef RF, London SD, Reddy S V. (2007). RANK ligand signaling modulates the matrix metalloproteinase-9 gene expression during osteoclast differentiation. *Exp Cell Res,* 313:168–178.

Szeto C-C, Chow K-M, Kwan BC-H, Chung K-Y, Leung C-B, Li PK-T (2008). Oral calcitriol for the treatment of persistent proteinuria in immunoglobulin A nephropathy: an uncontrolled trial. *Am J Kidney Dis,* 51:724–31.

Taguchi Y, Yamamoto M, Yamate T, Lin SC, Mocharla H, DeTogni P, et al. (1998). Interleukin-6-type cytokines stimulate mesenchymal progenitor differentiation toward the osteoblastic lineage. *Proc Assoc Am Physicians,* 110:559–74.

Takahashi N, Udagawa N, Kobayashi Y, Takami M, Martin TJ, Suda T (2008). Osteoclast Generation. Principles of bone biology. San Diego, CA, USA: Academic Press.

Takahashi N, Udagawa N, Udagawa N, Suda T (2014). Vitamin D endocrine system and osteoclasts. *Bonekey Rep,* 3:495.

Takasu H, Sugita A, Uchiyama Y, Katagiri N, Okazaki M, Ogata E, et al. (2006). c-Fos protein as a target of anti-osteoclastogenic action of vitamin D, and synthesis of new analogs. *J Clin Invest,* 116:528–35.

Tang X, Pan Y, Zhao Y (2013). Vitamin D inhibits the expression of interleukin-8 in human periodontal ligament cells stimulated with Porphyromonas gingivalis. *Arch Oral Biol,* 58:397–407.

Teitelbaum SL, Ross FP (2003). Genetic regulation of osteoclast development and function. *Nat Rev Genet,* 4:638–49.

Tengvall P, Lundström I (1992). Physico-chemical considerations of titanium as a biomaterial. *Clin Mater,* 9:115–134.

Termine JD, Kleinman HK, Whitson SW, Conn KM, McGarvey ML, Martin GR (1981). Osteonectin, a bone-specific protein linking mineral to collagen. *Cell,* 26:99–105.

Thadhani R (2009). Is calcitriol life-protective for patients with chronic kidney disease? *J Am Soc Nephrol,* 20:2285–90.

Thevenot P, Hu W, Tang L (2008). Surface chemistry influences implant biocompatibility. *Curr Top Med Chem,* 8:270–80.

Thornton B, Basu C (2011). Real-time PCR (qPCR) primer design using free online software. *Biochem Mol Biol Educ,* 39:145–54.

Tilg H, Trehu E, Atkins MB, Dinarello CA, Mier JW (1994). Interleukin-6 (IL-6) as an anti-inflammatory cytokine: induction of circulating IL-1 receptor antagonist and soluble tumor necrosis factor receptor p55. *Blood,* 83:113–8.

Tilyard MW, Spears GF, Thomson J, Dovey S (1992). Treatment of postmenopausal osteoporosis with calcitriol or calcium. *N Eng J Med*, 326:357-362.

Tu Q, Valverde P, Chen J (2006). Osterix enhances proliferation and osteogenic potential of bone marrow stromal cells. *Biochem Biophys Res Commun,* 341:1257–65.

Türker NS, Özer a. Y, Kutlu B, Nohutcu R, Sungur A, Bilgili H, et al. (2014). The effect of gamma radiation sterilization on dental biomaterials. *Tissue Eng Regen Med,* 11:341–349.

Väänänen HK, Zhao H (2008). Osteoclast Function. Biology and Mechanisms. Principles of bone biology. San Diego, CA, USA: Academic Press.

Väänänen HK, Zhao H, Mulari M, Halleen JM (2000). The cell biology of osteoclast function. *J Cell Sci,* 113:377–381.

Vallet-Regí M (2014). Bio-Ceramics with Clinical Applications. Chichester, UK: John Wiley & Sons, Ltd.

Van Driel M, Van Leeuwen J PTM (2014). Vitamin D endocrine system and osteoblasts. *Bonekey Rep,* 3:493.

Van Tienhoven EAE, Korbee D, Schipper L, Verharen HW, De Jong WH (2006). In vitro and in vivo (cyto)toxicity assays using PVC and LDPE as model materials. *J Biomed Mater Res A,* 78:175–82.

Verhaar HJ, Samson MM, Jansen PA, de Vreede PL, Manten JW, Duursma SA (2000). Muscle strength, functional mobility and vitamin D in older women. *Aging,* 12:455–60.

Vitale RF, Ribeiro F de AQ (2007). The role of tumor necrosis factor-alpha (TNF-alpha) in bone resorption present in middle ear cholesteatoma. *Braz J Otorhinolaryngol,* 73:117–21.

Wang W, Poh CK (2013). Titanium Alloys in Orthopaedics. Titanium alloys - Advances in properties control. InTech.

Wang Y-H, Liu Y, Maye P, Rowe DW (2006). Examination of mineralized nodule formation in living osteoblastic cultures using fluorescent dyes. *Biotechnol Prog,* 22:1697–701.

Willems E, Mateizel I, Kemp C, Cauffman G, Sermon K, Leyns L (2006). Selection of reference genes in mouse embryos and in differentiating human and mouse ES cells. *Int J Dev Biol,* 50:627–635.

Wilson CJ, Clegg RE, Leavesley DI, Pearcy MJ (2005). Mediation of biomaterial-cell interactions by adsorbed proteins: a review. *Tissue Eng,* 11:1–18.

Wilson SR, Peters C, Saftig P, Brömme D (2009). Cathepsin K activity-dependent regulation of osteoclast actin ring formation and bone resorption. *J Biol Chem,* 284:2584–2592.

Wu Q, Merchant F, Castleman K (2010). Microscope Image Processing. San Diego, CA, USA: Academic Press.

Wu Y, Yu T, Yang X, Li F, Ma L, Yang Y, et al. (2013). Vitamin D3 and insulin combined treatment promotes titanium implant osseointegration in diabetes mellitus rats. *Bone,* 52:1–8.

Yagi M, Miyamoto T, Sawatani Y, Iwamoto K, Hosogane N, Fujita N, et al. (2005). DC-STAMP is essential for cell-cell fusion in osteoclasts and foreign body giant cells. *J Exp Med,* 202:345–51.

Yakar S, Courtland H-W, Clemmons D (2010). IGF-1 and bone: New discoveries from mouse models. *J Bone Miner Res,* 25:2543–52.

Yakar S, Rosen CJ, Beamer WG, Ackert-Bicknell CL, Wu Y, Liu JL, et al. (2002). Circulating levels of IGF-1 directly regulate bone growth and density. *J Clin Invest,* 110:771–781.

Yamaguchi A, Komori T, Suda T (2000). Regulation of osteoblast differentiation mediated by bone morphogenetic proteins, hedgehogs, and Cbfa1. *Endocr Rev,* 21:393–411.

Yamaguchi M, Weitzmann MN (2012). High dose 1,25(OH)2D3 inhibits osteoblast mineralization in vitro. *Int J Mol Med,* 29:934–8.

Yaszemski MJ, Trantolo DJ, Lewandrowski KU, Hasirci V, Altobelli DE (2003). Tissue Engineering And Novel Delivery Systems. New York, NY, USA: CRC Press.

Yucel-Lindberg T, Båge T (2013). Inflammatory mediators in the pathogenesis of periodontitis. *Expert Rev Mol Med,* 15:e7.

Yucel-Lindberg T, Brunius G (2006). Epidermal growth factor synergistically enhances interleukin-8 production in human gingival fibroblasts stimulated with interleukin-1β. *Arch Oral Biol,* 51:892–898.

Zhao G, Raines AL, Wieland M, Schwartz Z, Boyan BD (2007). Requirement for both micron- and submicron scale structure for synergistic responses of osteoblasts to substrate surface energy and topography. *Biomaterials,* 28:2821–9.

Zhou C, Li Y, Wang X, Shui X, Hu J (2012). 1,25Dihydroxy vitamin D(3) improves titanium implant osseointegration in osteoporotic rats. *Oral Surg Oral Med Oral Pathol Oral Radiol,* 114:S174–8.

Zhou S, Glowacki J, Kim SW, Hahne J, Geng S, Mueller SM, et al. (2012). Clinical Characteristics Influence In Vitro Action of 1,25-Dihydroxyvitamin D3 in Human Marrow Stromal Cells. *Connect Tissue Res,* 27:1992–2000.

Zhou X, Zhang Z, Feng JQ, Dusevich VM, Sinha K, Zhang H, et al. (2010). Multiple functions of Osterix are required for bone growth and homeostasis in postnatal mice. *Proc Natl Acad Sci USA*, 107:12919–12924.

Zhou Y, Liu Y, Tan J (2006). Is 1, 25-dihydroxyvitamin D3 an ideal substitute for dexamethasone for inducing osteogenic differentiation of human adipose tissue-derived stromal cells in vitro? *Chin Med. J (Engl),* 119:1278–86.

Zoppi N, Gardella R, De Paepe A, Barlati S, Colombi M (2004). Human fibroblasts with mutations in COL5A1 and COL3A1 genes do not organize collagens and fibronectin in the extracellular matrix, down-regulate alpha2beta1 integrin, and recruit alphavbeta3 Instead of alpha5beta1 integrin. *J Biol Chem,* 279:18157–68.